

University of Southampton Research Repository

Copyright © and Moral Rights for this thesis and, where applicable, any accompanying data are retained by the author and/or other copyright owners. A copy can be downloaded for personal non-commercial research or study, without prior permission or charge. This thesis and the accompanying data cannot be reproduced or quoted extensively from without first obtaining permission in writing from the copyright holder/s. The content of the thesis and accompanying research data (where applicable) must not be changed in any way or sold commercially in any format or medium without the formal permission of the copyright holder/s.

When referring to this thesis and any accompanying data, full bibliographic details must be given, e.g.

Thesis: Author (Year of Submission) "Full thesis title", University of Southampton, name of the University Faculty or School or Department, PhD Thesis, pagination.

Data: Author (Year) Title. URI [dataset]

University of Southampton

Faculty of Environmental and Life Sciences

School of Biological Sciences

**Investigating the role of PIP4K in Immune System Regulation and P53-Inactivated
Cancers**

by

Shidqiyyah Abdul Hamid

Thesis for the degree of Doctor of Philosophy

May 2021

University of Southampton

Abstract

Faculty of Environmental and Life Sciences

School of Biological Sciences

Thesis for the degree of Doctor of Philosophy

Investigating the Role of PIP4K in Immune System Regulation and P53-Inactivated Cancers

by

Shidqiyyah Abdul Hamid

Phosphatidylinositol 5-phosphate 4-kinase (PIP4K) catalyses the formation of phosphatidylinositol 4,5 bisphosphate (PtdIns(4,5)P₂) which is a messenger involved in important cellular signalling pathways including the PI3K/Akt/mTOR pathway and the phospholipase C pathway. Three isoforms of PIP4K have been identified, namely PIP4K2 α , PIP4K2 β , and PIP4K2 γ , which have been shown to play roles in cellular activities such as growth, stress response, immune system regulation, and tumour formation. However, the exact mechanisms engaged by the kinases are still obscure. This study focused on investigating the role of PIP4K in modulating the immune system through regulatory T cells (Tregs), and in growth of cancer cells with inactivated p53. Findings from this study showed that PIP4K2 β and 2 γ isoforms regulate PI3K/Akt/mTOR signalling in Tregs to control cell proliferation, survival, and immunosuppressive activity. This study also suggested that PIP4K controls FOXP3 expression, the master transcriptional regulator of Tregs through a novel PI3K/UHRF1/FOXP3 pathway. Previously PIP4K had been shown to play roles in cancer cell growth, and a discovery of possible synthetic lethal interaction with p53 in cancer cells has made this kinase a promising target for cancer therapy. Findings from this study indicate that the synthetic lethality of PIP4K and p53 is not present in all types of cancer. Rather, it is suggested to depend on the specific mutation of p53 and alteration in expression of PIP4K in the cells. Inhibition of PIP4K also regulates the PI3K/Akt pathway differently in different cancer cells. Together, findings from this study suggested that PIP4K modulates both the immune system and cancer cell growth, and its different role in regulating PI3K/Akt/mTOR pathway could be the key to understand how PIP4K modulates the systemic immune response, and how different cancers can benefit from the expression of this family of lipid kinases.

Table of Contents

Table of Contents	i
Table of Tables	vii
Table of Figures	ix
Research Thesis: Declaration of Authorship	xiii
Acknowledgements	xv
Definitions and Abbreviations	xvii
Chapter 1 Introduction	1
1.1 Introduction to Phosphoinositides and their Kinases	1
1.1.1 Phosphatidylinositol and Polyphosphoinositides	1
1.1.2 Phosphoinositide Kinases.....	3
1.1.3 General Functions of PPIs and Phosphoinositide Kinases	4
1.1.3.1 PI3K/Akt pathway and PTEN	5
1.1.3.2 PPI in p53 regulation	7
1.2 Phosphatidylinositol 5-phosphate 4-kinase (PIP4K)	8
1.2.1 PIP4K Isoforms: Structure, localization, and activity	8
1.2.2 PIP4K roles on PI3K/Akt pathway.....	9
1.2.3 Functional Roles of PIP4Ks in Physiological and Pathological Processes	10
1.2.4 PIP4K and Immune System Regulation: Current Evidence and Potential Role in Regulatory T Cells Activity	14
1.2.5 PIP4K and Cancer Cells Growth: Current Evidence and Potential Interaction with p53.....	20
1.3 Study Aims.....	25
Chapter 2 Materials and Methods	27
2.1 Chemicals, reagents and other materials	27
2.2 Buffers and solutions.....	29
2.3 Methods for investigating the role of PIP4K in regulatory T cells activation pathway	30

2.3.1	Generation of Tregs and naïve T cells lysates, expansion, transduction, and stimulation	31
2.3.2	PBMC Immunostaining	32
2.3.3	T cell Proliferation assay	32
2.3.4	Suppression Assay.....	32
2.3.5	T cell lysate preparation	33
2.4	Methods for investigating the role of PIP4K in tumour cell growth.....	33
2.4.1	Cell Biology.....	33
2.4.1.1	Cell Lines	33
2.4.1.2	Cell Culture.....	34
2.4.1.3	Cell lysis for protein extraction	34
2.4.1.4	RT-qPCR for RNA from adherent cells.....	34
2.4.1.5	Transient transfection of cells	35
2.4.1.6	Generating lentiviral supernatant.....	35
2.4.1.7	Generating retroviral supernatant.....	36
2.4.1.8	Cell transduction and antibiotic selection	36
2.4.1.9	Single colony growth.....	37
2.4.1.10	Generation of auxin-inducible degron (AID)-tagged U2OS cell line for conditional PIP4K protein degradation.....	38
2.4.1.11	Etoposide treatment for p53 pathway activation	38
2.4.1.12	Cell morphology.....	38
2.4.1.13	Cell Attachment assay.....	38
2.4.1.14	Anchorage-independent clonogenic growth assay (Soft agar)	38
2.4.1.15	Cell proliferation assay.....	39
2.4.1.16	Cell migration assay	39
2.4.1.17	Cell viability assay	39
2.4.1.18	Senescence assay.....	40
2.4.2	Protein Biochemistry	40
2.4.2.1	Immunocytochemistry.....	40
2.4.2.2	Protein Assay.....	41
2.4.2.3	Protein sample preparation for western blot.....	41
2.4.2.4	Western Blot	41

2.4.3	Molecular Biology.....	43
2.4.3.1	Making DH5 α competent cells	43
2.4.3.2	DNA gel purification	44
2.4.3.3	Oligo annealing.....	45
2.4.3.4	DNA ligation.....	45
2.4.3.5	Bacterial Transformation.....	45
2.4.3.6	DNA plasmid miniprep	46
2.4.3.7	cDNA synthesis and qPCR.....	47
2.4.3.8	Designing a single guide RNA (sgRNA) for CRISPR/Cas9	49
2.4.4	Statistical Analysis	49
Chapter 3 Role of PIP4K in T cell signalling through the PI3K/Akt/mTOR and MAPK		
	Signalling Pathway	51
3.1	Introduction.....	51
3.2	Results	57
3.2.1	Effect of PIP4Ks modulation on PI3K/Akt/mTOR and ERK signalling pathway in Tregs	57
3.2.2	PIP4K2B and PIP4K2C signalling controls the expression of FOXP3 and Treg's function through PI3K/UHRF1.....	60
3.2.3	Pharmacological inhibition of PIP4K2 γ phenocopies <i>PIP4K2C</i> silencing.....	63
3.2.4	Effect of PIP4K2B and PIP4K2C modulation on PI3K/Akt/mTOR and ERK signalling pathway in naïve T cells	65
3.3	Discussion	68
3.3.1	PIP4K depletion modulates Tregs and Naïve T cells signalling and activity.....	68
Chapter 4 Different Methods of Manipulating P53 and PIP4K in Tumour Cells		
4.1	Introduction.....	73
4.2	Results	74
4.2.1	P53 modulation in cells	74
4.2.1.1	Generation of <i>TP53</i> knockdown cells through shRNA method	74
4.2.1.2	Generation of <i>TP53</i> knockout cells through CRISPR/Cas9 method	76
4.2.1.3	P53 activities and mutation in BT474 cells.....	78

4.2.2	Generation of PIP4K depleted cells through shRNA and CRISPR/Cas9 methods 80	
4.2.3	Generation and characterisation of auxin inducible degron (AID)-tagged PIP4K for protein degradation	82
4.3	Discussion.....	88
4.3.1	Advantages and limitations of the different methods in depleting TP53 and PIP4K used in this study	88
Chapter 5 Investigating the relationship between PIP4K and p53 in cancer cells		93
5.1	Introduction	93
5.2	Results.....	93
5.2.1	Effect of PIP4K isoforms and p53 depletion on cancer cells proliferation	93
5.2.2	Effect of PIP4K isoforms and p53 depletion on anchorage-independent growth.....	97
5.2.3	Temporal effect of PIP4K isoforms knockdown on the clonogenic activity of cancer cells.....	107
5.2.4	Effect of PIP4K isoforms and p53 depletion on cell migration, adherence, viability, and senescence.	112
5.3	Discussion.....	117
5.3.1	Synthetic lethal interaction between p53 and PIP4K in tumour cells: a mutation-specific effect.....	117
Chapter 6 Investigating the role of PIP4K in PI3K/Akt signalling and possible interaction with p53.....		123
6.1	Introduction	123
6.2	Results.....	124
6.2.1	Effect of <i>PIP4K2A</i> and <i>2B</i> depletion and p53 deletion on the PI3K/Akt pathway activation	124
6.2.2	Identifying the effect of <i>PIP4K2A</i> and <i>PIP4K2B</i> acute depletion on the PI3K/Akt pathway activation and PTEN expression.....	134
6.3	Discussion.....	139

6.3.1 *PIP4K2A* and *PIP4K2B* depletion modulates PI3K/Akt signalling through PTEN.

139

Chapter 7 Final Discussion.....	143
7.1 Role of PIP4K in the immune system and cancer cells.....	143
7.2 Different roles of PIP4K in PI3K/Akt signalling pathway	144
7.3 The future direction of PIP4K as a target for immune-related disorder and cancer therapy	146
7.4 Final Conclusion.....	147
Appendix A PIP4K Isoforms Sequence Comparison	149
Appendix B Structure of PIP4K Isoforms.....	151
Appendix C Auxin Inducible Degron (AID) Construct.....	152
Appendix D Expression of PTEN in U2OS and BT474	153
List of References	155

Table of Tables

Table 1.1 Effect of PIP4K depletion in tumour cell growth.....	24
Table 2.1 List of chemicals and reagents	27
Table 2.2 List of buffers and solutions	29
Table 2.3 Antibodies used for immunostaining with FACS.....	32
Table 2.4 Mammalian cell line used	33
Table 2.5 List of plasmids used for transient transfection and their target sequence.....	35
Table 2.6 List of mammalian expression vectors used for retroviral transduction	36
Table 2.7 List of shRNA constructs used for lentiviral transduction.....	37
Table 2.8 List of CRISPR SgRNA constructs used for lentiviral cell transduction	37
Table 2.9 Composition of stacking and separating gel (1.0 mm) for protein electrophoresis	42
Table 2.10 List of antibodies used and their descriptions	43
Table 2.11 List of qPCR primers and their sequences.....	48

Table of Figures

Figure 1.1 Structures of phosphatidylinositol and myo-inositol.....	2
Figure 1.2 Structure of seven polyphosphoinositides derived from phosphatidylinositol and their converting kinases and phosphatases.	3
Figure 1.3 PI3K-Akt-mTOR signalling pathway.....	6
Figure 1.4 Effect of PIP4K depletion in physiological processes of organisms.	11
Figure 1.5 Activation and differentiation of naïve CD4+ T cells, and immune suppression mechanisms by regulatory T cells.	15
Figure 1.6 PI3K/Akt/mTOR pathway's roles in Treg activities.	18
Figure 2.1. Flowchart of Tregs sample obtainment and processing.	30
Figure 3.1 PIP4K2B and 2C affect FOXP3 expression in TCR stimulated CD4+ Naïve T cells.	52
Figure 3.2 PIP4K2B and 2C affect Tregs' proliferation, viability, and survival.	55
Figure 3.3 PIP4K2B and 2C silencing reduced FOXP3 expression and impaired the immunosuppressive activity.	56
Figure 3.4 Depletion of PIP4K2B and 2C affect the TCR dependent PI3K/Akt/mTOR and ERK pathways.....	58
Figure 3.5 Overexpression of <i>PIP4K2B</i> does not affect the TCR dependent PI3K/Akt/mTOR pathway.	59
Figure 3.6 Inhibition of PI3K, together with silencing of <i>PIP4K2B</i> and <i>PIP4K2C</i> decrease FOXP3 expression.	61
Figure 3.7 Depletion of <i>PIP4K2B</i> or <i>2C</i> , or inhibition of p110 δ in nTregs reduces the UHRF1 expression that further decreases the expression of FOXP3 and CTLA4 as well as immunosuppressive capability.	62
Figure 3.8 Pharmacological inhibition of PIP4K2 γ in nTregs resulted in decreased activation of the PI3K/Akt/mTOR and ERK pathways, reduced proliferation and FOXP3 expression.	64
Figure 3.9 <i>PIP4K2B</i> or <i>2C</i> depletion modulates the activation of PI3K/Akt and ERK pathways in naïve T cells.....	66

Figure 3.10 Pharmacological inhibition of PIP4K2 γ in naïve T cells does not affect the activation of PI3K/Akt/mTOR and ERK pathways.	67
Figure 3.11 Effect of <i>PIP4K2B/2C</i> inhibition on Treg activities.	69
Figure 4.1 Changes in p53 and expression of its downstream targets in etoposide treated <i>TP53</i> knockdown U2OS cells and its downstream signalling.	75
Figure 4.2 Changes in the expressions of p53 and its downstream targets in etoposide treated <i>TP53</i> KO cells.	77
Figure 4.3 Changes in the expressions of p53 and its downstream targets in BT474 cells grown at two different temperatures.	79
Figure 4.4 mRNA and protein expression of PIP4K isoforms following knockdown or knockout in U2OS cells.	81
Figure 4.5 Morphological changes of cells following different method of PIP4K depletion.	82
Figure 4.6 Endogenous tagging of PIP4K isoforms results in auxin-dependant protein degradation.	84
Figure 4.7 Comparison between different PIP4K degradation techniques.	85
Figure 4.8 Low expression of AID-tagged PIP4K is not due to proteasomal degradation.	87
Figure 5.1. Double depletion of <i>PIP4K</i> and <i>TP53</i> does not cause U2OS proliferation arrest.	94
Figure 5.2 <i>PIP4K2B</i> knockout stops BT474 with inactive p53 from growing.	96
Figure 5.3 Depletion of <i>PIP4K2A</i> affects colony formation in U2OS cells irrespective of the p53 status.	98
Figure 5.4 PIP4K knockout does not affect clonogenic potential of U2OS cells.	99
Figure 5.5 Deletion of p53 and PIP4K does not affect colony growth of HCT116.	101
Figure 5.6 <i>PIP4K2A</i> knockdown with diminished p53 activity reduced large colony formation in BT474.	103
Figure 5.7 Depletion of PIP4K with diminished p53 activity significantly reduced large colony formation in BT474.	104

Figure 5.8 Depletion of p53 reduced proliferation and anchorage independent growth, and diminished the synthetic lethal interaction with <i>PIP4K2B</i>	106
Figure 5.9 <i>PIP4K2A</i> knockdown colony phenotype is temporal.	108
Figure 5.10 <i>PIP4K2A</i> overexpression in cells.	110
Figure 5.11 <i>PIP4K2A</i> knockdown colony phenotype could not be rescued by <i>PIP4K2A</i> overexpression.....	111
Figure 5.12 Effect of PIP4K and p53 depletion on U2OS cell migration activity.....	113
Figure 5.13 PIP4K depletion reduces cell adhesion activity.....	114
Figure 5.14 Effect of PIP4K and p53 depletion on cell viability and senescence.	116
Figure 6.1 Changes in Akt and S6 phosphorylation and PTEN expression in U2OS cells with <i>PIP4K2A</i> and/or <i>2B</i> knockdown and <i>TP53</i> knockout.....	125
Figure 6.2 The effect of <i>PIP4K2A</i> , <i>PIP4K2B</i> and <i>TP53</i> knockout on Akt and S6 phosphorylation and PTEN expression in U2OS cells.....	127
Figure 6.3 Effects of <i>PIP4K2A</i> , <i>PIP4K2B</i> and <i>TP53</i> modulation on PTEN mRNA expression.	129
Figure 6.4 Effect of <i>PIP4K2A</i> and/or <i>2B</i> knockout on PI3K/Akt pathway activation and PTEN expression in BT474 cells.	131
Figure 6.5 Effect of <i>PIP4K2A</i> and/or <i>2B</i> knockdown on PI3K/Akt pathway activation and PTEN expression in BT474 cells.	133
Figure 6.6 Attempts to determine the effects of acute depletion of PIP4K2 α and 2 β on PI3K/Akt/mTOR signalling and PTEN levels.	135
Figure 6.7 Administration of doxycycline and auxin affect PI3K/Akt/mTOR signalling and PTEN levels in U2OS cells.	136
Figure 6.8 Administration of auxin with and without doxycycline being removed show different effects on PTEN expression and Akt and S6 phosphorylation.	138
Figure 6.9 Suggested PIP4K involvement in the PTEN-Akt-p53-MDM2 regulatory network in U2OS cells.	140

Research Thesis: Declaration of Authorship

Print name: Shidqiyyah Abdul Hamid

Title of thesis: Investigating the Role of PIP4K in Immune System Regulation and P53-Inactivated Cancers

I declare that this thesis and the work presented in it are my own and has been generated by me as the result of my own original research.

I confirm that:

1. This work was done wholly or mainly while in candidature for a research degree at this University;
2. Where any part of this thesis has previously been submitted for a degree or any other qualification at this University or any other institution, this has been clearly stated;
3. Where I have consulted the published work of others, this is always clearly attributed;
4. Where I have quoted from the work of others, the source is always given. With the exception of such quotations, this thesis is entirely my own work;
5. I have acknowledged all main sources of help;
6. Where the thesis is based on work done by myself jointly with others, I have made clear exactly what was done by others and what I have contributed myself;
7. Parts of this work have been submitted for publication as:-

Poli, A., Abdul-Hamid, S., Zaurito, A. E., Campagnoli, F., Bevilacqua, V., Sheth, B., Fiume, R., Pagani, M., Abrigani, S., and Divecha, N. (2020) 'PIP4Ks impact on PI3K, FOXP3 and UHRF1 signaling and modulate human regulatory T-cell proliferation and immunosuppressive activity', *Manuscript submitted for publication*.

Signature:

Date:06/05/2021

Acknowledgements

First and foremost, I would like to express my gratitude to Prof. Nullin Divecha for giving me the opportunity to work in his lab. Through his expert advice, I have learned so much about science in general and phosphoinositides in particular. Thank you also to Dr. Katrin Deinhardt for always being there to give me support and encouragement and keeping my motivation up. My appreciation also goes to Dr. Alessandro Poli who was working with the INGM, Milan back then and currently with the IFOM, Milan for his great help in this project. Dr. Poli also has granted the permission to reproduce figures from his research to be used in this thesis. I would like to express the deepest appreciation to all the previous and current members of Inositide Lab (IL), University of Southampton: Dr. Bhavwanthi Sheth, Dr. Zahid Shah, Magdalena Castellano-Vidalle, Francesca Campagnoli, and Dr. Scott Kimber for their continuous help and support. To all the staff of the School of Biological Sciences, University of Southampton, fellow Ph.D. friends, Post-Docs, and the Malaysian community in Southampton, which I humbly failed to individually mention in this acknowledgement, I truly appreciate all of your help and friendship.

I wish to sincerely thank my dearest parents, and to my siblings, for their continuous pray, support, and encouragement. Their emotional support and belief in me had kept me strong to finish this Ph.D. journey. Thank you also to the Ministry of Education Malaysia and my employer, IIUM for providing the funding and opportunity for me to further my study up to this level.

Definitions and Abbreviations

AID	auxin-inducible degron
AML	acute myeloid leukemia
ARF	auxin response transcription factor
BCA	bicinchoninic acid
CD25	interleukin-2 receptor α chain
cDNA	complementary DNA
CRISPR	clustered regularly interspaced short palindromic repeats
CTLA-4	cytotoxic T lymphocyte-associated antigen 4
DAG	diacylglycerol
DMEM	Dulbecco's Modified Eagle Medium
DMSO	dimethyl sulfoxide
DNA	deoxyribonucleic acid
DNMT1	DNA methyltransferase 1
dNTP	deoxyribonucleotide triphosphate
ERBB2	Erb-B2 receptor tyrosine kinase 2
FBS	fetal bovine serum
FOXO	Forkhead box O
GBM	glioblastoma
GFP	green fluorescent protein
GSK3	glycogen synthase kinase
H ₂ O ₂	hydrogen peroxide
HDR	homology directed repair
HER2	human epidermal growth factor receptor 2
IL-10	interleukin 10
IL-2	interleukin 2
Indel	insertion and deletion
ING2	inhibitor of growth protein 2
INGM	The National Institute of Molecular Genetics
IPEX	immune dysfunction, polyendocrinopathy, enteropathy, X-linked
KD	knockdown
KO	knockout
LB	lysogeny/Luria broth
mAID	mini-AID
MAPK	mitogen-activated protein kinase
MDM2	murine double minute 2
MEF	mouse embryonic fibroblast
mRNA	messenger RNA
mTOR	mammalian target of rapamycin
MTT	3-(4,5-dimethylthiazol-2-yl)-2,5-diphenyl tetrazolium bromide
NHEJ	non-homologous end joining
OD	optical density
OV	overexpress
PBS	phosphate buffer solution
PCR	polymerase chain reaction
PDK1	3-phosphoinositide-dependent protein kinase 1
PHD	plant homeodomain

PHLDA3	pleckstrin homology like domain family A member 3
PHLPP	PH domain leucine-rich repeat protein phosphatase
PI	phosphoinositide
PI3K	phosphoinositide 3-kinase
PIP2	phosphatidylinositol (4,5)-bisphosphate
PIP3	phosphatidylinositol (3,4,5)-trisphosphate
PIP4K	phosphatidylinositol-5-phosphate 4-kinase
PIP4K2A/PIP4K2 α	PIP4K type 2 alpha
PIP4K2B/PIP4K2 β	PIP4K type 2 beta
PIP4K2C/PIP4K2 γ	PIP4K type 2 gamma
PIP5K	phosphatidylinositol-4-phosphate 5-kinase
PKC	protein kinase C
PLC	phospholipase C
PPIns	polyphosphoinositide
PtdIns	phosphatidylinositol
PtdIns(3,4,5)P ₃	phosphatidylinositol (3,4,5)-trisphosphate
PtdIns(4,5)P ₂	phosphatidylinositol (4,5)-bisphosphate
PtdIns4P	phosphatidylinositol 4-phosphate
PtdIns5P	phosphatidylinositol 5-phosphate
PTEN	phosphatase and tensin homolog
PUMA	p53 upregulated modulator of apoptosis
RT-qPCR	quantitative reverse transcription PCR
RNA	ribonucleic acid
RNAi	RNA interference
ROS	reactive oxygen species
sgRNA	single guide RNA
SHIP	Src homology 2-containing inositol 5' phosphatase / Phosphatidylinositol 3,4,5-trisphosphate 5-phosphatase 1
shRNA	short hairpin RNA
Tconv	conventional T cell
TCR	T cell receptor
Teffs	effector T cells
TGF-B	transforming growth factor β
TIGAR	TP53 Induced Glycolysis Regulatory Phosphatase
TIR1	protein transport inhibitor response 1
TOR	target of rapamycin
Tregs	regulatory T cells
UHRF1	ubiquitin-like, PHD and ring finger-containing 1
UTR	untranslated region
UV	ultraviolet
WT	wild type

Chapter 1 Introduction

1.1 Introduction to Phosphoinositides and their Kinases

1.1.1 Phosphatidylinositol and Polyphosphoinositides

Inositol is a derivative of cyclohexane containing six hydroxyl groups that are found naturally as nine isomers with myo-inositol as the major isomer occurring in eukaryotes (Balla, 2013; Irvine, 2016). Phosphatidylinositol (PtdIns) refers to a myo-inositol ring structure connected to a diacylglycerol backbone through a phosphodiester bond (Figure 1.1). It makes up approximately 10% of the total cell glycerophospholipids (Pendaries *et al.*, 2003) with the diglyceride consisting of two fatty acids; usually stearic acid and arachidonic acid (Figure 1.1A) (Pizer and Ballou, 1959; Brown *et al.*, 1961). The orientation of the hydroxyl group on the myo-inositol ring of PtdIns is illustrated using Agranoff's turtle model of PtdIns (Agranoff, 2009; Irvine, 2016) (Figure 1.1B). The cyclohexane structure of the myo-inositol ring has been described as similar to a chair conformation with one –OH group being axial and the other five being equatorial (Balla, 2013). To ease the understanding of the hydroxyl group numbering, the inositol ring has been likened to a body of a turtle with its right front flipper representing the carbon D1, assuming that the turtle is 'right flippered'. The D numbering convention then continues anticlockwise, with the turtle's axial head numbered as D2, left front and back limb as D3 and D4, tail as D5 and finally end at the right-back flipper as D6 (Figure 1.1C).

The –OH group at the D1 position of PtdIns is coupled to the diacylglycerol backbone by the phosphodiester bond that theoretically leaves the other five positions free for phosphorylation (Balla, 2013; Divecha, 2016). However, *in vivo*, only the D3, D4, and D5 have been found to be reversibly phosphorylated by kinases and phosphatases. Phosphorylation of the hydroxyl groups of the inositol ring on the three, four, and five positions generate seven phosphorylated derivatives of PtdIns, called polyphosphoinositides (PPIs) (Balla, 2013). To date, seven PPIs have been identified, which are 1) phosphatidylinositol 3 phosphate (PtdIns3P); 2) phosphatidylinositol 4 phosphate (PtdIns4P); 3) phosphatidylinositol 5 phosphate (PtdIns5P); 4) phosphatidylinositol 3,4-bisphosphate (PtdIns(3,4)P₂); 5) phosphatidylinositol 4,5-bisphosphate (PtdIns(4,5)P₂ or PIP₂); 6) phosphatidylinositol 3,5-bisphosphate (PtdIns(3,5)P₂); and 7) phosphatidylinositol 3,4,5-trisphosphate (PtdIns(3,4,5)P₃ or PIP₃) (Strahl and Thorner, 2007; Balla, 2013) (Figure 1.2). Although PPIs only represent a minor group of phospholipids, they have diverse cellular functions (Michell, 2011; Echard, 2012; Balla, 2013) as they act as transducers that enable multiple external cues to impact important intracellular processes such as transmembrane receptor signal transduction,

vesicular trafficking, defence against pathogens, control of ion channel function, and also transcriptional output control (Balla, 2013).

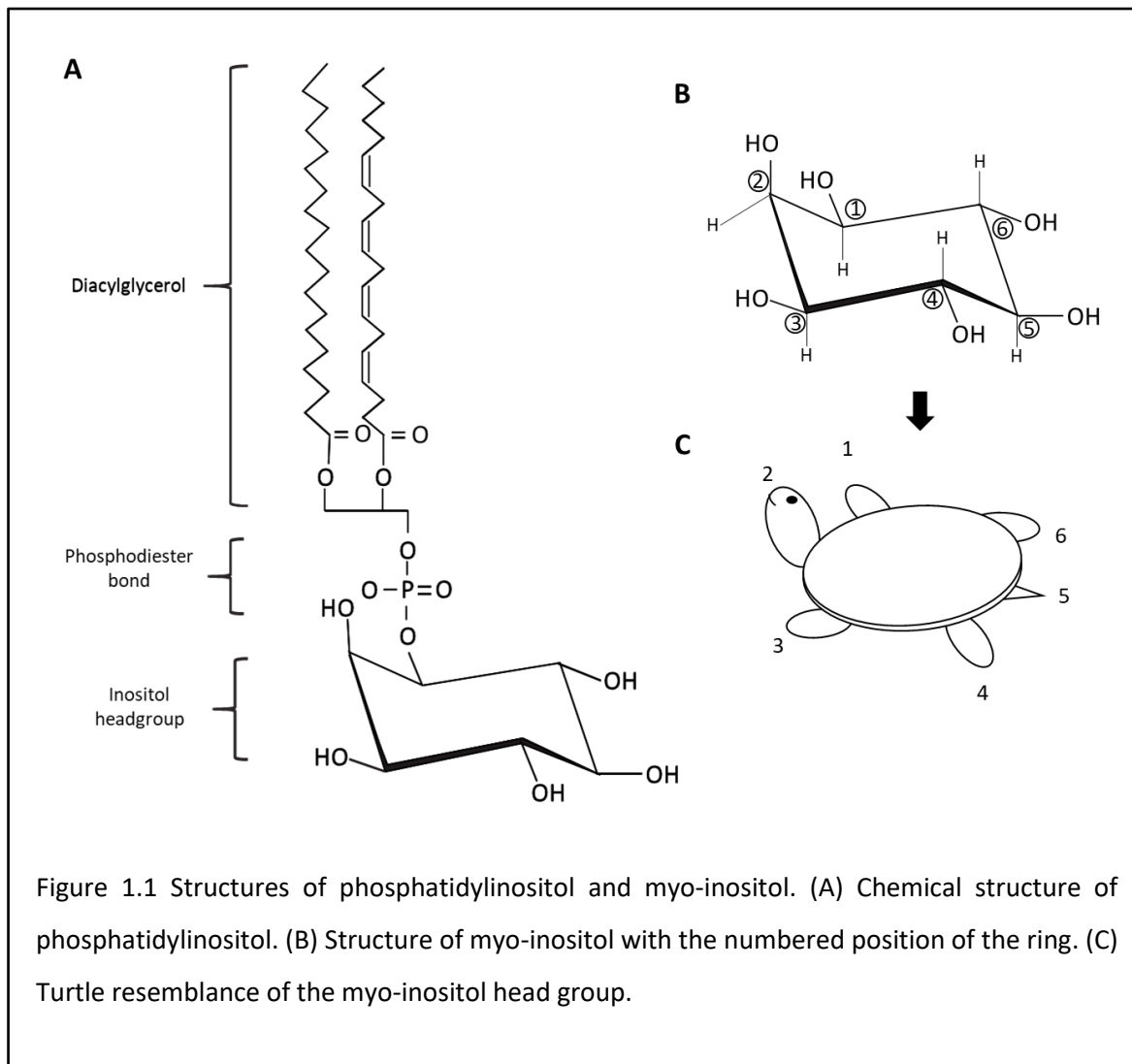
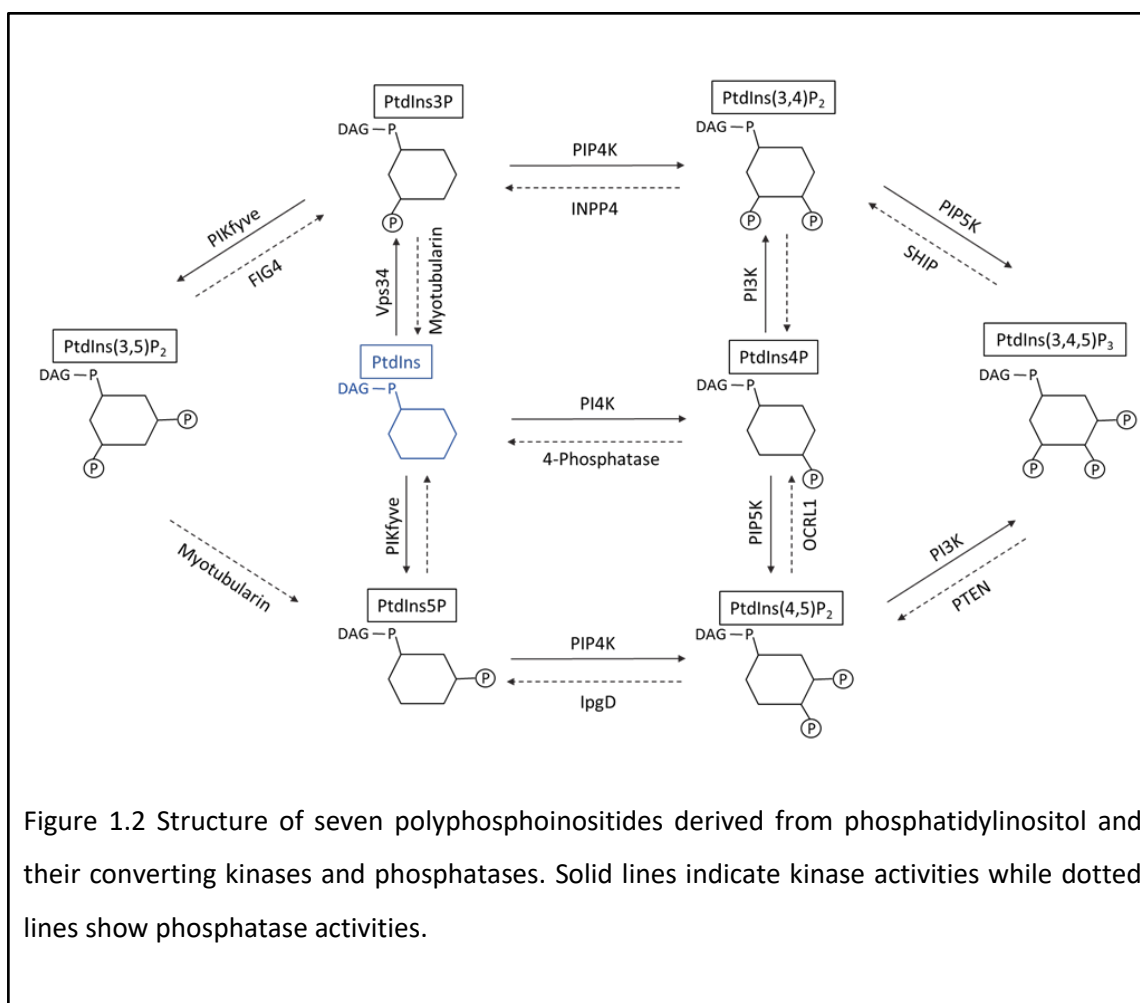


Figure 1.1 Structures of phosphatidylinositol and myo-inositol. (A) Chemical structure of phosphatidylinositol. (B) Structure of myo-inositol with the numbered position of the ring. (C) Turtle resemblance of the myo-inositol head group.

Synthesis of PtdIns occurs in the endoplasmic reticulum, before being transported to other compartments such as the Golgi apparatus and plasma membrane and modified by kinases and phosphatases (McCrea and De Camilli, 2009). The localisations of the PPIs were identified through high-resolution imaging techniques using protein domains that bind to specific phosphoinositides. The domains were coupled with fluorescent proteins to generate genetically encoded fluorescent probes that can be used to localise PPIs in cells. PtdIns(3,4)P₂, PtdIns(4,5)P₂ (PIP₂) and PtdIns(3,4,5)P₃ (PIP₃) reside predominantly at the plasma membrane, PtdIns3P on early endosomes, while PtdIns4P can be found both at the plasma membrane and Golgi apparatus (Viaud *et al.*, 2016). Sub-cellular localisations of the specific PPIs have enabled them to serve as cellular

or specific organelle markers (Wang *et al.*, 2003; Schulze *et al.*, 2006; Hammond *et al.*, 2012), and have been suggested to be important in the maintenance of cell polarity (Fabian *et al.*, 2010).



1.1.2 Phosphoinositide Kinases

PPIs metabolism is highly active and strictly controlled by the specific actions of over eighty isoforms of PPIs kinases, phosphatases and phospholipases (Czech, 2000; Pendaries *et al.*, 2003; Irvine, 2005; McCrea and De Camilli, 2009; Divecha, 2010). PPIs kinases were first categorized based on their biochemical properties such as their respective substrate preference and how they were modulated by stimulators or inhibitors (Strahl and Thorner, 2007). The current agreed nomenclature is based on their substrate and the site they phosphorylate. For example, PtdIns 5-phosphate 4-kinase (PIP4K) phosphorylates PtdIns5P at the D4 position to form PtdIns(4,5)P₂; while the phosphorylation activity of some phosphoinositide 3-kinases (PI3Ks) on PtdIns(4,5)P₂ will generate PtdIns(3,4,5)P₃. As shown in Figure 1.2, some PPIs can be generated from the actions of more than one PPIs kinases, such as PtdIns(4,5)P₂ which can be derived from PtdIns4P or PtdIns5P.

The distinct sub-cellular patterns of PPIs are partly the consequence of their metabolism by differentially localised kinases, phosphatases, and phospholipases.

1.1.3 General Functions of PPIs and Phosphoinositide Kinases

The phosphorylated head groups of PPIs interact with a variety of proteins with different degrees of affinity and specificity (McCrea and De Camilli, 2009). They function to generate novel regulated binding surfaces that recruit proteins through these specific binding domains to drive downstream signalling (Hodgkin *et al.*, 2000; Gozani *et al.*, 2003). One way that PPIs control downstream signalling is by their direct interaction with protein domains such as the Pleckstrin Homology (PH), FYVE (Fab-1, YGL023, Vps27, and EEA1), phox (PX), Epsin N-Terminal Homology (ENTH) (Viaud *et al.*, 2016), and plant homeodomain (PHD) fingers (Gozani *et al.*, 2003). The phosphoinositide-protein domain interaction can lead to changes in protein localisation, activity, or interaction with other proteins that drive downstream signalling. Among the seven PPIs, PtdIns(4,5)P₂ has roles in two major signalling cascades, namely the phospholipase C (PLC) pathway and the phosphoinositide 3-kinase (PI3K) pathway (Toker, 1998; Rameh and Cantley, 1999). Their roles in the PI3K pathway will be discussed in detail later. In the PLC pathway, PtdIns(4,5)P₂ is hydrolysed by a family of phospholipases C to produce two second messengers, which are diacylglycerol (DAG) and inositol 1,4,5-trisphosphate (Ins(1,4,5)P₃). Ins(1,4,5)P₃ binds to its cognate receptor in the endoplasmic reticulum (ER) and triggers Ca²⁺ release from the ER into the cytoplasm, while DAG activates members of the protein kinase C (PKC) family (Berridge, 1984).

PPIs kinases have specific roles in regulating PPIs and impaired activities of these kinases are implicated in diseases. Several PPIs metabolising enzymes are causative for pathogenic bacterial invasion as well as disorders such as myopathy, neurodegenerative disorders, genetic disorder, metabolic disorder, and cancer (reviewed in Pendaries *et al.*, 2003; McCrea and De Camilli, 2009). For instance, hyperactivation of the PI3K pathway drives increased cell proliferation, decreased apoptosis and increased resistance to treatment that then promotes the development of some types of cancer (Yao and Cooper, 1995; Sun *et al.*, 1999; Zhou, Liao, Xia, Spohn, *et al.*, 2001; Bacus *et al.*, 2002). Deregulation of the PI3K activity can be due to several factors such as mutation that increases its catalytic activity, or disruption/deletion of phosphatases that regulates PtdIns(3,4,5)P₃ by removing its phosphate, such as the phosphatase and tensin homolog (PTEN), leading to hyperactivation of the kinase pathway (Oda *et al.*, 2005; Saal *et al.*, 2005). Consequently, the pharmaceutical industry has invested heavily in developing several inhibitors targeting different components of the PI3K-dependent pathway for cancer therapy. For example, inhibitors targeting PI3K are currently being tested (reviewed in Zhao, Qiu and Kong, 2017). Being one of the most

studied pathways, understanding the PI3K activity and its connection with different PPIs is crucial to understand the physiological and pathological processes in various systems.

1.1.3.1 PI3K/Akt pathway and PTEN

PI3K is divided into three classes, namely class I, class II and class III PI3Ks. Class I PI3Ks have been extensively studied for their roles in several cellular functions, including regulation of metabolism and in the immune system (Fruman *et al.*, 2017). Class I PI3Ks have their catalytic subunit bound to p85 regulatory subunits that modulate the enzyme activity and subcellular localisation (Fruman *et al.*, 2017). There are four distinct class I catalytic isoforms in mammals, namely p110 α , p110 β , p110 γ , and p110 δ , which are encoded by *PIK3CA*, *PIK3CB*, *PIK3CG*, and *PIK3CD* respectively. Class I PI3Ks preferentially utilised PtdIns(4,5)P₂ to produce PtdIns(3,4,5)P₃, although *in vitro* studies reported that they are also capable of synthesising PtdIns3P from PtdIns and PtdIns(3,4)P₂ from PtdIns4P (Rameh and Cantley, 1999; Vanhaesebroeck *et al.*, 2010). PtdIns(3,4,5)P₃ recruits several proteins containing the PH domain to cell membrane. The most studied effector molecule is the Akt/Protein kinase B (PKB) which also acts as a surrogate indicator of class I PI3K activation (Fruman *et al.*, 2017). PtdIns(3,4,5)P₃ recruits Akt to the plasma membrane together with 3-phosphoinositide-dependent protein kinase 1 (PDK1) which leads to phosphorylation of Akt on threonine 308 (Thr308) (Alessi *et al.*, 1997). For Akt to achieve its optimal activity, phosphorylation at Ser473 residue by kinases such as mammalian target of rapamycin complex 2 (mTORC2) is required (Sarbasov *et al.*, 2005) (Figure 1.3). Complete activation of Akt is essential for the activation of downstream targets, such as transcription factors Forkhead box O (FOXO) and mammalian target of rapamycin complex 1 mTORC1 (Manning, 2004). mTORC1 and mTORC2 are two distinct mTOR complexes found in mammalian cells. They share the catalytic mTOR subunit with other associated proteins, but also different proteins such as their adaptor, Raptor and Rictor that regulate specific functions of mTORC1 and mTORC2, respectively (Chapman and Chi, 2014). Activation of mTORC1 leads to the phosphorylation of 4E-binding protein 1 (4EBP1) and p70 ribosomal protein S6 kinase (S6K), which further leads to phosphorylation of ribosomal protein S6. This downstream PI3K/Akt pathway activation resulted in increased translation of proteins necessary for cell growth and proliferation (Ma and Blenis, 2009). In addition, *in vitro* experiments also showed that mTOR facilitates Thr308 phosphorylation by PDK1 (Sarbasov *et al.*, 2005).

Termination of this pathway can take place in two ways: 1) Akt inactivation through dephosphorylation of Akt by enzymes such as the PH domain leucine-rich repeat protein phosphatase (PHLPP) family (Grzechnik and Newton, 2016); and 2) Dephosphorylation of PtdIns(3,4,5)P₃ into PtdIns(4,5)P₂ by PTEN (Maehama and Dixon, 1998). PTEN is the most important

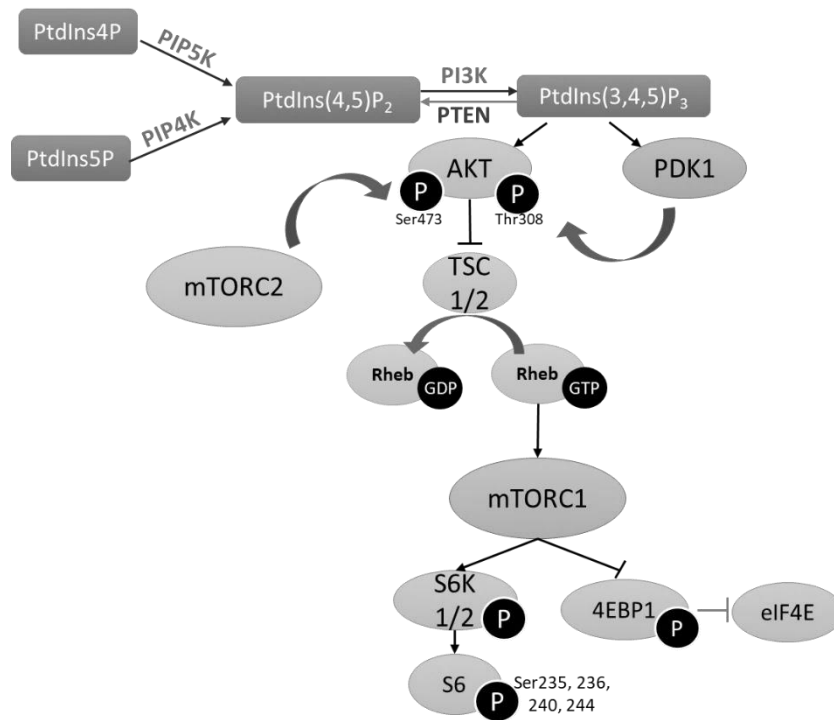


Figure 1.3 PI3K-Akt-mTOR signalling pathway. PIP4K and phosphatidylinositol-4-phosphate 5-kinase (PIP5K) contribute to the production of PtdIns(4,5)P₂ that will be converted by PI3K into another lipid second messenger, PtdIns(3,4,5)P₃. PtdIns(3,4,5)P₃ mediates the phosphorylation of Akt at Thr308 by PDK1, and mTORC2 phosphorylates Akt at Ser473. These events lead to the phosphorylation of tuberous sclerosis 2 (TSC2). TSC1/TSC2 protein complex is one of the immediate downstream proteins of Akt. TSC2 contains a GTPase-active protein (GAP) that converts active, GTP-bound Rheb (Ras homologue enriched in brain) into its inactive, GDP-bound Rheb. Phosphorylation of TSC2 impairs the TSC1/2 complex's ability to act as a GAP towards Rheb-GTPs, allowing them to accumulate. Rheb-GTP activates mTORC1, which phosphorylates S6K1/2 and 4E-binding protein 1 (4EBP1). These actions activate S6K1/2, which lead to phosphorylation of ribosomal S6 protein at multiple sites. Phosphorylation of 4EBP1 by mTORC1 prevents its binding to the 5' cap-binding protein eukaryotic translation initiation factor 4E (EIF4e), a translation initiation factors, thereby allowing translation initiation to proceed. PTEN terminates the PI3K pathway by dephosphorylating PtdIns(3,4,5)P₃.

PI3K/Akt negative regulator and a classical tumour suppressor that is often mutated or deleted in various human cancers (Milella *et al.*, 2015). Its tumour suppressor activity could also be through its protein phosphatase activity, independent of the PI3K/Akt pathway (Hlobilkova *et al.*, 2000). The level of PTEN gene or protein is crucial during tumour development, and insufficient PTEN could promote the growth of certain cancers such as breast and colorectal cancers, melanoma, and leukaemia (Milella *et al.*, 2015). P53, another widely studied tumour suppressor has been reported to have a positive effect on PTEN's transcriptional regulation of mRNA and protein (Stambolic *et al.*, 2001). In addition, the same study also showed that in immortalised mouse embryonic fibroblasts

(MEF), PTEN is required for p53-mediated apoptosis, suggesting a complex interplay between them in the Akt pathway and tumour suppression.

1.1.3.2 PPI in p53 regulation

P53 is a transcription factor encoded by *TP53* genes. It is a major tumour suppressor protein that is also known as the 'guardian of the genome' (Lane, 1992). P53 is activated in response to cellular stress such as hypoxia, DNA damage, and cellular oncogenic transformation (Lowe and Earl Raley, 1993; Nelson and Kastan, 1994; Graeber *et al.*, 1996; Bieging *et al.*, 2014). Although the exact mechanism is still under investigation, it is known that p53 senses the presence of a stressor signal and induces transient cell cycle arrest, senescence, DNA repair, or apoptosis, thus preventing any unhealthy cells from spreading (Giaccia and Kastan, 1998). It also triggers various DNA repair mechanisms such as excision repair and non-homologous end-joining (NHEJ) (Powell *et al.*, 1995; Seo *et al.*, 2002). Similar to PTEN, p53 is frequently mutated in more than 50% of human tumours (Hainaut and Hollstein, 1999). Expression of a mutant p53 is often the result of missense mutations (Muller and Vousden, 2014). P53 binds to MDM2 (murine double minute 2), a family of E3 ligases, which negatively regulates the level of p53. Upon the exposure to a stress signal, MDM2 detaches from its main substrate, p53, which then stabilises and activates the tumour suppressor (Hu *et al.*, 2012).

As stated before, p53 exerts positive control on PTEN transcription and has also been reported to have a connection with the PI3K/Akt pathway. The PI3K/Akt pathway affects the expression of p53 by modulating the level of MDM2 (Zhou *et al.*, 2001). Akt acts by phosphorylating MDM2 at Ser166 and Ser186, promoting translocation of MDM2 into the nucleus and degradation of p53. Furthermore, PTEN is also capable of facilitating MDM2 degradation by inhibiting PI3K/Akt signalling, thus increasing the level of p53 (Zheng *et al.*, 2010). In cancer cells with mutated proteins upstream of PI3K/Akt, such as human epidermal growth factor receptor 2 (HER-2) amplification, p53 is often dysfunctional and is suggested to be due to suppression by the oncogenic signals. Activation of Akt in these cells increases the ubiquitination and degradation of p53 by MDM2. Recent evidence demonstrated that PIP5K and its product PtdIns(4,5)P₂ enhances p53 stability (Choi *et al.*, 2019). Upon stress, PIP5K binds to p53 and promotes the synthesis of PtdIns(4,5)P₂ which binds to p53. This interaction then leads to nuclear p53 stabilisation. The deletion of specific PIP5K isoform, namely PIP5K α , resulted in decreased p53 protein levels but without changes to mRNA levels. The study also found that only inhibition of PIP5K α , but not another isoform, PIP5K γ , or two isoforms of PIP4K, namely PIP4K2 α and β , could affect the p53 protein level. However, PIP4K2 β can indirectly affect p53 acetylation that modulates its response to DNA damage (Gozani *et al.*, 2003; Jones *et al.*, 2006). Interestingly, another study also reported that amplification of

PIP4K2 β correlates with a *TP53* mutation in cancer cells, and is suggested to be a novel relevant cancer therapeutic target (Emerling *et al.*, 2013). As a focus of this study, PIP4K will be discussed in detail in the following sections.

1.2 Phosphatidylinositol 5-phosphate 4-kinase (PIP4K)

1.2.1 PIP4K Isoforms: Structure, localization, and activity

PtdIns 5-phosphate 4-kinase (PIP4K) phosphorylates PtdIns5P at the D4 position to form PtdIns(4,5)P₂, and PtdIns3P into PtdIns(3,4)P₂ to a lesser extent (Clarke *et al.*, 2007). In mammals, the PIP4K family consists of three isoforms, being PIP4K2 α , PIP4K2 β , and PIP4K2 γ , and are encoded by the genes *PIP4K2A*, *2B* and *2C*, which in humans are located on chromosome 10p12.2, 17q12 and 12q13.3 respectively (Clarke and Irvine, 2012; Fiume *et al.*, 2015). Different isoforms have a high degree of similarity by crystallography structure comparison in which their catalytic core domain has the most sequence homology (Rao *et al.*, 1998; Anderson *et al.*, 1999; Clarke and Irvine, 2018). The amino acid sequence of *PIP4K2B* is 77% similar to *PIP4K2A* while *PIP4K2C* resembles 64% to the *PIP4K2A* and *PIP4K2B* (Clarke and Irvine, 2018) (Also Appendix A and B). Their distributions in tissues and subcellular localization also differ from one isoform to the other, possibly explaining the requirement for all three isoforms to be present within a cell performing different functions (Bultsma *et al.*, 2010). All three isoforms are highly expressed in the brain, although they are differently expressed according to different brain compartments and stages of development (Clarke *et al.*, 2009; Noch *et al.*, 2020). Their presence, however, varies in other tissues. The α isoform is highly expressed in the spleen and peripheral blood, the β is highly expressed in muscle and heart, while the γ isoform is predominantly expressed in the kidney and specific neurons in the brain (Divecha *et al.*, 1995; Itoh *et al.*, 1998; Clarke *et al.*, 2008, 2009). Differences in expression level suggest that different PIP4K isoforms could have specific functions in each organ. At the cellular level, PIP4K2 α is predominantly cytoplasmic (Ciruela *et al.*, 2000; Bultsma *et al.*, 2010; Droubi *et al.*, 2016) and membrane-bound (Wang *et al.*, 2010), although it can also be found in the nucleus (Bultsma *et al.*, 2010; Wang *et al.*, 2010). PIP4K2 β contains an α -helix insert sequence that localises it predominantly to the nucleus (Ciruela *et al.*, 2000; Wang *et al.*, 2010), while PIP4K2 γ 's localization is currently not specified to any intracellular vesicular compartment (Clarke and Irvine, 2013).

Each isoform shows a different amount of intrinsic PIP4K activity. PIP4K2 α was reported to be 2000-fold more active than the PIP4K2 β isoform (Bultsma *et al.*, 2010), while PIP4K2 γ appears to have little activity in *in vitro* studies (Clarke *et al.*, 2008). A sequence rich in Glycine (G-loop) in PIP4Ks plays a role in controlling these different levels of PIP4K activity (Appendix B). Introducing the loop sequence of PIP4K2 α into PIP4K2 β increases its activity by 400 folds, while introducing it

into the PIP4K2 γ leads to a 50-fold increase in activity (Clarke and Irvine, 2013). Surprisingly, knockdown of PIP4K2 γ leads to increase in PtdIns5P even though it appears to lack PIP4K activity. This could be explained by PIP4Ks' ability to form homo and heterodimers with each other, suggesting heterodimerisation self-regulation (Rao *et al.*, 1998). An important domain within all lipid kinases is the activation loop consisting of a 20 to 25-amino acid region in the C terminus, which determines substrate specificity (Kunz *et al.*, 2000). Swapping the activation loop of PIP5K into PIP4K switches the substrate specificity of PIP4K to utilising PtdIns4P instead of PtdIns5P. Due to its function to produce PtdIns(4,5)P₂, PIP4Ks have been studied for their role in PI3K/Akt, as well as other pathways such as ERK, Notch1, and Hippo (Jude *et al.*, 2015; Zheng and Conner, 2018; Lima *et al.*, 2019; Hong *et al.*, 2020).

1.2.2 PIP4K roles on PI3K/Akt pathway

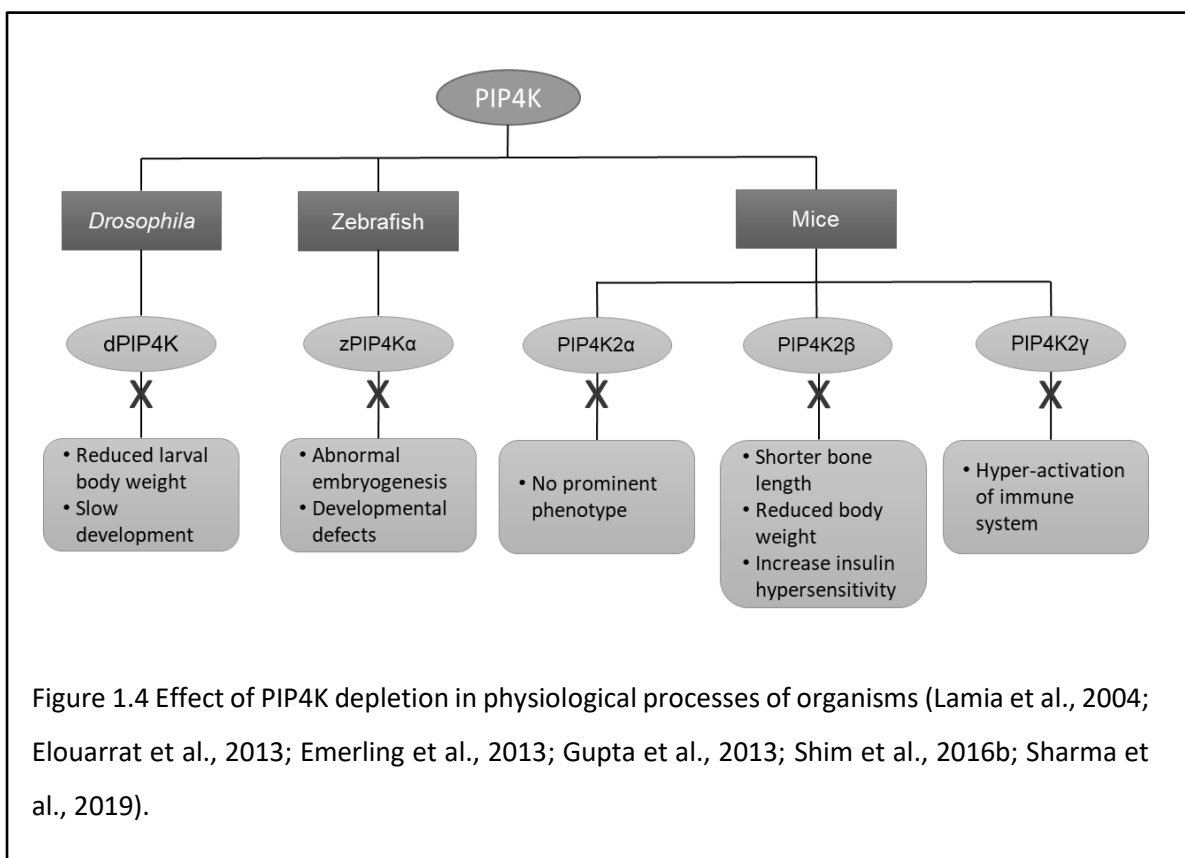
As part of the PI3K-Akt signalling pathway, PIP4K has been studied to understand its role in the various regulation of cellular processes. PtdIns(4,5)P₂ is one of the most abundant PPIs and acts as an essential lipid messenger involved in various cellular signalling pathway including the PI3K/Akt, PKC, and Hippo pathway, which plays crucial role balancing cell proliferation and differentiation (Choi *et al.*, 2015; Hong *et al.*, 2020). Being able to control PtdIns(4,5)P₂ production makes the kinases significant and could be a target of therapeutic research. However, PIP4K contribution on PtdIns(4,5)P₂ production in the cells is smaller compared to its canonical production by PIP5K; partly due to the higher level of PtdIns4P in cells (Toker, 2002; van den Bout and Divecha, 2009). Although changes in PIP4K levels do not always significantly impact on PtdIns(4,5)P₂ levels, they do lead to changes in the level of the substrate, PtdIns5P (Carricaburu *et al.*, 2003; Emerling *et al.*, 2013; Jones *et al.*, 2013; Jude *et al.*, 2015; Bulley *et al.*, 2016; Shim *et al.*, 2016), and the level of PtdIns5P had also been shown to significantly affect the levels of PtdIns(3,4,5)P₃ in cells (Grainger *et al.*, 2011; Al-Ramahi *et al.*, 2017).

Data obtained in cell lines and organisms concerning the role of PIP4K in PI3K/Akt activation varies across different studies, which demand further investigation of possible factors explaining the discrepancies (Lamia *et al.*, 2004; Emerling *et al.*, 2013; Gupta *et al.*, 2013; Jude *et al.*, 2015; Kitagawa *et al.*, 2017; Sharma *et al.*, 2019). Moreover, different effects on downstream mTORC1 activation were also reported (Mackey *et al.*, 2014; Shim *et al.*, 2016). Despite its known function in PtdIns(4,5)P₂ production, most of the evidence suggested that PIP4K plays a negative role in the activation of the PI3K/Akt pathway (Carricaburu *et al.*, 2003; Emerling *et al.*, 2013; Sharma *et al.*, 2019; Shin *et al.*, 2019; Wang *et al.*, 2019). The way PIP4K controls the activation of the Akt pathway is still under investigation. It was previously proposed that PIP4K activates a PtdIns(3,4,5)P₃-specific phosphatase and that PtdIns5P plays a role in stabilising the PtdIns(3,4,5)P₃ by acting as an inhibitor

of this specific 5-phosphatase, rather than controlling the synthesis of PtdIns(3,4,5)P₃ (Carricaburu *et al.*, 2003). Another study has also proposed that PtdIns5P inhibits Akt dephosphorylation (Ramel *et al.*, 2009). A recent study showed that PIP4K negatively controls the insulin-activated PI3K/Akt pathway through its physical interaction with PIP5K and inhibition of PtdIns(4,5)P₂ synthesis (Wang *et al.*, 2019), while others suggested that this negative effect arose from inhibition of PIP4K that upregulates PI3K activities (Sharma *et al.*, 2019; Shin *et al.*, 2019). Bulley *et al.* (2016) reported that removal of PIP4K2 α activity in chicken DT40 B cells reduced PtdIns(3,4,5)P₃ levels and Akt activation in response to insulin. Overexpression of this protein restored the Akt activity, while acute depletion of the kinase resulted in the opposite effect. The researchers suggested that the different roles of PIP4K may occur as a consequence of temporal effects after PIP4K inhibition (Bulley *et al.*, 2016). This suggested that the primary function of PIP4K is to control the level of PtdIns(4,5)P₂, and adaptive consequence might take place following a long-term removal of the kinase. While this suggestion seems promising, identifying other possible reasons behind the observed differences in the studies is crucial. For example, Shin *et al.*, (2019) highlighted PTEN deficiency as a source of negative regulation of PI3K by PIP4K. For all these proposed mechanisms, their generalisability to all types of cells needs to be elucidated.

1.2.3 Functional Roles of PIP4Ks in Physiological and Pathological Processes

The roles of PIP4Ks in various cellular processes have been studied in several species by knocking out, overexpressing, or interfering with the expression of PIP4K isoforms. To date, PIP4K has been found to have roles in the developmental process (Elouarrat *et al.*, 2013; Gupta *et al.*, 2013; Mathre *et al.*, 2019), insulin sensitivity (Carricaburu *et al.*, 2003; Lamia *et al.*, 2004; Sharma *et al.*, 2019), autophagy (Droubi *et al.*, 2016; Al-Ramahi *et al.*, 2017; Lundquist *et al.*, 2018), and immune system activity (Shim *et al.*, 2016) in transgenic animals (Figure 1.4) as well as a role in oxidative stress response in cell lines (Gozani *et al.*, 2003; Jones *et al.*, 2013) and cancer development (Emerling *et al.*, 2013; Keune *et al.*, 2013; Jude *et al.*, 2015; Shin *et al.*, 2019). The demonstrated roles played by PIP4K through in vitro and organism studies might suggest that PIP4K can be a biological target for therapy. Several inhibitors for PIP4K isoforms have been developed that can potentially be used as therapeutic agents for disorders such as type 2 diabetes and cancer (Voss *et al.*, 2014; Clarke *et al.*, 2015; Kitagawa *et al.*, 2017; Sivakumaren *et al.*, 2020).



Development process

PIP4K has been identified to have roles in both pre- and post-neonatal developmental processes. In zebrafish, PIP4K2 α is important during normal embryogenesis (Elouarrat *et al.*, 2013). The depletion of the PIP4K2 α gene (zPIP4K2 α) caused several developmental defects such as heart failure, malformation of the eyes, and severe mid-body winding. Subsequently, delayed hatching from the chorion and altered swimming patterns were observed. In mice, PIP4K2 α and 2 β together are essential for early postnatal development, with double knockout pups often dying within 12 hours (Emerling *et al.*, 2013). Mice with a homozygous deletion of *PIP4K2B* showed a decrease in bone length by 5 to 10% compared to wild-type mice at all ages (Lamia *et al.*, 2004), whereas deletion of PIP4K2 α or 2 γ alone did not cause any noticeable phenotypes (Emerling *et al.*, 2013; Shim *et al.*, 2016). Differences in the requirement for α and β isoforms to be present during different stages of life suggested that they must have both redundant and non-redundant roles during development. In *Drosophila*, loss of the single PIP4K gene (*dPIP4K*) resulted in reduced salivary gland size *in vivo* and reduced larval body weight following a delayed larval development at multiple points after hatching (Gupta *et al.*, 2013; Mathre *et al.*, 2019).

Insulin Regulation

Activation of the PI3K pathway is essential for insulin-mediated uptake of glucose and compared to wild-type littermates, PIP4K2 β knockout mice showed better glucose control as the

mice age, with increased Akt activation in skeletal muscle and liver (Lamia *et al.*, 2004). In addition to increased insulin hypersensitivity, the mice also showed reduced body weights compared to the wild-type littermates when fed on high-fat diets. This is in line with a study showing that overexpression of PIP4K in cultured cells negatively regulates insulin-dependent Akt phosphorylation in part by decreasing the cellular level of PtdIns(3,4,5)P₃ (Carricaburu *et al.*, 2003). This showed that PIP4K2 β plays important role in determining insulin sensitivity and adiposity, and could be a suitable enzyme to target in type 2 diabetes (Carricaburu *et al.*, 2003; Lamia *et al.*, 2004). A similar outcome was seen with inactivation of dPIP4K in *Drosophila* in which PtdIns(3,4,5)P₃ levels were increased in the organism along with suppressed insulin resistance (Sharma *et al.*, 2019). However, the deletion of PIP4K2 γ in mice, showed no changes in insulin sensitivity (Shim *et al.*, 2016).

Autophagy

Recent studies have linked PIP4K with autophagy (Vicinanza *et al.*, 2015; Droubi *et al.*, 2016; Al-Ramahi *et al.*, 2017; Lundquist *et al.*, 2018). PtdIns5P is one of the lipids involved in the formation of autophagosome, the key structure in the autophagy system. Deletion of *PIP4K2B*, but not *PIP4K2A* enhanced autophagy in chicken DT40 cells (Droubi *et al.*, 2016), while silencing all three isoforms of PIP4K in HeLa cells resulted in increased levels of PtdIns5P as well as autophagosome and lysosome numbers (Vicinanza *et al.*, 2015). Overexpression of active PIP4Ks, attenuated the autophagy process while inactive PIP4K mutant overexpression showed no changes, further underlining the function of PtdIns5P in the induction of autophagy. It was also shown that PIP4K2 γ which had the most prominent association in terms of localization with autophagosome gave the strongest effect. PIP4K2 γ has also been associated with mTORC1 signalling that is intimately involved in regulating autophagy (Mackey *et al.*, 2014; Al-Ramahi *et al.*, 2017). The exact relationship between PIP4K2 γ and mTORC1 is still unclear but each appears to impact the others' output (Mackey *et al.*, 2014). MEF lacking both *PIP4K2A* and *PIP4K2B* showed defects in autophagy and autophagosome clearance activity during a period of fasting (Lundquist *et al.*, 2018). However, this observation was reported in the context of p53 loss. It was suggested that loss of PIP4Ks kinase activity prevents the acidification of the autophagosome which reduces nutrients supply to the cells, and p53 loss in the cells had further blunted cellular responses to nutrient scarcity. Direct metabolite supplementation was reported to rescue the autophagy defect.

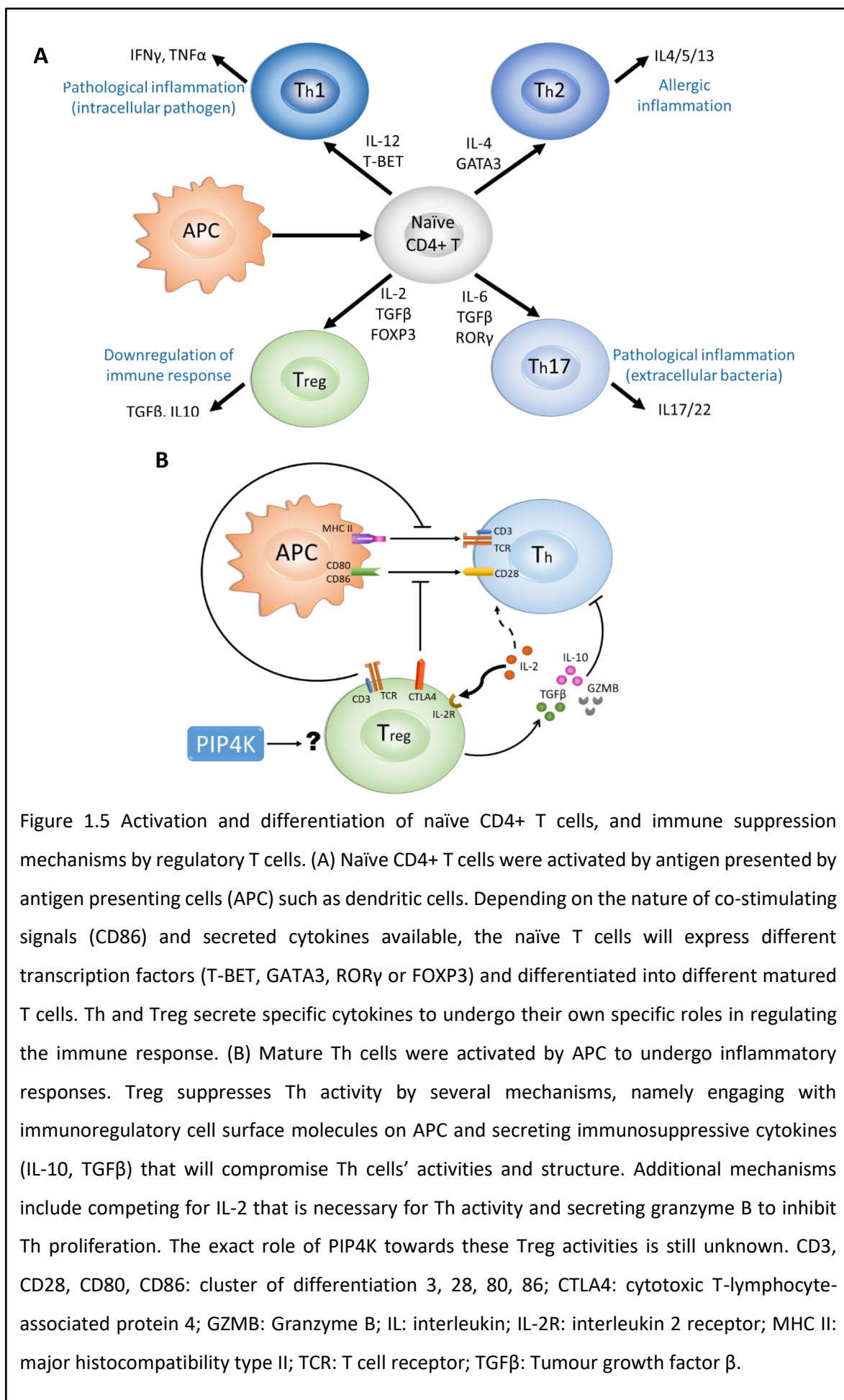
Stress Response: Evidence from *in vitro* studies

Following exposure of cells to cellular stressors such as UV radiation, PIP4K2 β is phosphorylated at threonine 322 and serine 326 by the p38 mitogen-activated protein kinase (MAPK) pathway, which leads to its inactivation and results in an increase in nuclear PtdIns5P (Jones *et al.*, 2006). Increased PtdIns5P leads to the translocation and activation of the inhibitor of growth protein 2 (ING2), a tumour suppressor gene, which contains a PHD finger that binds to PtdIns5P. This interaction induces the acetylation of the tumour suppressor p53 that leads to the activation of p53 dependent pathways such as apoptosis (Gozani *et al.*, 2003; Keune *et al.*, 2012; Jones *et al.*, 2013). It was suggested that under low-stress conditions, PIP4K might suppress the PI3K/Akt pathway and upon high cellular stress, PIP4K could mediate responses through the p38 MAPK pathway. Together, these data suggested that the interactions between ING2 and PtdIns5P can regulate nuclear responses to DNA damage (Gozani *et al.*, 2003).

1.2.4 PIP4K and Immune System Regulation: Current Evidence and Potential Role in Regulatory T Cells Activity

When the immune system is triggered following host detection of infectious microorganisms the resulting chain of actions includes the recruitment of T helper (Th) cells to execute defensive mechanisms. This is followed by the action of regulatory T cells (Tregs) to control the T helper activity from hyperactivation and potential tissue damage (Vignali *et al.*, 2008). Both T helper and Tregs originate from CD4⁺ T cells that can differentiate into different T cell subtypes according to signals from various microenvironments and cytokines (Boyton and Altmann, 2002) (Figure 1.5A). Strict regulation of this system is crucial to ensure balanced activity between the two. The role of PIP4K in the immune system was brought into attention by reports showing a single nucleotide polymorphism (SNP) at the *PIP4K2C* locus, being associated with autoimmunity disorders such as rheumatoid arthritis and diabetes type 1 (Raychaudhuri *et al.*, 2008; Fung *et al.*, 2009). Our lab has also shown that the level of PIP4K in a group of cancer cell lines derived from hematopoietic tissue is higher (Barretina *et al.*, 2012; Jude *et al.*, 2015), which increased our interest to further investigate the role of this kinase in the immune system. Another study discovered that the deletion of PIP4K2 γ in mice resulted in increased inflammation, T-cell activation, and cytokine production despite having normal growth and viability (Shim *et al.*, 2016). Some mice also developed spontaneous chronic inflammation with increased pro-inflammatory cytokines and immune cell infiltration in several organs. The mice exhibited increased mTORC1 signalling in immune system organs such as the spleen with increased T cell proliferation and T helper cell populations, and had lower numbers of immune suppressor regulatory Tregs. Such significant effects of PIP4K2 γ depletion towards the immune system had raised curiosity on the molecular role played by this kinase; either it is through the Tregs or other T helper cells. This study will focus on discovering the role of PIP4K towards Tregs, particularly through their effect on the cells' activation of the Akt pathway.

Tregs represent only 5-10% of the total CD4⁺ T cell population. They function to regulate immunological tolerance and thus play an important role in autoimmune diseases such as inflammatory bowel disease, cancer and also post organ transplantation (Sakaguchi *et al.*, 2001; Ohkura and Sakaguchi, 2010b). Tregs can be defined by the expression of interleukin 2 (IL-2) receptor α -chain (CD25), cytotoxic T lymphocyte-associated antigen 4 (CTLA-4) or CD125, and absence of CD127 surface markers (Santegoets *et al.*, 2015). However, the most specific molecular marker is the expression of the Foxp3 transcription factor that also partly drives the immune suppressive ability (van der Vliet and Nieuwenhuis, 2007; Soond *et al.*, 2012). Mice harbouring Foxp3 mutations or Foxp3 deficiencies develop a condition known as immune dysfunction, polyendocrinopathy, enteropathy, X-linked (IPEX), an autoimmune disorder affecting multiple



organs of a person, commonly the intestine and skin (Bennett *et al.*, 2001; Brunkow *et al.*, 2001). Tregs can be categorized into three subsets: 1) thymus-derived Tregs (tTregs; also known as natural Tregs or nTregs), 2) peripherally derived Tregs (pTregs), and 3) in vitro-induced Tregs (iTregs) (Abbas *et al.*, 2013). The iTregs develop from naïve CD4⁺ T cells in response to T cell receptor (TCR) co-stimulated in the presence of transforming growth factor β (TGF- β 1) (Chen *et al.*, 2003). The different roles played by nTregs and iTregs are still under debate (Bilate and Lafaille, 2011). Tregs generally suppress immune responses by secreting suppressive cytokines like interleukin 10 (IL-10) and TGF- β that inhibit T cells and leukocytes activities (Pandiyan *et al.*, 2007), as well as by expressing high levels of IL-2 receptor to bind and sequester IL-2, competing with effector T cells. CTLA-4 that is also highly expressed on Tregs disturbs dendritic cell function to inhibit their stimulation of T effector cells (Yokosuka *et al.*, 2010) (Figure 1.5B).

TCR consists of α and β antigen-binding chains ($\alpha\beta$ TCR) with five CD3 subunits and a membrane receptor known as CD28. CD28 acts as a co-stimulatory receptor that aids in various T cell processes such as differentiation and homeostasis (Tang *et al.*, 2003; Guo *et al.*, 2008). The TCR recognises and binds with antigens bound to the cell surface major histocompatibility complex (MHC) complex. Following the ligand-binding event, CD3 induces T cell activation (Rudolph *et al.*, 2006). Although TCR activation leads to the downstream activation of pathways such as PI3K/Akt and Mapk/ERK (mitogen-activated protein kinases/extracellular signal-regulated kinases) pathways, the exact mechanism is unknown (Rincón *et al.*, 2001; Ward and Cantrell, 2001; Fayard *et al.*, 2010; Okkenhaug, 2013). It is suggested that the activated TCR/CD3 complex leads to phosphorylation of tyrosine at the cytoplasmic tail of CD28 that will then mediate the activation of downstream pathways (August and Dupont, 1994). While TCR is expressed by all CD4⁺ T cells, different subsets of these T cells carry a slightly distinct feature from each other. Tregs possess a TCR repertoire slightly different in breadth and charge compared to conventional T cells (Tconv), a group of T lymphocytes that also expresses an $\alpha\beta$ T cell receptor, but differs than Tregs in terms of their migratory behaviour in organs (Wong *et al.*, 2007; Roberts and Girardi, 2008; Tong *et al.*, 2019). Further studies demonstrated that the signal elicited by TCR is dampened in Treg cells, which is caused by low phosphorylation of CD3 ζ , one of the key components of MHC receptor (Yan *et al.*, 2015). The reduced signal then radiates along with the downstream signalling of Akt, S6, and ERK1/2. Interestingly, this dampened signalling effect only exhibits upon TCR stimulation, but not stimulation from cytokines and other intercellular signals; implying that Tregs will get less stimulated due to pathogens compared to the other CD4⁺ effector T cells (Teffs) that actively respond to combat the pathogens. This enables the immune system to execute an appropriate mechanism to defend the body against pathogens. Moreover, different strength and stimulation of

signal on TCR also play a significant role for Tregs transcriptional program and development through TGF- β stimulation (Marie *et al.*, 2005; Miskov-Zivanov *et al.*, 2013).

PI3K/Akt/mTOR pathway in general controls various aspects of Treg cell functions (Figure 1.6). Previous studies showed that inactivating mutations of p110 δ PI3K in BALB/c mice caused increased Tregs in the thymus (Patton *et al.*, 2006) and retroviral overexpression of Akt reduced the number of nTregs (Haxhinasto *et al.*, 2008), indicating a negative effect of PI3K/Akt pathway on Tregs production. The negative effect of PI3K/Akt may be due to their inactivation of FOXO transcription factors that are crucial for differentiation and Tregs cell function (Kerdiles *et al.*, 2010; Ouyang *et al.*, 2010). The FOXO transcription factor belongs to the Forkhead box family of transcription factors and is required for the appropriate expression of Foxp3 (Ohkura and Sakaguchi, 2010a). Activated Akt will cause FOXO to be excluded from the nucleus and thus interferes with nTreg development (Soond *et al.*, 2012). Prolonged treatment with mTOR inhibitor rapamycin, partially inhibited Akt phosphorylation, thus maintaining FOXO in the nucleus (Sarbasov *et al.*, 2006). In addition, suppressing mTOR signalling with rapamycin promotes oxidative metabolism that is required by Tregs for cellular differentiation (Michalek *et al.*, 2011).

Another significant role of the PI3K/Akt pathway is that PI3K activity is needed for Treg function. In mice lacking p110 δ PI3K activity, the production of IL-10 by Tregs was reduced, resulting in low T cell suppressive activity and increased development of autoimmune colitis (Okkenhaug, 2002; Patton *et al.*, 2006; Uno *et al.*, 2010). Also, inhibition of the PI3K pathway showed enhanced anti-tumour activity, while Tregs infusion restored tumour growth (Abu-Eid *et al.*, 2014). On the contrary, Tregs overexpressing an active form of Akt had reduced ability to suppress T cell proliferation (Crellin *et al.*, 2007; Patterson *et al.*, 2011). Evidence suggested that some PI3K activities are needed for Treg mediated suppression, but very high Akt activity can also inhibit this suppressive function (Soond *et al.*, 2012).

The role of PI3K signalling in Tregs is also controversial as different studies have shown contradicting results. For example, evidence showed that PI3K could both enhance and block peripheral conversion of naïve CD4⁺ T cells into iTreg (Harada *et al.*, 2010; Patterson *et al.*, 2011; Patton *et al.*, 2011). There is no clear explanation as to why these differences are observed but it may lie in the amount of co-stimulation provided which could compensate the lack of PI3K activity, and the intensity of PI3K/Akt activity such that very high PI3K/Akt activation may be unsuitable for iTreg conversion (Soond *et al.*, 2012). Similar contradicting results were also observed on homeostasis and the expansion of peripheral Tregs. In mice with inactivated PI3K, and despite increased nTregs generation, the levels of peripheral Tregs in spleen and lymph nodes of mice were low indicating that PI3K is required for their growth and maintenance. (Patton *et al.*, 2006). In

contrast, the administration of either PI3K or Akt inhibitors resulted in proliferation inhibition in Tregs. In the case of mTOR, activation of this pathway contributes to Treg proliferation and suppression (Chapman and Chi, 2014), while using rapamycin to block mTOR signalling showed increased expansion of Tregs (Battaglia *et al.*, 2005).

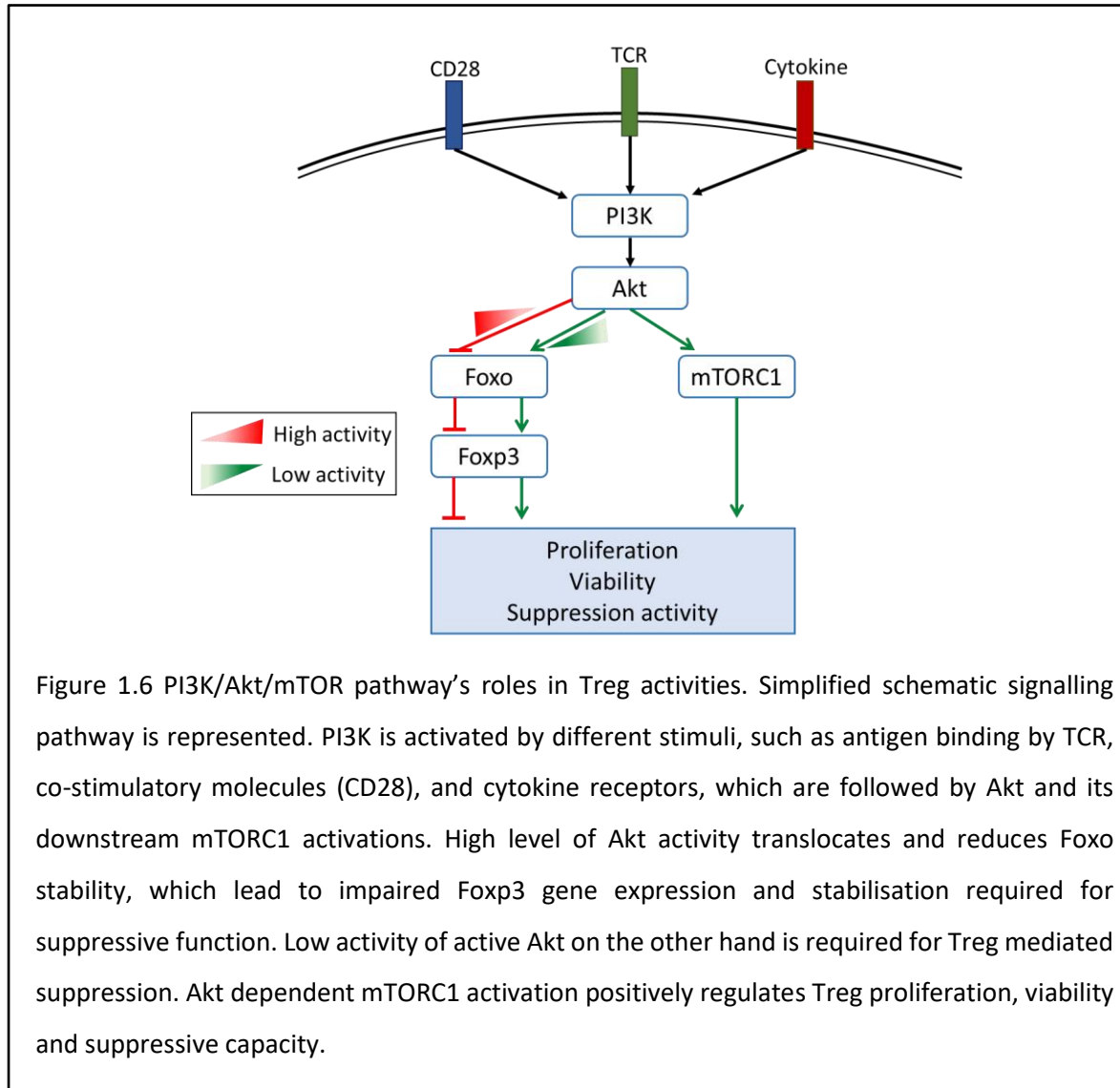


Figure 1.6 PI3K/Akt/mTOR pathway's roles in Treg activities. Simplified schematic signalling pathway is represented. PI3K is activated by different stimuli, such as antigen binding by TCR, co-stimulatory molecules (CD28), and cytokine receptors, which are followed by Akt and its downstream mTORC1 activations. High level of Akt activity translocates and reduces Foxo stability, which lead to impaired Foxp3 gene expression and stabilisation required for suppressive function. Low activity of active Akt on the other hand is required for Treg mediated suppression. Akt dependent mTORC1 activation positively regulates Treg proliferation, viability and suppressive capacity.

Another pathway studied in relation to T cells is the ERK pathway. One of the ERK downstream cascades that consists of Ras, Raf, Mek1/2, and ERK1/2 controls the phosphorylation of the same PI3K/Akt downstream signalling S6 ribosomal protein, suggesting a cross-talk between the two pathways (Chow *et al.*, 2006; Yoon and Seger, 2006). This pathway is also found to regulate T cells differently, and as with PI3K/Akt studies, discrepancies between ERK studies have been reported. One study showed that inhibition of ERK showed suppressed iTregs differentiation (Lu *et al.*, 2010). Others, however, reported that ERK inhibitor increase the TGF- β epigenetic regulation of Foxp3 in Tregs (Luo *et al.*, 2008). Another study also reported that knockdown of the ERK-activating enzyme Mek enhanced TGF- β induced Foxp3 expression and development of Tregs (Liu *et al.*, 2013). The contrasting findings were suggested to be due to different mechanisms of ERK inhibitors utilised by the different studies that affect different transcription factors and DNA methylation. Therefore, a proper plan is required in order to study changes in the activation of different pathways in Tregs with a careful interpretation of the outcome.

Although the role of PIP4K in Tregs is not well characterised, the involvement of PIP4K2 γ in the immune system suggests that PIP4Ks might have an important role in Treg cell function and activation. Shim *et al.* (2016) reported that deletion of PIP4K2 γ leads to hyperactivation of the immune system and it is possible that PIP4K2 γ positively regulates the immunosuppressive activity. They also found that the mTORC1 signalling complex, which is important in T-cell differentiation and activation, was hyperactivated in several tissues of the PIP4K2 γ knockout mice (Shim *et al.*, 2016). In addition, PIP4K2 γ knockout mice also appeared to have fewer Tregs. Therefore, investigating the role of PIP4K in Tregs activity could be the first step to understand the role of PIP4K in modulating the immune system.

1.2.5 PIP4K and Cancer Cells Growth: Current Evidence and Potential Interaction with p53

Cancer is viewed as one of the major health burdens worldwide (Wang *et al.*, 2016). New therapeutic approaches are being actively researched, taking into account genetic and epigenetic factors, as well as any molecular changes in the microenvironment. Six alterations in the normal cellular signals have been identified as hallmarks of cancer (Hanahan and Weinberg, 2000, 2011), which enable cells to acquire the functional capabilities of cancer, including the ability to sustain proliferative signalling, circumvent apoptosis, and avoid growth suppressors. Deregulations of several components leading to the activated cancer capabilities have been identified. This include modulation of the PI3K/Akt pathway and Ras oncogene, which is a GTPase (guanosine triphosphate hydrolase enzyme) family member that regulates the ERK pathway (Vivanco and Sawyers, 2002; Luo *et al.*, 2009). PI3K pathway and Ras are somehow interacting with each other through the Ras-binding domain expressed by the class I PI3K catalytic isoforms (Gupta *et al.*, 2007). The PI3K/Akt pathway is closely studied with cancer development due to its role in cell growth, proliferation, and apoptosis, which control the survival and growth of cancer cells (Janku *et al.*, 2018). The regulation of the PI3K pathway, while well documented, is not well characterised at the molecular level.

PI3K/Akt is one of the most commonly dysregulated pathways in human cancers with its substrate, PtdIns(3,4,5)P₃, elevated in many cancers (Fruman and Rommel, 2014). For certain cancers such as head and neck cancer, this pathway is reported to be the most frequently mutated and could serve as a predictive biomarker (Lui *et al.*, 2013). In the case where PI3K is normal, dysregulation of other components related to PI3K might take place that in turn activates the PI3K signalling pathway; examples are activated Ras, Akt, and loss of PTEN activity (Engelman, 2009). Due to the evidence and the drugability of the pathway components, this pathway has been a continuous target for cancer therapy with the idea to inhibit the central oncogenic driver through this signalling network. However, as PI3K/Akt regulates numerous processes in normal cells, counterbalancing the requirement in normal cells compared to tumour cells is a challenge (Engelman, 2009; Fruman and Rommel, 2014; Janku *et al.*, 2018). Since deregulation of this pathway is common in cancer, there is a chance to discover a factor that can help in directing the therapeutic PI3K/Akt inhibition selectively towards oncogenic cells with mutated PI3K activity instead of cancers bearing wild type PI3K gene. To identify this factor, expanding the knowledge of this extensive PI3K-cancer network needs to be continued. For example, studying the role of other kinases indirectly involved with the pathway (Morrow *et al.*, 2014; Ikononov *et al.*, 2019) could also help to broaden our understanding of this field.

While the PIP4K2 γ isoform is found to be involved in modulating immune system function, the 2 α and 2 β strongly impact on cancer cell growth (Table 1.1). A recent study reported a strong protein co-expression between the phospholipase C delta (PLCD), a potential prognostic marker of pancreatic ductal adenocarcinoma, with several PIPs kinases including *PIP4K2A* and *PIP4K2B* (Zhou *et al.*, 2019). Multiple studies involved in modulation of PIP4K exhibited different outcomes in different cancer cells. For example, depletion of *PIP4K2A* showed a reduced clonogenic potential of acute myeloid leukaemia (AML) in both human and murine AML cells (Jude *et al.*, 2015). *PIP4K2A* depletion induced arrest of AML cells in G1 of the cell cycle and caused apoptosis. In contrast, overexpression of *PIP4K2A* in PTEN-deficient glioblastoma (GBM) cells caused inhibition of tumour growth *in vitro* and *in vivo* (Shin *et al.*, 2019). *PIP4K2A* also downregulated the Akt/S6 pathway in PTEN-deficient GBMs, but not in the GBMs with wild type PTEN. The authors suggested that *PIP4K2A* enhanced the expression of the p85 regulatory subunit of PI3K degradation by competing with the low level of PTEN for p85 interaction. In human breast cells, high level of PIP4K2 α can be more frequently observed in cancerous cells (Emerling *et al.*, 2013). Status of PIP4K2 β , however, varies across different breast cancer cell lines. A study conducted on several cancer cells showed that PIP4K2 β was highly expressed in only 38% of the cancer cells and could not be detected in normal cells (Emerling *et al.*, 2013). In contrast, another study that examined the expression of *PIP4K2B* across 489 tissue microarrays of human breast tumour patients showed that both high and low expression of the gene associated with poor patient survival (Keune *et al.*, 2013). Cells with low *PIP4K2B* gene expression were found to associate with high-grade tumour characteristics and metastatic activity, while high *PIP4K2B* gene expression was associated with the human epidermal growth receptor *ERBB2* amplification, similar to what had been reported previously (Luoh *et al.*, 2004; Emerling *et al.*, 2013; Keune *et al.*, 2013). Further observations indicated that depletion of *PIP4K2B* in both normal and tumour breast cells reduced the expression of the tumour suppressor E-cadherin, which enhanced TGF- β induced epithelial to mesenchymal transformation (Keune *et al.*, 2013).

In addition to the various roles between different cancer cells, changing levels of PIP4K also exhibits distinct effects between oncogenic cells and normal cells. In acute leukaemia cells, *PIP4K2A* downregulation reduced growth, but a similar phenotype was absent in normal human hematopoietic stem and progenitor cells (Jude *et al.*, 2015). Although the exact reason behind this interesting observation remains to be elucidated, this study indicates that *PIP4K2A* can be a potential anti-leukaemia therapeutic (Fiume *et al.*, 2015; Jude *et al.*, 2015). Moreover, inhibition of *PIP4K2A* was also shown to be capable of inhibiting the growth of normal cells activated human BJ cells, but not the Ras activated cells, suggesting a cross-talk between PI3K and Ras pathways in cancer growth (Kitagawa *et al.*, 2017). Although the detailed mechanism is still under investigation,

the data suggested that PIP4K can be a good therapeutic target for certain types of cancer without harming normal cells. The literature in general suggests that PIP4K function is highly cell-specific and should not be generalised even within similar types of cancer.

The roles of PIP4Ks in cancer cell development has also been studied in relation to p53 (Emerling *et al.*, 2013). It was reported that in a subset of breast cancer that lacks p53 activity, the expression of PIP4K2 α or 2 β was high compared to normal breast epithelial tissues. Depletion of both PIP4K2 α and 2 β in p53 mutated cells resulted in senescence, reduced cell proliferation and growth, although depletion of either alone did not show a similar outcome (Emerling *et al.*, 2013). In other breast cancer cells with wild type p53 such as MCF7, such effects were not observed; leading to a possibility that PIP4K2 α /2 β expression is essential for tumour development under mutated p53 condition. Knocking out p53 in mice led to the development of spontaneous tumours such as lymphomas and soft tissue sarcomas in mice. The deletion of both *TP53* and *PIP4K2B* was lethal at an early stage of development, while the loss of either alone did not lead to any obvious developmental abnormalities. Homozygous deletion of *PIP4K2A* also did not reduce the tumour-dependent death due to the loss of p53. Surprisingly, the homozygous deletion of *PIP4K2A* combined with a heterozygous loss of *PIP4K2B* prevented tumour development and significantly increased the tumour free survival following p53 deletion. This study suggested a synthetic lethal phenotype between loss of P53 and *PIP4K2B*, suggesting that compromising PIP4K activity in tumours that have lost p53 could be a useful anti-tumour therapy.

A theory has been proposed to explain the mechanism of tumour growth arrest following the loss of PIP4K and p53 (Emerling *et al.*, 2013; Jones *et al.*, 2013). PtdIns5P has been identified as a second messenger for reactive oxygen species (ROS)-dependent cell damage that leads to cell cycle arrest. PIP4K reacts to a high level of PtdIns5P by producing intracellular PtdIns(4,5)P₂ that helps to suppress rates of ROS production by maintaining glucose metabolism. Since p53 also plays an important part in regulating glucose and ROS homeostasis (Itahana and Itahana, 2018), the absence of both PIP4K and p53 could not be tolerated by the cells. Reduced cellular response to nutrient scarcity following defect in autophagosome activity due to loss of p53 and PIP4K could also explain the synthetic lethal phenotype observed in mice (Lundquist *et al.*, 2018). In addition, PtdIns5P is also involved in regulating p53-dependent apoptosis *via* interaction with ING2 (Gozani *et al.*, 2003). ING2 is another candidate for a tumour suppressor gene that aids in activating p53 by enhancing its acetylation, stability, and activation process (Pedeux *et al.*, 2005). It contains a PHD finger that binds to PtdIns5P, and localisation of ING2 into the chromatin was found to be modulated by the level of nuclear PtdIns5P (Jones *et al.*, 2006). The absence of both PIP4K and p53 might have disrupted this mechanism, causing the cells to opt for another defensive mechanism. Another possible mechanism could be through the PI3K/Akt itself as p53 is also involved with the pathway.

Hence, studying the synthetic lethal interaction between PIP4K and p53 through this pathway is a promising approach to investigate the possible mechanism that leads to the tumour growth arrest.

Table 1.1 Effect of PIP4K depletion in tumour cell growth

Types of cancer	Cell line/organism	PIP4K modulation	P53 modulation	Effect
Acute myeloid leukaemia (AML) (Jude <i>et al.</i> , 2015)	THP 1 (human)	<i>PIP4K2A</i> knockdown	No	Reduced proliferation and clonogenic potential.
	Primary cell line (human)	<i>PIP4K2A</i> knockdown	No	Reduced frequency of clonogenic cells.
	MLL-AF9 (murine)	<i>PIP4K2A</i> knockdown	No	Reduced clonogenic potential.
Breast cancer	BT474 (human) (Emerling <i>et al.</i> , 2013)	<i>PIP4K2A</i> and <i>PIP4K2B</i> knockdown	Yes (E258K – p53 functional at 32°C)	At 37°C, cell growth inhibited and tumour formation impaired in xenografts (mice). Impaired tumour formation in xenografts (mice).
	MCF7 (human)	<i>PIP4K2A</i> and <i>PIP4K2B</i> knockdown (Emerling <i>et al.</i> , 2013)	No	No effect on growth.
		<i>PIP4K2B</i> knockdown (Keune <i>et al.</i> , 2013)	No	No significant differences in growth rate, cell-cycle distribution, or anchorage-dependent clonogenic growth. Reduce colony growth in anchorage-dependent growth.
Spontaneous cancer (e.g. lymphomas & sarcomas) (Emerling <i>et al.</i> , 2013)	Mice	No	<i>TP53</i> knockout	Formation of a spontaneous tumour.
		<i>PIP4K2A</i> homozygous + <i>PIP4K2B</i> heterozygous knockout	<i>TP53</i> knockout	Dramatic reduction in spontaneous tumour formation and tumour death.
Glioblastoma (Shin <i>et al.</i> 2019)	PTEN-deficient GBMs (patient-derived)	Overexpress	No	Reduced cellular proliferation, clonogenic growth, and Akt signalling pathway.

1.3 Study Aims

PIP4K has been shown to play several physiological and pathological roles. Among the crucial functions, the kinase's roles in the immune system and cancer growth have been chosen to be further studied in this two-part project. Collaboration work with a laboratory in Milan had brought us to further investigate the mechanism played by PIP4K in modulating the regulatory T cells (Tregs). This project focused on identifying how PIP4K affects the Akt and ERK pathways in Tregs and naïve T cells, which will form the first part of this study. The second and major component involved studying the role of PIP4K in p53 inactivated cancer cells, as well as regulations of Akt pathway by PIP4K.

Chapter 2 Materials and Methods

2.1 Chemicals, reagents and other materials

Table 2.1 List of chemicals and reagents

Acros	Sodium orthovanadate Sodium phosphate dibasic dehydrate 10x reverse transcriptase buffer Multiscribe reverse transcriptase
Amersham / GE Healthcare	Nitrocellulose Blotting Membrane High Performance chemiluminescence film
FMC Bio Products	NuSieve® GTG® agarose
Invitrogen	SeeBlue® Plus2 Prestained Standard (1X)
Life Technologies	Dulbecco's Modified Eagle Medium (DMEM) 1X Foetal Bovine Serum LDS sample buffer 4x Nupage® McCoy's 5a Medium Modified MOPS SDS running buffer 20x Nupage® Penicillin-Streptomycin (Pen strep) Stable trypsin replacement enzyme TrypLE™ Express (1x) Glycin N,N,N',N' – tetramethylethylenediamine (TEMED)
Melford	<i>Bis</i> -TRIS
Millipore	Immobilon™ Western Chemiluminescent HRP Substrate
Polysciences, Inc	Polyethylenimine (PEI)
Primerdesign	Precision 2X qPCR Mastermix
Roche	Bovine serum albumin fraction V Western Blocking Reagent
Scientific Laboratory Supplies	Medical Blue Sensitive X-ray Film

Sigma-Aldrich	<p>3-Indoleacetic acid (Auxin)</p> <p>Acetic acid</p> <p>Ammonium persulfate (APS)</p> <p>Ampicillin sodium salt</p> <p>Crystal Violet</p> <p>Hexadimethrine bromide (Polybrene)</p> <p>IGEPAL® CA-630 (NP40)</p> <p>Insulin solution human</p> <p>Nuclease Benzonase®</p> <p>Ponceau S Solution</p> <p>Tween® 20</p>
Thermo Fisher	<p>Acrylamide: Bis-Acrylamide 37.5:1 Electrophoresis 40% solution</p> <p>Dithiothreitol (DTT)</p> <p>dNTP mix 10mM</p> <p>Ethanol</p> <p>Formaldehyde</p> <p>Isopropanol/ 2-propanol</p> <p>Magnesium Chloride 50mM</p> <p>Methanol</p> <p>Pierce™ BCA Protein Assay Kit</p> <p>Potassium chloride</p> <p>Potassium dihydrogen orthophosphate</p> <p>Pre-cast gel Bolt™ 4-12% Bis-Tris Plus. 15 wells</p> <p>Random hexamer primer</p> <p>RiboLock</p> <p>RNAse inhibitor</p> <p>Sodium fluoride</p> <p>Supersignal® West Femto Maximum Sensitivity substrate</p> <p>Tris base</p>

2.2 Buffers and solutions

Buffers and solutions used are listed in alphabetical order below. Final concentrations or volumes used to prepare are stated. Solutions are always prepared with ultrapure Millipore water (resistivity: 18.2 M Ω .cm@25°C) unless stated.

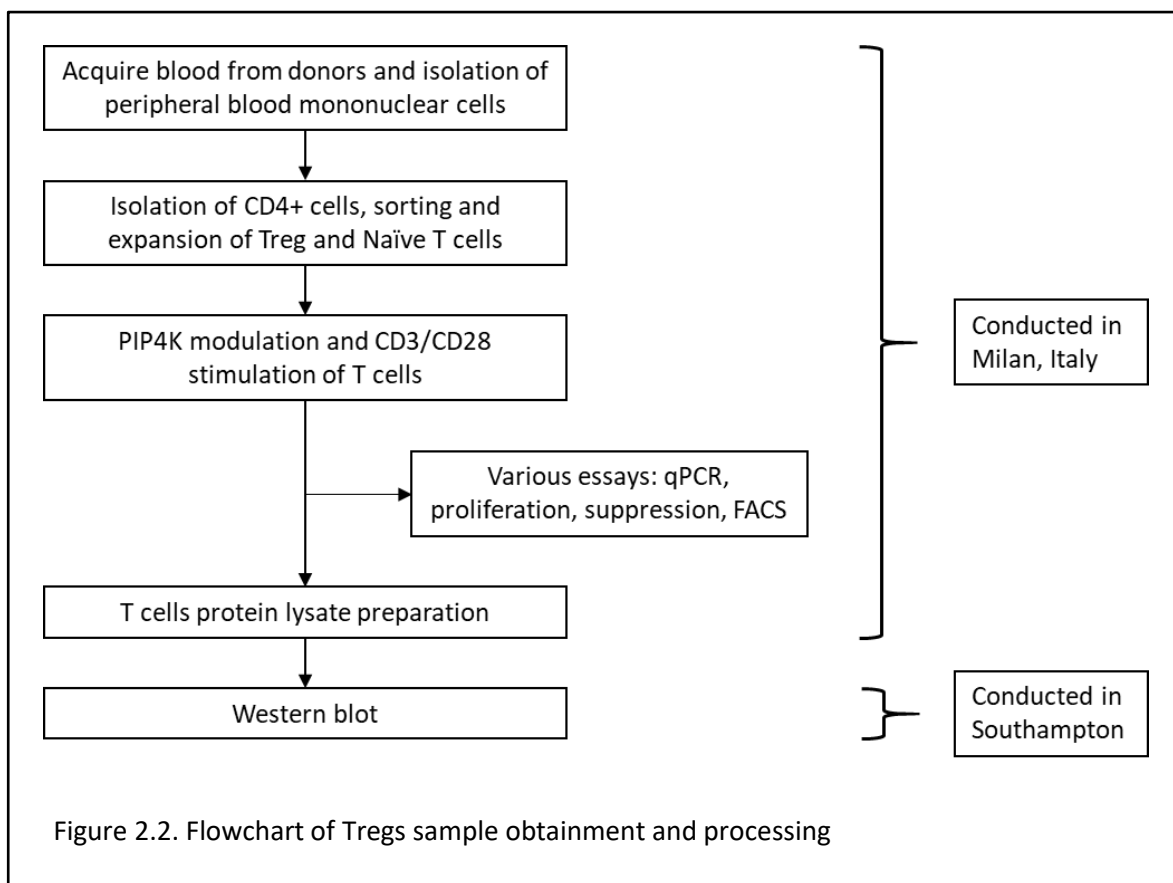
Table 2.2 List of buffers and solutions

Bis-Tris Gel buffer (3x) 1) 1.0 M Bis-Tris HCl pH 6.5	Cell freezing media 1) 90% (v/v) fetal bovine serum (FBS) 2) 10% (v/v) dimethyl sulphoxide (DMSO)
Crystal Violet (0.5%) 1) 0.5% (w/v) crystal violet 2) 20% (v/v) methanol	Elution buffer 1) 10 mM Tris-HCl, pH 8.0
Formaldehyde (4%) 1) 4% formaldehyde 2) Dilute in 1x PBS	Inoue buffer 1) 55 mM MnCl ₂ 2) 15 mM CaCl ₂ 3) 250 mM KCl 4) 10 mM PIPES (0.5 M, pH 6.7 stock)
N3 (Neutralisation buffer) 1) 4.2 M guanidine hydrochloride 2) 0.9 M potassium acetate, pH 4.8	P1 (resuspension buffer) 1) 50 mM Tris-HCl 2) 10 mM EDTA, pH 8.0 3) 50-100 μ g/ml RNase A
P2 (Lysis buffer) 1) 200 mM NaOH 2) 1% SDS	P3 (neutralisation buffer) 1) 3 M potassium acetate, pH 5.5
PB wash buffer 1) 5 M guanidine hydrochloride 2) 30% Isopropanol	PE wash buffer (5x) 1) 80 mM NaCl 2) 8 mM Tris-HCl, pH 7.5 (25°C) 3) 80% ethanol (add prior to dilution)
Phosphate buffer solution (PBS) (10x) 1) 1.4 M NaCl 2) 27 mM KCl 3) 101 mM Na ₂ HPO ₄ 4) 18 mM KH ₂ PO ₄	PBS / 0.1% Tween 20 (10x) 1) 1.4 M NaCl 2) 27 mM KCl 3) 101 mM Na ₂ HPO ₄ 4) 18 mM KH ₂ PO ₄ 5) 1% Tween 20

QG buffer 1) 5.5 M guanidine hydrochloride 2) 30% isopropanol	RIPA buffer 1) 1% NP-40 2) 1% Deoxycholate (DOC) 3) 0.1% SDS 4) 150 mM NaCl 5) 10 mM NaPO ₄ pH7.2 6) 2 mM EDTA
Solution D 1) 4 M guanidine thiocyanate 2) 25 mM sodium citrate 3) 0.5% sarkosyl	TAE buffer (50x) 1) 2 M Tris 2) 50 mM EDTA 5.71% Acetic acid
TFB1 1. 30 mM KAc 2. 10 mM CaCl ₂ 3. 50 mM MnCl ₂ 4. 100 mM RbCl 5. 15% glycerol *Adjust to pH5.8 with 1M HAc	TFB2 1. 10 mM MOPS, pH6.5 2. 75 mM CaCl ₂ 3. 10 mM Rbcl 4. 15% glycerol 5. *Adjust to pH 6.5 with 1M KOH, filter sterilize
X-gal staining solution 1. 1 mg/ml X-gal solution 2. 40 mM citric acid/sodium phosphate buffer pH6.0 3. 5 mM potassium ferricyanide 4. 5 mM potassium ferrocyanide 5. 150 mM NaCl 6. 2 mM MgCl ₂	Wash buffer (Gel extraction & PCR purification) 1. 20 mM NaCl 2. 2 mM Tris-HCl, pH 7.5 3. 70% ethanol
Western Blot Transfer buffer (10x) 1. 1.2 M Tris base 2. 400 mM glycine	Western Blot Transfer buffer (1x) 1. Diluted from 10x WB transfer buffer 2. Methanol 20% (v/v) 3. Dilute in H ₂ O

2.3 Methods for investigating the role of PIP4K in regulatory T cells activation pathway

T cell work is a collaborative project with Dr. Alessandro Poli (National Institute of Molecular Genetics (INGM), Milan). T cells were obtained and processed in Milan and protein lysates were sent to the University of Southampton. Methods for investigating the role of PIP4K in regulatory T cells and tumour cells activities will be discussed separately. This is necessary for clarity as different methods of protein lysates preparation for T cells and cancer cells were used. Diagram 2.1 (below) illustrates the flow of the T cells sample processing.



2.3.1 Generation of Tregs and naïve T cells lysates, expansion, transduction, and stimulation

T cells were isolated from buffy coat of healthy donors of Fondazione IRCCS Ca'Granda Ospedale Maggiore Policlinico, Milan. Peripheral blood mononuclear cells (PBMC) were isolated by Ficoll-hypaque density gradient centrifugation. The use of PBMC from healthy donors was approved by the ethical committee of Fondazione IRCCS Ca'Granda Ospedale Maggiore Policlinico for research purposes. Informed consent was obtained from subjects before blood withdrawal.

From the PBMC, CD4⁺ cells were isolated using a human CD4⁺ T cell isolation kit (Miltenyi Biotec). Tregs were extracted and sorted with different surface markers, namely: CD4⁺, CD127_{low}, CD25_{high}, CD45RO_{low}, and CD62L_{low}. For Tregs and naïve T cell expansion, 10,000,000 cells were collected in a 96-well plate, washed in PBS and resuspended in a serum-free RPMI medium with IL2. The cells then received stimulation with anti-CD3/CD28 beads for different time courses, ranging from one minute to two hours. Cells with PIP4K knockdown were produced through viral transduction with pLKO.1 expressing shRNA constructs and were sorted for GFP. Overexpression cells were produced by transduction with a virus containing the pCDH vector with CMV promoter driving the expression of PIP4K2 β while NIH-12848 (20 μ M) was used as a PIP4K2 γ inhibitor (Clarke *et al.*, 2015).

2.3.2 PBMC Immunostaining

For cell surface marker staining, PBMC were washed with PBS before directly stained with specific conjugated antibodies for 30 minutes at 37°C in the dark. For intracellular staining, PBMC were washed with PBS before resuspension in Fixation/Permeabilisation Buffer (eBioscience) for 30 minutes at 4°C. Cells were washed with PBS and further permeabilised in Permeabilisation Buffer (Life Technologies) before conjugated antibodies for intracellular targets added and the cells incubated for 30 minutes at room temperature in the dark. Cells were washed and resuspended in PBS before analysed by fluorescence-activated cell sorting (FACS) (Canto II (BD)). Data analysis was done by FlowJo8 and geometric mean of fluorescence intensity value was used to express the mean fluorescence intensity (MFI). Table 2.3 below listed the antibodies used for immunostaining analysed by FACS.

Table 2.3 Antibodies used for immunostaining with FACS

Antibody	Company	Additional Information
Anti-FOXP3 eFluor450/APC	eBiosciences	Clone: 236A/E7, FJK-16S
Anti-GATA3 BV421	BD Biosciences	Clone: L50-823
Anti-Tbet PE	eBiosciences	Clone: 4B10
Anti-CTLA-4 APC	BioLegend	Clone: L3D10
Ki67 PE	BioLegend	Clone: 11F6

2.3.3 T cell Proliferation assay

Primary Treg cells were labelled with CellTrace/carboxyfluorescein diacetate succinimidyl ester (CFSE) (Violet/CFSE, Thermo Fisher) and stimulated with CD3/CD28 at a ratio of 1 cell: 0.1 beads. The cells were incubated in complete RPMI 1640 medium supplemented with IL-2 for 4 days. Proliferation was read as the dilution of Cell Trace/CFSE using FACS. Data analysis was done by FlowJo 8.

2.3.4 Suppression Assay

20,000 Naïve T cells from healthy donors were labelled with CellTrace/CFSE and co-cultured with nTreg cells at ratios of 1:1, 1:0.5, and 1:0.25 respectively. The cells were stimulated with CD3/CD28 Dynabeads at a ratio of 1 cell to 0.1 beads in the absence of IL-2 for 96 hours. Naïve T

cells cultured alone, with or without receiving stimulation, were used as positive and negative controls respectively for the assay. Proliferation of Naïve T cells was determined by the dilution of Cell Trace/CFSE using FACS before the data analysed using FlowJo 8. The suppressive capacity of Treg cells was determined by the lack of proliferation of the Naïve T cells.

2.3.5 T cell lysate preparation

Generated Treg and Naïve T cells with PIP4K2B/2C knockdown and overexpression; as well as cells treated with PIP4K2 γ inhibitor were mixed and incubated with Laemmli buffer for 30 minutes to lyse the cells. The lysates were sent to the University of Southampton by courier service. Prior to western blot analysis, the cell lysates were boiled at 95°C for 5 minutes.

2.4 Methods for investigating the role of PIP4K in tumour cell growth

2.4.1 Cell Biology

2.4.1.1 Cell Lines

Mammalian cell lines used in this study were previously obtained by Prof. Nullin Divecha's lab unless otherwise stated. HCT 116 cell line was a gift from Dr. Rob Ewing (School of Biological Sciences, University of Southampton). All the cell lines and their description are listed in Table 2.4

Table 2.4 Mammalian cell line used

Cell line	Description	Type	Culture media
U2OS eco	Human bone osteosarcoma epithelial cells, expressing ecotropic retrovirus receptor	Adherent	DMEM (1X), 10% FBS
HEK293FT	Human embryonal kidney cells transformed with SV40 large T antigen	Adherent	DMEM (1X), 10% FBS
Platinum E (Plat-E)	Derived from 293T cells, contains gag, pol and env genes for retrovirus packaging	Adherent	DMEM (1X), 10% FBS
BT 474	Human epithelial mammary gland; ductal carcinoma	Adherent	DMEM (1X), 10% FBS
HCT 116	Human epithelial colorectal carcinoma	Adherent	McCoy's 5A, 10% FBS

2.4.1.2 Cell Culture

U2OS, HEK293FT, Plat-E, and BT 474 cells were grown in DMEM (1x) supplemented with 10% foetal bovine serum (FBS) and 1% penicillin (100 U/ml) streptomycin (100 µg/ml) (pen/strep). HCT 116 was grown in McCoy's 5A supplemented with 10% FBS and 1% pen/strep. All cell lines were grown at 37°C, 5% CO₂ in a 10 cm dish until the cells were about 80% confluent before the cells were passaged. For sub-culturing, cells were washed once with sterile PBS before incubated with 1 ml of 0.25% trypsin at 37°C for 5 minutes. Following the incubation, cells were re-suspended in complete media to inactivate the trypsin and the mixture was gently pipetted up and down several times to disrupt any cell aggregation. Approximately 2x10⁶ Cells were then seeded in a sterile dish. Cell cryopreservation was conducted by harvesting cells through centrifugation (1200 rpm for 3 minutes) and re-suspended in freezing media (10% DMSO in FBS) before being transferred to a cryogenic vial. The vial was placed in a cell freezing container before being transferred to a liquid nitrogen vessel (-180°C). For thawing, cells were thawed at 37°C and quickly transferred to a 15 ml falcon tube containing approximately 5 ml of cell culture medium. The tube was centrifuged at 1200 rpm for 3 minutes. Supernatant was removed and the cells re-suspended with 1 ml of media before transferred to a 10 cm dish containing 10 ml of complete media.

2.4.1.3 Cell lysis for protein extraction

Media was removed and cells were washed with ice-cold 1x PBS before being placed on ice. RIPA buffer (1% NP-40, 1% DOC, 0.1% SDS, 150 mM NaCl, 10 mM NaPO₄, 2 mM EDTA) containing 5 mM NaF and 1 mM Orthovanadate was added to the cells. After 15 minutes incubation on ice, cells were scrapped by a silicone scraper and the cell lysate transferred into an Eppendorf tube. Cells were sonicated using an ultrasonic bath for 5 minutes and cell debris removed by centrifugation at 11,000 rpm for 10 minutes, with the supernatant being transferred to a clean Eppendorf tube and stored at -20°C.

2.4.1.4 RT-qPCR for RNA from adherent cells

Total RNA was extracted from a 12-well plate. Media was removed and cells were washed with ice-cold 1x PBS before placing the plate on ice. 350 µl of Solution D (4 M guanidine thiocyanate, 25 mM sodium citrate, 0.5% sarkosyl) with 350 mM β-mercaptoethanol was added to lyse the cell and 350 µl of 70% ethanol was added before the lysate loaded on to a DNA mini-spin silica column. The column was centrifuged in a microcentrifuge for 1 minute at 11,000 rpm and washed once with 450 µl of 4 M sodium acetate and centrifuged as before. The column was washed twice with 400 µl of 70% ethanol and centrifuged as before between each wash and finally centrifuged for 2 minutes

at 14,000 rpm to dry the column. RNA was eluted by applying 50 μ l of RNase free water to the column, left to stand for 1 minute and centrifuged at 10,000 rpm for 1 minute. The RNA was incubated on dry ice prior to storage at -80°C .

2.4.1.5 Transient transfection of cells

Cells were plated at $2-4 \times 10^5$ per well in a 6-well plate and left for two hours to overnight. A total of 2 μ g plasmid was made up to 94 μ l with serum and antibiotic-free media in an Eppendorf tube and left to incubate at room temperature for 10 minutes. 6 μ g of PEI (3:1 ratio of PEI to DNA; or 6 μ l of the 1 mg/ml PEI) stock was added to the tube and incubated for another 20 minutes. The transfection mixture was then added dropwise to the cells and the cells were left overnight in the incubator at 37°C , 5% CO_2 . Cells were selected for puromycin resistance by the addition of fresh media containing 2 μ g/ml puromycin for 24 hours only.

Table 2.5 List of plasmids used for transient transfection and their target sequence

Plasmid	Sequence targeted/expressed
pSPCas9(BB)-2A-puro-p53-guide1	TCGACGCTAGGATCTGACTG
pSpCas9nickase(BB)-2A-puro-p53-guide2	AGGAAACATTTTCAGACCTA
pSpCas9n(BB)-2A-puro-PIP4K2A-exon10-left arm	CGCAGGAGGTTACGTCAAGATG
pSPCas9n(BB)-2A-puro-PIP4K2A-exon10-right arm	GCCTCGGACAGACATGAACAT
pSpCas9(BB)-2A-puro-PIP4K2B-exon10-left arm	AGGTAGAAGAGAACTACGTC
pSpCas9(BB)-2A-puro-PIP4K2B-exon10-right arm	CTGGATATGGGGTCGGGGAT
pcDNA3-PIP4K2A-mAID-P2A-Clover	mini-AID sequence with <i>PIP4K2A</i> homology sequence
pcDNA3-PIP4K2B-AID-P2A-Clover	AID sequence with <i>PIP4K2B</i> homology sequence

2.4.1.6 Generating lentiviral supernatant

HEK293FT cells were plated 1×10^6 in a single well of a 6-well plate. Virus was generated using lentiviral vector pLKO.1 containing a short hairpin RNA (shRNA)-targeting sequence or pLenti vector containing sgRNA of a target sequence. The plasmids were co-transfected with lentivirus packaging plasmids encoding GAG-Pol and VSVG in a ratio of 4:2:1 respectively, with a total of 2 μ g DNA. The

DNA mixture was made up to 94 μ l with serum-free DMEM without antibiotics and incubated for 10 minutes at room temperature. 6 μ g of PEI was added and the transfection mixture was incubated for another 20 minutes before added to the HEK293FT cells. After 24 hours of incubation, the media containing virus particles were harvested and transferred into a 15 ml falcon tube. The media was replaced with fresh DMEM media containing 10% FBS and 1% pen/strep. The viral harvest was repeated on days two and three and the collected viral supernatants were pooled together. Viral supernatants were filtered through a 0.45 μ m membrane filter prior to transduction. The remaining viral supernatant was stored at -80°C until required.

2.4.1.7 Generating retroviral supernatant

Plat-E cells were plated at 1×10^6 per well of a 6-well plate. 2 μ g of retroviral plasmid was transfected to generate virus of interest. Transfection and viral supernatant collection were conducted as the lentiviral method above.

2.4.1.8 Cell transduction and antibiotic selection

U2OS cells were plated at 2.5×10^5 per well of a 6-well plate and left overnight at 37°C , 5% CO_2 . The media was removed and replaced with 2 ml of fresh media containing 0.5 ml of the collected viral supernatant and 5 $\mu\text{g}/\text{ml}$ of polybrene. In the control well, the media was replaced with fresh media. The cells were left for one night at 37°C , 5% CO_2 before the media was replaced with 2 ml of complete media and left for another day. Cells were selected for puromycin resistance by the addition of fresh media containing 2 $\mu\text{g}/\text{ml}$ puromycin for two to three days.

Table 2.6 List of mammalian expression vectors used for retroviral transduction

Plasmid	Sequence expressed
RT3-HA-Tir1	TIR1 <i>Oryza Sativa</i> coding sequence
pBabe-Puro-PIP4K2A	PIP4K2Ahu coding sequence

Table 2.7 List of shRNA constructs used for lentiviral transduction

shRNA	Sequence
Sh-x	CAACAAGATGAAGAGCACCAA
ShTP53	CACCATCCACTACAACACTACAT
ShPIP4K2A #1	CCTCGGACAGACATGAACATT
ShPIP4K2A #2	CCAGCATCGTTCTAGCTATTT
ShPIP4K2B #1	CAAACGCTTCAACGAGTTTAT
ShPIP4K2B #2	GCAAGATCAAGGTGGACAATC

Table 2.8 List of CRISPR SgRNA constructs used for lentiviral cell transduction

SgRNA	Sequence
SgPIP4K2A #1	GGGGTAAACCACTCGGTAAG
SgPIP4K2A #2	AGAGGACCCTAGGTTGCCG G
SgPIP4K2B #1	CGATCCTCAGCGTCCTGATG
SgPIP4K2B #2	CCCGGAATAGCTTCACTTTC

2.4.1.9 Single colony growth

Cells were plated at 5×10^2 in a 25 cm plate and gently shaken to ensure a proper spread of the cells. The cells left to grow at 37°C, 5% CO₂ for several days until colonies can be seen from the bottom of the plate by naked eyes. Colonies were selected by marking with a marker pen and numbered accordingly. Media was removed from the plate and the cells washed once with PBS. Sterilized round filter papers, approximately 6mm in diameter were immersed in trypsin EDTA for several minutes. With sterile forceps, the immersed filter papers were transferred on top of the selected colonies, and the plate incubated at 37°C, 5% CO₂ for 5 minutes. Cells were observed under a microscope to determine whether trypsinisation had occurred. The filter papers were individually transferred to a single well of a 12-well plate containing 1 ml of media. Cells were left to grow for three days. Filter papers were removed and cell growth was monitored daily. Colonies that grew in patches were trypsinised and re-plated, and colonies that grew to confluence were transferred to a larger plate for expansion.

2.4.1.10 Generation of auxin-inducible degron (AID)-tagged U2OS cell line for conditional PIP4K protein degradation

U2OS cells were transiently transfected with CRISPR/Cas9 vector directed against the last exon (exon 10) of *PIP4K2A* or *PIP4K2B*, together with vector expressing homology directed repair sequence with AID construct as well as green fluorescent protein (GFP) (Table 2.5, Appendix C). Following 24 hours of antibiotic selection, cells were sorted by fluorescence-activated cell sorting (FACS) for GFP positive cells. The sorted cells were grown in single colonies to select for potential correct clones. Screening for correct clones that contain AID-tagged endogenous PIP4K was conducted by western blotting. Selected clones were grown and transduced with retroviral vector expressing TIR1 sequence from *Oryza sativa* under tetracycline-controlled transcriptional activation (Table 2.6).

2.4.1.11 Etoposide treatment for p53 pathway activation

Cells were plated and left overnight or until they reached 60-70% confluency. Media was removed and replaced with fresh media containing 30 μ M etoposide. Cells were left in at 37°C, 5% CO₂ for 24 hours.

2.4.1.12 Cell morphology

Cells were plated at 3×10^5 per well in a 6-well plate. Photos of cells from each well were taken using an EVOS imaging system at 10x magnification to observe cells' morphology and spreading pattern.

2.4.1.13 Cell Attachment assay

Cells were plated at 6×10^4 per well in a 6-well plate in triplicate and prepared in three sets. The plates were left in the incubator for one, two and four hours respectively. Media was removed and the cells were washed three times with PBS followed by addition of 300 μ l of 0.25% trypsin EDTA and incubated for 5 minutes at 37°C, 5% CO₂. The detached cells were resuspended in 1 ml of complete media and were counted with a haemocytometer. The percentage of cells attached was counted as a total number of cells counted over the total number of cells initially plated.

2.4.1.14 Anchorage-independent clonogenic growth assay (Soft agar)

Two layers of 1% NuSieve™ low-melting agarose in DMEM with 10% FBS and pen/strep, and 0.35% NuSieve™ low-melting agarose in DMEM with 10% FBS and pen/strep containing 15,000 cells soft agar respectively were plated in each well of a 12-well plate. The agar was first boiled in a serum-free DMEM, with concentration double of the final concentration needed. Melted agar was

kept in a 42°C incubator to maintain the agar in solution. The agar was mixed with DMEM supplemented with 20% FBS in a 1:1 ratio to get the desired final concentration of 10% FBS. The first layer (1% agarose; as above) of soft agar was created by pipetting 1 ml into each well and incubated at 4°C for 3 hours to overnight. The second layer (0.35% agarose containing 15,000 cells; as above) of soft agar was created by carefully pipetting 0.5 ml on top of the previous layer to avoid bubbles. The plates were incubated at room temperature for 20 minutes and the inter-well spaces of the plate were filled with PBS prior to incubation at 37°C to prevent the agar from drying out. The cells were grown for 15 days for U2OS, 25 days for BT474 and 7 days for HCT116 cells, before their images captured using the EVOS imaging system. Number and size of colonies were analysed by ImageJ.

2.4.1.15 Cell proliferation assay

Cells were plated at 3×10^4 per well in a 12-well plate. Four sets of plates were prepared to measure the proliferation rate for four days. After the specified time, cells were washed with 1x PBS and fixed with 4% formaldehyde for 15 minutes. Cells were washed once with water and stained with 0.5% crystal violet for 20 minutes. Excess stain was removed by washing the cells three times with water and the plate dried in a fume hood. Addition of 1 ml of 10% acetic acid to each well followed and the plate was gently shaken to dissolve the stain. A sample of 50 μ l of the solution from each well was transferred into a well of a 96-well plate containing 150 μ l of water. The OD₅₉₀ reading was measured with an optical plate reader. For day 0, the plate was processed 6 hours after the cells were plated.

2.4.1.16 Cell migration assay

Cells were grown in a 6-well plate until confluent and with a P200 pipette tip, a vertical 'wound' was created across each well by scratching the monolayer of cells. Cells were washed with 1x PBS three times to remove detached cells before supplementing with fresh serum-free media. A photo of each well was taken using an EVOS imaging system, 10x magnification at 0, 6, 12, and 24 hours. A line was drawn on each well to mark the same spot to monitor the cells. To determine the migration distance of each cell line, the width of the wound was measured using ImageJ and compared with the initial size at 0 hours.

2.4.1.17 Cell viability assay

Cells were seeded at $1-2 \times 10^4$ per well in a 96-well plate in a triplicate and incubated for 18-24 hours at 37°C, 5% CO₂. Medium was replaced with 100 μ l of media containing the appropriate drug (etoposide: 50 μ M, or erastin: 10 μ M) and incubated for 24 hours at 37°C, 5% CO₂. The medium was removed and gently washed once with 1x PBS and replaced with 100 μ l of DMEM (without

phenol red) with 1:10 of MTT (thiazolyl blue tetrazolium bromide) solution. The plate was incubated for 4 hours at 37°C, 5% CO₂ or until a precipitate could be seen. The media was carefully removed and the cells washed once with 1x PBS. Addition of 100 µl of sterilised filtered DMSO to each well was used to dissolve the formazan blue crystal by gently pipetting. The plate was then incubated at 37°C, 5% CO₂ for 15 minutes or covered with aluminium foil and shaking until the crystal dissolved. The absorbance was immediately measured at OD₅₇₀.

2.4.1.18 Senescence assay

Cells were plated at 3,000 per well in a 6-well plate and incubated overnight at 37°C, 5% CO₂. The cells were treated with 2 µM of etoposide and incubated for 48 hours at 37°C, 5% CO₂ to induce senescence, leaving one untreated well to serve as a negative control. The media was replaced and the cells remained growing for five days to develop the senescence phenotype. Cells were washed twice with 1x PBS before being fixed with 4% formaldehyde in 1x PBS for 3-5 minutes at room temperature. Cells were then washed and 2 ml of X-gal staining solution (1 mg/ml X-gal, 40 mM citric acid/sodium phosphate buffer pH 6.0, 5 mM potassium ferricyanide, 5 mM potassium ferrocyanide, 150 mM NaCl, 2 mM MgCl₂) was added. Cells were left to incubate at 37°C (without CO₂) for at least overnight or until blue staining is observable. Cells were washed with distilled water twice before viewed under an inverted bright-field microscope. The percentage of stained cells was counted. The preparation of the X-gal staining solution is based on a method previously described by Itahana, Campisi and Dimri (2007).

2.4.2 Protein Biochemistry

2.4.2.1 Immunocytochemistry

Cells were plated in a plate containing sterilised coverslip until they reached 50-60% confluency. Cells were washed with PBS twice before incubated with 4% formaldehyde for 10 minutes for fixation. Cells were then washed with PBS twice and permeabilised with 0.2% Triton X-100 for 10 minutes. Cells were incubated with 3% BSA in 1x PBS, 0.1% Tween 20 (PBS-T) and washed with 1x PBS-T twice for five minutes before primary antibody added and the cells incubated for overnight in cold room. After three times washes with 1x PBS-T, cells were incubated with Alexa Fluor conjugated secondary antibody for one hour in dark and washed twice in PBS-T and once in PBS for five minutes. Coverslip was mounted upside down on slide with a drop of Invitrogen™ ProLong™ Gold Antifade Mountant with DAPI and let to incubate overnight in the dark at 4°C before viewing under microscope.

2.4.2.2 Protein Assay

Protein quantitation was conducted using the bicinchoninic acid (BCA) protein assay method with the Pierce™ BCA protein assay kit according to the protocol provided. Briefly, samples and BSA standards were each mixed with BCA working reagent in a 96-well plate and incubated at 37°C for 30 minutes. The plate was allowed to cool to room temperature for 10 minutes before the plate was centrifuged for 1 minute at 1,000 rpm. Absorbance readings were measured at 562 nm on a plate reader.

2.4.2.3 Protein sample preparation for western blot

Lysates containing 15 to 30 µg of protein were mixed with a 3x LDS sample buffer containing 250 mM DTT and boiled at 95°C for 5 minutes. Samples were cooled to room temperature and centrifuged at 13,000 rpm for 30 seconds before being loaded on a Bis-Tris protein gel.

2.4.2.4 Western Blot

Protein sample was loaded onto a 10% or 12% acrylamide Bis-Tris gel (Table 2.9). Proteins were separated in MOPS running buffer at constant voltage (100 V) for the first 15 minutes followed by 160 V until the blue dye front reaches the bottom of the chambers using the Thermo Scientific XCell SureLock Mini-Cell chamber system. The composition of the gel is listed in table 2.4. Molecular weights were determined by comparison with SeeBlue® Plus2 Prestained Standard molecular weight marker.

Separated proteins were transferred to a nitrocellulose membrane at 65 V for 2 hours using the Transfer-Blot® cell (Biorad). At 4°C After blotting, the membrane was stained with Ponceau S to visualise protein transfer before washed with 1x PBS, 0.1% Tween 20 (PBS-T) to remove excess staining. The membrane was blocked with 5% dried skimmed milk (Marvel) in PBS-T for 30 minutes at room temperature to prevent non-specific binding. Membranes were incubated with 3 ml 3% BSA in PBS-T containing Roche western blocking reagent (1 in 50) and primary antibody overnight with rotation at 4°C. Antibodies used and their dilutions are listed in table 2.10. After overnight incubation, membranes were washed with PBS-T three times for 10 minutes before incubated with secondary antibodies conjugated to either fluorescent indicators or horseradish peroxidase (HRP), diluted in 3% BSA in PBS-T for 1 to 1.5 hours at room temperature. The membrane was washed three times with PBS-T and two times with 1x PBS for 5 minutes and the signals visualised using a LI-Cor Odyssey Infrared Imager (LI-COR Bioscience), or using chemiluminescent HRP substrate and captured using Syngene chemiluminescence imaging system.

Table 2.9 Composition of stacking and separating gel (1.0 mm) for protein electrophoresis

Stacking gel (5%)		
H ₂ O	1 ml	
1.0 M Bis-Tris HCl pH 6.5	0.67 ml	
30% acrylamide	0.33 ml	
10% APS	8 µl	
TEMED	4 µl	
Total volume	2 ml	
Separating gel	10%	12%
H ₂ O	2 ml	1.6 ml
1.0 M Bis-Tris HCl pH 6.5	2ml	2 ml
30% acrylamide	2 ml	2.4 ml
10% APS	24 µl	24 µl
TEMED	12 µl	12 µl
Total volume	6 ml	6 ml

Table 2.10 List of antibodies used and their descriptions

Antibody	Species	Dilution used	Company	Product code
Akt	Rabbit	1:3000	Cell Signalling Technology	9272
Actin clone C4	Mouse	1:10000	Millipore	MAB1501
GAPDH 14C10	Rabbit	1:3000	Cell Signalling Tech	2118
Histone H3	Rabbit	1:3000	Cell Signalling Technology	4499
p44/42 MAPK (Erk1/2)	Rabbit	1:3000	Cell Signalling Technology	4695
P53 DO1	Mouse	1:3000	Santa Cruz	SC-126
Phospho-Akt (Ser473)	Rabbit	1:3000	Cell Signalling Technology	4060
Phospho-p44/42 MAPK (Erk1/2) (Thr202/Tyr204)	Rabbit	1:3000	Cell Signalling Technology	9101
Phospho-S6 (Ser235/236)	Rabbit	1:3000	Cell Signalling Technology	2211
PIP4K2 α	Rabbit	1:3000	Cell Signalling Technology	5527
PIP4K2 α P19	Rabbit	1:3000	In-house	-
PIP4K2 β	Rabbit	1:3000	Cell Signalling Technology	9694
PIP4K2 β P6	Rabbit	1:3000	In-house	-
PTEN A2B1	Mouse	1:200	Santa Cruz	SC-7974
Uhrf1	Rabbit	1:1000	Invitrogen	PA5-29884

2.4.3 Molecular Biology

2.4.3.1 Making DH5 α competent cells

Initially, the modified Hanahan method (Sambrook and Russell, 2000) was used to prepare DH5 α competent cells and later, the modified Inoue method (Im *et al.*, 2011) was also used due to its simpler procedure; besides having a comparable transformation efficiency with the former method. Both protocols are listed below:

Modified Hanahan Method

DH5 α glycerol stock from -80°C was streaked and inoculated in 2 ml of Luria-Bertani (LB) media and the cells grew during the day at 37°C, shaking at 220 rpm. The culture was diluted into 4 tubes containing 2.5 ml of LB media and incubated overnight at 37°C, 220 rpm. The culture was diluted into 1 L (2x 0.5 L) of LB media containing 20mM of MgSO₄. The cells were grown to an OD₆₀₀ of between 0.4 – 0.6 and transferred into four sterile buckets containing 0.5 L of LB media and pelleted at 4,500 g (500 rpm in ultra-centrifuge, using JA-14 rotor) for 5 minutes at 4°C. The cell pellet of each bucket was gently resuspended in 50 ml of TFB1, making up a total of 200ml. The solution was transferred into four separate 50 ml falcon tubes and incubated for 5 minutes on ice. The cells were centrifuged as previous. The pellet was gently resuspended in 10 ml ice-cold TFB2 followed by a further 30 ml and the tube swirled. The cells were incubated overnight on ice at 4°C. The cellular solution was made into 200 μ l of aliquots in sterile microfuge tubes, snap-frozen in liquid nitrogen and stored at -80°C until required.

Modified Inoue Method

DH5 α glycerol stock from -80°C was streaked and inoculated in 10 ml of LB media and the cells grown overnight at 37°C, 220 rpm. The cells were diluted 100-fold (2 ml of the overnight culture in 200 ml of LB media). The cells were grown at 26°C until OD₆₀₀ reached 0.5-0.6 and the culture vessel transferred to ice for 10 minutes. Cells were harvested by centrifugation at 2,500 g for 10 minutes at 4°C. The medium was discarded and the residual media removed by placing the open centrifuge bottles upside down on paper towels for 2 minutes. A vacuum aspirator was used to remove any remaining drops adhering to the bottles' walls or necks. Cell pellets were re-suspended into 50 ml (1/4 of the original volume) of ice-cold Inoue buffer. The cells were gently resuspended by swirling, transferred to a 50 ml falcon tube and stored on ice for 5 minutes. The cells were harvested by centrifugation as above. The medium was discarded and removed as previous. The cell pellets were gently resuspended by swirling in 10 ml of ice-cold Inoue buffer and 0.74 ml of DMSO was added, the bacterial suspension mixed by swirling and incubated on ice for 10 minutes. The cellular solution was made into 200 μ l of aliquots in sterile microfuge tubes, snap-frozen in liquid nitrogen and stored at -80°C until required.

2.4.3.2 DNA gel purification

Digested DNA run on a 0.8 – 1.0% agarose gel-TAE buffer were viewed under the UV illuminator and the DNA band of interest cut out using a clean scalpel, taking as little gel as possible and placed in a 1.5 ml Eppendorf tube. The gel was weighed and three times the gel weight (mg) in volume (μ l) of QG buffer was added to the gel piece. The tube was incubated at 37°C with shaking

for 10 minutes or until the gel fully dissolved. 2-propanol was added to the solution as 1x volume of the original weight. The solution was transferred to a spin column and centrifuged at 11,000 rpm for 1 minute in a microcentrifuge. To the column, 750 μ l of wash buffer for gel extraction was added and centrifuged at 11,000 rpm for 1 minute in a microcentrifuge. The elution buffer pre-warmed at 60°C and 35-50 μ l was added to the centre of the column and the tube left to incubate at room temperature for 2-5 minutes. The tube was centrifuged at 10,000 rpm for 2 minutes in a microcentrifuge. To estimate the concentration of the purified DNA product, 5 μ l was run on a 10% agarose gel alongside a standard DNA with known concentration.

2.4.3.3 Oligo annealing

In a thin-walled PCR tube, the following reaction was prepared:

- 1) 7 μ l H₂O
- 2) 1 μ l 10x T4 ligation buffer
- 3) 1 μ l oligo forward (100 μ M)
- 4) 1 μ l oligo reverse (100 μ M)

With a thermocycler, the following annealing protocols were used:

- 1) 37°C for 30 minutes
- 2) 95°C for 5 minutes
- 3) Cooldown to 4°C @ 5°C/min

2.4.3.4 DNA ligation

10 μ l of ligation mix was prepared in a tube as follows:

- 1) 1 μ l of 10x ligation buffer
- 2) 30 ng of digested vector
- 3) 1 μ l of annealed oligo (diluted 1:200)
- 4) 1 μ l of T4 DNA ligase 3 u/ul
- 5) H₂O up to 10 μ l

The tube was incubated at room temperature for 1 hour or as recommended by the T4 ligase protocol. For bacterial transformation 5 μ l of the reaction was used.

2.4.3.5 Bacterial Transformation

An aliquot of competent cells (stored at -80°C) was thawed and stored on ice. Plasmid DNA added to 90 μ l of competent cells and incubated on ice for 20 minutes. The cells were heat-shocked

for exactly 60 seconds at 42°C. The cells were transferred to ice and allowed to cool for 2 minutes, followed by addition of 1 ml antibiotic-free LB media. The cells were incubated at 37°C with shaking at 220 rpm, for 40-50 minutes (to allow the bacteria to recover and to express the antibiotic resistance marker encoded by the plasmid). All or part of the transformed bacterial culture can be plated on agar containing the appropriate antibiotic selection. To plate all of the cultures, the cells were pelleted at 4,400 rpm for 2.5 minutes in a microcentrifuge and 1 ml of the supernatant was gently removed by pipette, leaving approximately 90 µl of media in the tube. The pellet was gently resuspended by pipetting before plating on an agar plate.

2.4.3.6 DNA plasmid miniprep

A single bacterial colony was picked and grown overnight in 5 ml of LB media containing 1µg/ml ampicillin in a shaking incubator set at 220 rpm, 37°C. The bacterial culture was centrifuged at 4,000 rpm, 4°C for 10 minutes in a microcentrifuge. The supernatant was removed and the pellet re-suspended in 250 µl of P1 buffer (50 mM Tris-HCl, 10mM EDTA, pH 8.0, 100 µg/ml RNase A) before transferred to an Eppendorf tube. Following the addition of 250 µl of P2 buffer (200 mM NaOH, 1% SDS) and the solution was quickly mixed by inverting the tube 4-6 times. The isolation was incubated for a maximum of 5 minutes at room temperature before 300 µl of P3 buffer (3.0 M potassium acetate, pH 5.5) was added and mixed by inversion four to six times. The solution was centrifuged at 13,000 rpm for 5-10 minutes in a microcentrifuge. The supernatant was transferred to a spin column and centrifuged at 11,000 rpm for 1 minute in a microcentrifuge and the flow-through was discarded. The column was washed once with 600 µl of PB buffer (5 M guanidine hydrochloride, 30% isopropanol), followed by a one-time wash with 750 µl of PE buffer (80 mM NaCl, 8 mM Tris-HCl, pH 7.5, 80% ethanol) each by centrifugation at 11,000 rpm for 1 minute each in a microcentrifuge. The column was dried to remove any remaining ethanol from the silica membrane by further centrifugation at 11,000 rpm for 2 minutes. The column was placed in a clean 1.5 ml Eppendorf tube and 50 µl of elution buffer (EB) (10 mM Tris-HCl, pH 8.0), pre-warmed to 60°C, was added to the column. The column was incubated for 5 minutes at room temperature before the column centrifuged at 10,500 for 2 minutes in a microcentrifuge. The eluted plasmid DNA was stored at -20°C.

2.4.3.7 cDNA synthesis and qPCR

RNA extraction was conducted as discussed under subheading 2.4.1.4 and the following protocol was used for cDNA synthesis and qPCR:

1. 20 μ l of reverse transcription mix for cDNA synthesis prepared according to the protocol below

Component	Each reaction
RNA	500 ng
50 mM MgCl ₂	2.2 μ l
10x reverse transcriptase buffer	2.0 μ l
10 mM dNTPs	0.25 μ l
Random Hexamer primer	1.0 μ l
RNase guard/block	0.4 μ l
Reverse transcriptase	0.5 μ l
H ₂ O	Up to 20 μ l

2. Reverse transcription was carried out using a thermocycler machine as follows:
 - 1) Incubate 25°C for 10 minutes
 - 2) Incubate 48°C for 30 minutes
 - 3) Incubate 95°C for 5 minutes
 - 4) Incubate 4°C for infinity
 - 5) End
3. The 20 μ l of cDNA was diluted with 80 μ l H₂O, whereby 5 μ l of the mix was used for qPCR. Fast 2 x qPCR Precision™ Mastermix with SYBR green was used for qPCR analysis, and the following mix was prepared:

Component	Each reaction
Forward primer (20 μ M)	0.1 μ l
Reverse primer (20 μ M)	0.1 μ l
Fast 2x qPCR Mastermix	5 μ l

4. The 5.2 μ l mix added into each well according to the planned experimental plate set up.
5. 5 μ l of the diluted cDNA added to each well accordingly.

6. Samples were analysed in triplicate and amplification conducted on Applied Biosystem SetpOnePlus™ Real-Time PCR machine with the following protocol:

Stage	Step.	Time	Temperature	Cycle
Holding	1	20 sec	95°C	1x
Cycling	2	3 sec	95°C	40x
	3	30 sec	64°C	
Melt curve (step and hold)	4	15 sec	95°C	1x
	5	1 min	60°C	
	6			
	7	Ramp to 95°C with an increment of 0.3°C per minute		
		15 sec	95°C	

7. The amplification of each mRNA was measured by the comparative Ct method normalized to GAPDH (Schmittgen and Livak, 2008; Wilcox and Hinchliffe, 2008).

Table 2.11 List of qPCR primers and their sequences

Gene	Primers	Sequences
PIP4K2A	Forward	ATGGAATTAAGTGCCATGAAAAC
	Reverse	GCATCATAATGAGTAAGGATGTCAAT
PIP4K2B	Forward	TGCATGTGGGAGAGGAGAG
	Reverse	TCTTCAGCTGTGCCAAGAAC
TP53	Forward	CCTCTCCCCAGCCAAAGAAG
	Reverse	TCTCGGAACATCTCGAAGCG
Actin	Forward	ATTGGCAATGAGCGGTTC
	Reverse	GGATGCCACAGGACTCCAT
GAPDH	Forward	CCCCGGTTTCTATAAATGAGC
	Reverse	CACCTTCCCCATGGTGTCT

2.4.3.8 Designing a single guide RNA (sgRNA) for CRISPR/Cas9

A list of possible gRNA sequences was obtained from websites that offer CRISPR guide design such as the Broad Institute GPP (<https://portals.broadinstitute.org/gpp/public/analysis-tools/sgrna-design>). The desired sequence had the NGG (PAM site) removed and a G base added in front of the sequence for POL1 activity. Appropriate restriction site sequences based on the vector were then added in front of both forward and reverse complement sequences.

2.4.4 Statistical Analysis

Data were analysed using two-way or one-way Analysis of Variance (ANOVA) with Dunnett's Multiple Comparison tests as the posthoc test unless stated otherwise. All analyses were conducted using SPSS software version 20.

Chapter 3 Role of PIP4K in T cell signalling through the PI3K/Akt/mTOR and MAPK Signalling Pathway

3.1 Introduction

Our lab has previously shown that the expression of *PIP4K2A* was higher in hematopoietic cell lines compared to cell lines derived from other tissues (Jude *et al.*, 2015). This suggested that this family of kinases plays a significant role in the hematopoietic system. We decided to further elucidate the specific role of PIP4K in immune system activity, especially in regulatory T (Treg) cells. This study is a collaboration with Dr. Alessandro Poli, a postdoctoral researcher who worked in Prof. Nullin Divecha's laboratory at the INGM in Milan.

Some of the initial findings obtained by Dr. Poli are illustrated in Figure 3.1 – 3.3 (Poli *et al.*, 2020). The project was initiated by studying the potential role of PIP4K isoforms in naïve T cells. Changes in transcription factors regulating different T helper and Tregs differentiation were carefully examined. Naïve T cells were transduced using lentivirus encoding a short hairpin RNA (shRNA) targeting *PIP4K2A*, *PIP4K2B*, and *PIP4K2C* (Figure 3.1A). GFP or mCherry fluorescent protein expression was also introduced into the vector to be used for cell sorting by FACS. The transduced cells that are either GFP or mCherry positive were then sorted by FACS before the level of *PIP4K2A*, *2B*, and *2C* mRNA was determined (Figure 3.1B). The sorted cells were used to analyse the level of several transcription factors in Naïve T cells. Depletion of the three isoforms did not result in significant changes in the level of transcription factors *T-BET* and *GATA3*, which control Th1 and Th2 differentiation respectively (Figure 3.1C & D). *PIP4K2B* and *2C* knockdown however decreased *FOXP3* mRNA, which plays a crucial role in the generation and function of Tregs (Fontenot *et al.*, 2003), whereas *PIP4K2A* knockdown did not show a similar effect. Thus, the project focused on the role of PIP4K2 β and 2 γ in Treg differentiation and function.

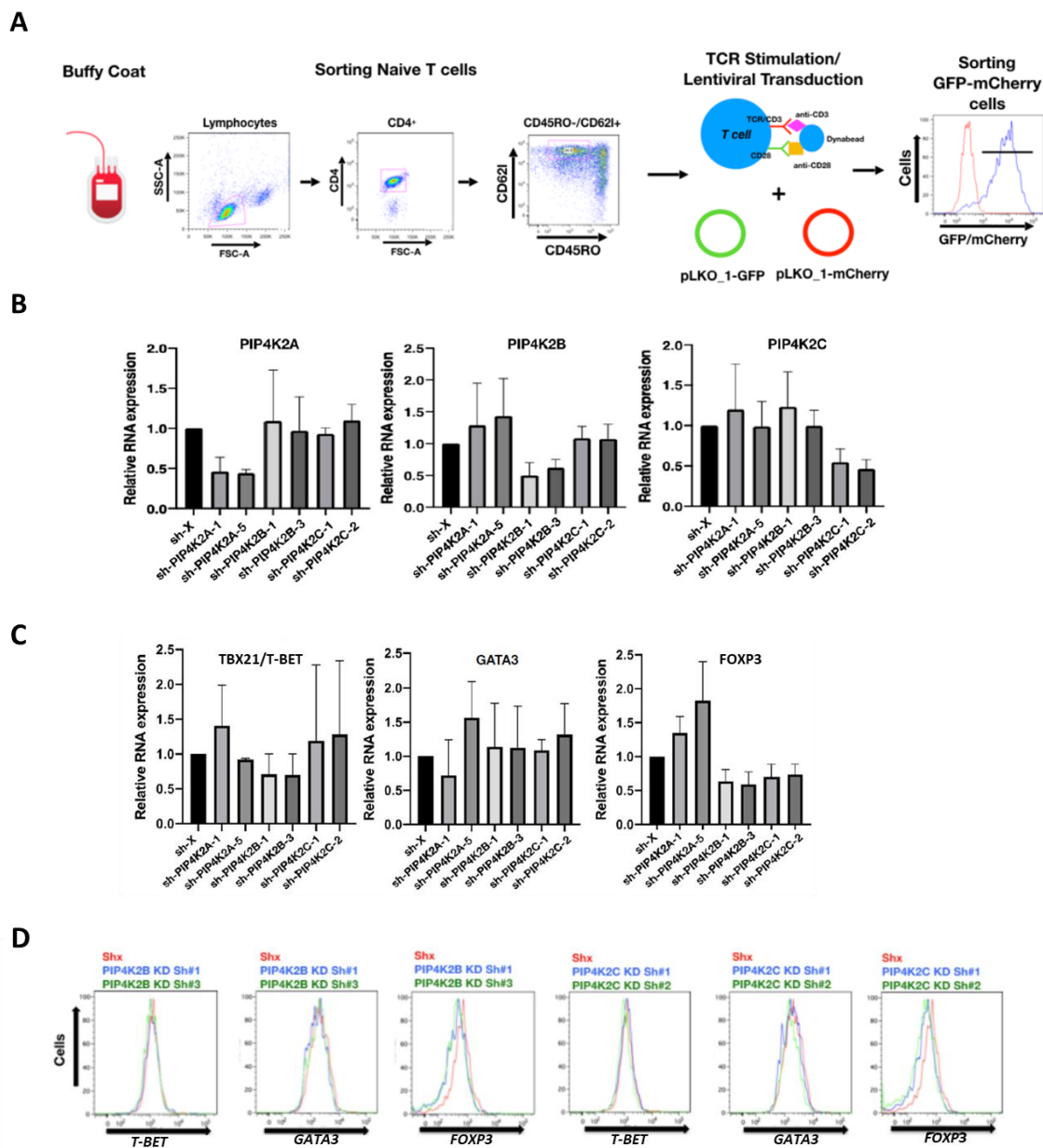


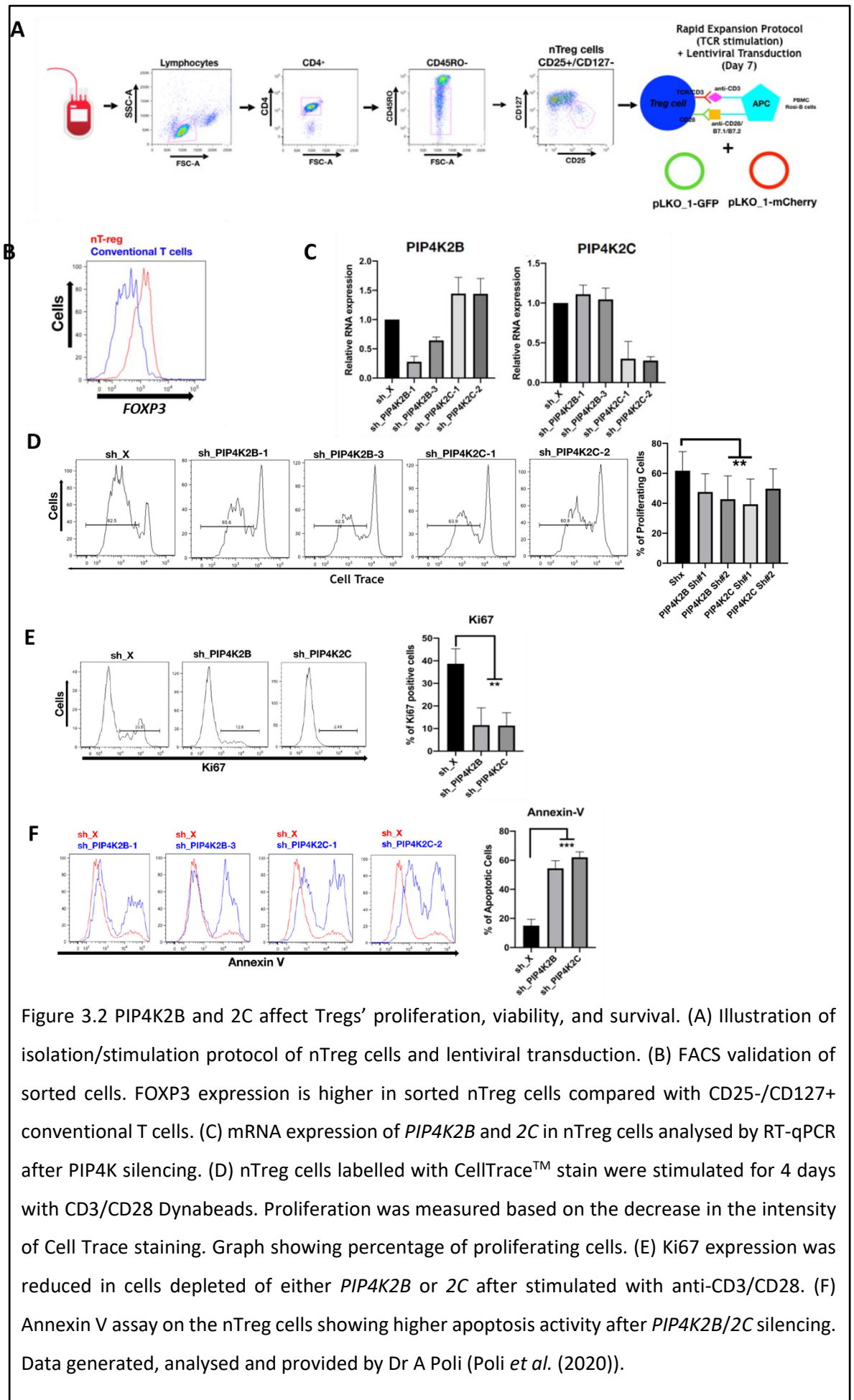
Figure 3.1 PIP4K2B and 2C affect FOXP3 expression in TCR stimulated CD4+ Naïve T cells. (A) Illustration of isolation/stimulation protocol of Naïve CD4+ T cells and lentiviral transduction. Naïve T cells were sorted and stimulated, before transduced with lentivirus encoding specific shRNA sequences targeting each isoform of PIP4K (sh-PIP4K2A, sh-PIP4K2B, and sh-PIP4K2C) or empty pLKO-1 vector as a control (sh-X). The vector also expressed fluorescent protein (GFP or mCherry) to be used for FACS sorting. (B) mRNA expression of PIP4Ks after gene silencing. (C) qPCR and (D) FACS analyses of T-BET, GATA3 and FOXP3 protein level after *PIP4K2B* and *2C* silencing. Graph showing fluorescence intensity on the x-axis and number of events (cell count) on the y-axis. Data generated, analysed and provided by Dr A Poli (Poli *et al.* (2020)).

Studying Tregs is challenging due to the scarcity of the cells, poor *in vitro* proliferation, and lack of reliable cell-surface makers (Crellin *et al.*, 2007). Most T cell subtypes exhibit T regulatory activity and the Tregs utilised in this study are the CD4⁺ T cells expressing high level of CD25⁺ and FOXP3 transcription factor; commonly used by other researchers (Reviewed in Rudensky, 2011). Natural tregs (nTregs) obtained were cell-sorted by FACS for CD4⁺/CD25⁺/CD127⁻CD45RO⁻ before being expanded by a rapid expansion protocol (REP) (Dudley *et al.*, 2003; Somerville *et al.*, 2012) (Figure 3.2A). Cells were analysed by FACS to validate the high expression of FOXP3 in sorted nTreg compared to conventional T cells (Figure 3.2B). The Tregs were transduced to knockdown *PIP4K2B* and *PIP4K2C* and the mRNA levels of the kinases were determined using RT-qPCR (Figure 3.2C). Depletion of *PIP4K2B* or *2C* attenuated cell proliferation, as shown by diminished dye dilution of cell tracer (Figure 3.2D) and reduction in staining of proliferation marker Ki67 (Figure 3.2E). In addition, there was an increase in annexin V-labelled cells which indicates an increase in cell apoptosis (Figure 3.2F).

Foxp3 expression is crucial for development and function of Tregs (Fontenot *et al.*, 2003). Therefore, lysates of Treg cells with depletion of either *PIP4K2B* or *2C* were probed with a FOXP3 antibody using western blotting to determine if there are any changes in the expression of the transcription factor. Results showed that the expression of FOXP3 is decreased in cells lacking *PIP4K2B* and *2C* compared to control cells (Figure 3.3.A). Tregs were also produced with double knockdown of *PIP4K2B* and *2C* (double sorting for cells expressing GFP and mCherry), and the mRNA expression showed a reduction in the expression of both *PIP4K2B* and *2C* (Figure 3.3B). The level of FOXP3 was compared between control, single PIP4K isoform knockdown, and double PIP4K isoforms knockdown using FACS. Depletion of both *PIP4K2B* and *2C* showed a stronger decrease in FOXP3 expression compared to the single PIP4K isoform knockdown (Figure 3.3C). Performing a suppression assay when either *PIP4K2B* and/or *2C* were depleted in Treg indicates that double depletion of *PIP4K2B* and *2C* decreases the Treg's ability to suppress T conventional cell proliferation even more than single PIP4K depletion (Figure 3.3D). The decrease in suppression activity corresponds with the stronger decrease in FOXP3 expression induced by the double knockdown of *PIP4K2B* and *2C*. Expression of CTLA-4, which is one of FOXP3 downstream targets and a fundamental immunosuppressive protein expressed by Tregs was also reduced following depletion of *PIP4K2B* or *2C* (Williams and Rudensky, 2007) (Figure 3.3E).

PI3K/Akt signalling pathway is reported to have a positive effect in regulating Tregs function (Soond *et al.*, 2012; Pompura and Dominguez-Villar, 2018). PIP4K depletion has been observed to both upregulate and downregulate the PI3K/Akt signalling pathway in different cells (Carricaburu *et al.*, 2003; Lamia *et al.*, 2004; Emerling *et al.*, 2013; Jones *et al.*, 2013), and the kinase's role in Treg cells is not yet defined. Gene set enrichment analysis (GSEA) was conducted on RNA-Seq

samples of Tregs upon depletion of *PIP4K2B* or *2C* in comparison to sh-x control (Figure 3.3F). Genes involved in the PI3K/AKT signalling pathway were shown to be deregulated in Treg cells with depleted *PIP4K2B* (left panel) and *PIP4K2C* (right panel). Therefore, we decided to further investigate the effect of PIP4K2 β /2 γ depletion in Tregs in the PI3K pathway. In addition, we also studied the activation of two other pathways involved in T cell regulation, namely the mTOR and ERK signalling pathways. Phosphorylation of Akt at Serine 473, ribosomal protein S6 at Serine 235/236, and phospho-p44/42 Mapk (ERK1/2) at Threonine 202/ Tyrosine 204 are associated with the respective proteins' activation. Therefore, Treg cell lysates were used to examine changes in these phosphorylations that serve as surrogate for PI3K/Akt, mTOR, and ERK pathway activation respectively. To ensure a better understanding of the whole project, the results presented in this chapter will also include several data from Dr. Poli.



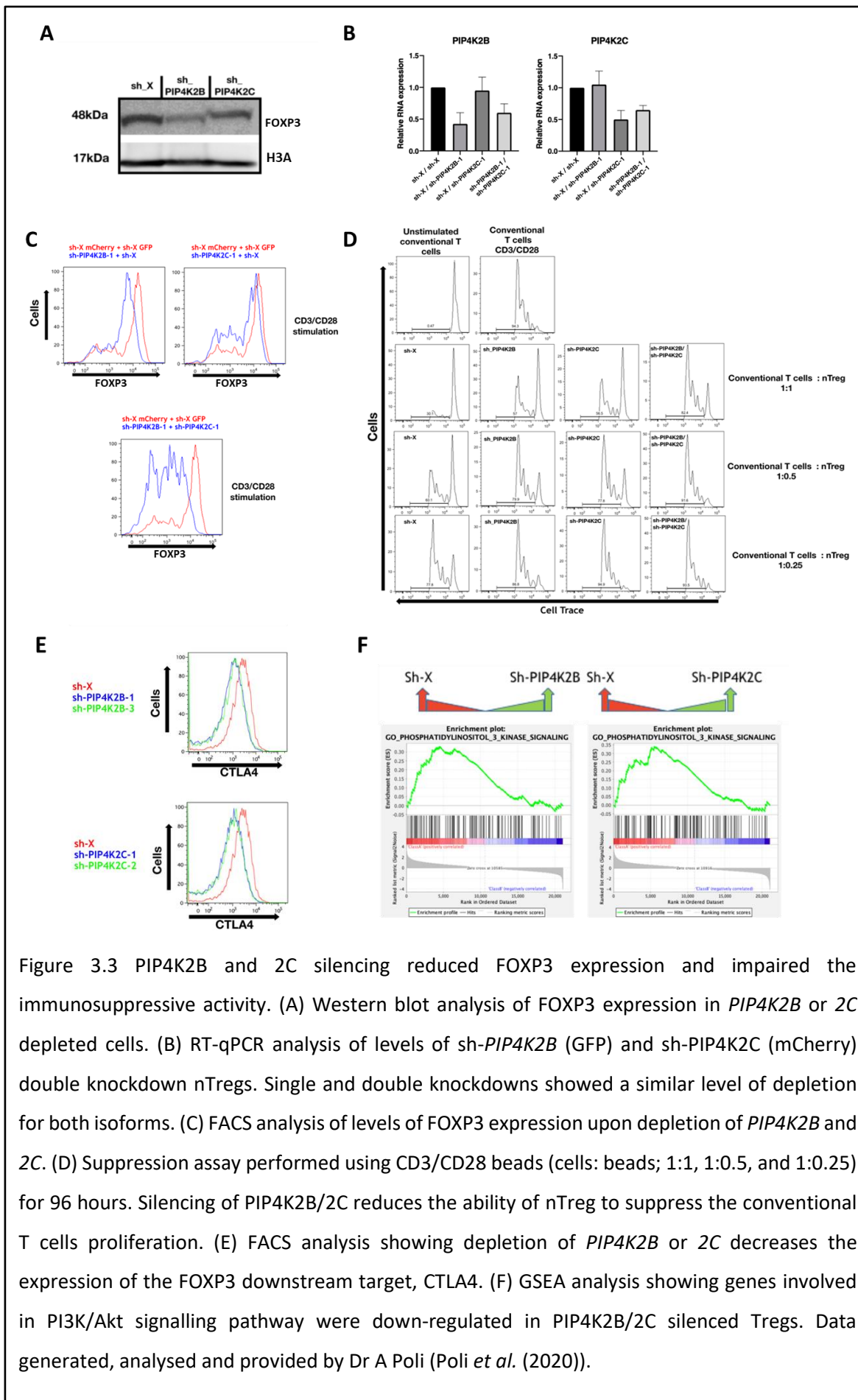


Figure 3.3 PIP4K2B and 2C silencing reduced FOXP3 expression and impaired the immunosuppressive activity. (A) Western blot analysis of FOXP3 expression in *PIP4K2B* or *2C* depleted cells. (B) RT-qPCR analysis of levels of sh-*PIP4K2B* (GFP) and sh-*PIP4K2C* (mCherry) double knockdown nTregs. Single and double knockdowns showed a similar level of depletion for both isoforms. (C) FACS analysis of levels of FOXP3 expression upon depletion of *PIP4K2B* and *2C*. (D) Suppression assay performed using CD3/CD28 beads (cells: beads; 1:1, 1:0.5, and 1:0.25) for 96 hours. Silencing of *PIP4K2B/2C* reduces the ability of nTreg to suppress the conventional T cells proliferation. (E) FACS analysis showing depletion of *PIP4K2B* or *2C* decreases the expression of the FOXP3 downstream target, CTLA4. (F) GSEA analysis showing genes involved in PI3K/Akt signalling pathway were down-regulated in *PIP4K2B/2C* silenced Tregs. Data generated, analysed and provided by Dr A Poli (Poli *et al.* (2020)).

3.2 Results

3.2.1 Effect of PIP4Ks modulation on PI3K/Akt/mTOR and ERK signalling pathway in Tregs

To examine the activation of PI3K/Akt/mTOR and ERK pathways in Tregs following T cell receptor (TCR) activation, the cells were stimulated with CD3/CD28 for the duration indicated in the figure. Cell lysates were probed with antibodies to phosphorylated Akt at Ser473, phosphorylated S6 at Ser235/236, and phospho-p44/42 Mapk (Erk1/2) at Thr202/Tyr204. Changes in the phosphorylation of these proteins were observed through immunoblotting. An increase in the phosphorylation of Akt, S6, and Erk1/2 was seen following stimulation (Figure 3.4A). Moreover, the increment of phosphorylation was also time-dependent. This observation indicates that TCR stimulation activates PI3K/Akt/mTOR and ERK pathways in nTreg. Depletion of *PIP4K2B* and *2C* attenuated the activation of Akt, S6, and Erk1/2 following 1-hour CD3/CD28 stimulation (Figure 3.4B & C). This finding suggested that both PIP4K isoforms have a positive effect on these pathways in the Tregs.

To understand whether overexpression of the PIP4K would cause the opposite effect of the gene knockdown, Tregs overexpressing *PIP4K2B* and *PIP4K2C* were produced by Dr. Poli and RT-qPCR analysis was used to determine the mRNA expression levels of *PIP4K2B* (Figure 3.5A). Cell lysates receiving similar TCR stimulation were used for immunoblotting to examine the changes in protein phosphorylation. Overexpression of the PIP4K2 β and 2 γ isoforms did not show any differences in Akt pathway activation compared to control cells (Figure 3.5B & C).

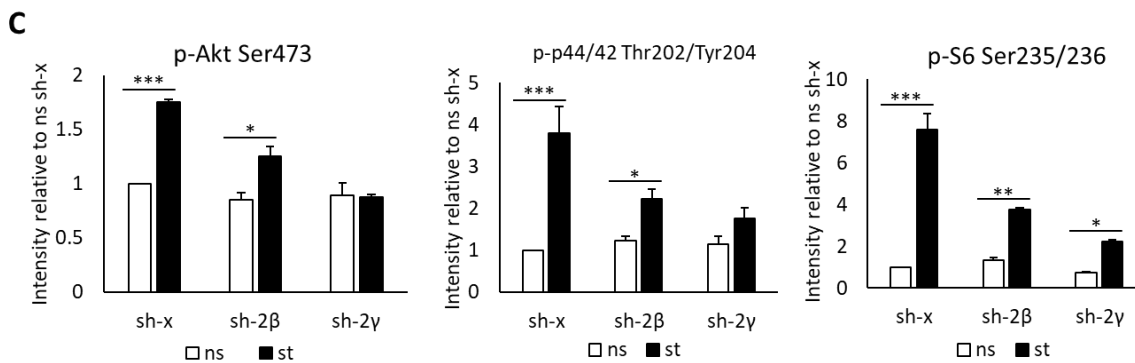
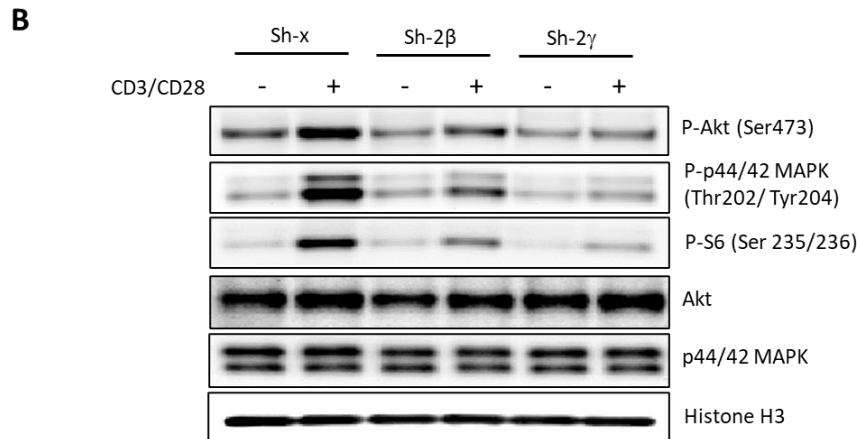
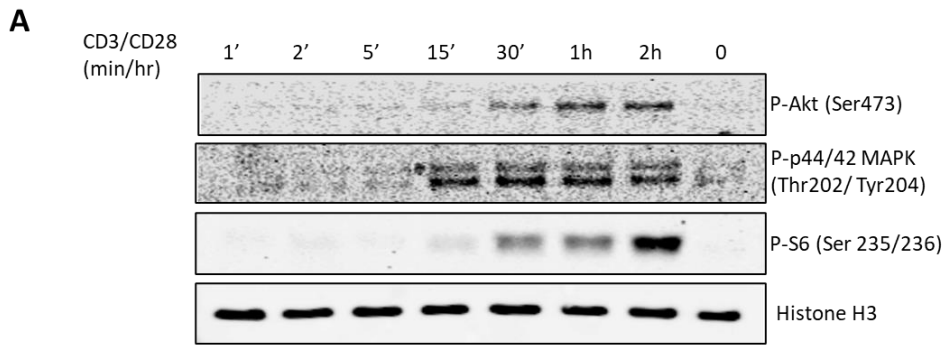
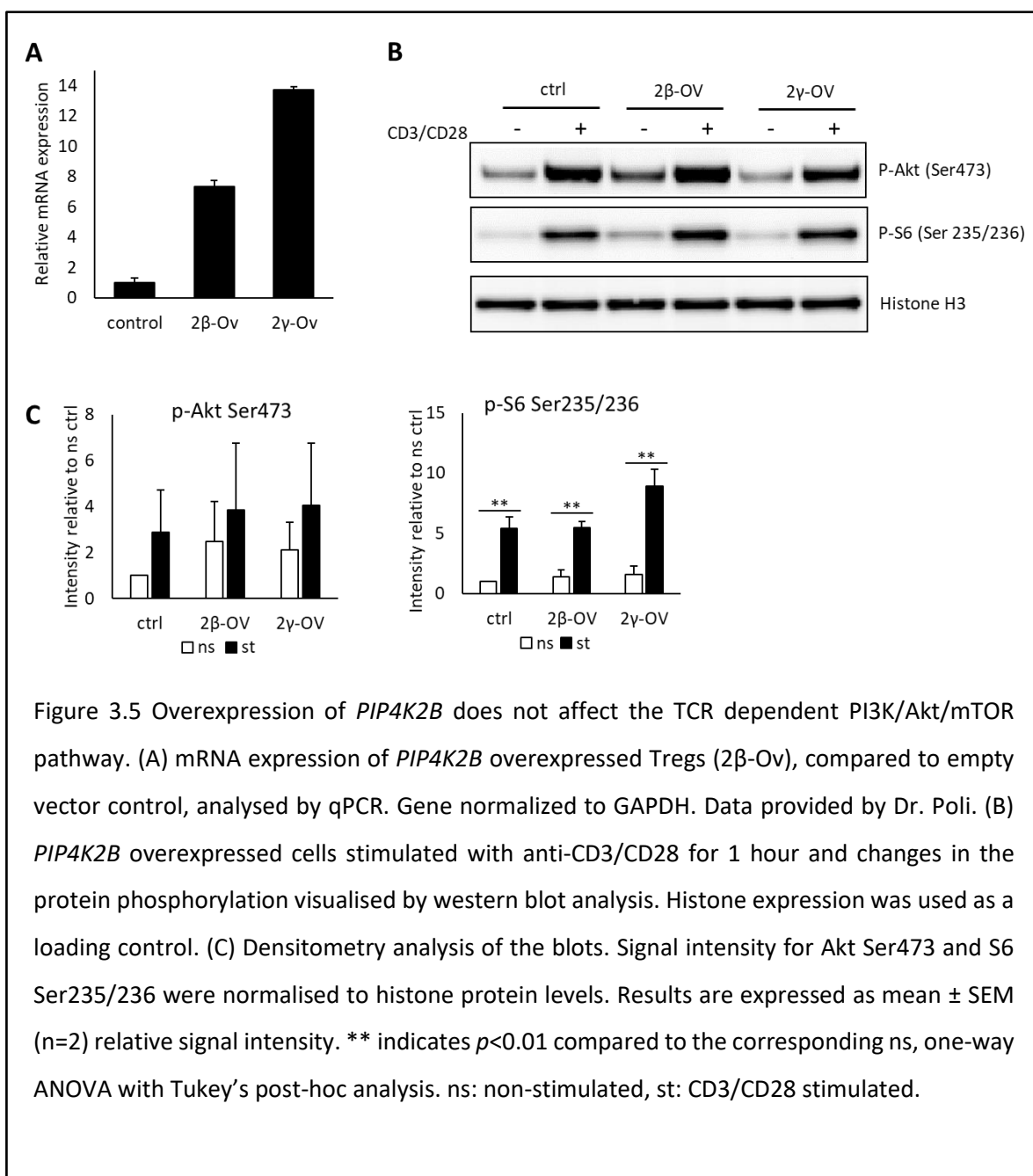


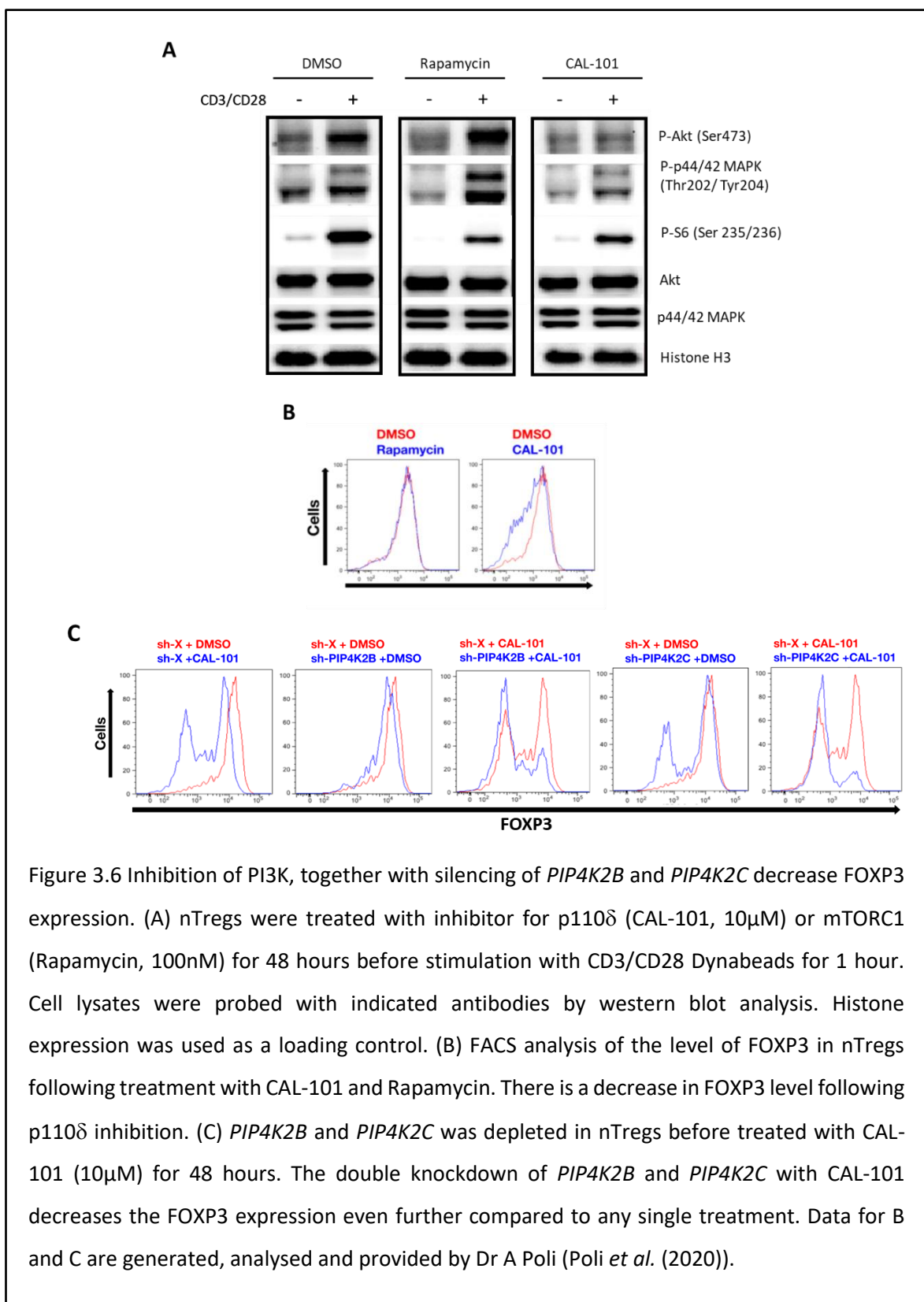
Figure 3.4 Depletion of PIP4K2B and 2C affect the TCR dependent PI3K/Akt/mTOR and ERK pathways. (A) Tregs stimulated with CD3/CD28 for the specified time and changes in the protein phosphorylation visualised by western blot analysis. Histone expression was used as a loading control. (B) PIP4K2 β or 2 γ depletion from nTreg (shown in Figure 3.2A and B) prior stimulation with anti-CD3/CD28 for 1 hour. Lysates were obtained and used for western blot analysis. Histone expression was used as a loading control. (C) Densitometry analysis of the blots. Signal intensity for Akt Ser473, S6 Ser235/236, and Erk1/2 Thr202/Tyr204 were normalised to histone protein levels. Results are expressed as mean \pm SEM (n=3) relative signal intensity. *, **, and *** indicate $p < 0.05$, 0.01, and 0.01 respectively compared to the corresponding ns, one-way ANOVA with Tukey's post-hoc analysis. ns: non-stimulated, st: CD3/CD28 stimulated.

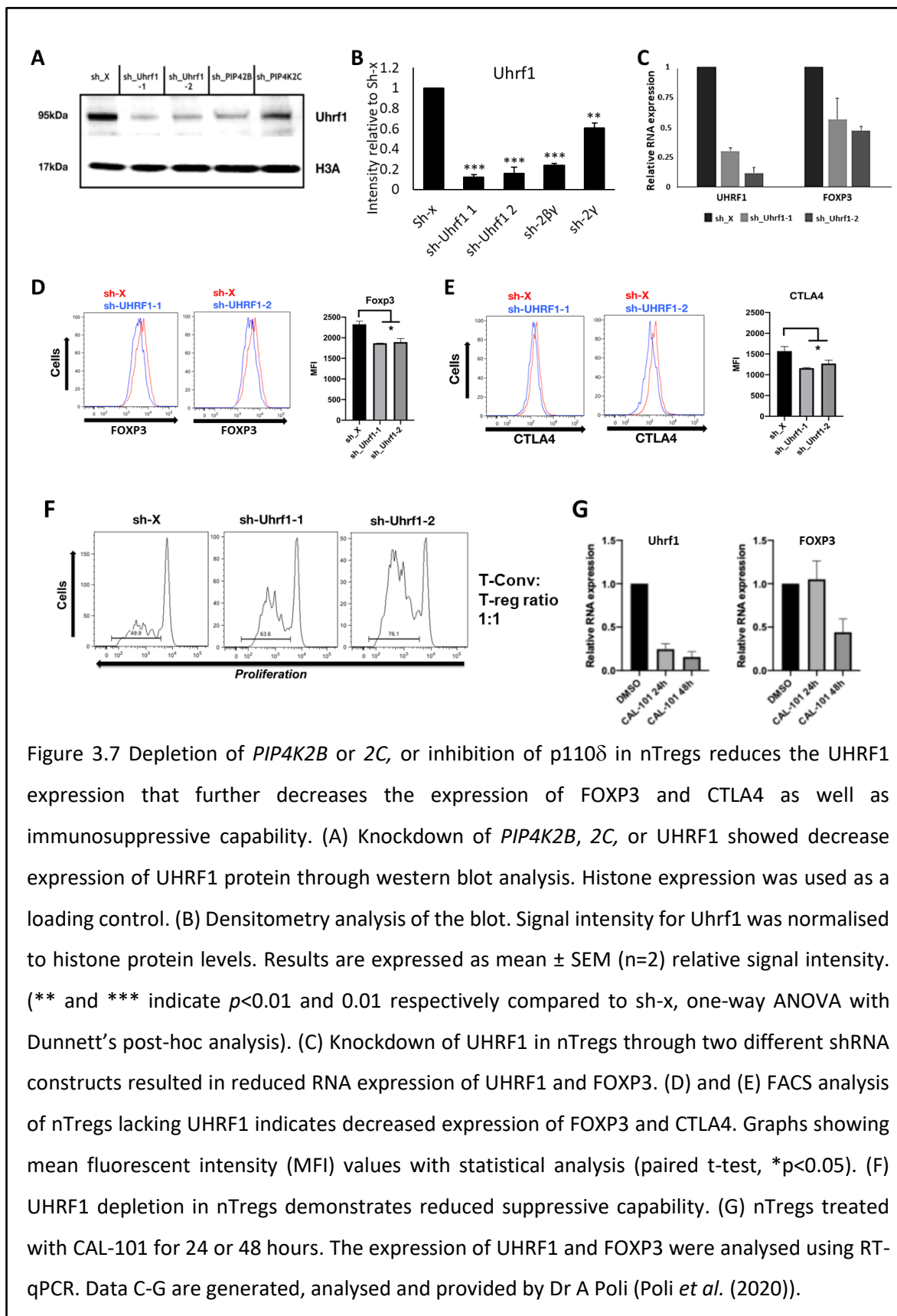


3.2.2 PIP4K2B and PIP4K2C signalling controls the expression of FOXP3 and Treg's function through PI3K/UHRF1

Data shown in Figure 3.3A and C indicate that single and double depletion of *PIP4K2B* and *2C* attenuate the level of FOXP3 protein in Tregs. To identify which pathway controls the FOXP3 expression, Tregs were either treated with PI3K p110 δ isoform inhibitor (CAL-101) or mTORC1 inhibitor (Rapamycin) before stimulation with CD3/CD28. p110 δ became the target as it is the main PI3K signal transducer in Tregs, which reported to have roles in Tregs development, differentiation, and function (Patton *et al.*, 2006; Chellappa *et al.*, 2019). Lysates of the Tregs were then obtained and the inhibition of the pathway was validated by western blot analysis. Cells treated with CAL-101 showed a slight decreased in phosphorylation of Akt compared to the DMSO control while rapamycin led to reduced S6 phosphorylation (Figure 3.6A). Level of FOXP3 protein was further analysed by FACS following the treatment with inhibitors on Tregs that showed that CAL-101 treatment decreased FOXP3 expression. However, Rapamycin showed no changes in FOXP3 protein levels in Tregs (Figure 3.6B). The combination of CAL-101 treatment together with depletion of *PIP4K2B* or *PIP4K2C* resulted in a stronger decrease in FOXP3 protein expression compared to either intervention alone (Figure 3.6C). These data suggested that PIP4K partly regulates the expression of FOXP3 through PI3K-dependent pathway, but not mTORC1.

PIP4K2B and *2C* regulation of FOXP3 expression through the PI3K-dependent pathway needs to be further defined and thus a possible additional factor involved in the downstream signalling needs to be identified. Ubiquitin-like, PHD and ring finger-containing 1 (UHRF1) is a nuclear E3-ubiquitin ligase that can be regulated through the PIP4K/PtdIns5P pathway (Gelato *et al.*, 2014). Deletion of UHRF1 in mouse Tregs was reported to decrease their proliferation and immunosuppressive function, leading to the development of spontaneous colitis (Obata *et al.*, 2014). Data showed that *PIP4K2B* or *2C* depletion in Tregs leads to reduced expression of the UHRF1 protein (Figure 3.7A & B), and therefore the role of UHRF1 in Tregs was further investigated. Depletion of UHRF1 in Tregs decreased expression of FOXP3 mRNA and protein (Figure 3.7C & D). In addition, UHRF1 silencing also reduces the expression of CTLA-4 (Figure 3.7E) and a suppression assay conducted on the UHRF1 depleted Tregs indicated that lack of UHRF1 reduced the Tregs capability to suppress conventional T cell proliferation (Figure 3.7F). To investigate the potential effect of PI3K as a downstream signalling molecule of PIP4K but upstream of UHRF1 expression, Tregs were treated with CAL-101 and the expression of UHRF1 was determined by RT-qPCR. Inhibition of PI3K δ decreased the expression of UHRF1 as well as FOXP3 (Fig 3.7G). These data are in agreement with a model that PIP4K regulates FOXP3 expression through downstream signalling of PI3K and UHRF1.





3.2.3 Pharmacological inhibition of PIP4K2 γ phenocopies *PIP4K2C* silencing.

As gene depletion of PIP4Ks impaired the PI3K/Akt pathway activation, an inhibitor for PIP4K2 γ , NIH-12848 (Clarke *et al.*, 2015) was also used in this study to determine if pharmacological inhibition of this PIP4K isoform induces similar effects. Tregs were treated with NIH-12848 before receiving CD3/CD28 stimulation. Western blot analysis showed that PIP4K2 γ inhibition significantly reduced activation of the PI3K/Akt/mTOR and ERK pathways in Tregs (Figure 3.8A & B), similarly to *PIP4K2C* knockdown. NIH-12848 treatment at 10, 20, and 30 μ M reduced cell proliferation by about 11, 29, and 39 percent respectively (Figure 3.8C). In addition, the inhibitor treatment also inhibited FOXP3 expression (Fig 3.8D) in a dose-dependent manner. These observations indicate that PIP4K2 γ inhibition phenocopies the effect of PIP4K2 γ depletion.

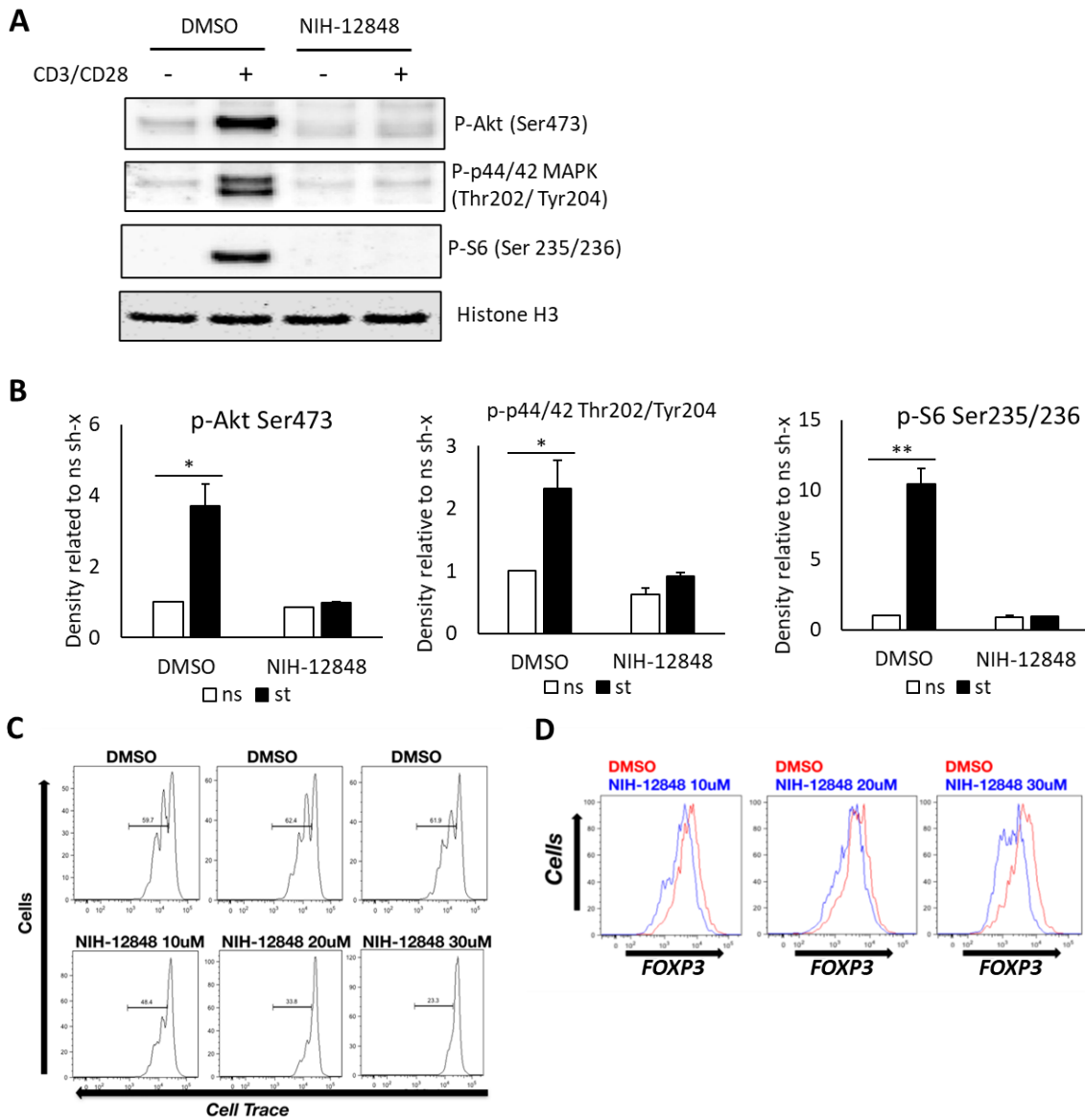


Figure 3.8 Pharmacological inhibition of PIP4K2 γ in nTregs resulted in decreased activation of the PI3K/Akt/mTOR and ERK pathways, reduced proliferation and FOXP3 expression. (A) Western blot analysis of nTregs lysates treated with PIP4K2 γ inhibitor NIH-12848 (20 μ M) or DMSO for 48 hours and subjected to CD3/CD28 coated Dynabeads stimulation for 1 hour. Histone H3 expression was used as a loading control. (B) Densitometry analysis of the blots. Signal intensity for Akt Ser473, S6 Ser235/236, and Erk1/2 Thr202/Tyr204 were normalised to histone H3 protein levels. Results are expressed as mean \pm SEM (n=3) relative signal intensity. (* and ** indicate $p < 0.05$ and 0.01 respectively compared to ns DMSO, one-way ANOVA with Tukey's post-hoc analysis. ns: non-stimulated, st: CD3/CD28 stimulated). (C & D) nTregs were treated with 10, 20, or 30 μ M of NIH-12848 for 48 hours followed by TCR stimulation. (C) Effect of PIP4K2 γ inhibition on nTreg cell proliferation. Proliferation was assessed for 4 days. (D) FACS analysis of FOXP3 level. PIP4K2 γ inhibition 30uM reduces FOXP3 level. Data C and D are generated, analysed and provided by Dr A Poli (Poli *et al.* (2020)).

3.2.4 Effect of PIP4K2B and PIP4K2C modulation on PI3K/Akt/mTOR and ERK signalling pathway in naïve T cells

PI3K/Akt/mTOR and ERK pathways in naïve T cells are required for differentiation and function of various CD4⁺ cells. While activation of PI3K/Akt and ERK are needed for effector T cell differentiation, induced Tregs (iTregs) differentiation requires minimal activation with a transient decrease in PI3K/Akt pathway activation and a reduced ERK activation (Chang *et al.*, 2012; Han *et al.*, 2012; Etemire *et al.*, 2013). Data from section 3.2.1 showed that PIP4K2 β and 2 γ depletion impacts Tregs' pathway activation. Therefore, it is important to determine the role of these kinase isoforms in naïve T cells' activity. Pathway activation of naïve T cells stimulated for different time courses were analysed by western blot. Similar to Tregs, CD3/CD28 stimulation of naïve T cells induced phosphorylation of Akt at Serine 473, S6 at Serine 235 and 236, and p44/42 Mapk at Threonine 22/ Tyrosine 24 (Figure 3.9A).

To examine the effect of PIP4K modulation on naïve T cells pathways, cells with silenced PIP4K2 β or 2 γ were produced as in Figure 3.1A and B. Similar to Tregs, the naïve T cells were stimulated and pathway activations were observed. Stimulation of TCR on naïve T cells depleted of PIP4K2 β /2 γ showed a trend towards an increase in Akt phosphorylation while depletion of PIP4K2 γ prominently increased the S6 phosphorylation (Fig 3.9B & C). Phosphorylation of Erk1/2 however, showed no clear changes, which is different from that observed in Tregs. However, the slight increase in Akt activation in naïve T cells data suggest that depletion of *PIP4K2B* and *2C* can lead to increased number of T helper cells.

To determine whether inhibiting the activity of PIP4K2 γ pharmacologically will lead to similar outcome, naïve T cells were treated with 20 μ M of NIH-12848 for 48 hours or DMSO as a control before receiving CD3/CD28 stimulation. Lysates generated from the cells were utilised for western blot analysis. Results indicated that PIP4K2 γ inhibition did not cause any effect on the expression of phosphorylated Akt, S6, or Erk1/2 upon stimulation (Figure 3.10A & B). The increased S6 phosphorylation shown by *PIP4K2C* depletion was also not observed. The difference in outcome between PIP4K2 γ pharmacological inhibition and gene depletion could be due to a difference in the level of PIP4K2 γ activity in the cells after either method of inhibition. Increasing the concentration of NIH-12848 may result in an outcome similar to *PIP4K2C* knockdown.

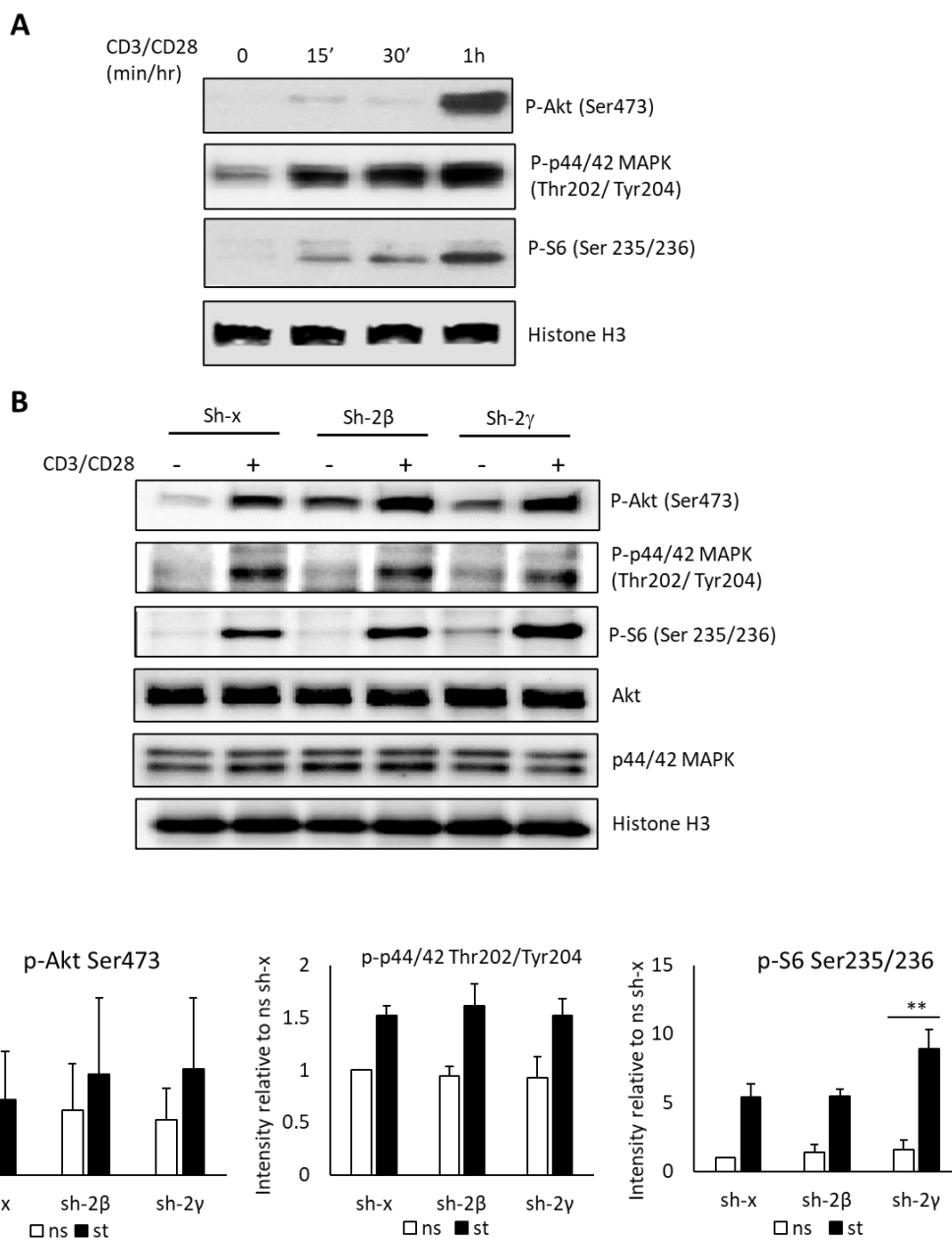
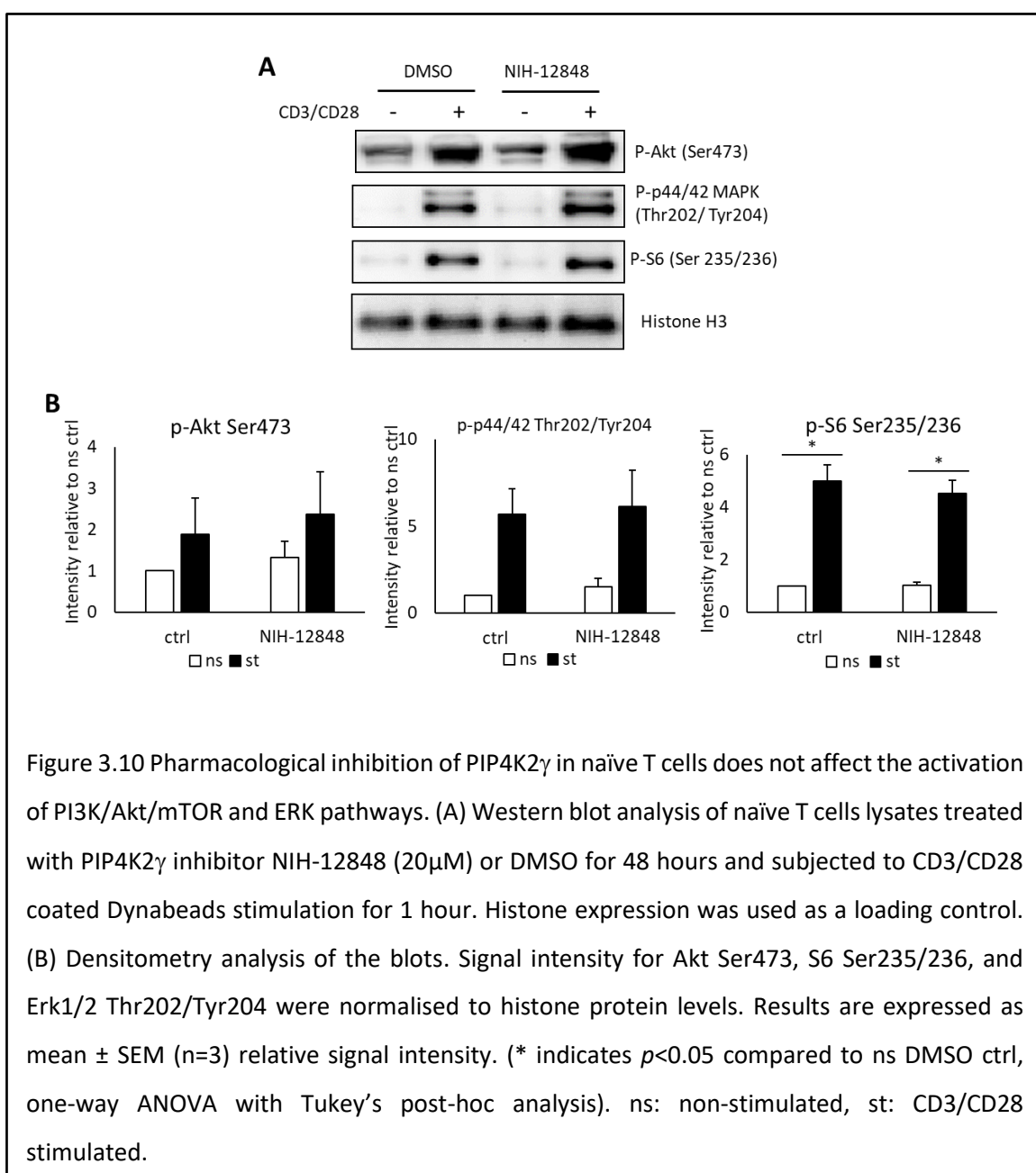


Figure 3.9 *PIP4K2B* or *2C* depletion modulates the activation of PI3K/Akt and ERK pathways in naïve T cells. (A) Western blot analysis of changes in protein phosphorylation in naïve T cells stimulated with CD3/CD28. (B) Western blot analysis of changes in protein phosphorylation in *PIP4K2B/2C* silenced naïve T cells stimulated with CD3/CD28 for one hour. Histone expression was used as a loading control. (C) Densitometry analysis of the blots. Signal intensity for Akt Ser473, S6 Ser235/236, and Erk1/2 Thr202/Tyr204 were normalised to histone protein levels. Results are expressed as mean \pm SEM ($n=2$) relative signal intensity. (** indicates $p<0.01$ compared to the corresponding ns, one-way ANOVA with Tukey's post-hoc analysis). ns: non-stimulated, st: CD3/CD28 stimulated.



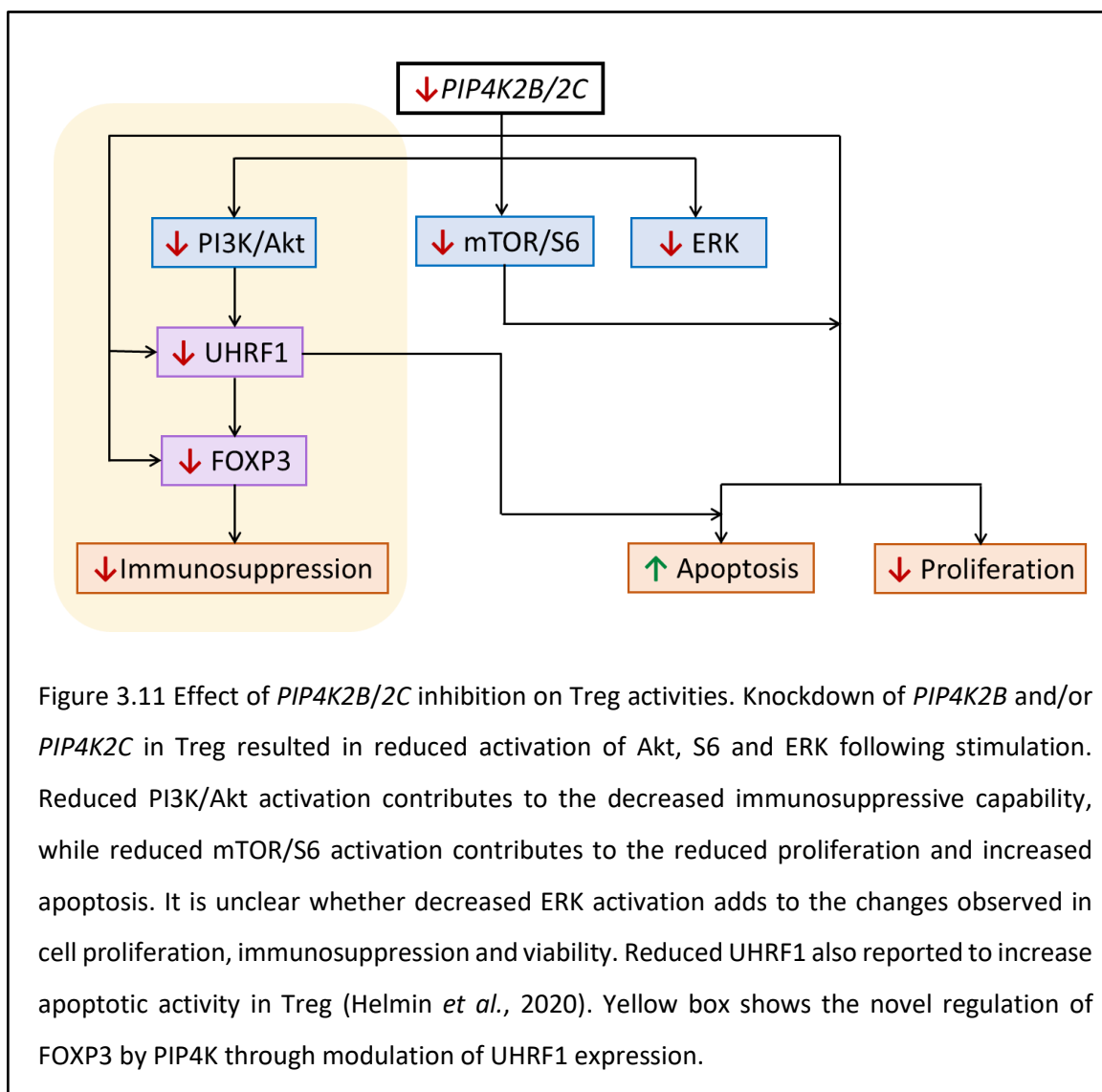
3.3 Discussion

3.3.1 PIP4K depletion modulates Tregs and Naïve T cells signalling and activity

Our data showed that depletion of PIP4K2 β or 2 γ has a negative effect on Tregs suppressive function, proliferation, and survival. Depletion of *PIP4K2B* or *2C* in Tregs causes downregulation of *FOXP3* and CTLA-4 (Poli *et al.*, 2020), which are crucial for Tregs immunosuppressive activity (Williams and Rudensky, 2007; Klocke *et al.*, 2017). Decreased expression of these genes indicated that *PIP4K2B* or *2C* depletion abrogates the suppressive activity of Tregs. *PIP4K2B* or *2C* knockdown also attenuates the activation of PI3K/Akt/mTOR and ERK pathways following TCR stimulation. Therefore, PIP4K is suggested to regulate Tregs through these pathways. Inhibition of PI3K and Akt was previously shown to attenuate Tregs proliferation and suppressive activities (Abu-Eid *et al.*, 2014), and adding ERK inhibitor into a melanoma treatment regime also stimulated antitumor activity in part through decreasing Tregs number (Hu-Lieskovan *et al.*, 2015).

Our data further reveal how PIP4K signalling regulates FOXP3 expression and Treg activity. Treatment of Tregs with a PI3K δ or mTORC1 inhibitor showed that activation of PI3K, but not mTOR stimulates FOXP3 expression. Our findings support previous studies showing that inhibition of the PI3K p110 δ inhibits Tregs suppressive function (Patton *et al.*, 2006; Ali *et al.*, 2014; Chellappa *et al.*, 2019). In addition, we showed that CAL-101 treatment reduced FOXP3 expression and together with the depletion of either *PIP4K2B* or *2C*, FOXP3 expression was further reduced. The potentiation effect shown by the simultaneous administration could be due to PIP4K effect on ERK pathway on top of PI3K/Akt pathway inhibition.

Another protein found to be involved in Tregs modulation by PIP4K signalling is UHRF1 that regulates gene expression by recruiting the methyltransferase DNMT1 to modify chromatin structure (Bostick *et al.*, 2007). *PIP4K2B* and *2C* knockdown led to a reduction in UHRF1 expression, while depletion of UHRF1 by shRNA in Tregs phenocopied the depletion of PIP4K isoforms. The cells also showed a lower expression of FOXP3 and CTLA-4 and exerted reduced suppressive function. Moreover, inhibition of PI3K also reduced the expression of UHRF1 similar to PIP4K knockdown. It has also been reported that the deletion of UHRF1 in mice leads to decreased proliferation and functional maturity of Tregs (Obata *et al.*, 2014). PIP4K regulates PtdIns5P and PtdIns5P modulates UHRF1 by binding to a poly basic region to control the localisation of UHRF1. PtdIns5P appears to act as a positive allosteric regulator of UHRF1 (Gelato *et al.*, 2014). Although no direct connection between PIP4K depletion and downregulation of UHRF1 had been reported so far, our observation suggests that PIP4K regulates Tregs activity through PI3K and its downstream signalling of UHRF1 which modulates the expression of FOXP3 (Figure 3.11).



Similar to Tregs, activation of the PI3K/Akt and ERK pathways were also observed in naïve T cells following TCR stimulation. Modulation of PIP4K2 β and 2 γ in naïve T cells however showed different effects in the activation of pathways compared to Tregs. PIP4K2 β depletion resulted in a slight increase in the PI3K/Akt/mTOR pathway while PIP4K2 γ silencing leads to increased mTOR activation with no effect on ERK phosphorylation. Activation of PI3K/Akt/mTOR and ERK pathways in naïve T cells are necessary for the development of T helper cells (Chang *et al.*, 2012; Han *et al.*, 2012; Liu *et al.*, 2013; Pennock *et al.*, 2013). Therefore, current observations suggest that depletion of *PIP4K2B* or *2C* in naïve T cells might have a positive impact on helper T cell activity through PI3K/Akt/mTOR activation, despite not showing any effect on the expression of transcription factor T-bet or GATA3. It is interesting that depletion of *PIP4K2B* or *2C* in naïve T cells negatively affects expression of Tregs transcription factor but shows a positive effect on pathway activation that

benefit the development of helper T cells. These observations suggest that PIP4K depletion plays multiple roles in naïve T cells that might be coordinated to enhance the immune response.

Data from this study demonstrated the contradicting roles of PI3K pathway activation in Tregs development and homeostasis. Soond *et al.* (2012) attempted to elucidate the discrepancies by addressing the role of PI3K activation on different stages of Treg differentiation and maintenance separately. PI3K activation in Treg during thymic development and *in vitro* differentiation can lead to nuclear exclusion of transcription factor Foxo. Foxo was found to directly bind to Foxp3 and is necessary for Foxp3 expression (Harada *et al.*, 2010; Ouyang *et al.*, 2010). Therefore, attenuation of the PI3K pathway may facilitate the differentiation process. However, PI3K activation is necessary for Treg homeostasis since both TCR and IL-2 signals which control Treg number and expansion require downstream activation of PI3K (Soond *et al.*, 2012). Different stimulation used in a study also needs to be carefully considered as it could result in different responses. For example, Tregs exhibit lower Akt and ERK phosphorylation compared to Tconv cells upon TCR stimulation (Yan *et al.*, 2015) and this lower phosphorylation response was not observed following Treg stimulation by cytokines. Therefore, a detailed description of the experiments and the cells being used are necessary in order to progress our understanding of Tregs signalling.

In this study, depletion of the PIP4K isoforms showed a more robust effect in Tregs compared to naïve T cells. Tregs were reported to have a higher susceptibility towards PI3K/Akt inhibitor (Abu-Eid *et al.*, 2014; Chellappa *et al.*, 2019), and less sensitive TCR activation compared to conventional T cells (Yan *et al.*, 2015). Tregs have also been reported to express a higher level of PTEN compared to the CD25⁻ cells (Strauss *et al.*, 2009), which might explain why Tregs are more sensitive to PIP4K depletion which reduced Akt activation even further, rather than overexpressed PIP4K that may increase Akt activation. However, it is too early to suggest PTEN as the sole reason while PTEN is also involved in controlling other complex protein phosphatase activity (Li *et al.*, 1997).

Overall findings on PIP4K signalling indicate that PIP4K2 β and 2 γ positively affect the pathways in Tregs while showing the opposite effect in naïve T cells. Low PI3K/Akt/mTOR and ERK activations following PIP4K depletion in Tregs suppressed the proliferation and suppressive activity. In contrast, depletion of PIP4K2 β and 2 γ in naïve T cells could suppress their differentiation into FOXP3⁺ iTregs, while increasing the development of other T conventional cells. These findings could partly explain the previous observation on the effect of PIP4K2 γ deletion in mice (Shim *et al.*, 2016), since mice lacking PIP4K2 γ exhibited increased inflammation activity alongside an increased T helper cell population and decreased Tregs population. Taken together, this study suggested that the silencing of PIP4K2 β and 2 γ could cause hyperimmune response partly due to the downregulation of Tregs activity and differentiation. Pharmacological inhibition of PIP4K2 γ also

confirmed the outcomes shown by gene depletion, which suggests that PIP4K is a good target for therapeutic intervention to suppress Tregs immunosuppressive activity. One limitation faced in this study was the low number of CD4⁺ CD25⁺ FOXP3⁺ Tregs obtained that made it difficult to conduct additional western blot experiments to study the pathways in greater detail. However, the data obtained is already helpful to understand a bigger picture of how PIP4K affects the immune system through Tregs. More pre-clinical research is required to understand the role of PIP4K in other T cell types in order to confirm the suitability of modulating PIP4K in managing immune-related disorders.

Chapter 4 Different Methods of Manipulating P53 and PIP4K in Tumour Cells

4.1 Introduction

A previous study showing a synthetic lethal interaction between PIP4K and p53 in cancer cells (Emerling *et al.*, 2013) has brought new hope for potential new therapeutic strategies for cancers with loss of p53 function, which accounts for more than 50% of total cancers. The study reported that depletion of PIP4K2 α and 2 β in a p53 inactivated cancer cell line impaired tumour growth. In *TP53* deleted mice, depletion of *PIP4K2A/2B* also led to a significant reduction in tumour formation with increased survival from tumour-dependent death, which also suggests the presence of a synthetic lethal interaction between p53 and PIP4Ks (Emerling *et al.*, 2013). However, the *in vitro* evidence came from a single cancer cell line with a unique *TP53* mutation, and the effect seen in mice could be a result of other physiological factors such as increased tumour surveillance activity of the immune system. Therefore, it is too early to extrapolate the synthetic lethal phenomenon between p53 and PIP4K as a universal cell-autonomous effect. Thus, the second part of this project aims to reveal if there is a synthetic lethal interaction between loss of p53 and loss of PIP4K activity that can be exploited as a potential therapeutic in cancer, and if so, to find the potential mechanism that underlies this interaction. To answer this question, the expression of *TP53* and *PIP4K* were modulated in the human cell lines U2OS, BT474, and HCT116, which derived from osteosarcoma, ductal breast carcinoma, and colorectal carcinoma respectively. For this project, the *TP53* gene was depleted using shRNA or CRISPR/Cas9 gene editing. *PIP4K2A* and *2B* expression was depleted using three different methods: (1) shRNA, (2) CRISPR/Cas9, and (3) auxin-inducible degron (AID). These methods target RNA, DNA, and the protein respectively. It is hoped that modulating protein expression with different techniques will prevent us from relying on data based on one method while further validating any result.

4.2 Results

4.2.1 P53 modulation in cells

4.2.1.1 Generation of *TP53* knockdown cells through shRNA method

Knockdown of *TP53* in U2OS cells was achieved through lentiviral transduction of the cells with virus particles containing short hairpin RNA (shRNA) targeting *TP53* for RNAi-mediated gene knockdown. The virus was produced from pLKO.1 derivative plasmid with a U6 promoter to drive shRNA synthesis and SV40 promoter to drive GFP expression for selection (Figure 4.1A). Cells were sorted for GFP positive cells by FACS following transduction. To identify the effectiveness of the gene knockdown and how it affected the p53 downstream activity, cells were treated with DNA-damaging agent etoposide to induce DNA damage. In cells with functioning p53, DNA damage will cause p53 stabilisation followed by activation of its downstream transcription genes such as p21, PUMA and TIGAR that leads to growth arrest or apoptosis; a process that is absent in p53-null cells (Itahana and Itahana, 2018). In this project, the expression of p53 and its downstream targets were observed through western blot and qPCR analysis (Figure 4.1B & C). P53 was still expressed at a lower amount in the knockdown cells and qPCR analysis showed a 70% knockdown of *TP53*. Knockdown of *TP53* also reduced the etoposide-induced p53 activation pathway as demonstrated by the lower level of p53 and p21 protein induction compared to p53 wild type cells. Furthermore, the induction of mRNA expression of p53 downstream targets p21, PUMA, and TIGAR was also slightly reduced following 24 hours of etoposide stimulation (Figure 4.1C).

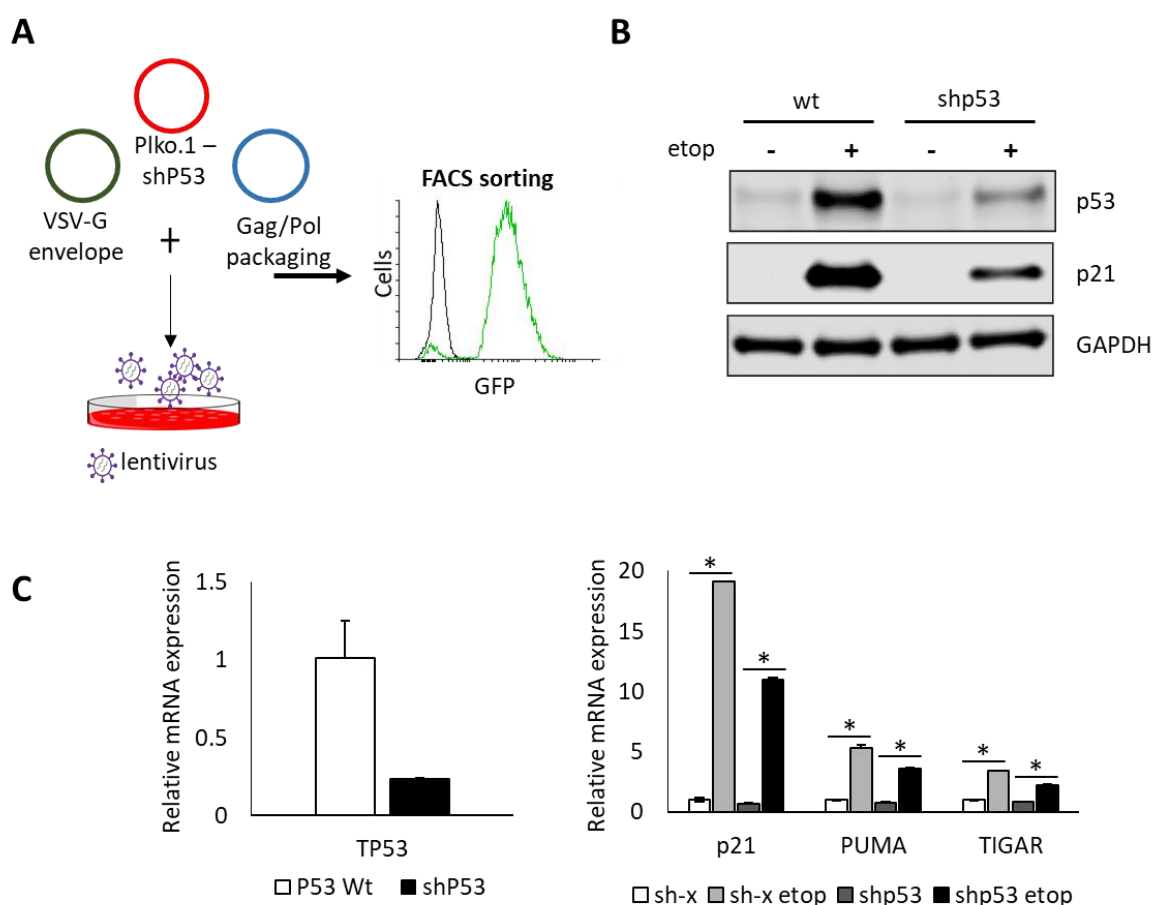
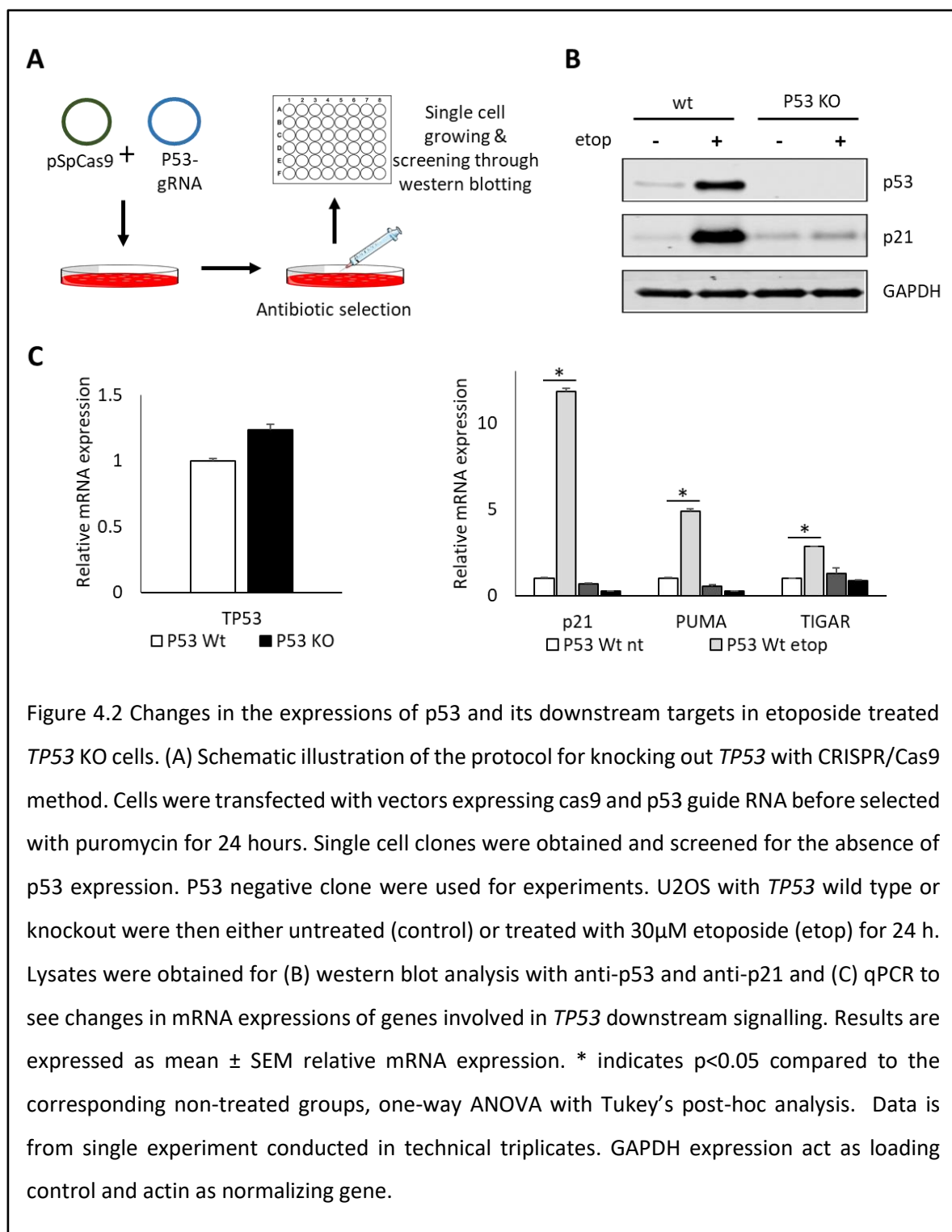


Figure 4.1 Changes in p53 and expression of its downstream targets in etoposide treated *TP53* knockdown U2OS cells and its downstream signalling. (A) Schematic illustration of the protocol used to knockdown *TP53* in cells. Lentivirus containing the shRNA sequence for *TP53* was transduced into cells. Viral particles were generated in HEK293FT cells using pLKO-based vector and plasmid encoding VSV-G for envelope and GAG/pol for viral packaging. Cells were FACS sorted for a positive GFP signal and used for experiments. Cells with *TP53* wild type (wt) or knockdown (KD) were either untreated (control) or treated with 30 μ M etoposide (etop) for 24 h. (B) Western blot analysis of p53 and P21 upon etoposide stimulation in cell lysates. GAPDH expression was used as a loading control. (C) *TP53* baseline mRNA level (left) and relative mRNA expressions of *TP53* and its downstream signalling following etoposide stimulation (right). Results are expressed as mean \pm SEM relative mRNA expression. * indicates $p < 0.05$ compared to the corresponding non-treated groups, one-way ANOVA with Tukey's post-hoc analysis. Experiment was conducted in technical triplicates and represents three independent experiments ($n=3$). Actin expression was used as a normalizing gene.

4.2.1.2 Generation of *TP53* knockout cells through CRISPR/Cas9 method

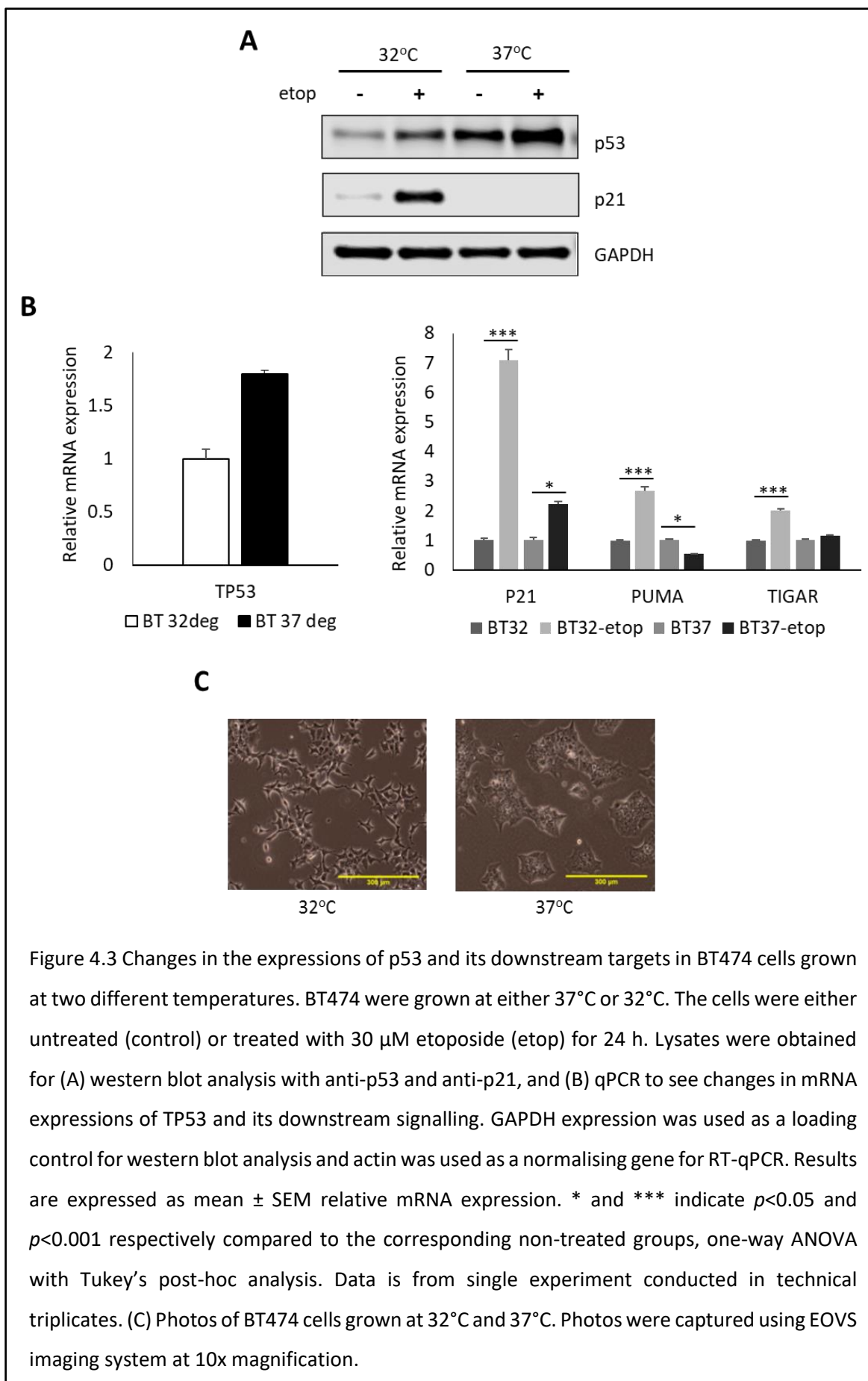
CRISPR/Cas9 gene editing was used to generate *TP53* knockout U2OS cells (Figure 4.2A). Briefly, cells were transiently transfected with a CRISPR/Cas9 plasmid containing a guide sequence targeting the *TP53* gene at nucleotides 47 to 67. After selection with puromycin for 24 hours, single colonies were isolated and grown in a 96-well plate. Several colonies were treated with etoposide to study the induction of p53 and its downstream targets and were screened by western blot analysis. Clone 13 (containing the correct knockout) was studied for changes in protein and mRNA expressions of *TP53* and its downstream target compared to control (Figure 4.2B & C). Expression of p53 and p21 in *TP53* KO cells were dramatically reduced following etoposide stimulation compared to p53 wild type cells (Figure 4.2B). *TP53* mRNA was expressed comparably in wild type and knockout cells, suggesting a frameshift or a missense mutation is responsible for the loss of p53 protein. Induction of mRNA encoding P21, PUMA, and TIGAR were almost totally attenuated following etoposide treatment (Figure 4.2C). The expression of p53 and p21 following *TP53* knockout were much lower compared to the previous *TP53* knockdown cells (Figure 4.1B), with a more dramatic reduction of p21 and PUMA induction. This indicates that the total loss of p53 protein from gene deletion exerts a stronger effect than gene knockdown.



4.2.1.3 P53 activities and mutation in BT474 cells

Human ductal breast carcinoma cell line BT474 possesses a temperature-sensitive mutation (E285K) in the p53 gene, causing a wild-type conformation if grown at 32°C and a mutant conformation of p53 at 37°C with reduced transcriptional activity (Jia *et al.*, 1997; Müller *et al.*, 2005). Although p53 was not directly manipulated per se in this experiment, the cells were grown at the two different temperatures and activation of the p53 activity through etoposide treatment was observed (Figure 4.3). As observed in previous studies, at 32°C the p53 pathway was activated following etoposide treatment, as shown by the increase in the protein and mRNA expression of p53 and its downstream target (Figure 4.3A & B). Whereas, at 37°C the p53, which is in a mutated condition, failed to exert a normal downstream response towards the DNA-damaging process. Despite the high basal p53 expression, further induction of expression after etoposide treatment led to a higher expression of p53 but without P21 expression observed, which indicates that mutant p53 has lost its ability to induce downstream target.

Changes in the cell morphology following the alteration in p53 activity were also observed (Figure 4.3C). At 32°C, BT474 had an elongated and spiky appearance, a characteristic of basal epithelial cells grown in 2D culture (Holliday & Speirs 2011). In contrast at 37°C, they adopt a cobblestone shape that is more characteristic of luminal-like epithelial cells. This change in phenotype, however, was not observed in a previous study (Christgen *et al.*, 2012).

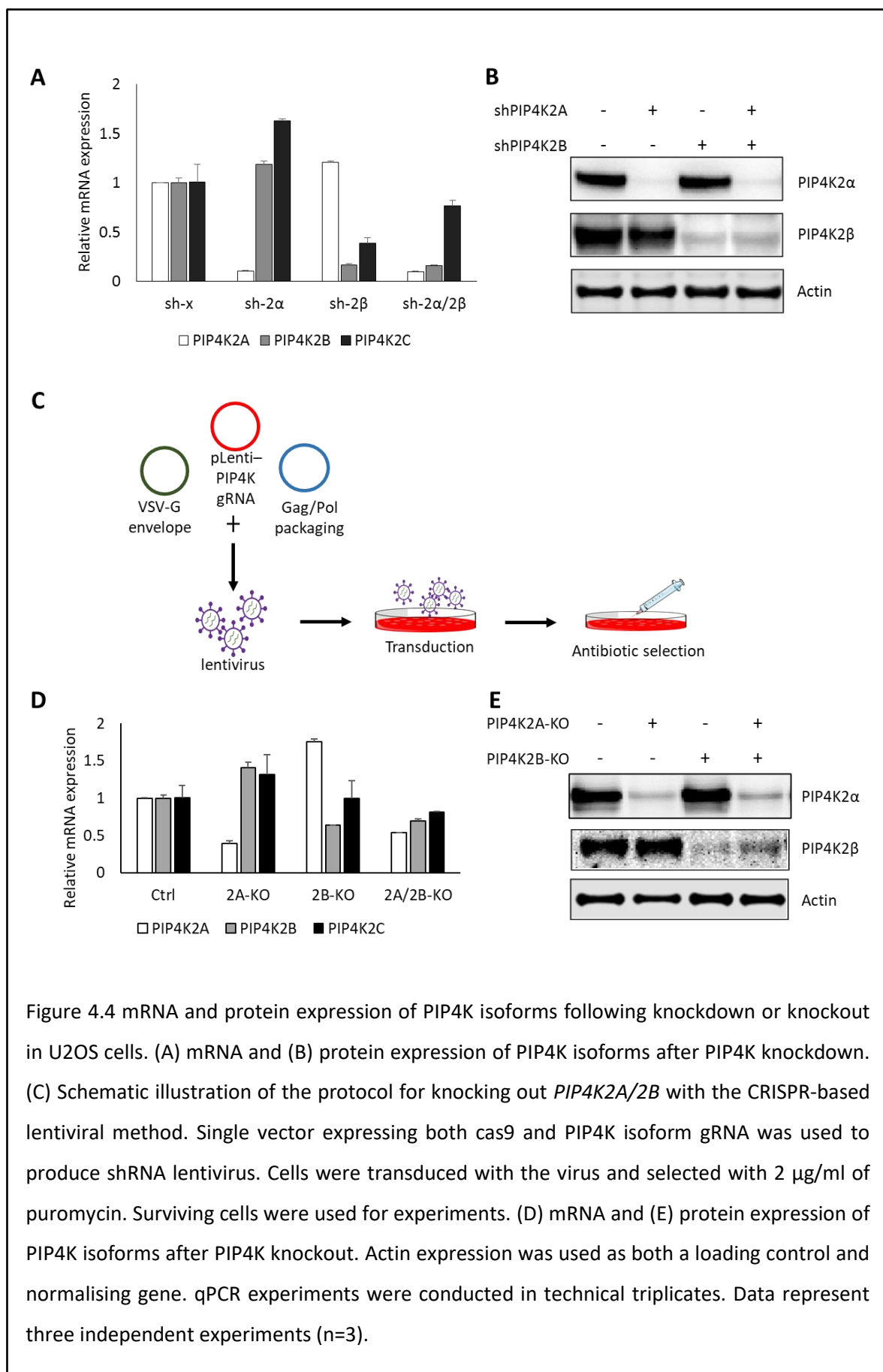


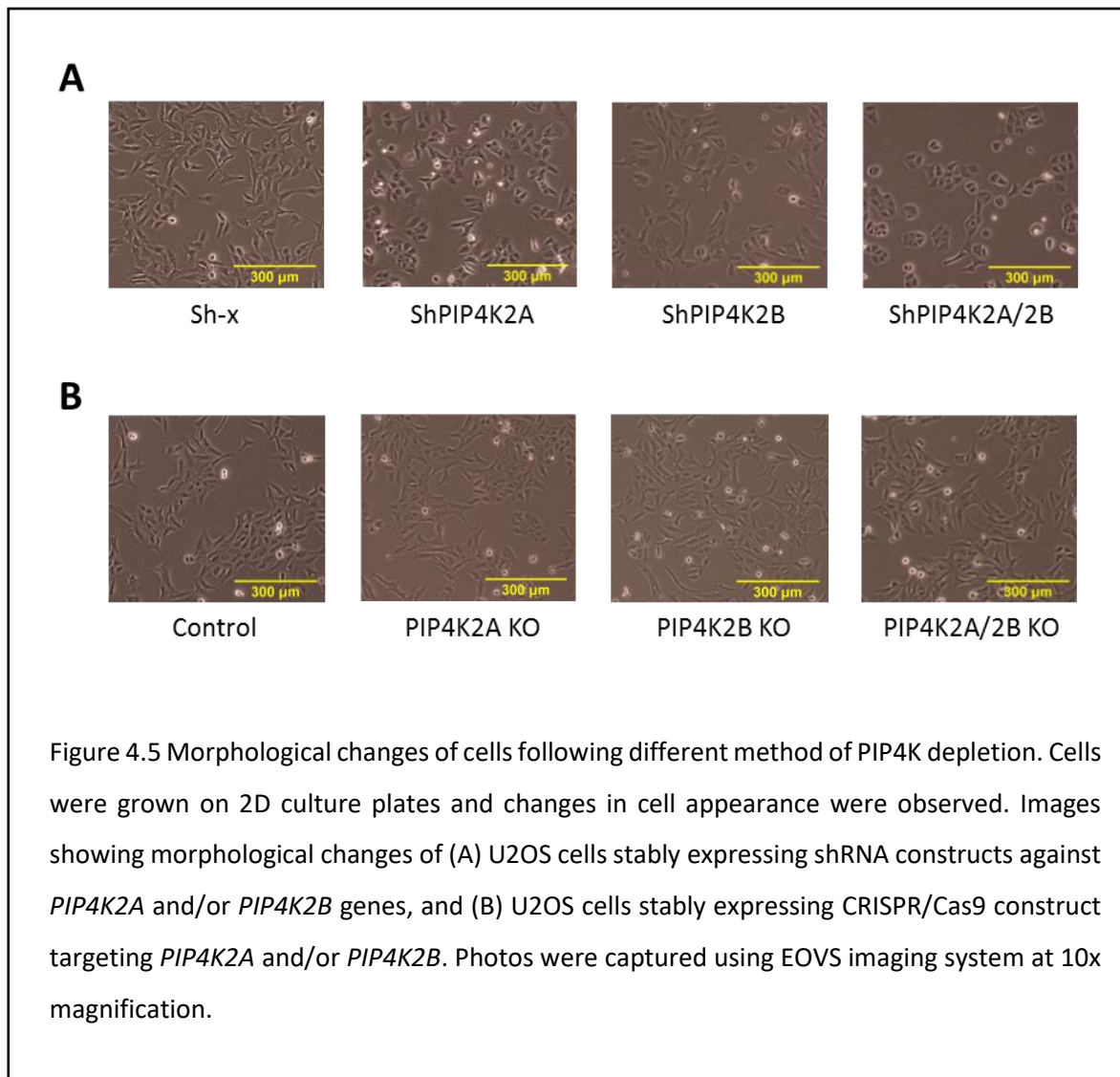
4.2.2 Generation of PIP4K depleted cells through shRNA and CRISPR/Cas9 methods

To study a synthetic lethal interaction, the expression of PIP4K2 α and 2 β isoforms were silenced in cells containing p53 depletion using knockdown or knockout approaches. PIP4K isoforms were silenced either individually or simultaneously. To achieve PIP4K2 α and/or 2 β knockdown, human osteosarcoma cell line U2OS was infected with virus particles containing shRNA constructs targeting each isoform. The protocol used is the same as previously described for sh-p53 cells. The CRISPR/Cas9 method was also used to produce cells with *PIP4K2A* and/or *2B* knockout. However, the approach used was slightly different than the deletion method used for *TP53*. Single lentiviral plasmid system with pLentiCRISPR backbone (Shalem *et al.*, 2014) was used to produce lentivirus particles containing Cas9 and a PIP4K sgRNA construct with a puromycin selection marker. Similar to shRNA, HEK293 FT cells were used to produce the viral supernatant. The virus was transduced into the cells and after selection with puromycin, the cells were screened by western blot analysis and used for experiments. Thus, instead of cells selected from single clone, whole population of antibiotic selected cells was utilised for experiments. Figure 4.4 illustrates the mRNA and protein expression of PIP4K2 α /2 β following both depletion methods.

Depletion of PIP4K by shRNA reduced gene expression by 70-80% compared to a control vector transduction which was reflected by a strong reduction in protein expression (Figure 4.4A & B). CRISPR-based lentiviral gene knockout also caused a reduction in the gene expression of the targeted PIP4K, which ranged from 20-50% knockdown compared to the control (Figure 4.4C & D). CRISPR/Cas9 utilises the non-homologous end joining (NHEJ) repair mechanism after a DNA double strand break to generate a genetic knockout. The repair mechanism often introduces various kinds of insertion/deletion (indel) mutations in the cell pool. This resulted in a mix of long and short mRNA sequences that could not be detected by the RT-qPCR primers and therefore showed a higher gene expression compared to shRNA. This observation, however, is different compared to the knockout method used to delete *TP53* whereby no changes in mRNA expression were observed (Figure 4.2C). As *TP53* knockout cells were grown from a single cell, the whole cell population had a uniform indel; such as a frameshift mutation. The expression of PIP4Ks after Cas9-targeting was also strongly reduced compared to the control (Figure 4.4E).

Prominent changes in cell morphology were observed following PIP4K modulation, particularly the 2 α isoform. *PIP4K2A* knockdown caused a significant alteration in the cell morphology, in which the cells seem to adopt a more rounded shape compared to the elongated control cells (Figure 4.5A). This phenotype was also more obvious in the double isoform knockdown and was independent of the presence or absence of *TP53*. However, these changes were not observed in the cells with PIP4K knocked out using plentiCRISPR (Figure 4.5B).





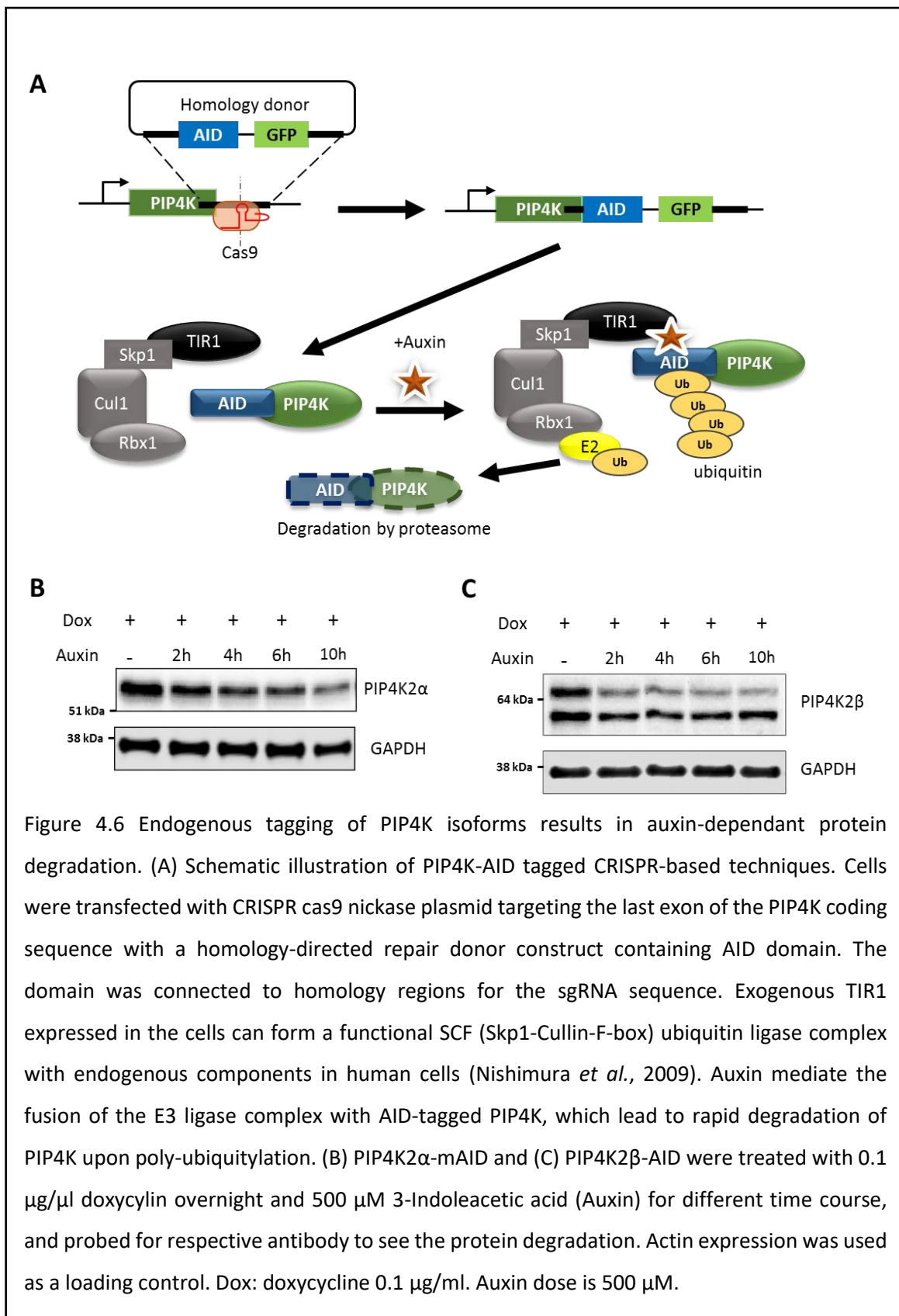
4.2.3 Generation and characterisation of auxin inducible degron (AID)-tagged PIP4K for protein degradation

An additional approach used in this study to reduce PIP4K2 α and 2 β expression is a conditional depletion system adopted from a unique plant-specific degradation mechanism, which utilises an auxin inducible degron (AID). This method requires tagging the endogenous PIP4K isoforms with an AID domain, and exogenously expressing the TIR1 E3 ligase, which in the presence of the auxin leads to the degradation of the AID-tagged protein (Nishimura *et al.*, 2009). Initially, U2OS cells were co-transfected with the CRISPR/Cas9 nickase plasmid containing the guide sequence targeting the final exon of the *PIP4K* coding sequence, and a donor construct containing the AID sequence (Figure 4.6A). Endogenous *PIP4K2A* gene was tagged with mini-AID (mAID) sequence, an 8 kDa minimal domain derived from the full-length 25 kDa AID, to produce mAID-

tagged PIP4K2 α . Endogenous *PIP4K2B* gene of U2OS cells was also tagged with AID sequence, and the cells expressing PIP4K2 β -AID used for this project were already available in our lab and were tagged with the full-length AID structure. The AID construct was also fused to a kanamycin/neomycin resistant marker; porcine teschovirus-1 2A (P2A), and GFP (Appendix C). Cells were plated at low density to pick single cell clones that were screened by western blot analysis.

Correctly identified clones were transduced with pRetro-Tet-On plasmid to stably express doxycycline-inducible TIR1. The AID-TIR1 clones were treated with doxycycline and auxin to activate the system and degrade the protein of interest. Figure 4.6B & C show the degradation of the tagged protein following the addition of 0.1 μ g/ml doxycycline and 500 μ M auxin (Natsume *et al.*, 2016). The PIP4K2 α protein degradation started after 2 hours of auxin treatment and continued with a longer exposure (Figure 4.6B). PIP4K2 β showed a stronger degradation following 2 hours of auxin treatment compared to the 2 α (Figure 4.6C). However, there were two bands of PIP4K2 β -AID cells observed on the blot. The first band appeared above the 64 kDa marker which is close to the estimated 73 kDa size, and a second band below the 64 kDa marker. The smaller size bands showed a weaker degradation compared to the top bands. A possible explanation for this observation will be discussed in the discussion section.

It is also crucial to assess to what extent each of the three methods can deplete protein levels. To compare the efficiency of these three methods, samples from each of the methods, U2OS cells transduced with shRNA for *PIP4K2A*, lentivirus for CRISPR-*PIP4K2A*, and auxin treated PIP4K2 α -mAID cells, were run on a single bis-Tris protein gel. A similar PIP4K2 β isoform depletion set was also run. Figure 4.7A & B illustrate the differences in PIP4K expression across the three different methods. The knockdown and knockout methods had a comparable efficiency of protein removal. These results also demonstrate that in both AID-tagged PIP4K2 α and 2 β , no endogenous PIP4K2 α or 2 β can be viewed, which might indicate homozygous knockout. However, in comparison to the endogenous PIP4K level, the AID-tagged PIP4K level for both isoforms was conspicuously low and even after 24 hours of auxin treatment, the proteins were still present. To identify whether AID-tagging also affected transcription of the kinases, RT-qPCR was conducted. The mRNA expressions of both PIP4K isoforms in their corresponding AID-tagged cells were comparable, if not slightly higher compared to wild type cells (Figure 4.7C). This suggested that the low protein expression of AID-tagged cells was not due to low mRNA level.



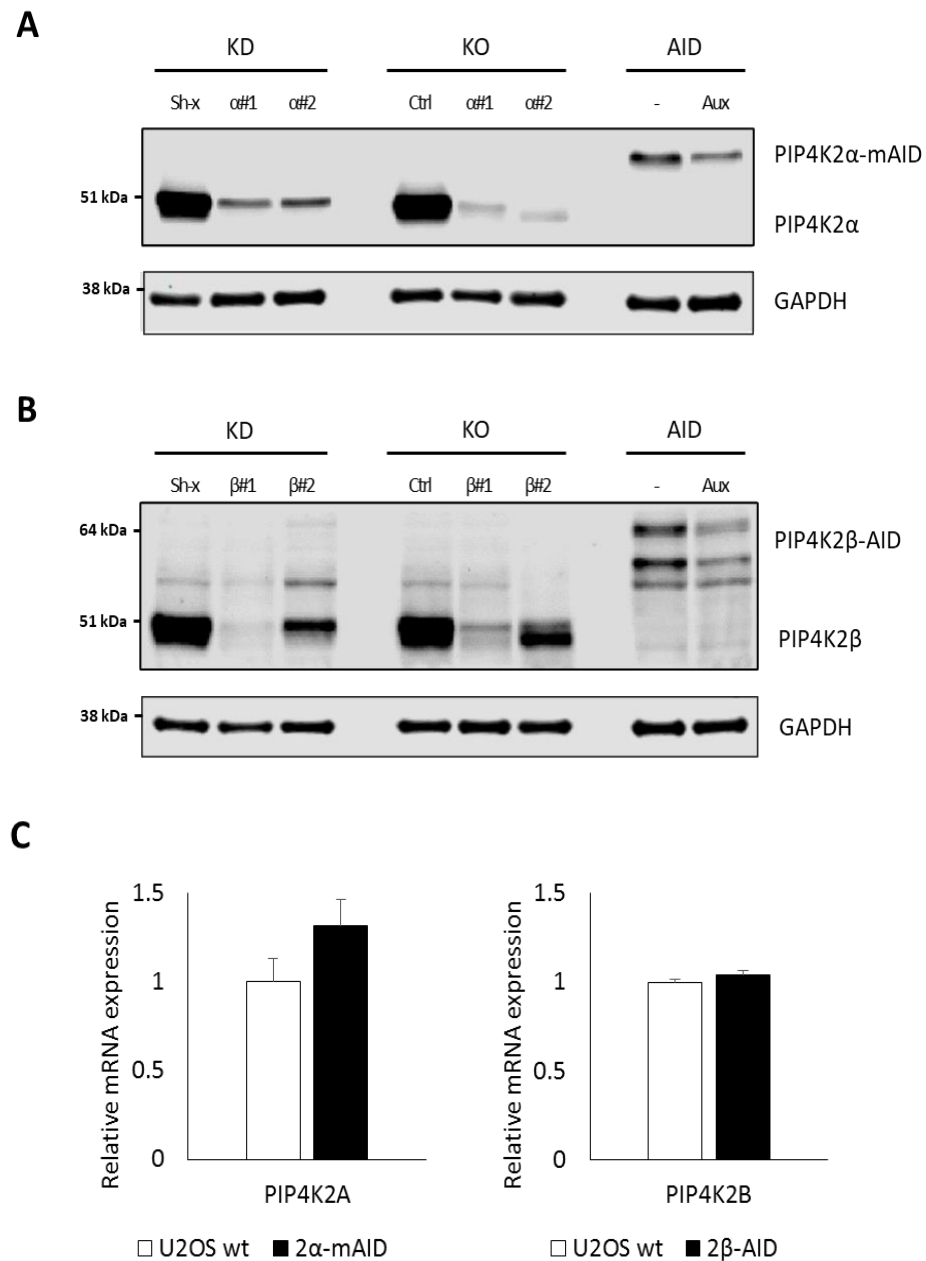
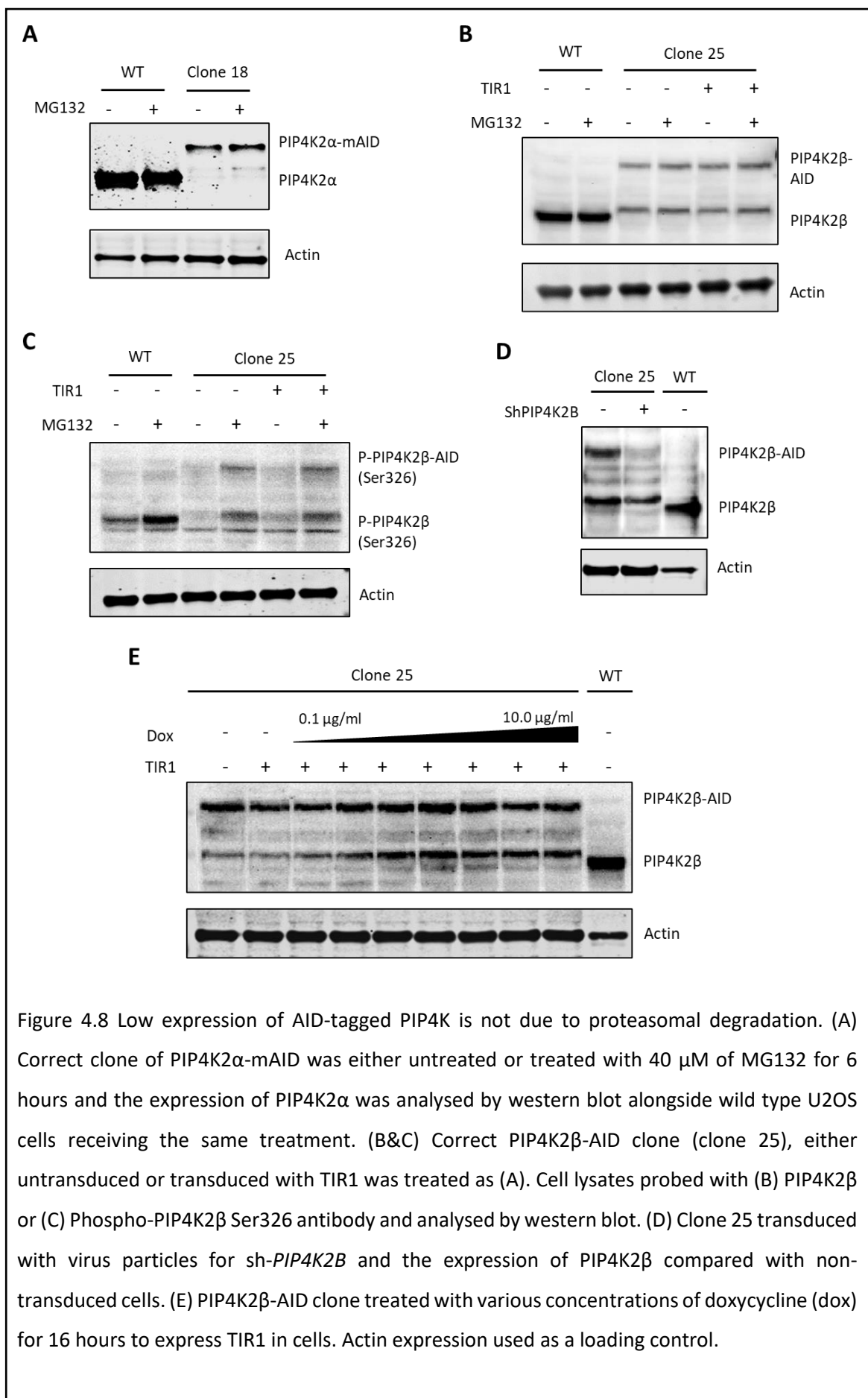


Figure 4.7 Comparison between different PIP4K degradation techniques. Lysates of PIP4K knockdown (KD), PIP4K knockout (KO), and AID-tagged PIP4K (AID) cells received auxin treatment were analysed by western blot to compare the level of (A) PIP4K2 α and (B) PIP4K2 β depletion. GAPDH expression was used as a loading control. (C) qPCR results of *PIP4K2A* expression in PIP4K2 α -mAID cells (left) and *PIP4K2B* expression in PIP4K2 β -AID cells (right). Data normalized to actin expression. Data is from single experiment conducted in technical triplicates, and represents two independent experiments (n=2). Aux: Auxin 500 μ M for 24 hours.

Increased protein degradation could be one of the possible reasons for the low expression of AID-tagged PIP4Ks. To test this hypothesis, the correct clones for AID-tagged PIP4Ks were treated with the proteasome inhibitor MG132 to inhibit proteasomal degradation. Clone 18 containing PIP4K2 α -mAID with no TIR1 transduced were treated with 40 μ M of MG132 for 6 hours. The expression of PIP4K2 α was compared to wild type U2OS receiving similar treatment. Western blot analysis indicated that inhibition of proteasome degradation pathway by MG132 treatment did not affect PIP4K2 α expression in the clones and wild type cells (Figure 4.8A). A similar experiment was conducted on PIP4K2 β -AID clone 25 cells, with the addition of clone 25 transduced with doxycycline-inducible TIR1. There was no difference in total PIP4K2 β expression between clone 25 transduced with or without TIR1 following the MG132 treatment (Figure 4.8B). Expression of PIP4K2 β phosphorylated at serine 326 was however increased (Figure 4.8C). Ser326 phosphorylation of PIP4K2 β was reported to inhibit its kinase activity (Jones *et al.*, 2006). The exact mechanism of how inhibition of proteasome increases PIP4K2 β phosphorylation is currently unknown. However, PIP4K2 β can be directly phosphorylated by p38 stress-activated protein kinase, and MG132 had been reported to activate p38 (Meriin *et al.*, 1998; Jones *et al.*, 2006). Therefore, inhibition of proteasome might have increased stress kinases such as p38 which lead to increase PIP4K2 β phosphorylation. Despite the increase in the level of phosphorylated PIP4K2 β , MG132 did not affect the total expression of the protein. These data indicated that proteasomal degradation did not cause the low expression of the AID-tagged PIP4Ks.

To determine if the expression of TIR1 could contribute to the degradation of AID-tagged PIP4Ks in the absence of auxin, clone 25 was treated with different doses of doxycycline (0.1, 0.25, 0.5, 1.0, 2.0, 5.0, and 10.0 μ g/ml) for 16 hours. The expression of PIP4K2 β was compared with non-treated cells or cells with no TIR1 by western blot analysis, and no clear differences in PIP4K2 β expression were observed between all the AID-tagged PIP4K2 β cells (Figure 4.8E). Therefore, the expression of TIR1 alone will not cause the AID-tagged PIP4K to be degraded. Figure 4.8B, C, and E showed that clone 25 had multiple bands that possibly indicate PIP4K2 β -AID since the bands were absent in the wild type cells. This observation is similar to data shown in Figures 4.6 and 4.7, although the size of the bottom band varies between experiments. To ascertain whether the bottom bands were also PIP4K2 β , clone 25 stably expressing sh-*PIP4K2B* was created and the expression of PIP4K2 β was compared with control cells by western blot analysis. The result showed that the expression of the top or 'main' PIP4K2 β -AID band was strongly reduced in *PIP4K2B* depleted cells while the bottom band showed a slight decrease in expression (Figure 4.8D). This indicates that the bottom band also belongs to PIP4K2 β , however, the reason for the bottom band being less affected by the knockdown remains to be elucidated.



4.3 Discussion

4.3.1 Advantages and limitations of the different methods in depleting TP53 and PIP4K used in this study

Choosing the right method to modulate proteins of interest is extremely important especially when a slight difference in the level of gene or protein expression could change cellular function. Different p53 levels in tumour cells, for example, will determine their survival fate and the basal level could affect the initiation response to cellular stress (Espinosa *et al.*, 2003; Zilfou and Lowe, 2009). In this study, we utilised three different methods for modulating the level of proteins of interest in cells, namely shRNA-mediated gene knockdown, CRISPR/Cas9 gene knockout, and auxin induced degradation of protein.

Both shRNA and CRISPR/Cas9 were used to deplete p53 in this study. To confirm the gene silencing effect, etoposide that induces DNA-induced damage by inhibiting DNA topoisomerase II was administered and the resulting induction of p53 downstream signalling proteins P21 and PUMA were observed. Cells transduced with the shRNA construct still showed some downstream activation as approximately 30% of p53 mRNA expression was present in cells. *TP53* knockout cells exhibited no activation in the pathway despite the slightly higher mRNA expression compared to the control. The CRISPR/Cas9 gene deletion method requires double strand breaks (DSBs) and non-homologous end joining repair (NHEJ) to produce a knockout phenotype through random short deletion and insertion mutations (indels) (Valerie and Povirk, 2003; Shi *et al.*, 2015). The expression of mRNA with no detection of protein indicates that a frameshift mutation had possibly occurred. Changes in single nucleotides were reported to be the most common form of p53 mutation that commonly resulted in missense mutation (Hainaut and Hollstein, 1999).

Modulation of PIP4K expression was also conducted by shRNA and CRISPR/Cas9 techniques. However, instead of transiently transfecting the cells with the CRISPR/Cas9 and gRNA constructs as for p53 knockout, the cells were stably transduced with lentivirus to produce the constructs necessary for the gene knockout and antibiotic resistance. With this method, the cells can be utilised after the selection process, and without having to grow them from a single clone. This method is quicker, does not depend on single cell cloning and obviates the requirement for experiments to be carried out on multiple clones. The lentivirus CRISPR method also allows the production of a new batch of cells with genetic deletion for every different experiment. However, different transductions might result in a different pool of mutations, which cause variation between experiments. These random indel mutations could probably explain the slight changes in mRNA expression in the cell pool that could be a mix of nonsense and frameshift mutation, and whether

it affected the intron/axon architecture conservation. Also, some cells will have a mutation in one or both alleles, while some mutated proteins may retain some functionality (Shi *et al.*, 2015). Since the chance of having the correct knockout clone is higher due to the stable expression of Cas9 and antibiotic selection, it is better to invest time to pick several single clones that subsequently are proven to bear null mutations and perhaps to pool these together; given that the effect of acute gene deletion is not the studied subject. Furthermore, the sequences used to target the genes are selected based on the highest knockout efficiency. Targeting the Cas9 to the critical domain of the protein of interest should be considered in the future as this will increase the chance of having a null mutation even if in-frame mutations occur (Shi *et al.*, 2015).

While both PIP4K depletion methods resulted in reducing the expression of *PIP4K2A*, only *PIP4K2A* knockdown cells adopted a round morphology. This change in morphology was seen with all the different *PIP4K2A* shRNA constructs. There is no study reported on morphological changes induced by *PIP4K2A* depletion. However, stable expression of type I 4-phosphatase, which dephosphorylate PtdIns(4,5)P₂, to increase PtdIns5P also causes similar morphological changes in HeLa cells (Zou *et al.*, 2007). It is known that both high expression of type I 4-phosphatase, and low expression of total PIP4K either through knockdown or knockout, cause an increase in PtdIns5P (Zou *et al.*, 2007; Wang *et al.*, 2019). Therefore, increases in PtdIns5P may be responsible for the rounded morphology. It is hard to conclude whether the morphology phenotype is a true positive effect. However, as similar decreases in the PIP4K α protein level was observed for both knockdown and knockout method, it is more likely that the phenotype shown by *PIP4K2A* knockdown was due to off-target effect.

A previous study had examined the efficiency of RNAi and CRISPR/Cas9 against an identical set of targeted genes (Morgens *et al.*, 2016). They reported that both methods changed the expression of other genes besides the primary targeted genes, but the effect on off-target genes were inconsistent between the two methods. The discrepancies were suggested to be due to the differences of the techniques and the most prominent difference is that the former induces knockdown of gene expression while the other causes persistent damage on the target DNA, resulting in different levels of gene loss. However, in this current study, it was the knockdown method that produced a reduced gene that showed the morphological changes. One possible explanation of the different phenotypes between CRISPR/Cas9 and shRNA knockdown is the effect of microRNA (miRNA) activities. miRNA generally acts to control their target genes post-transcriptionally by binding to the 3' untranslated terminus (3'UTR) of the gene and repress protein production (Cannell *et al.*, 2008). shRNA utilises a set of processes to produce mature RNAi that are reported to often interfere with miRNA processing (Grimm *et al.*, 2006). Similar to shRNA, miRNA is commonly processed through RNA-induced silencing complex (RISC) complex, therefore, a high

level of shRNA in the cells can cause competition for the RISC processing unit, causing impaired miRNA activity. This will then lead to an abnormal level of target mRNA and resulted in a disease state. One study reported that shRNA could up- and downregulate miRNA expression and different shRNA constructs targeting the same gene could affect similar or different miRNAs (Masuda *et al.*, 2016). In this study, the rounded phenotype was also observed with other shPIP4K constructs (data not shown), suggesting that it is not a single shRNA construct's off-target effect. One possible way to test if it is due to miRNA activity is to use siRNA instead of shRNA, which should not interfere with the upstream RNAi components and allowing less competition with miRNA activity. The siRNA method however is not always as effective and miRNA interference has still been reported to take place (Reviewed in Jackson and Linsley, 2010).

The third method of PIP4K modulation utilised was the AID system. With this system, both PIP4K2 α and 2 β proteins were shown to degrade following doxycycline and auxin (dox-aux) treatment; although western blot analysis showed a weak expression that can still be observed after 24 hours of auxin treatment. The treatment was limited to 24 hours to observe the possible effect of acute depletion of PIP4K. AID was previously shown to deplete the AID-tagged PIP4K2 β within 45 minutes in chicken DT40 cells (Bulley *et al.*, 2016). They utilised cells stably expressing TIR1 while in this study, doxycycline is needed to induce expression of TIR1. However, overnight doxycycline treatment is sufficient to ensure stable expression of TIR1 prior to auxin administration, and therefore insufficient TIR1 expression is not an issue in this case. Difference in efficiency of the degradation system in different cell lines could be due to the different half-life of the protein and degradation efficiency.

The level of AID-tagged protein expressed in the cells compared to the endogenous protein is another concern. Western blot data indicated that the AID-tagged PIP4K bands were at most 1/5 of their endogenous counterpart. Bulley *et al.* (2016) also showed a weaker AID-tagged PIP4K band compared to the endogenous expression, although the difference was not as obvious as observed here. Other studies utilising the AID technique had also reported a slight reduction of tagged protein that was suggested to be due to the 'basal' activity of the AID-TIR1 degradation system, which might be triggered by any auxin-like structures present in the bovine serum and media (Natsume *et al.*, 2016; Nishimura and Fukagawa, 2017; Yesbolatova *et al.*, 2019). Recently, it was also found that the exogenous AID introduced to a native protein locus will result in continuous proteasomal degradation by the TIR1, independent of auxin (Li *et al.*, 2019; Sathyan *et al.*, 2019). These pieces of evidence, however, are still unable to explain the low level of AID-tagged PIP4Ks even before the introduction of TIR1 as observed in this study. Data from this study also showed that inhibition of the proteasome did not increase the level of PIP4K2 α and 2 β . We should not overlook the possibility that being a non-native structure in mammalian cells, the unstable AID itself could be a subject of

TIR1-independent degradation. The multiple bands seen with PIP4K2 β -AID could also be the result of this unknown mechanism of continuous degradation of the long AID sequence; thus producing different sizes of AID tagged PIP4K2 β . In addition to increased protein degradation, reduced protein translation could be another reason for the low expression of AID-tagged PIP4Ks. Increased coding sequence length is one of the contributing factors for reduced protein translation (Huang *et al.*, 2011), therefore the addition of AID sequence could have affected the rate of protein translation. It is also possible that the repair AID construct did not bind to all alleles following Cas9 endonuclease activity, resulting in loss of protein production. Finally, failure in recognising the AID-tagged PIP4K by antibody could be another reason for the observed low PIP4K-AID expression. Addition of AID sequence to the proteins could have altered the epitope for antibody binding thus reducing antibody affinity.

Some improvements suggested for this technique include introducing additional structures to the system which are critical for AID stabilisation. Auxin response transcription factor (ARF) is a component of native auxin signalling which acts to stabilise AID in the absence of auxin. The expression of this ARF significantly reduces the chronic degradation of AID-tagged proteins (Sathyan *et al.*, 2019). Other than providing an extra element to the already complicated system, another study took a different approach by utilising the F-box protein structure from *Arabidopsis thaliana* called AtAFB2, instead of the widely used *OsTIR1* (Li *et al.*, 2019). They also identified that the best degron sequence to be used with the AFB2 F-box protein, termed 'miniIAA7', is also derived from the same species. This method has been shown to dramatically reduce the rate of chronic degradation shown by the current method.

Another common issue with the AID system that was also encountered in this project was the time taken to obtain the clone with correct homologous AID sequence. It is known that the cells will naturally prefer the NHEJ system to repair the DSBs caused by Cas9 rather than adopting the homology directed repair (HDR) pathway using an introduced repair construct (Liu *et al.*, 2019). However, continuous efforts are being made to increase the chance of the HDR system being used in the cells. A recent example includes the introduction of pro-HDR factors into the CRISPR repair system which increased the HDR/NHEJ ratio up to several folds (Nambiar *et al.*, 2019; Tran *et al.*, 2019). These new techniques should be considered to be used in the future to ensure the preserved function of the tagged protein.

To conclude, three methods of protein/gene modulation were used, each with its advantages and disadvantages; which are widely discussed in the literature. Adopting several methods for an experiment is important to verify the function of the proteins investigated. However, through cell line development, differences in the level of protein expression and cell morphology can already be seen across the different techniques and thus discrepancies in the experimental outcomes are not unexpected. It is hoped that these results will serve as a reference for future studies in selecting the right gene/protein modulation technique for use in investigations.

Chapter 5 Investigating the relationship between PIP4K and p53 in cancer cells

5.1 Introduction

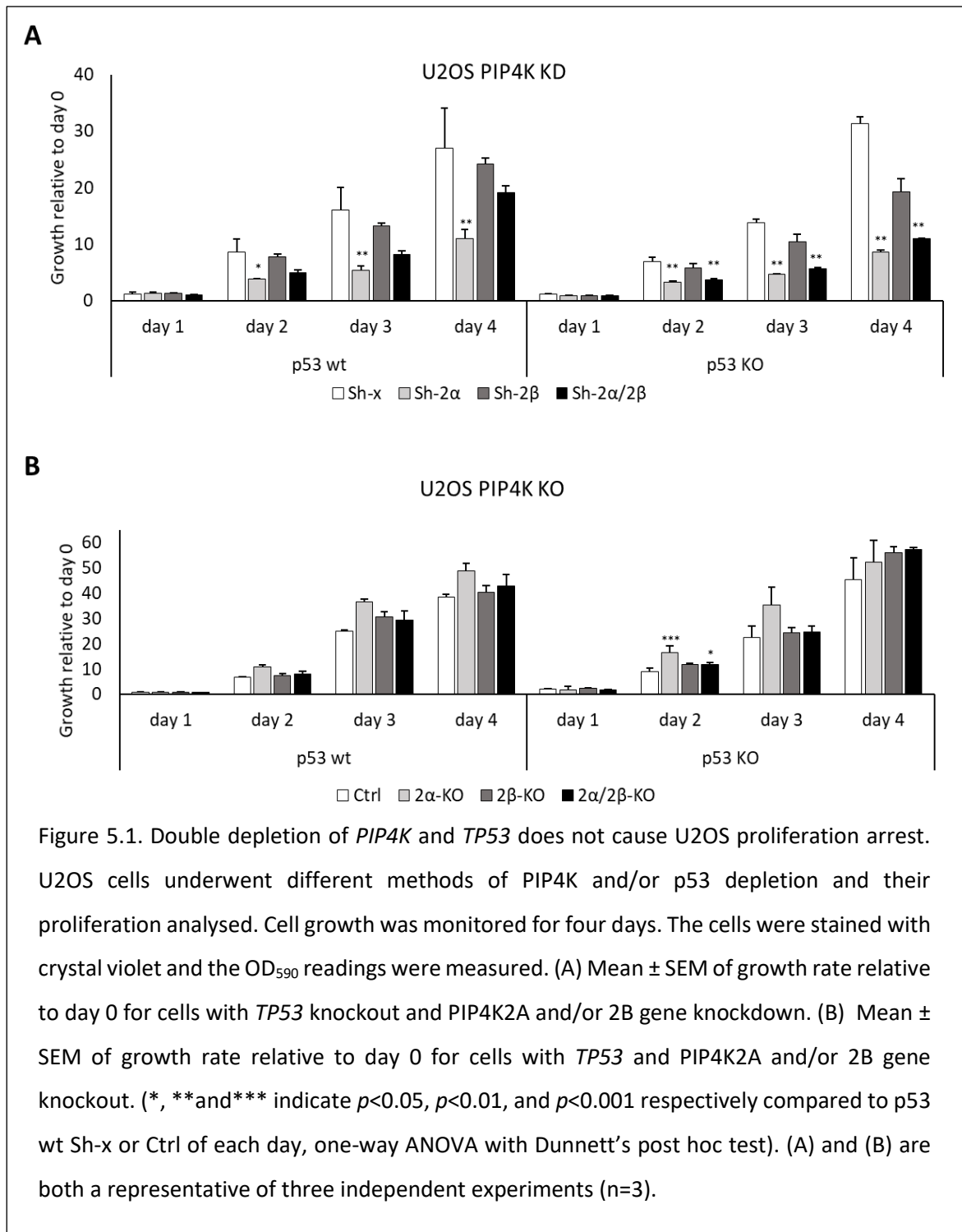
The *TP53* and *PIP4K* knockdown and knockout cell lines produced in chapter 4 were utilised to determine the presence of synthetic lethal interaction between loss of p53 and PIP4K2 α and/or 2 β . Cell growth was assessed through anchorage-dependent and independent assays, while other experiments were conducted to determine if depletion of *TP53* together with *PIP4K2A* and/or *2B* will affect other cell properties such as migration and viability. It is hoped that the findings will elucidate the role of PIP4K in p53 inactivated cancer and help in making future decisions for developing a PIP4K inhibitor(s) as a possible therapeutic agent for cancer.

5.2 Results

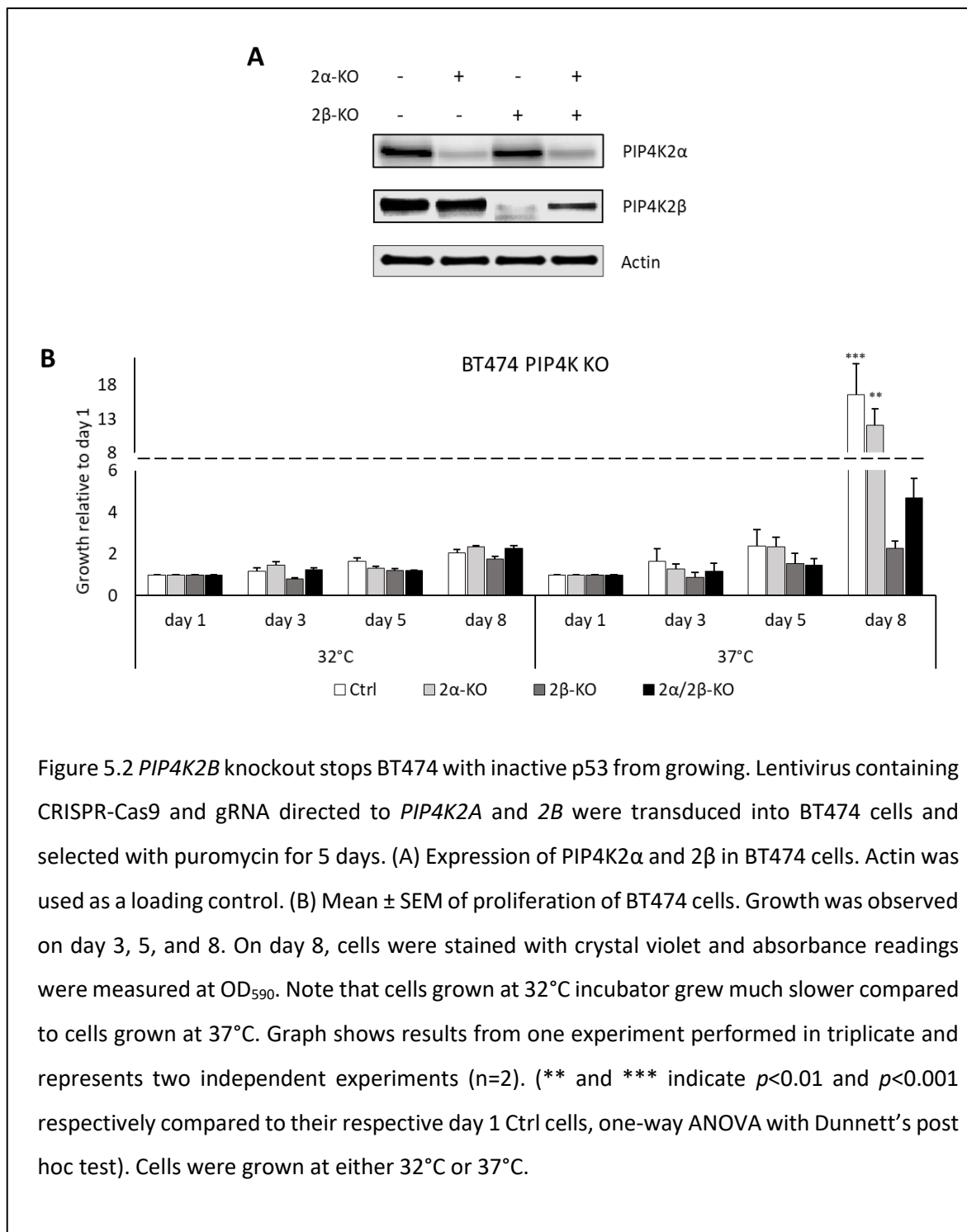
5.2.1 Effect of PIP4K isoforms and p53 depletion on cancer cells proliferation

Investigations were conducted to identify potential defects in cell growth when the expression of *PIP4K2A*, *PIP4K2B*, or both (*PIP4K2A/2B*) are depleted, in the context of either wild type or depleted p53. A total of eight cell lines with different p53 and PIP4K status were generated and their proliferation was observed for four days. *PIP4K2A* knockdown significantly reduced cell proliferation in both p53 wild type and deleted cells (Figure 5.1A). Although depletion of *PIP4K2A/2B* attenuated the growth of p53 deleted cells more than wild type cells, the interaction between p53 and PIP4K on cell growth was not statistically significant ($p>0.05$, 2-way ANOVA), which indicates that a synthetic lethal interaction between co-depletion of PIP4K and *TP53* was absent. Since double *PIP4K2A/2B* knockdown in p53 wild type cells already caused a slight reduction in cell growth, therefore, the growth suppression in *PIP4K2A/2B* and p53 depleted cells is not strong enough to indicate a synthetic lethality.

It is also crucial to understand if a slight presence of PIP4K signals in cells is enough to inhibit the synthetic lethal interaction. Therefore, *PIP4K2A* and *2B* knockout cells were generated in combination with *TP53* knockout and the effect on proliferation was observed. Analysis of the data showed that there was no significant interaction between p53 and PIP4K on cell growth for day 1 to day 4 ($p>0.05$, 2-way ANOVA) (Figure 5.1B). Moreover, in contrast to *PIP4K* knockdown, knocking out the *PIP4K* did not attenuate cell growth.



As no growth arrest was observed in U2OS following the *PIP4K* and *TP53* silencing, the BT474 cell line, in which a synthetic lethal interaction was previously observed (Emerling *et al.*, 2013), was utilised to replicate the findings by Emerling *et al.* (2013). In this cell line, PIP4Ks were knocked out using CRISPR/Cas9 lentiviral gene editing. Similar to CRISPR/Cas9 method utilised for U2OS cells, BT474 cells utilised for experiments were grown from a population of antibiotic selected cells and not from a clonally selected line. The experiment explored the effect of *PIP4K2A/2B* knockout on BT474 proliferation at 32°C and 37°C. As shown in Figure 5.2B, there was a strong reduction of growth for cells grown at 37°C with silenced *PIP4K2B* and a 2-way ANOVA indicated a significant interaction between p53 and PIP4K status on day 8 ($p=0.006$). Whereas, cells with depleted *PIP4K2A*, showed no strong difference in growth activity compared to control cells. Double knockout of the isoforms showed weaker growth retardation compared to the *PIP4K2B* knockout only cells, which could be due to the lower efficiency of *PIP4K2B* depletion in the double knockout cells (Figure 5.2A). The PIP4K knockout, however, did not show any significant effect towards BT474 cells grown at 32°C. These data suggest that a synthetic lethal interaction between loss of *PIP4K2B* and a temperature sensitive mutant of p53 can be observed in BT474 cells.



5.2.2 Effect of PIP4K isoforms and p53 depletion on anchorage-independent growth.

Previous studies showed that cells with a lack of p53 and PIP4K had impaired tumour formation in xenografts (Emerling *et al.*, 2013). For these investigations, growth in soft agar assay was utilised as a surrogate for xenograft assays. This assay is used to characterise the colony formation ability of cells, which is also a strong indicator of cellular transformation and their ability to form tumours in nude mice (Borowicz *et al.*, 2014). U2OS cells with various methods of PIP4K and p53 depletion were grown in soft agar and left to grow for 15 days before images of the colonies captured and the number of colonies and their size were analysed by ImageJ. Colonies bigger than 5000 μm^2 were categorised as large colonies. The size was chosen based on observation on colonies produced by each cell line, and large colonies were analysed to determine the differences in the cells' ability to form tumours in solid-free surface.

Regardless of the p53 status, cells with *PIP4K2A* and *PIP4K2A/2B* knockdown exhibited a lower number of large colonies, while knocking down *PIP4K2B* did not induce significant changes on the size of the colonies formed (Figure 5.3A, B, and C). Cells depleted p53, either through knockdown (Figure 5.3B) or knockout (Figure 5.3C & 5.4) produced slightly more large colonies, suggesting that the anchorage-independent growth depends on p53 function. Knocking out *PIP4K* did not cause any significant changes in colony growth, although there was a trend towards larger colonies (Figure 5.4A). 2-way-ANOVA analysis indicated no significant interaction between p53 and PIP4K on colony size ($p=0.89$). This observation is similar to the effect of *TP53* and PIP4K deletion on cell proliferation (Figure 5.1B), whereby no synthetic lethality was observed. P53 silencing only amplified the size of the colonies without changing the phenotypes shown by PIP4K knockout in p53 wild type cells (Figure 5.4B).

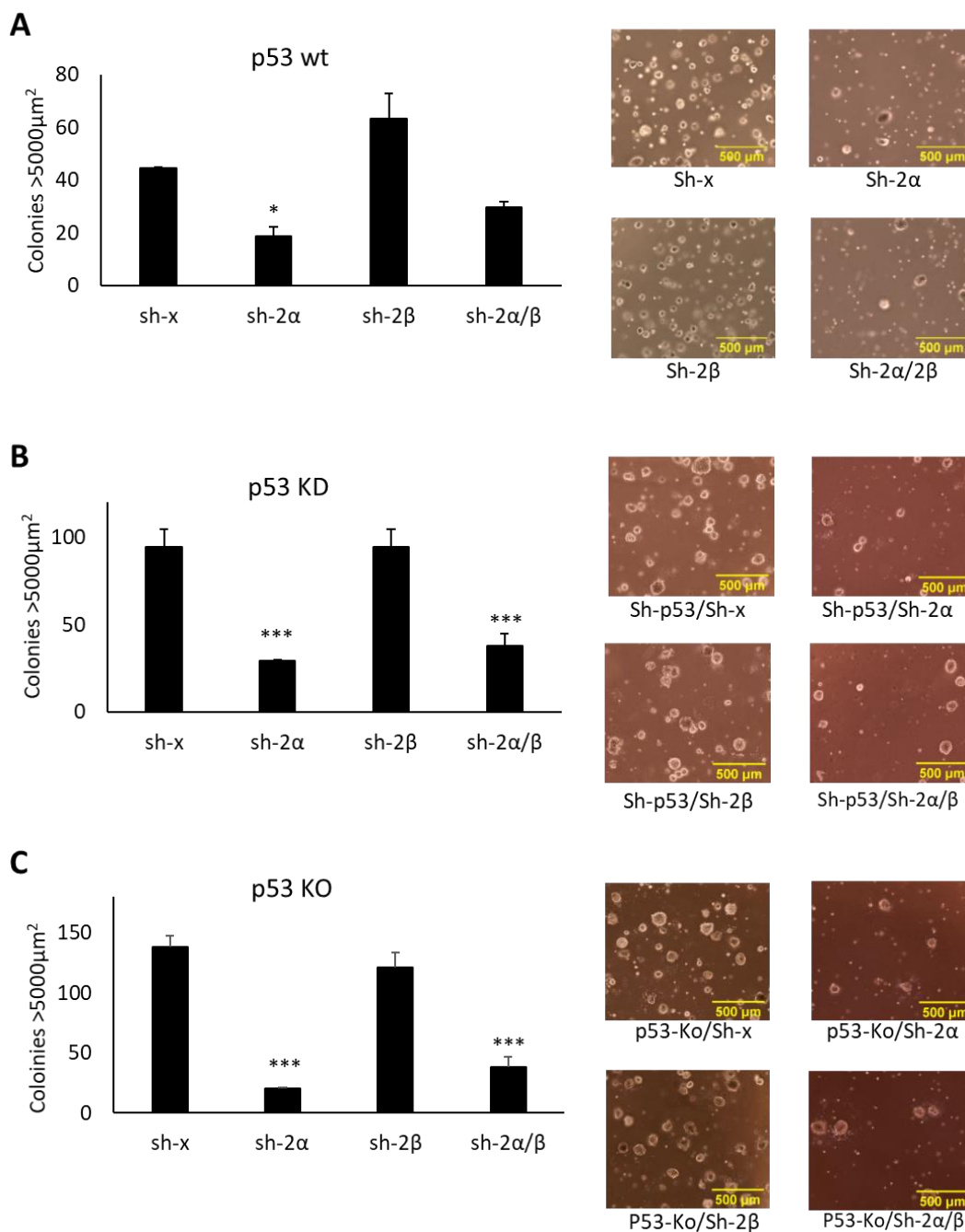


Figure 5.3 Depletion of *PIP4K2A* affects colony formation in U2OS cells irrespective of the p53 status. U2OS cells transduced with lentivirus bearing (A) shRNA construct for *PIP4K2A/2B*, (B) shRNA construct for both *TP53* and *PIP4K2A/2B*, and (C) shRNA construct for *PIP4K2A/2B*, with deleted *TP53* were grown in soft agar for 15 days. Graphs showing mean \pm SEM of large colonies. Data are from single experiment conducted in triplicates and represent of at least two independent experiments ($n=2$). (* indicates $p<0.05$ and *** indicates $p<0.001$ compared to sh-x control, one-way ANOVA). Photos of colonies were obtained with EVOS imaging system at 4x magnification and number of colonies were analysed with ImageJ.

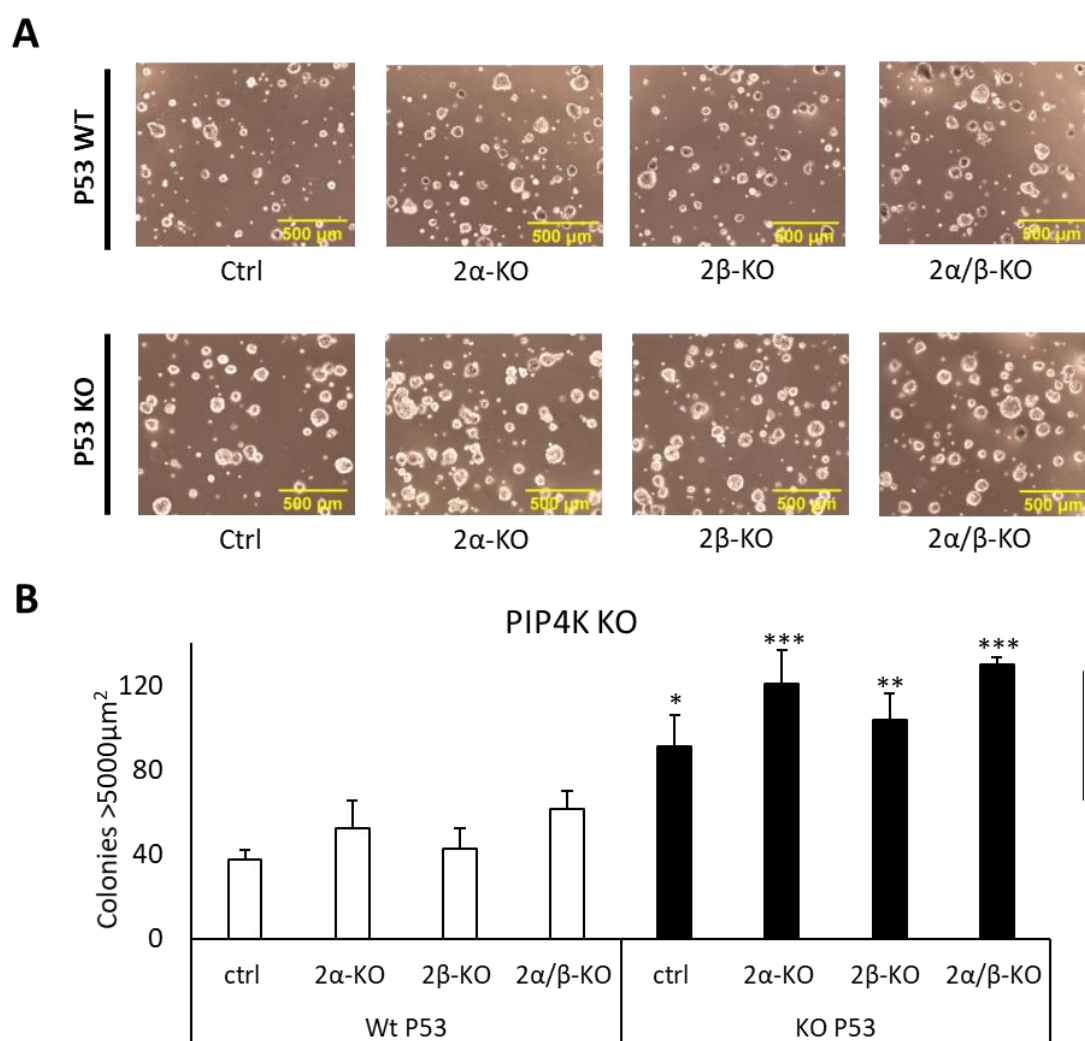
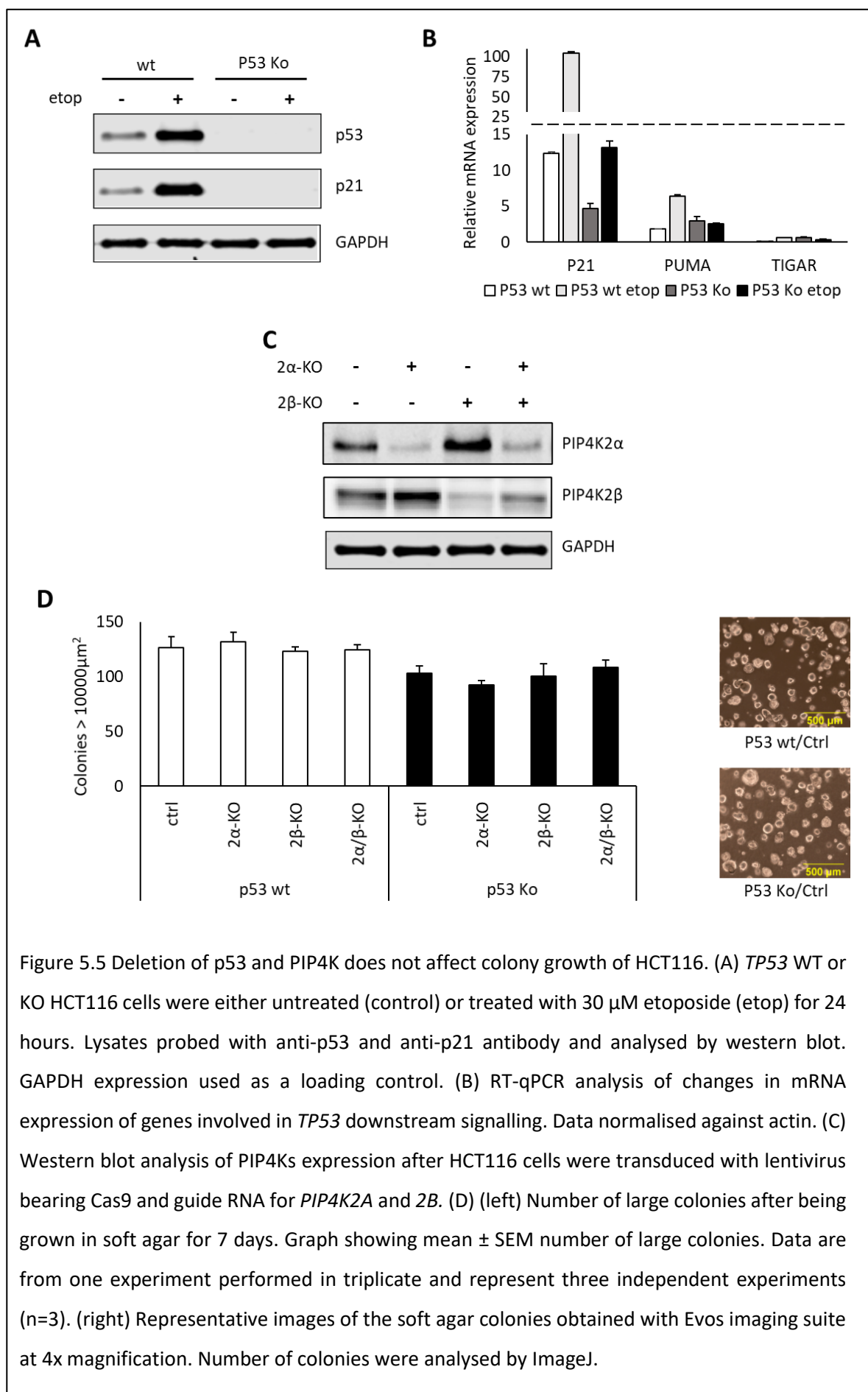


Figure 5.4 PIP4K knockout does not affect clonogenic potential of U2OS cells. U2OS cells transduced with lentivirus bearing Cas9 and guide RNA for *PIP4K2A* and *2B* with deleted *TP53* were grown in soft agar for 15 days. (A) Representative images of the colonies grown on soft agar. (B) Graph showing mean \pm SEM number of large colonies for each cell line. (*, **, and *** indicate $p < 0.05$, 0.01, and 0.01 respectively compared to WT p53 control, one-way ANOVA). Graph shows results from one experiment performed in triplicate and represents four independent experiments ($n=4$). Photos of colonies were obtained with EVOS imaging system at 4x magnification and number of colonies were analysed with ImageJ.

To determine if the absence of synthetic lethal interaction between p53 and PIP4K2 β observed in the U2OS cell is cell-specific, another human cancer cell line, HCT116, was used for the same experiment. Colorectal carcinoma cell line HCT116 is an adherent cell, similar to U2OS and BT474. It possesses wild type p53 (Liu and Bodmer, 2006) and no known PIP4K mutation like U2OS, which enable these genes to be modulated to study their potential synthetic lethality. A *TP53* knockout clone of the cell line was made using CRISPR/Cas9 and single cell cloning. Etoposide stimulation was conducted to confirm the absence of p53 activity (Figure 5.5A & B). *PIP4K2A* and *2B* were silenced by lentiviral delivery of CRISPR/Cas9 into HCT116 cells before undergoing a soft agar assay (Figure 5.5C). Initial observations demonstrated that colony growth of the HCT116 cell line in soft agar is rapid and therefore they were grown in soft agar for 7 days. Colonies bigger than 10,000 μm^2 were considered as large colonies. Analysis of the colony size showed no significant changes in colony number following PIP4K silencing (Figure 5.5D). No significant interaction was found between p53 and PIP4K on the colony size ($p=0.453$, 2-way-ANOVA), and therefore no synthetic lethal interaction was observed when both p53 and PIP4K were depleted. This observation is concurrent with the U2OS cell line in that there is an absence of synthetic lethality between PIP4K and p53.



To ascertain that growth in soft agar is suitable to detect synthetic lethal interaction between PIP4K and p53, BT474 cells with depleted PIP4K were grown in soft agar at 32°C and 37°C. Due to their slow growth, BT474 cells were grown in soft agar for 25 days and colonies bigger than 3000 μm^2 are considered as large. At 37°C, *PIP4K2A* knocked down cells showed a smaller number of large colonies compared to control cells (Figure 5.6B & C). This is a similar pattern to that shown by gene knockdown in U2OS cells. Knockdown of the PIP4K genes in BT474 cells grown at 32°C however, showed no significant changes in the number of large colonies, aside from a slight increase in the number of large colonies in cells depleted *PIP4K2B* and double *PIP4K2A/2B*. 2-way-ANOVA analysis indicated a significant interaction between p53 and PIP4K on colony size ($p=0.023$). This could be explained by the different impacts from the PIP4K knockdown as the cells were grown at different temperatures. Furthermore, no synthetic lethality effect can be seen in this experiment.

Similar soft agar experiments were conducted on BT474 cells with *PIP4K2A* and/or *2B* silenced by CRISPR/Cas9. Cells grown at 32°C did not show differences in the number of large colonies formed between cells lacking PIP4Ks and the control (Figure 5.7A & B). Note that cells grown at 32°C in general have smaller colonies compared to cells grown at 37°C. BT474 cells grown at 37°C however, showed a strong decrease in their ability to form large colonies when *PIP4K2B* was deleted (Figure 5.7A & B). There was a significant interaction between p53 and PIP4K on colony size ($p<0.001$, 2-way ANOVA), which refers to the loss of ability to form large colonies due to *PIP4K2B* being knocked out in cells where p53 was in the inactivated temperature sensitive state. *PIP4K2B* knockout in cells grown at 32°C also showed a slight reduction in the number of large colonies compared to the control, but these differences were small. This suggested that a synthetic lethal interaction between PIP4K and p53 can be observed in BT474 cells. However, the different phenotypes observed between PIP4K knockdown and knockout remain to be explained.

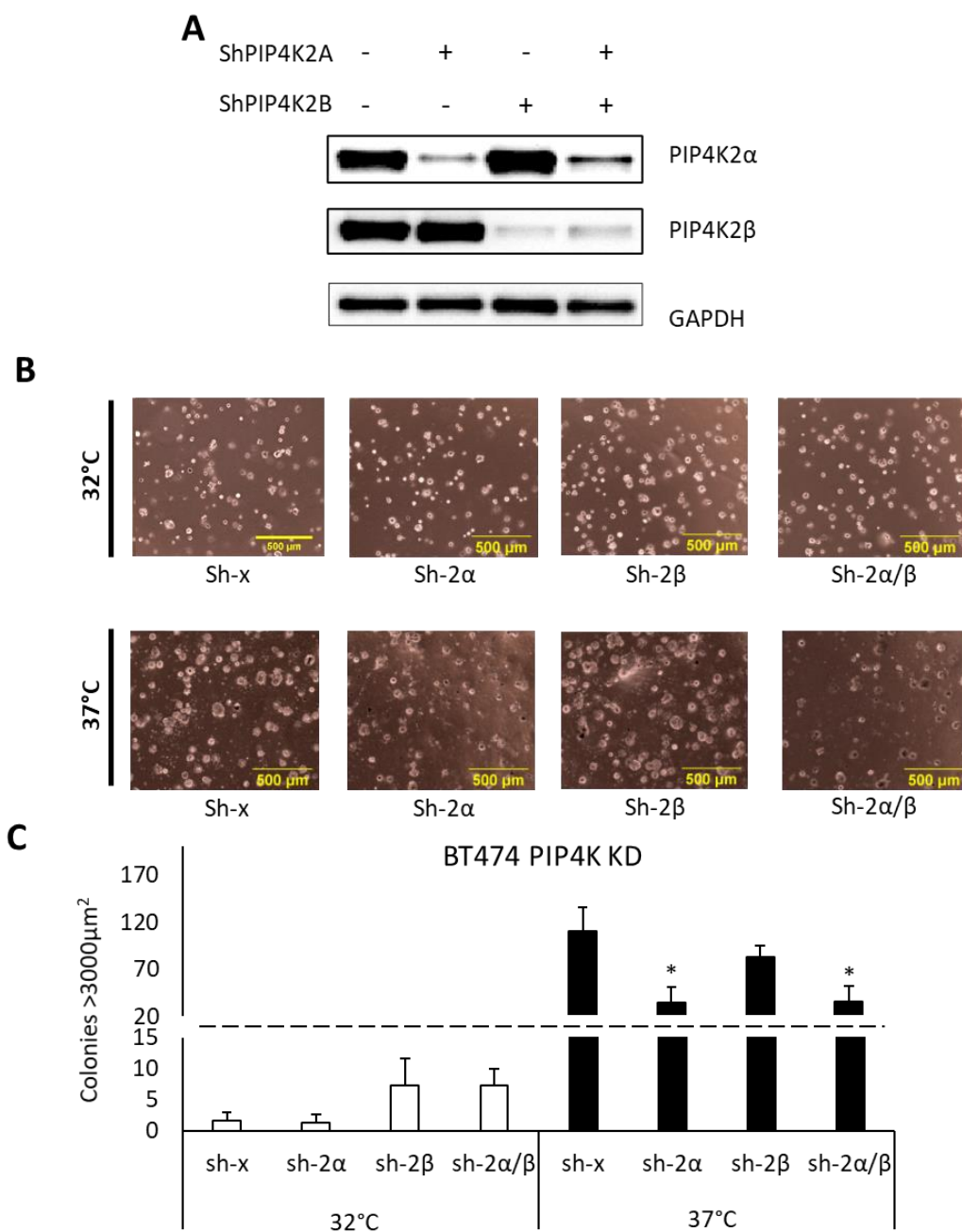


Figure 5.6 *PIP4K2A* knockdown with diminished p53 activity reduced large colony formation in BT474. BT474 cells transduced with lentivirus bearing shRNA sequence targeting *PIP4K2A* and *2B* were grown in soft agar for 25 days at 32°C or 37°C. (A) Western blot analysis showing the expression of PIP4K2 α and 2 β following knockdown. GAPDH expression used as a loading control. (B) Representative images of the colonies grown on soft agar. (C) Mean \pm SEM number of large colonies for each cell line. (* indicates $p < 0.05$ compared to sh-x of the corresponding temperature, one-way ANOVA). Graph shows results from one experiment performed in triplicate and represents two independent experiments ($n=2$). Data represents two independent experiments. Photos of colonies were obtained with EVOS imaging system at 4x magnification and number of colonies were analysed with ImageJ.

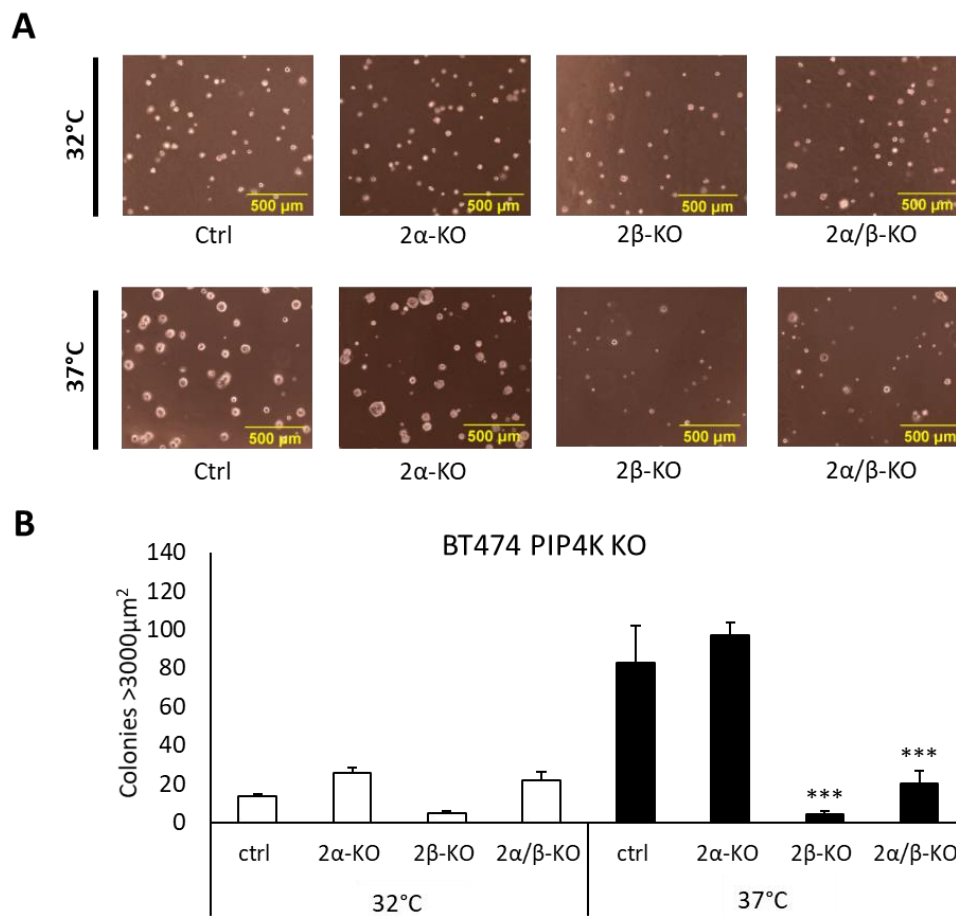


Figure 5.7 Depletion of PIP4K with diminished p53 activity significantly reduced large colony formation in BT474. BT474 cells transduced with lentivirus bearing Cas9 and gRNA for *PIP4K2A* and *2B* were grown in soft agar for 25 days at 32°C or 37°C. (A) Representative images of the colonies grown on soft agar. (B) Graph showing mean \pm SEM number of large colonies for each cell line. Data are from one experiment performed in triplicate and represent two independent experiments (n=2). (***) indicates $p < 0.001$ compared to control of the corresponding temperature, one-way ANOVA). Photos of colonies were obtained with EVOS imaging system at 4x magnification and number of colonies were analysed with ImageJ.

To determine whether the expression of mutant p53 is required for the synthetic lethal interaction between *PIP4K2B* and *TP53*, cells were transduced with lentiviral particles encoding shRNA to knockdown *TP53* with GFP expression (sh-p53). Control cells were transduced with lentiviral particles bearing non-targeted sequence (Sh-x) and expressing GFP as well. Transduced cells were analysed by flow cytometry (Guava® easyCyte™, Luminex Corporation) using the InCyte software to determine their GFP expression (Figure 5.8A). *PIP4K2B* was then removed from the cells by stably expressing Cas9 with gRNA directed against *PIP4K2B*. The cells were utilised to study changes in proliferation and anchorage-independent growth. *TP53* silencing in BT474 dramatically reduced cell proliferation and colony growth compared to wild type cells (Figure 5.8B, C & D). Analysis showed that there was a significant interaction between p53 and PIP4K on cell growth after nine days ($p > 0.05$, 2-way ANOVA) and colony size ($p = 0.019$, 2-way ANOVA), which suggested that the effects of reduced proliferation and ability to form large colonies due to *PIP4K2B* being knocked out were diminished in cells with silenced p53. *PIP4K2B* knockout significantly reduced proliferation and formation of large colonies compared to control in the presence of p53 (Figure 5.8B, C & D). However, in cells with silenced p53, there were no significant changes in proliferation and number of large colonies formed following *PIP4K2B* removal ($p = 1.00$, one-way ANOVA). Silencing p53 in BT474 cells produced phenotypes similar to that shown by BT474 cells grown at 32°C. These findings suggested that mutant p53 drives the rapid growth of BT474 and is necessary for the synthetic lethal interaction between p53 and PIP4K2 β to take place.

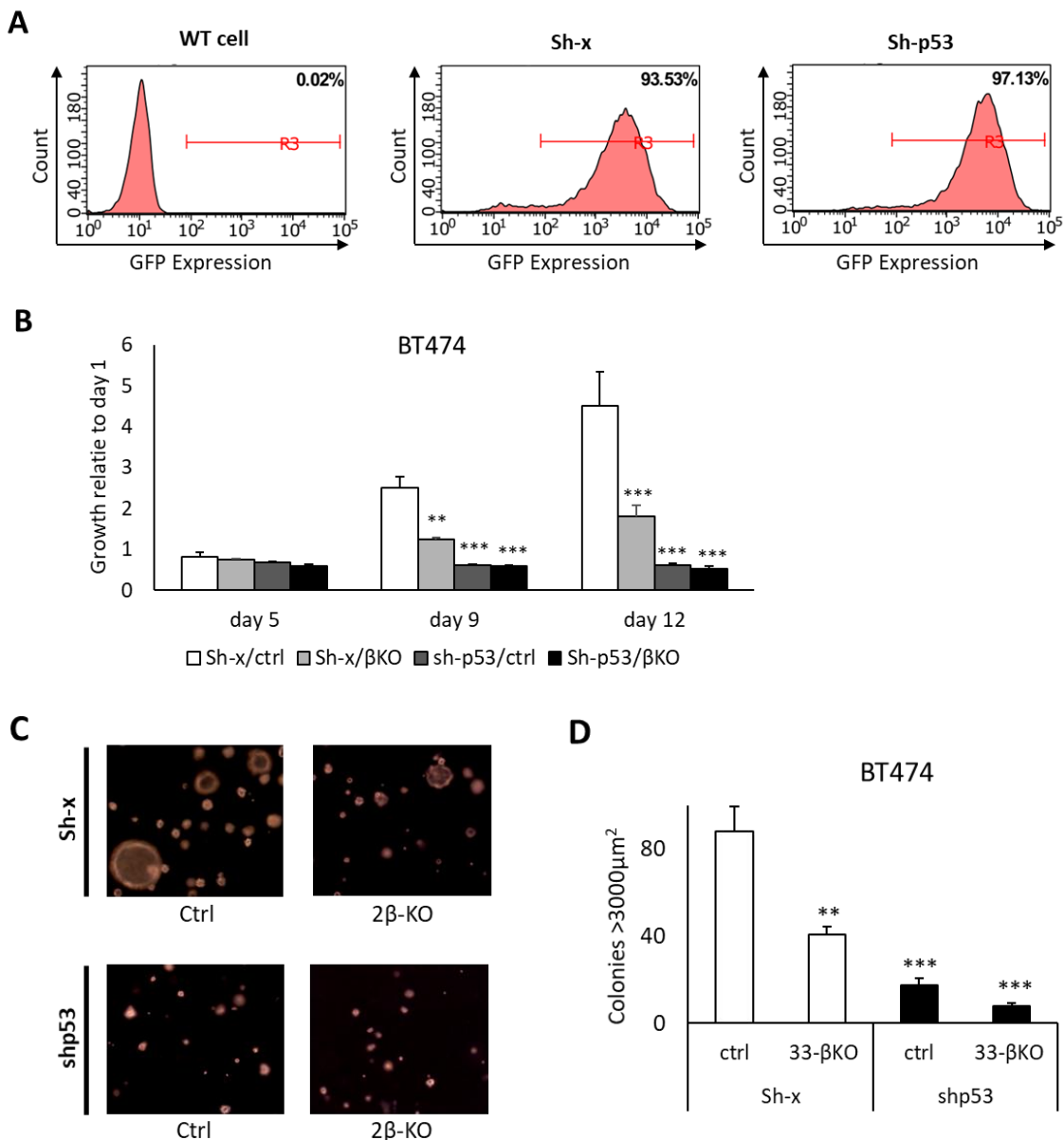


Figure 5.8 Depletion of p53 reduced proliferation and anchorage independent growth, and diminished the synthetic lethal interaction with *PIP4K2B*. BT474 cells transduced with lentivirus expressing shRNA for *TP53* and lentivirus stably expressing Cas9 and gRNA for *PIP4K2B* were utilised to study changes in proliferation and soft colony formation. (A) FACS analysis of cells transduced with Sh-x and sh-p53 lentivirus with GFP expression. (B) Mean \pm SEM of proliferation of BT474 cells. Growth was observed on day 5, 9, and 12. On day 12, cells were stained with crystal violet and absorbance readings were measured at OD₅₉₀. (C) 7,500 cells were plated on soft agar for 25 days. Representative images showing colonies grown on soft agar. (D) Graph showing mean \pm SEM number of large colonies for each cell line. (** and *** indicates $p < 0.01$ and $p < 0.001$ respectively compared to Sh-x control, one-way ANOVA). Graph shows results from one experiment performed in triplicate. Photos of colonies were obtained with EVOS imaging system at 4x magnification and number of colonies were analysed with ImageJ.

5.2.3 Temporal effect of PIP4K isoforms knockdown on the clonogenic activity of cancer cells

Throughout this project, U2OS cells were normally used for experiments six days after lentiviral transduction. The cells grown for another passage and plated on soft agar were seen to have a similar or slightly greater total number of large colonies compared to the control, regardless of whether the p53 is depleted or not for *PIP4K2A* knockdown cells (Figure 5.9A & B). The results indicated that there was no significant difference in colony sizes following PIP4K isoforms knockdown, either in p53 wild type cells ($p=0.732$), or in p53 deleted cells ($p=0.061$, one-way ANOVA). This suggested that the clonogenic phenotype demonstrated by *PIP4K2A* knockdown cells as shown in Figure 5.3 (above) is temporary. However, differences in colony growth between earlier and later passages were not observed in cells with knocked out PIP4K (result not shown). To ascertain that this finding was not due to the possibility of a higher PIP4K2 α expression after a greater period of growth, the expression of PIP4K2 α from the early and later passages were compared. This showed that there were no clear changes in protein expression when visualised (Figure 5.9C).

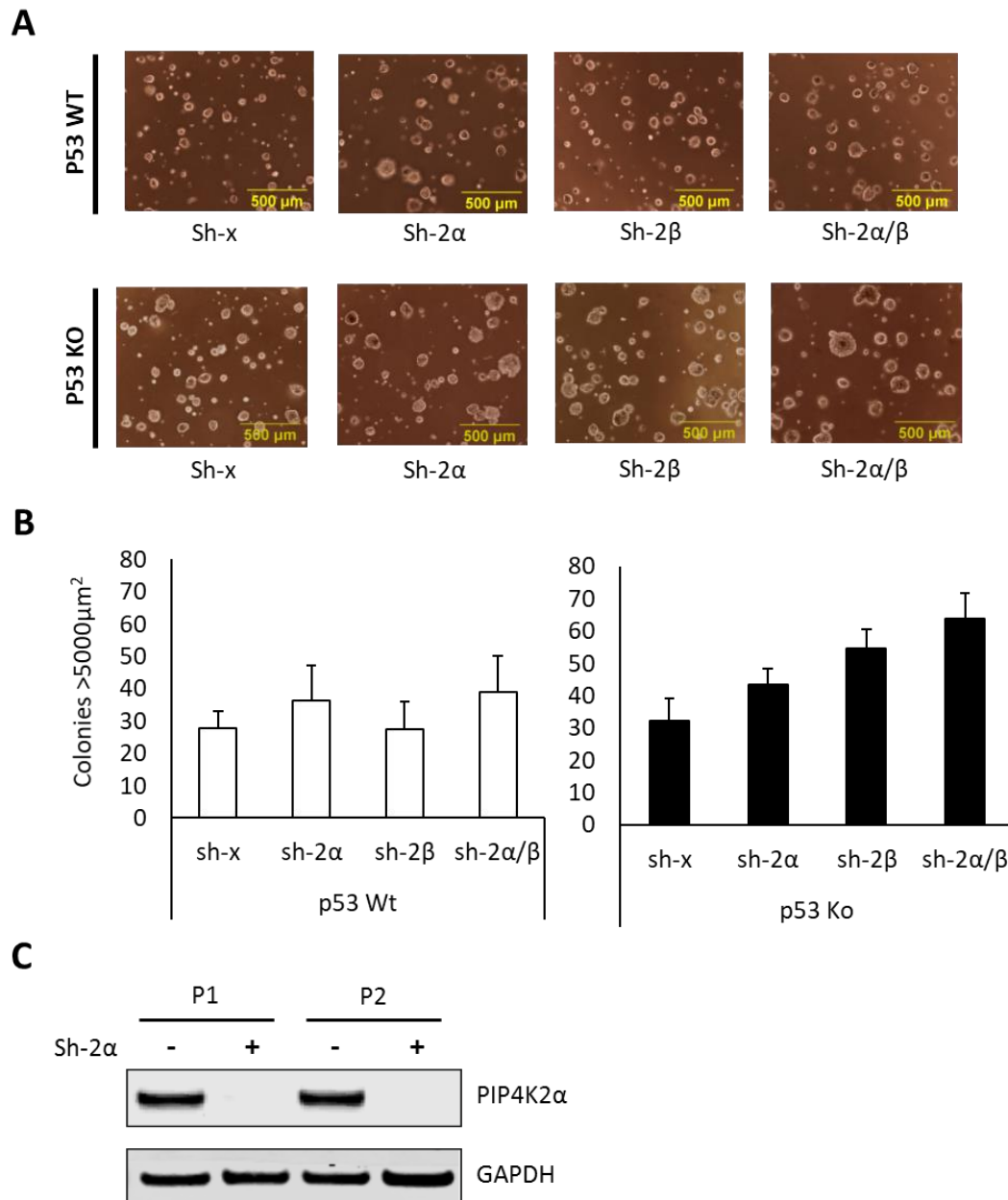
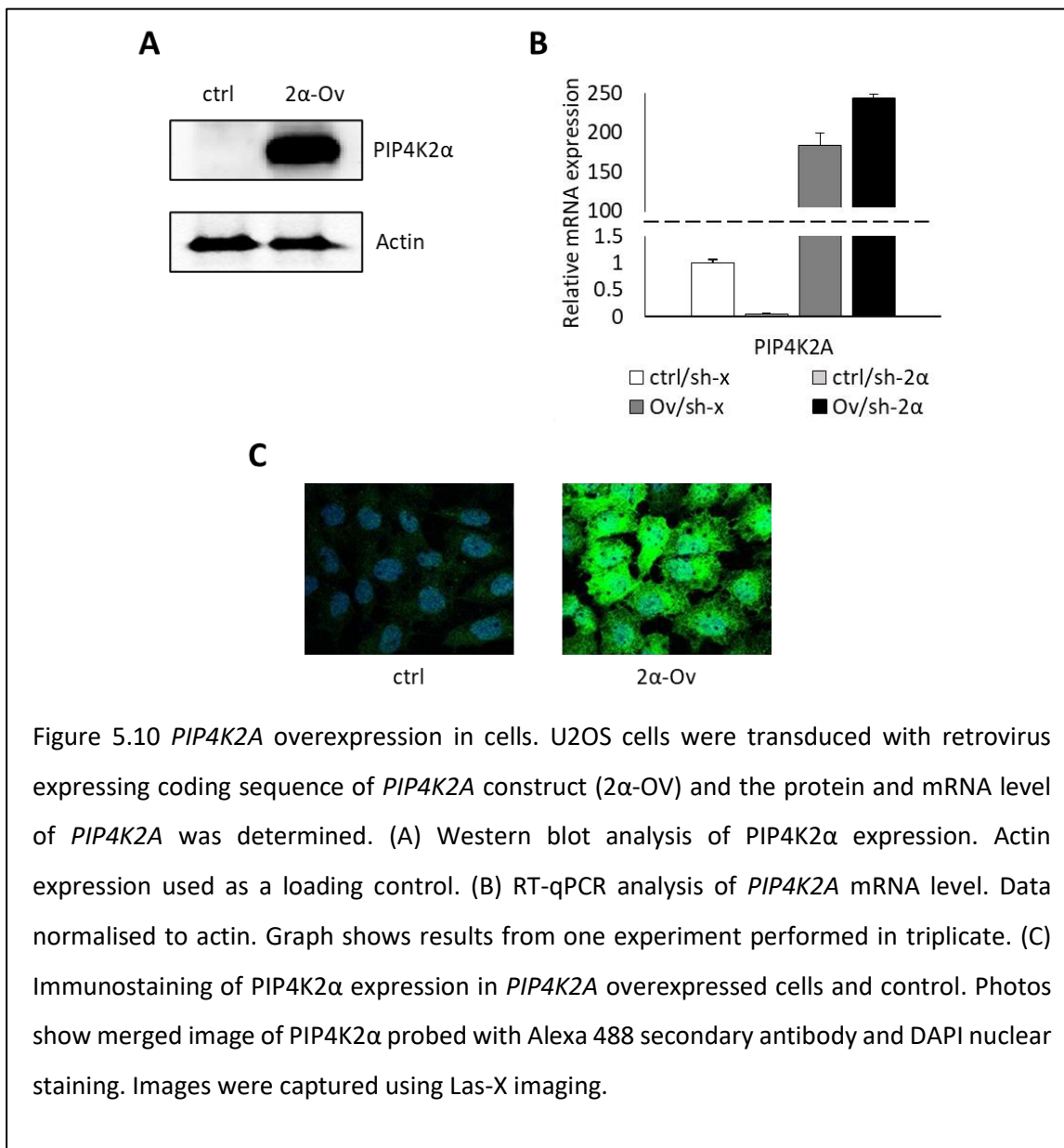


Figure 5.9 *PIP4K2A* knockdown colony phenotype is temporal. U2OS cells transduced with lentivirus bearing shRNA construct for *PIP4K2A/2B* with or without *TP53* were further passaged and grown in soft agar for 15 days. (A) Photos of colonies were obtained with Evos imaging suite at 4x magnification and number of colonies were analysed with imageJ. (B) Mean \pm SEM number of large colonies for each cell line. Graph shows results from one experiment performed in triplicate and represents two independent experiments (n=2). (C) Western blot analysis to compare the expression of *PIP4K2α* in U2OS with *PIP4K2A* knockdown harvested from earlier and later passages. GAPDH expression used as a loading control. P1: earlier passage, P2: later passage.

To understand whether the temporary effect of *PIP4K2A* knockdown is due to the acute removal of protein in the cells, a rescue experiment was conducted. U2OS cells were transduced with viral supernatant produced from pBABE retroviral vector to express myc-tagged *PIP4K2A*, before being transduced with *PIP4K2A* and/or *2B* lentiviral shRNA constructs. The expression of *PIP4K2A* was then confirmed through immunoblotting, qRT-PCR, and immunohistochemistry (Figure 5.10A, B, & C). The overexpression of PIP4K2 α was approximately 200 times more than the endogenous expression; thus making it hard to visualise the endogenous protein in the blot. The shRNA sequence which targeted the 3' UTR did not affect the exogenous expression of *PIP4K2A*.

The cells overexpressing *PIP4K2A* were then used for soft agar experiments to determine if the presence of exogenous *PIP4K2A* could rescue the phenotype of reduced colony size after *PIP4K2A* knockdown. Analysis of colony size demonstrated that there was no difference in colony size between cells overexpressing *PIP4K2A* and the control cells (Figure 5.11A & B). This indicates that PIP4K2 α expression failed to rescue colony growth size. The cells were also grown for another passage before being plated on soft agar to determine if *PIP4K2A* overexpression in the cells would cause a significant difference in colony growth of PIP4K depleted cells. As expected, the *PIP4K2A* knockdown cells had begun to produce larger colonies compared to cells of an earlier passage (Figure 5.11C & D). In addition, the cells overexpressing PIP4K2 α also had slightly fewer large colonies compared to their non-*PIP4K2A* overexpress control counterpart. These data might suggest that the effect shown by *PIP4K2A* knockdown on cell proliferation and clonogenic activity at an early passage of cells are artefactual.



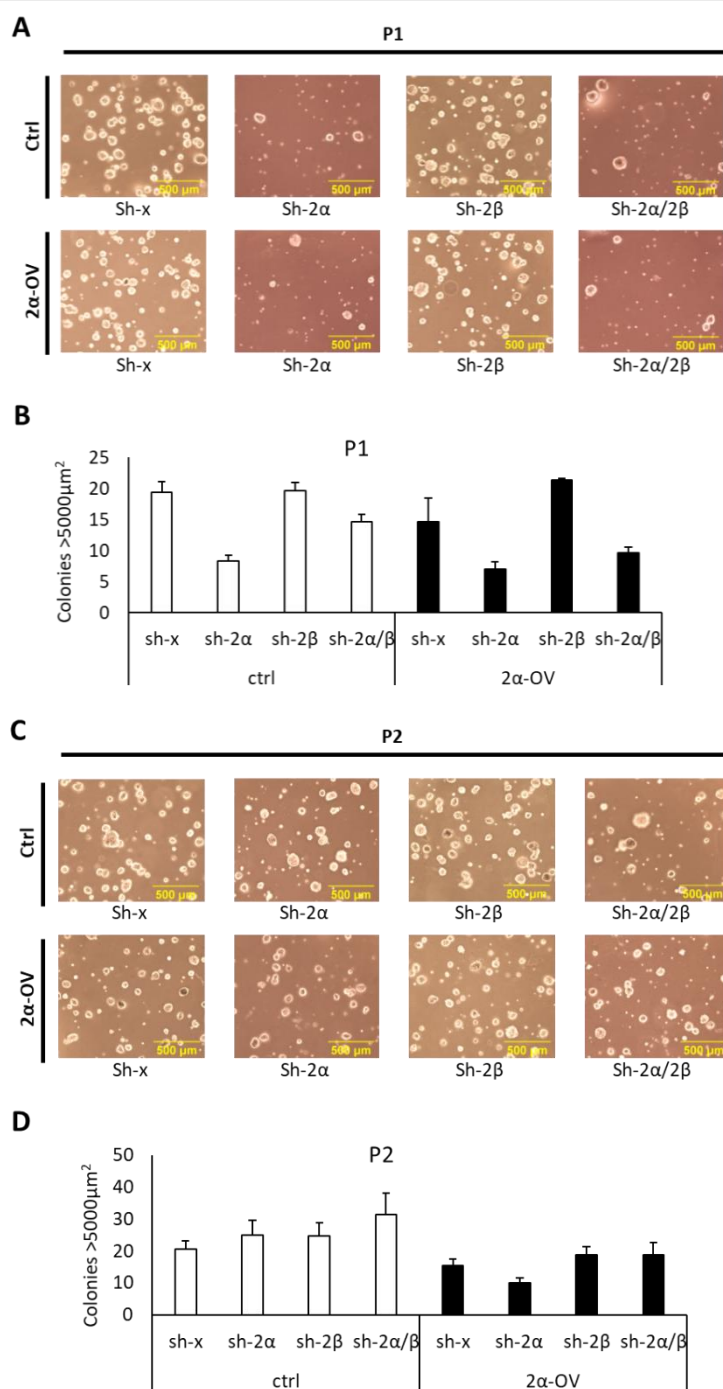


Figure 5.11 *PIP4K2A* knockdown colony phenotype could not be rescued by *PIP4K2A* overexpression. Cells overexpressing *PIP4K2A* (2α-Ov) were transduced with lentivirus expressing shRNA constructs targeting either *PIP4K2A*, *PIP4K2B*, or both and were grown in soft agar for 15 days. The colonies obtained were compared with a set of control cells (ctrl) not overexpressing the *PIP4K2α*. (A) Photos of colonies and (B) mean \pm SEM number of large colonies for each cell line (n=3). The cells were further passaged and grown in soft agar. (C) Photos of the colonies and (D) mean \pm SEM number of large colonies for each cell line (n=3). Photos of colonies were obtained with Evos imaging suite at 4x magnification and analysed with ImageJ. P1: earlier passage, P2: later passage.

5.2.4 Effect of PIP4K isoforms and p53 depletion on cell migration, adherence, viability, and senescence.

The effect of p53 and PIP4K loss on other cancer relevant phenotypes such as migration and senescence were also investigated in U2OS cells. To investigate whether there is a synthetic lethal effect in cell migration, cells were plated, allowed to grow to confluency and a wound was made by scratching the uniform monolayer of cells with a pipette tip, and 'wound closure' activity was monitored under serum-free conditions. Starving the cells are necessary to deplete any growth factor that could influence cell migration (Szustak and Gendaszewska-Darmach, 2020). The area of the wound after a certain time was compared to the wound size at zero hours (Figure 5.12A). Data showed that knocking down the expression of *PIP4K2A* or *2B* in cells attenuated the migration rate in the absence and presence of p53 in the cells (Figure 5.12B). 2-way-ANOVA analysis showed no significant interaction between p53 and PIP4K on cell migration ($p>0.05$). These results suggested that depletion of *PIP4K2A* and *2B* reduced the metastatic ability of the cells, while no synthetic lethal effect was observed.

Similar experiments were also conducted on cells with *PIP4K2A/2B* knocked out through CRISPR/Cas9. Different from the knockdown, *PIP4K2B* deletion significantly increased migration activity after 24 hours compared to the control, while deletion of *PIP4K2A* only showed a trend of increased migration activity (Figure 5.12C). 2-way-ANOVA analysis indicates that there is a significant relationship between p53 and PIP4K on cell migration ($p<0.05$), in which the higher migration activity in *PIP4K2B* knocked out cells was attenuated by the *TP53* knockout. A similar observation, between gene knockdown and knockout in cell migration experiments, is that the pattern of slightly higher migration activity shown by the *TP53* knocked out cells is dampened when PIP4K is also silenced. Although this observation suggests a cross-talk between the two genes in cellular migration, these changes altogether are still not enough to prove the existence of synthetic lethal interaction between PIP4K and p53 in U2OS cells.

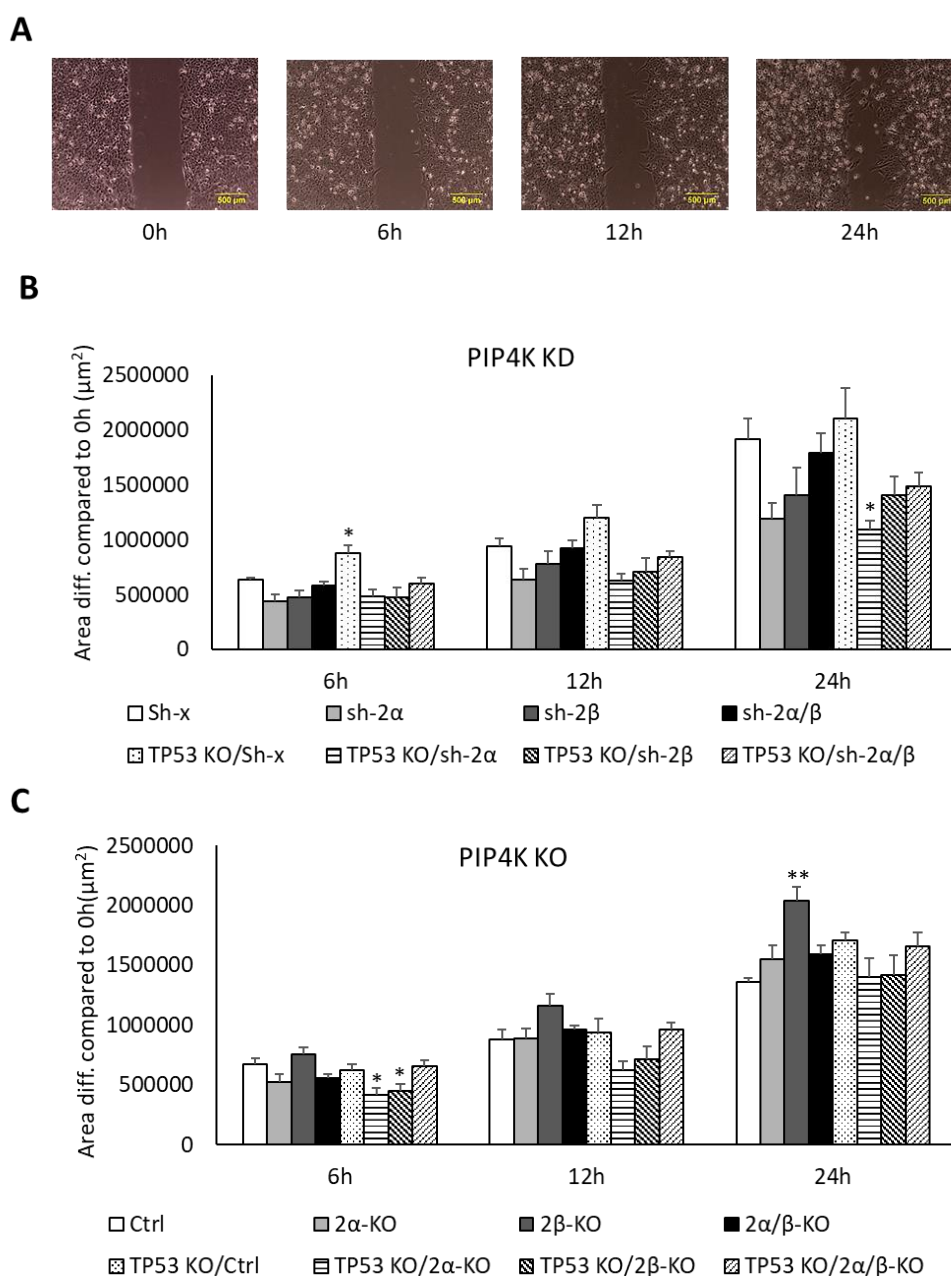


Figure 5.12 Effect of PIP4K and p53 depletion on U2OS cell migration activity. A wound was created and the closure rate was monitored after 6, 12, and 24 hours under serum-free media. (A) Representative of photos captured during the 24-hour period. (B) Graph showing mean \pm SEM of the wound area in U2OS cells transduced with lentivirus bearing shRNA construct for *PIP4K2A/2B* ($n=3$). (C) Mean \pm SEM of the wound area in cells transduced with lentivirus bearing Cas9 and gRNA for *PIP4K2A/2B*. Graph shows results from one experiment performed in triplicate and represent two independent experiments ($n=2$). (* and ** indicate $p<0.05$ and $p<0.01$ respectively compared to Ctrl, one-way-ANOVA). Photos of colonies were obtained with Evos imaging suite at 4x magnification. The changes in wound area were analysed with ImageJ.

As part of preliminary experiments to determine if a synthetic lethal interaction between PIP4K and p53 is present in U2OS cells, other experiments such as cell adherence, viability, and senescence were also conducted. These experiments were only conducted in cells that were silenced for both *PIP4K2A/2B* through gene knockdown. Cell adherence was considered to be a valuable phenotype to look for a lethal interaction as it is essential for cell communication and survival. It is also involved in several crucial processes including cell cycle and metastasis (Huang and Ingber, 1999). An attachment assay was used to determine U2OS cell adherence after depletion of *PIP4K2A/2B* and *TP53*. The attachment rate was determined by counting the percentage of cells attached on the plate after one, two, and four hours of plating from the initial number of cells plated. Depletion of both *PIP4K2A* and *2B* reduces the attachment percentage of the cells (Figure 5.13). The assay also showed that p53 depletion tends to slightly reduce the adhesion activity, while cells lacking both p53 and PIP4K demonstrated the lowest adhesion activity. No significant interaction between p53 and PIP4K was detected on the percentage of attached cells at the first and the second hour, while there was a significant interaction recorded at hour four ($p=0.02$, 2-way ANOVA). The significant interaction means that there was a reduced number of cells attached as the p53, *PIP4K2A*, and *PIP4K2B* were depleted. However, this could have been a false positive result since by the fourth hour, the Sh-x control cells had reached 100% cell attachment and therefore it appears that there is an interaction between loss of p53 and PIP4K in the cells. Data from one and two hours however showed that depletion of p53 or *PIP4K2A/2B* reduced the rate of attachment and that no synthetic lethal interaction was observed between p53 and PIP4Ks.

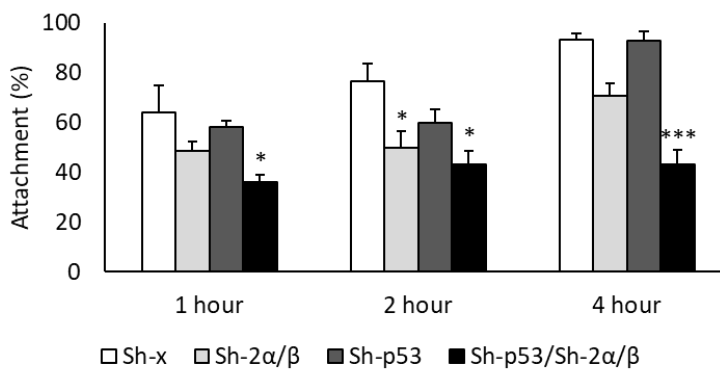


Figure 5.13 PIP4K depletion reduces cell adhesion activity. Cells were plated and monitored after 1, 2, and 4 hours of plating for adhesion activity. Cells were washed before trypsinisation after the stated hours of plating and the percentage \pm SEM of cells left in the well were counted. Graph shows results from one experiment performed in triplicate and represents three independent experiments ($n=3$). (* and *** indicate $p<0.05$ and $p<0.001$ respectively compared to Sh-x, one-way ANOVA).

The possible effect of double depletion of p53 and PIP4K on viability and senescence was also studied. These assays were conducted to partly understand the slower growth of PIP4K depleted cells. An MTT assay was utilised to monitor the effect of apoptosis agent etoposide and ferroptosis inducer erastin on cell viability, while senescence-associated β -galactosidase (SA- β gal) assays were used to study the effect of p53 and *PIP4K2A/2B* depletion on cellular senescence. Analysis of data from the MTT assay showed that depletion of *PIP4K2A/2B* reduced cell viability while p53 depletion increased cell viability with etoposide treatment. There was no clear effect on cell viability upon different backgrounds of PIP4K and p53 with erastin treatment (Figure 5.14A). 2-way ANOVA indicated no significant interaction between p53 and PIP4K on the cell viability for both etoposide ($p=0.81$) and erastin ($p=0.93$). This was most likely due to the depletion of PIP4Ks tending to reduce the cell viability in both wild type and depleted p53 backgrounds. Data from senescence assays showed that there was a trend of increasing number of senescing cells when *PIP4K2A/2B* was depleted, while silencing of p53 resulted in the opposite trend (Figure 5.14B). No significant interaction was found between p53 and PIP4K on senescent cells ($p=0.31$, 2-way-ANOVA), although depletion of the two PIP4K isoforms restored the senescence activity in p53 silenced cells. Data from both migration and senescence experiments suggested that there is an interesting interaction between p53 and *PIP4K2A/2B* in cell migration and senescence. Unfortunately, these data are not strong enough to prove the presence of synthetic lethal interaction.

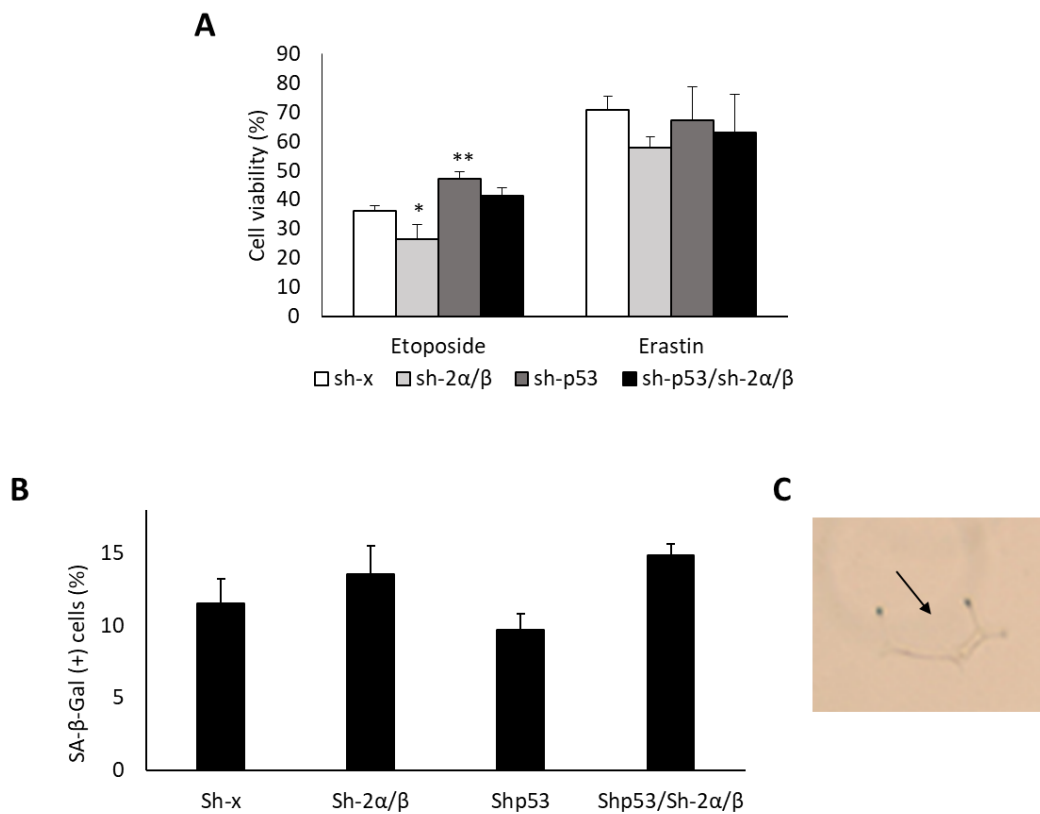


Figure 5.14 Effect of PIP4K and p53 depletion on cell viability and senescence. (A) Cells were treated with 100 μ M etoposide or 10 μ M erastin for 24 hours before incubation with MTT solution for 4 hours. The formazan blue crystals formed were dissolved with DMSO and the absorbance measured at 570nm. Graph indicates percentage \pm SEM of cell viability in each cell line. Graph shows results from one experiment performed in triplicate and represents three independent experiments (n=3). (* and ** indicate $p < 0.05$ and $p < 0.01$ respectively compared to Sh-x, one-way ANOVA). (B) Cells were treated with 2 μ M of etoposide for 48 hours before left growing for another 12 days in order to develop senescence. Cells then incubated with x-gal staining solution for 24 hours before observed under microscope and the x-gal positive cells counted. Graph showing percentage \pm SEM of x-gal positive cells for each studied cell line. Data show results from one experiment performed in triplicate and represent two independent experiments (n=2). (C) Images of x-gal positive cells. Photos were captured with Evos imaging suite at 10x magnification.

5.3 Discussion

5.3.1 Synthetic lethal interaction between p53 and PIP4K in tumour cells: a mutation-specific effect

TP53^{-/-}, *PIP4K2A*^{-/-}, *PIP4K2B*^{+/-} mice showed a dramatic reduction in spontaneous tumour formation compared to their *TP53*^{-/-}, *PIP4K2A*^{+/-}, *PIP4K2B*^{+/-} littermates (Emerling *et al.*, 2013), suggesting a synthetic lethal interaction between p53 and PIP4K in tumour cells. Current investigations intended to further explore the relationship between PIP4K and p53 in human tumour cell lines in a more controlled manner in order to elucidate how the two proteins cooperate to control cell transformation and growth. However, no synthetic lethal effect between p53 and *PIP4K2A/2B* was observed in U2OS cells. Another p53-wild type cell line, HCT116, was also used and similar to U2OS cells, a synthetic lethal effect was not observed in HCT116. Knockout of *PIP4K2B* or *PIP4K2A/2B* in the BT474 cell line however, did cause proliferation arrest and colony growth retardation under p53 inactivated condition as the cells were grown in 37°C. Thus, current investigations have reproduced the synthetic lethal effect in BT474 as shown by a previous study (Emerling *et al.*, 2013), and that this cell line can serve as good positive control. At this point, it is arguable whether the synthetic lethal interaction between PIP4K and p53 reported by Emerling *et al.*, (2013) was a 'universal' interaction present in all cancer cell types. Although this current study could be furthered in-depth by using the BT474 cell line as a model, the priority was to reveal whether this synthetic interaction initially observed in BT474 cells could be extended to other human cancer cell lines. This was in order to understand how this interaction could be exploited for the development of therapeutic interventions.

There are some differences between the findings from study by Emerling *et al.*, (2013) and this current study that should be highlighted. In this study, the synthetic lethal interaction was observed in BT474 cells with deleted *PIP4K2B* but not in cells in which the *PIP4K2B* gene was depleted through RNAi. Previously it was shown that the p53-PIP4K synthetic lethality was only observed when both 2A and 2B isoforms were silenced through the shRNA method, and depletion of single *PIP4K2A* or *PIP4K2B* did not show significant effect on cell growth. In the current study, it was shown that the knockdown of *PIP4K2A* or *PIP4K2A/2B* in BT474 cells could slightly reduce clonogenic growth, although the effect is not as strong as the *PIP4K2B* knockout. Although the same knockdown method was used, the different shRNA targeted sequences used could have caused the differences between the current study and the previous one. The position of a target site could affect the efficacy of the shRNA through formation of distinct secondary structure at different regions of the mRNA (Zhou and Zeng, 2009; Moore *et al.*, 2010). Using different target sequences for gene knockdown to get similar outcome is necessary to ensure target specificity. However, it is

intriguing to know whether findings from previous study could be replicated should similar shRNA target were used in this study, in order to ensure reproducibility across experiments. However, as the lethal interaction was found with the knockout method, the effort to produce the same shRNA construct directed towards 3' UTR of *PIP4K2B* like the previous study was halted.

This study showed that in U2OS cells, knockdown of both PIP4K isoforms increased senescence activity and triple depletion of *PIP4K2A/2B/TP53* slightly increased the senescence even more. The contribution showed by the reduction of p53 however was not significant compared to *PIP4K2A/2B* knockdown alone. Previous studies demonstrated that PIP4K could regulate senescence through its substrate, PtdIns5P, which is an oxidative stress regulator (Jones *et al.*, 2006, 2013; Keune *et al.*, 2012). PtdIns5P plays a role in H₂O₂-induced activation of Akt signalling, and PIP4K overexpression was reported to reduce the sensitivity of cancer cells to stress-induced cellular damage due to the reduction of PtdIns5P (Jones *et al.*, 2013). This suggested that inhibition of PIP4K signalling could be useful to increase tumour cell sensitivity to treatment with an oxidative stress approach. High reactive oxygen species and senescence activity were among other phenotypes previously reported in *PIP4K2A/2B* depleted BT474 cells which may have contributed to the lethal effect (Emerling *et al.*, 2013). In contrast, they observed no induction in senescence in p53 wild type cell lines, suggesting that deletion of p53 is necessary for the *PIP4K2A/2B* depletion-induced senescence to take place. However, data from the current study demonstrated that p53 deletion could not significantly increase the senescence activity following *PIP4K2A/2B* deletion, suggesting that the absence of p53 activity has different impact in U2OS and BT474 senescence.

The synthetic lethal phenotype which was observed in BT474 cells but not in U2OS and HCT116 cell lines, could suggest that there is a need for at least one or more factors to be present in addition to the absence of both p53 and PIP4K in order for the lethality to take place. BT474 expresses a mutated p53 protein that had been suggested by this study to be necessary for the synthetic lethal interaction to take place. Future studies should be conducted to compare the wild type BT474 with the cells having the endogenous mutated p53 removed and replaced with wild type p53 protein to further confirm the role of p53 in the cells. The activity of p53 in BT474 depends on the temperature that the cells are grown and another concern about this cell line are the changes in morphology with respect to the different temperatures as shown in Chapter 4. Differences in cell appearance in breast cancer cells were previously reported to be related to the expression of estrogen, progesterone and HER-2 receptor on the cells (Ibrahim *et al.*, 2009). Based on this data we can already expect that many changes take place aside from changes in p53 activity. What is more important is that these other temperature sensitive alterations may modulate how PIP4K knockdown affects cell behaviour.

BT474 also has an amplification of the *PIP4K2B* gene (Luoh *et al.*, 2004; Emerling *et al.*, 2013), leading to a high expression of *PIP4K2B* compared to other breast tumour cell lines. Thus, a relevant way to identify other cancer cells that could benefit from depleting PIP4K is by screening for other cancer cells with these two characteristics. In addition, the amplification of *PIP4K2B* could be due to the amplification of its adjacent gene *ERBB2*, as the co-amplification of both genes are highly correlated (Luoh *et al.*, 2004; Emerling *et al.*, 2013; Keune *et al.*, 2013). *ERBB2* is amplified in about 30% of breast cancer cell lines (Lacroix and Leclercq, 2004), and it is intriguing to know whether other p53 mutated cancer cell lines, with the intersection of *ERBB2* and *PIP4K2B* gene amplifications, will demonstrate a similar synthetic lethality interaction. Search results from the COSMIC (Tate *et al.*, 2019), Expression Atlas (Papatheodorou *et al.*, 2020) and GEMicCL (Jeong *et al.*, 2018) databases show that there are four cell lines with *TP53* bearing the temperature-sensitive E285K mutation including BT474. The other three cell lines however, do not have amplification of *PIP4K2B* or *ERBB2*. The databases also identified several other cell lines having a nonsense or frameshift *TP53* mutation with *PIP4K2B* and *ERBB2* gene amplification, which are the breast carcinoma cell lines EFM-192A, HCC202, and MDA-MB-361. These cell lines would be the most appropriate to investigate the synthetic lethal interaction, and if the interaction is then proven to exist, it will perhaps ease the path to study the molecular connection between the absence of p53 and the need for these cells to depend on PIP4K to survive.

P53 deletion alone could be insufficient to resemble the correct environment for synthetic interaction with loss of p53 activity shown by BT474. A study conducted in BT474 discovered a specific stress protein, Hsp90, to be essential for stabilisation of temperature-sensitive p53 mutation but showed no effect on wild type p53 (Müller *et al.*, 2005). This suggested that Hsp90 is a crucial factor for BT474 tumour activity. Hsp90 has been extensively studied in HER2 positive breast cancer cells and inhibition of Hsp90 was demonstrated to be effective in reducing BT474 growth on a xenograft model (Friedland *et al.*, 2014). We showed that BT474 transduced with shRNA against *TP53* had a dramatic reduction in clonogenic activity, which confirms the importance of the expression of mutant p53 in this cell line. Hsp90 and PI3K/Akt proteins also regulate each other's activity, and inhibition of both Hsp90 and PI3K/Akt activity showed a strong anti-tumour activity (Chatterjee *et al.*, 2013; Giulino-Roth *et al.*, 2017; Qin *et al.*, 2017). Therefore, there is a possibility that the synthetic lethal interaction observed in BT474 cells was due to alteration in the activity of PI3K pathway following *PIP4K2B* depletion that had affected Hsp90 activity. Future studies need to consider the involvement of this heat shock protein in studying the synthetic lethal interaction in mutated p53 cancer cells.

Another possible strategy to identify the special characteristic of BT474 that causes the p53-PIP4K interaction is by comparing the characteristics of the cells when grown at 37°C and 32°C. The

E285K mutation in p53 had also been studied in another cell line, IPH-926, which is a human infiltrating lobular breast cancer. Reconstitution of wild type p53 in the cells exposed about 60 genes differentially expressed compared to the mutated one (Christgen *et al.*, 2012). Among the highlighted genes were MDM2, CDKN1A, and PHLDA3 that were upregulated under wild type p53 activity. PHLDA3 is an Akt inhibitor regulated by p53, which also shows an anti-tumour activity (Kawase *et al.*, 2009). Thus, it is possible that in cells lacking PHLDA3 and aberrant p53 function, PIP4K is necessary for survival. While the possibilities could expand endlessly, a good strategy is needed to find the key factor determining the PIP4K-p53 synthetic lethal interaction. The lack of discovery for more cell lines showing similar interaction may suggest that it is exclusive for BT474 cells.

Apart from the lethal effect in the cells, Emerling *et al.* (2013) also demonstrated how depletion of *TP53* and *PIP4K2A/2B* in mice can dramatically reduce the formation of spontaneous tumours. While it is a very interesting finding, it is also important to understand that the genes were depleted in all tissues, thereby likely deregulating complex physiological processes. As discussed in the general introduction, PIP4Ks were found to have different roles in different physiological systems such as the immune system. Reduced spontaneous tumour formation shown by the mice with reduced PIP4K could in part be due to increased tumour surveillance activity of the immune system. Moreover, deletion of *PIP4K2B* in mice was reported to increase insulin sensitivity (Lamia *et al.*, 2004) and therefore could discourage development of spontaneous cancer caused by high insulin levels. The absence of spontaneous tumour formation observed in the mice is therefore not a perfect model for a cell-autonomous synthetic lethal interaction between p53 and PIP4K.

This study showed that inhibition of p53 does not always lead to similar phenotypes in different cancer cell lines. Although the deletion of p53 in U2OS resulted in higher clonogenic activity, such an effect is not observed in HCT116 cells. A study also reported no differences in HCT116 cell growth between HCT116 p53^{-/-} and p53^{+/+}, unless they are co-cultured with fibroblast (Hayashi *et al.*, 2016). HCT116 was reported to have wild type p53 (Liu and Bodmer, 2006). However, high point mutation rate in the cells could partly explain why some aspects of p53 functions are different (Kaeser *et al.*, 2004). Therefore, mutations in a cell line also need to be considered in order to determine the most appropriate model to study the synthetic lethal interaction.

The opposite phenotypes observed between different methods of PIP4K depletion are something that should not be left undiscussed. For example, *PIP4K2A* knockout leads to the formation of bigger colonies, whereas knockdown of the same gene inhibits the colony growth on soft agar. The knockdown phenotype however, was temporary and the effects seem 'reversed'

after one more passage of growth. Growing the PIP4K knocked down cells for a longer period of time led to slightly higher clonogenic activity, and partly resembles the phenotypes shown by cells with PIP4K gene knockout. This transient effect that was shown by all the knockdown constructs tested could probably depict the transition period of cells trying to overcome the modulation. shRNA actions are targeted at the mRNA level while CRISPR knockout method acts directly on the gene sequence. Although the PIP4K depleted cells produced through these two methods were used for experiments within a similar time frame, the different amount of time taken for both shRNA and the Cas9 process to take place in the cells might affect the phenotype shown when the cells were used for the experiment. However, there is no exact comparison between the timeline process between the two. Morgens *et al.* (2016) stated that the different timing of gene knockdown and knockout might be a reason they saw differences in gene expression, although it is not clear how long of a duration difference will be required to make a significant difference. A more stable effect shown by gene knockout could be a more accurate depiction of *PIP4K2A* action in the cells. Moreover, the slightly smaller size of colonies produced by cells overexpressing *PIP4K2A* grown for a longer duration, similar to a previous report (Jones *et al.*, 2013), might also support this argument. In addition, the *PIP4K2A* knockdown phenotypes could not be rescued by overexpression of exogenous *PIP4K2A*. This could suggest that the phenotype observed during the early passage could be an off-target effect although it is hard to explain why different shRNA constructs show similar observations. A global genomic study will be a useful method to try to understand the different events taking place in the cells following gene knockdown and knockout of PIP4K.

Findings from these results suggested that the p53-PIP4K synthetic lethality interaction is not universal but possibly limited to certain tumour cells bearing specific p53 mutation(s). Proper strategies and careful planning are needed in order to identify the complete conditions needed for the lethal effect to take place. The method used to modulate the gene of interest should also be verified in order to identify the true effect in our native physiological system. Should the synthetic lethal conditions be known in the future, it will be a significant contribution to oncology treatment as well as cancer signalling knowledge.

Chapter 6 Investigating the role of PIP4K in PI3K/Akt signalling and possible interaction with p53

6.1 Introduction

PI3K/Akt/mTOR signalling is commonly studied in relation to cancer due to their frequent dysregulation. Genomic alterations of components of the pathway, such as the α subunit of PI3K (PIK3CA), PTEN, and Akt in cancers, often lead to aberrant activation of the pathway. This has resulted in demand for an ideal inhibitor of the pathway to be used as an anticancer therapy (Janku *et al.*, 2018). PIP4K has been reported to both attenuate and increase the activation of the PI3K/Akt pathway in different cells, suggesting that this kinase could be a potential target for therapy in diseases including cancer (Carricaburu *et al.*, 2003; Bulley *et al.*, 2016; Shin *et al.*, 2019). This study has shown that depletion of *PIP4K2A* and *2B* isoforms in cancer cell lines could affect the cells' proliferation and clonogenic potential (see Chapter 5), which could be due to alteration in the activity of PI3K/Akt/mTOR signalling. To test this hypothesis, U2OS cells with *PIP4K2A* and *2B* depleted through knockdown, knockout, or the auxin-induced degradation technique (Natsume *et al.*, 2016), as well as BT474 cells with *PIP4K2A* and *2B* depleted through knockout were utilised to examine changes in PI3K/Akt/mTOR activation. As the insulin-PI3K signalling cascade is considered to be a pro-tumorigenic pathway (Hopkins *et al.*, 2020), cells in the experiments were stimulated with insulin and the activation of the PI3K/Akt/mTOR pathway was observed through the phosphorylation of Akt ser473 and S6 ser235/236. In addition to the depletion of *PIP4K2A* and *2B*, cells with deleted *TP53* were also used in this experiment, as this tumour suppressor is widely reported to be involved in PI3K/Akt signalling (Abraham and O'Neill, 2014). As the current study showed that the loss of p53 activity in different cancer cell lines showed different effects due to PIP4K depletion (Chapter 5), it will be interesting to identify any possible effects of combined loss of both PIP4K and p53 towards PI3K/Akt/mTOR pathway activation in different cell lines.

6.2 Results

6.2.1 Effect of *PIP4K2A* and *2B* depletion and p53 deletion on the PI3K/Akt pathway activation

U2OS cells with *PIP4K2A* and/or *2B* isoforms depleted through RNAi with deleted *TP53* were generated by the methods described in Chapter 4. The cells were stimulated with insulin and protein lysates were used for western blot analysis to study the changes in Akt ser473 and S6 ser235/236 phosphorylation. The results indicated that insulin stimulation causes an increase in Akt and S6 phosphorylation in all samples (Figure 6.1A & C). There was a trend of increased Akt phosphorylation in stimulated *PIP4K2A* and/or *PIP4K2B* depleted cells compared to the Sh-x control, while no differences in S6 phosphorylation can be observed. This suggests that modulation of PIP4K affects the upstream PI3K/Akt more than mTOR signalling. No clear differences in Akt phosphorylation were observed between cells with *PIP4K2A* and *PIP4K2B* knockdown, indicating that both isoforms have the same magnitude of effect towards the pathway. Cells with deleted p53 also showed higher Akt phosphorylation compared to the Sh-x control, which is in line with previous evidence (Feng, 2010). Depletion of *TP53* together with *PIP4K2B* or *PIP4K2A/2B* showed no changes in the Akt and S6 phosphorylation compared to removal of *TP53* only. This observation indicated that depletion of *PIP4K2A* and/or *PIP4K2B* can increase Akt phosphorylation without enhancing the effect of *TP53* depletion, suggesting crosstalk between PIP4K and p53 in the pathway.

To identify a possible factor connecting PIP4K and p53 in the PI3K/Akt pathway, PTEN expression, another factor potentially connecting the two proteins in the pathway, was examined. PTEN has a negative effect on Akt pathway activation (Sun *et al.*, 1999) and its expression is positively regulated by p53 (Stambolic *et al.*, 2001). However, there is no direct interaction between PIP4K and PTEN reported so far, raising an interest to determine the presence of a possible interaction between the two proteins. To test this hypothesis, U2OS cells with *PIP4K2A* and/or *2B* knockdown and *TP53* knockout were probed with a PTEN antibody and changes in the expression of this tumour suppressor protein were examined by western blot analysis (Figure 6.1B & D). Results demonstrated that deletion of *TP53* leads to a lower expression of PTEN; consistent with a previous study (Stambolic *et al.*, 2001). RNAi disruption of *PIP4K2A* and/or *PIP4K2B* also caused a reduction in PTEN expression, with the strongest reduction seen in *PIP4K2A* knockdown cells. This observation indicates that the changes in PI3K/Akt activation observed following the PIP4Ks and p53 depletion was partly due to decreased expression of PTEN.

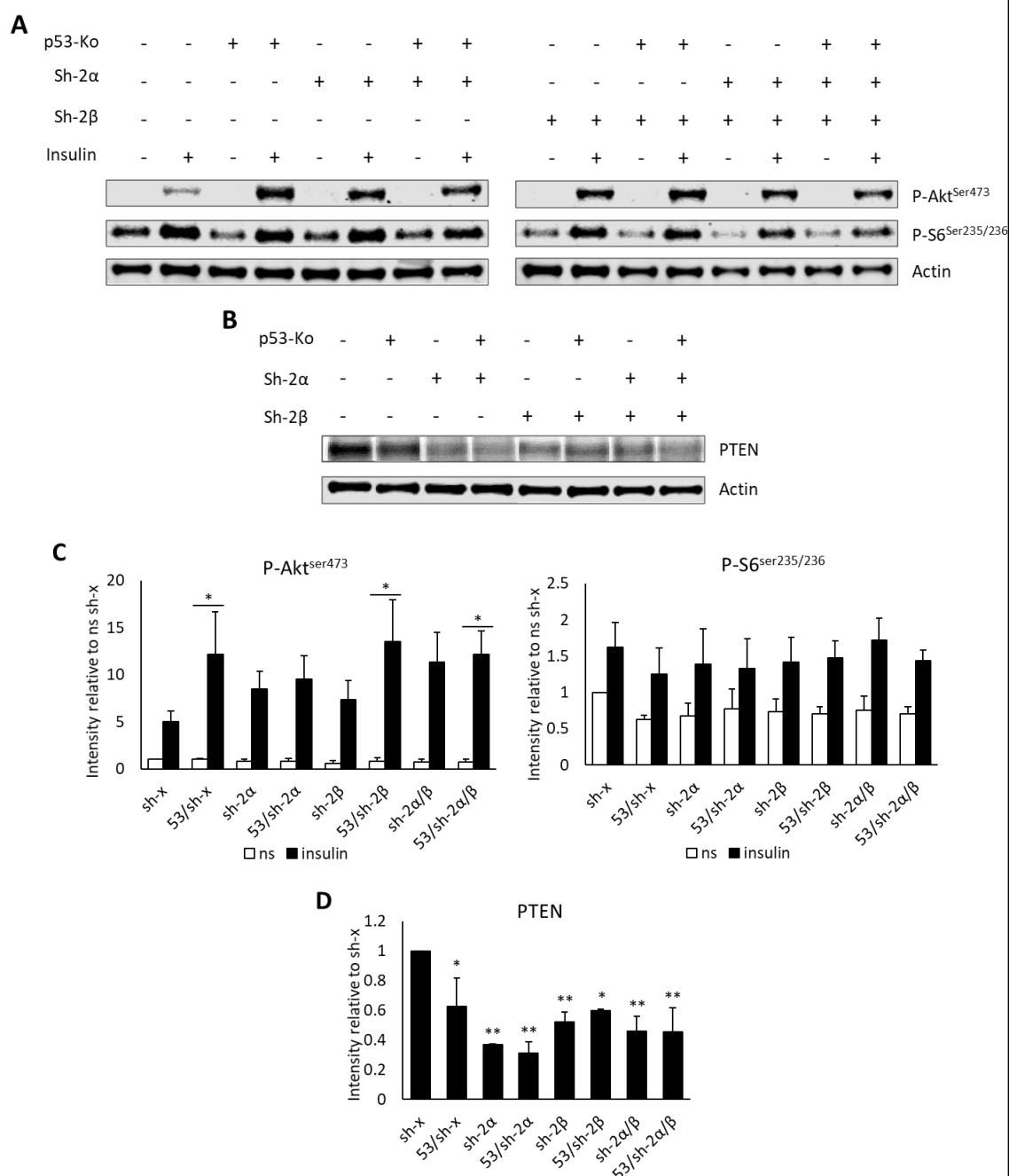


Figure 6.1 Changes in Akt and S6 phosphorylation and PTEN expression in U2OS cells with *PIP4K2A* and/or *2B* knockdown and *TP53* knockout. Cells were serum-starved for 24 hours before stimulated with 10 $\mu\text{g/ml}$ insulin for 10 minutes. Lysates obtained were utilised for western blot analysis to examine (A) changes in Akt and S6 phosphorylation and (B) PTEN expression. Actin acts as a loading control. (C&D) Densitometry analysis of the blots. Signal intensity for Akt Ser473, S6 Ser235/236, and PTEN were normalised to actin protein levels. Results are expressed as mean \pm SEM ($n=3$) relative signal intensity. For (C), * indicates $p<0.05$ compared to the corresponding ns, and for (D), * and ** indicate $p<0.05$ and 0.01 respectively compared to sh-x, one-way ANOVA with Tukey's (C) or Dunnett (D) post-hoc analysis. ns: non-stimulated.

A similar experiment as above was conducted in U2OS cells with *PIP4K2A* and *2B* isoforms knocked out through the lentiviral CRISPR/Cas9 method to confirm the role of PIP4K in the PI3K/Akt signalling. Findings indicated that there was an increase in Akt phosphorylation in cells with *PIP4K2A*, *PIP4K2B* and *TP53* knockout upon insulin stimulation (Figure 6.2A & C). However, *PIP4K2A* knockout cells only slightly increased the Akt phosphorylation compared to the control cells, while *PIP4K2B* knockout cells showed a stronger increase in Akt phosphorylation, comparable to the *TP53* only deleted cells. PTEN expression was also examined in these cells and results showed that there were no changes in PTEN expression in *PIP4K2A* knockout cells while *PIP4K2B* knockout cells showed a reduction in PTEN expression (Figure 6.2B & D). Both PIP4Ks knockdown and knockout methods showed that the high Akt phosphorylation following PIP4K isoform silencing was accompanied by reduced PTEN expression. The differences between PIP4K isoforms knockdown and knockout cells can be seen on *PIP4K2B* depletion, as knockout of this gene caused a strong increase in Akt phosphorylation while the gene knockdown only showed a slight effect on Akt phosphorylation. This discrepancy could be due to different levels of *PIP4K2B* presence in the cells, in which gene loss due to knockout produced a more significant effect.

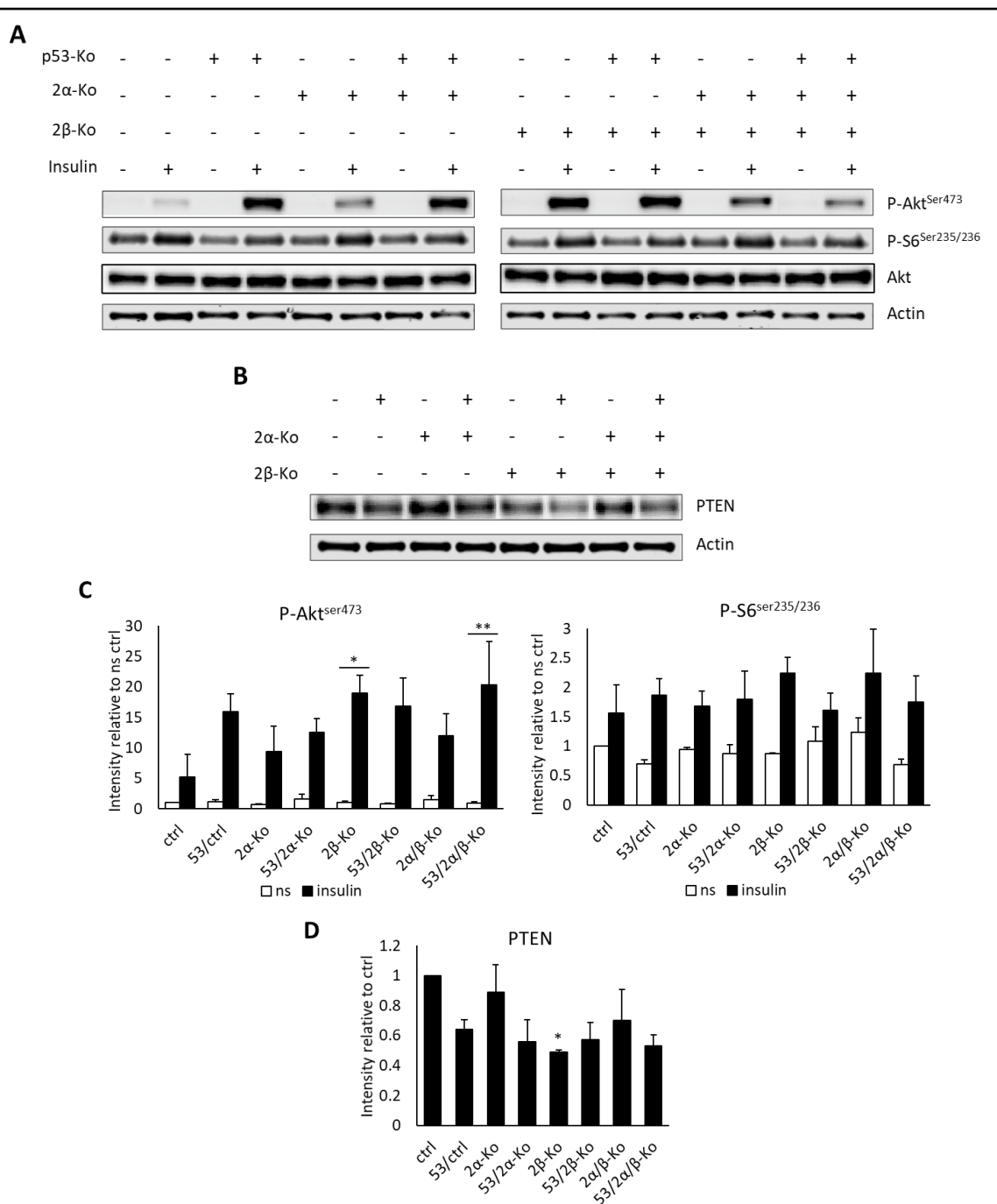
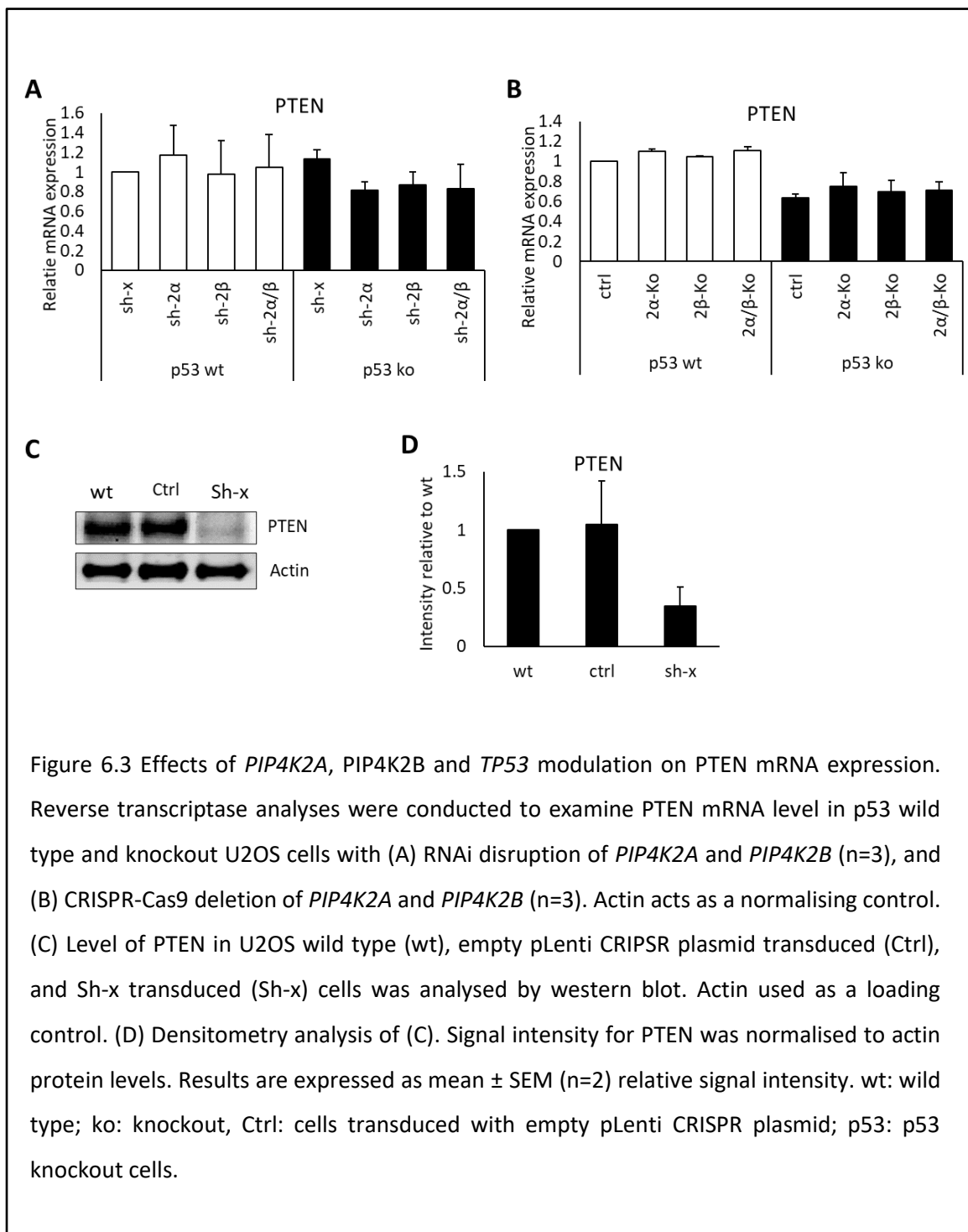


Figure 6.2 The effect of *PIP4K2A*, *PIP4K2B* and *TP53* knockout on Akt and S6 phosphorylation and PTEN expression in U2OS cells. Cells were serum-starved for 24 hours before stimulated with 10 $\mu\text{g/ml}$ insulin for 10 minutes. Lysates obtained were utilized for western blot analysis to study the (A) changes in Akt and S6 phosphorylation and (B) PTEN expression. Actin acts as a loading control. 2 α -Ko: *PIP4K2A* knockout, 2 β -Ko *PIP4K2B* knockout. (C&D) Densitometry analysis of the blots. Signal intensity for Akt Ser473, S6 Ser235/236, and PTEN were normalised to actin protein levels. Results are expressed as mean \pm SEM (n=3) relative signal intensity. For (C), * indicates $p < 0.05$ compared to the corresponding ns, and for (D), * and ** indicate $p < 0.05$ and 0.01 respectively compared to ctrl, one-way ANOVA with Tukey's (C) or Dunnett (D) post-hoc analysis. ns: non-stimulated.

P53 is known to positively regulate PTEN mRNA transcription (Stambolic *et al.*, 2001). However, it is unclear whether the low level of PTEN following *PIP4K2A* and *2B* isoforms removal was due to interruption at the mRNA level as well. Therefore, reverse transcriptase experiments were conducted to identify potential changes in PTEN mRNA level following the *TP53* and *PIP4K2A* and *2B* gene modulation. In PIP4Ks knockdown cells, there were no significant changes in PTEN mRNA expression in p53 knockout compared to p53 wild type cells (Figure 6.3A). Deletion of p53 in PIP4Ks knockout set also shows no significant changes in mRNA level. However, all four cell lines had a lower mRNA level by 20-30% compared to the control (Figure 6.3B). RNAi disruption of *PIP4K2A* and/or *2B* gene in p53 wild type cells caused no clear changes in the PTEN expression compared to their respective control, while in p53 knockout cells, *PIP4K2A* and/or *2B* knockdown tend to decrease the mRNA expression of PTEN (Figure 6.3A). In cells with *PIP4K2A* and *2B* knocked out by CRISPR-Cas9, silencing *PIP4K2A* and/or *2B* in both p53 wild type and knockout cells showed no changes in PTEN mRNA level compared to their respective control (Figure 6.3B). This suggests that depletion of p53, but not PIP4K, decreases PTEN transcription level. Between the two experiments, changes in PTEN mRNA level following p53 knockout, as shown by PIP4Ks knockout control were more consistent with the previously reported results (Stambolic *et al.*, 2001). This observation is perplexing as in both PIP4Ks knockdown and knockout experiments, the same p53 knockout cells were used. The difference was that for the PIP4Ks knockdown set, the p53 knockout control cells were transduced with lentivirus expressing a non-targeting shRNA (Sh-x) sequence, whereas the control cells for PIP4Ks knockout set were transduced with an empty pLenti CRISPR plasmid.

To identify possible factor that could explain the contradicting observation, PTEN protein levels in U2OS wild type, PIP4K knockout control (transduced with empty pLenti CRISPR plasmid), and PIP4K knockdown control (transduced with pLKO.1 plasmid expressing Sh-x sequence) cells were analysed and compared by western blot analysis. Results showed that there was a clear reduction in the level of PTEN in the PIP4K knockdown control compared to wild type cells (Figure 6.3C & D). There was no clear explanation for this observation, although possible factors will be addressed in the discussion. However, based on the results shown by PIP4Ks knockout cells' set alone, it could be concluded that p53 deletion reduces PTEN transcription level while the decreased PTEN protein level following PIP4K loss was not due to disruption in PTEN transcription activity.



Data from Chapter 5 (section 1.2.1) suggested that silencing *PIP4K2B* in the BT474 cell line by CRISPR knockout leads to growth arrest that was not observed in the U2OS cell line. Therefore, it is intriguing to analyse the insulin activated PI3K/Akt pathway experiment in this cell line, to determine whether changes in the Akt phosphorylation is also different from what was observed in U2OS cells. BT474 cells grown in 37°C incubator were serum starved for 24 hours before being stimulated with 10µg/ml of insulin for 30 minutes, and the lysates obtained were used to study Akt and S6 phosphorylation, as well as PTEN expression. A longer duration of insulin stimulation was used for this cell line due to its lack of growth response towards insulin (Mayer *et al.*, 2008). Result showed that deletion of *PIP4K2A* and/or *2B* reduced the phosphorylation of Akt at ser473, with a stronger effect shown by *PIP4K2A* knockout compared to *PIP4K2B* knockout cells (Figure 6.4A). *PIP4K2A* knockout cells also tend to attenuate S6 phosphorylation, suggesting that *PIP4K2A* depletion reduced activation of PI3K/Akt/mTOR pathway. Moreover, PTEN expression was slightly increased in BT474 cells with *PIP4K2A* and/or *2B* knocked out (Figure 6.4B), which is opposite to what was seen in U2OS cells. These data could suggest that in the BT474 cell line, *PIP4K2A* and *2B* knockout leads to reduced activation of PI3K/Akt pathway and increased PTEN level. However, there is also a possibility that the PIP4K isoforms depletion could have just delayed the phosphorylation, instead of inhibited the pathway activation. Since the insulin stimulation was administered in single time frame only (30 minutes), it is hard to make any conclusion regarding this matter.

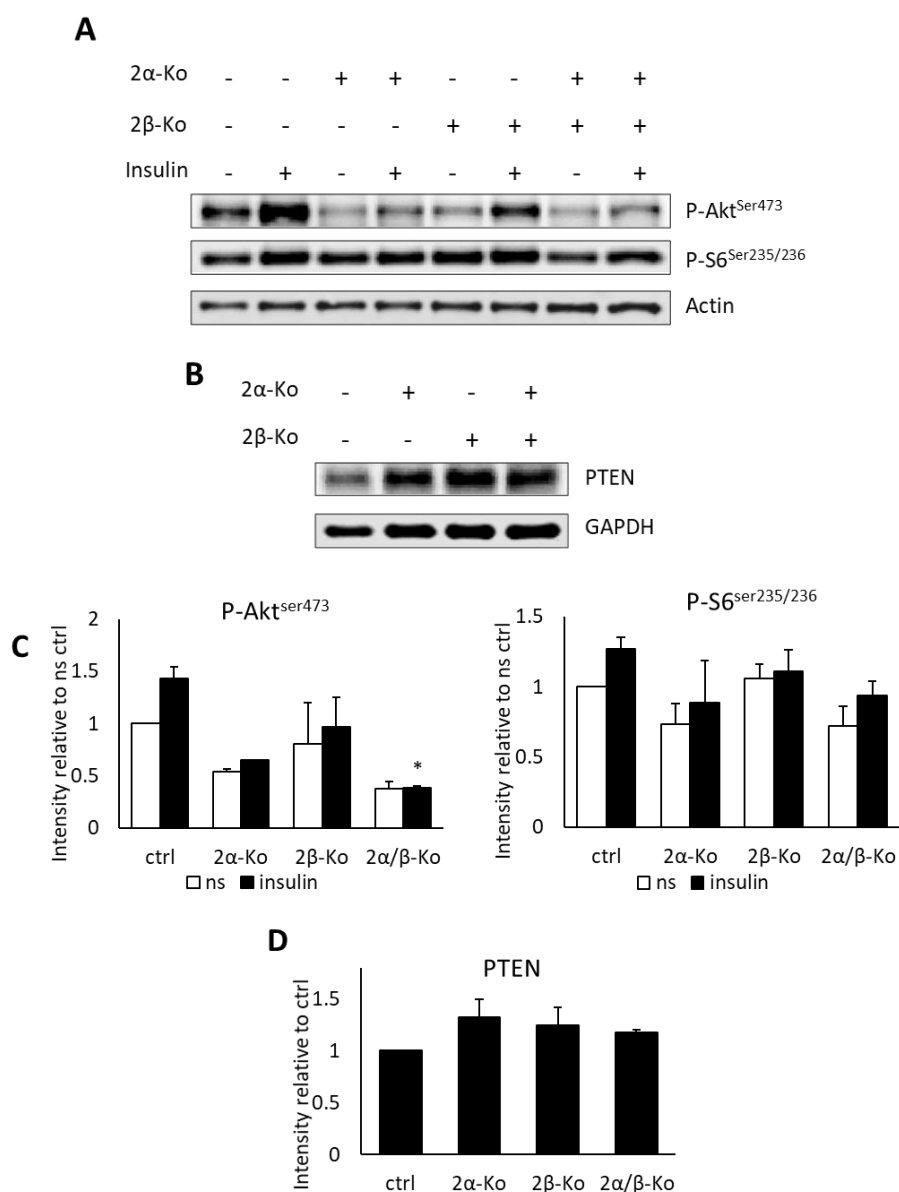
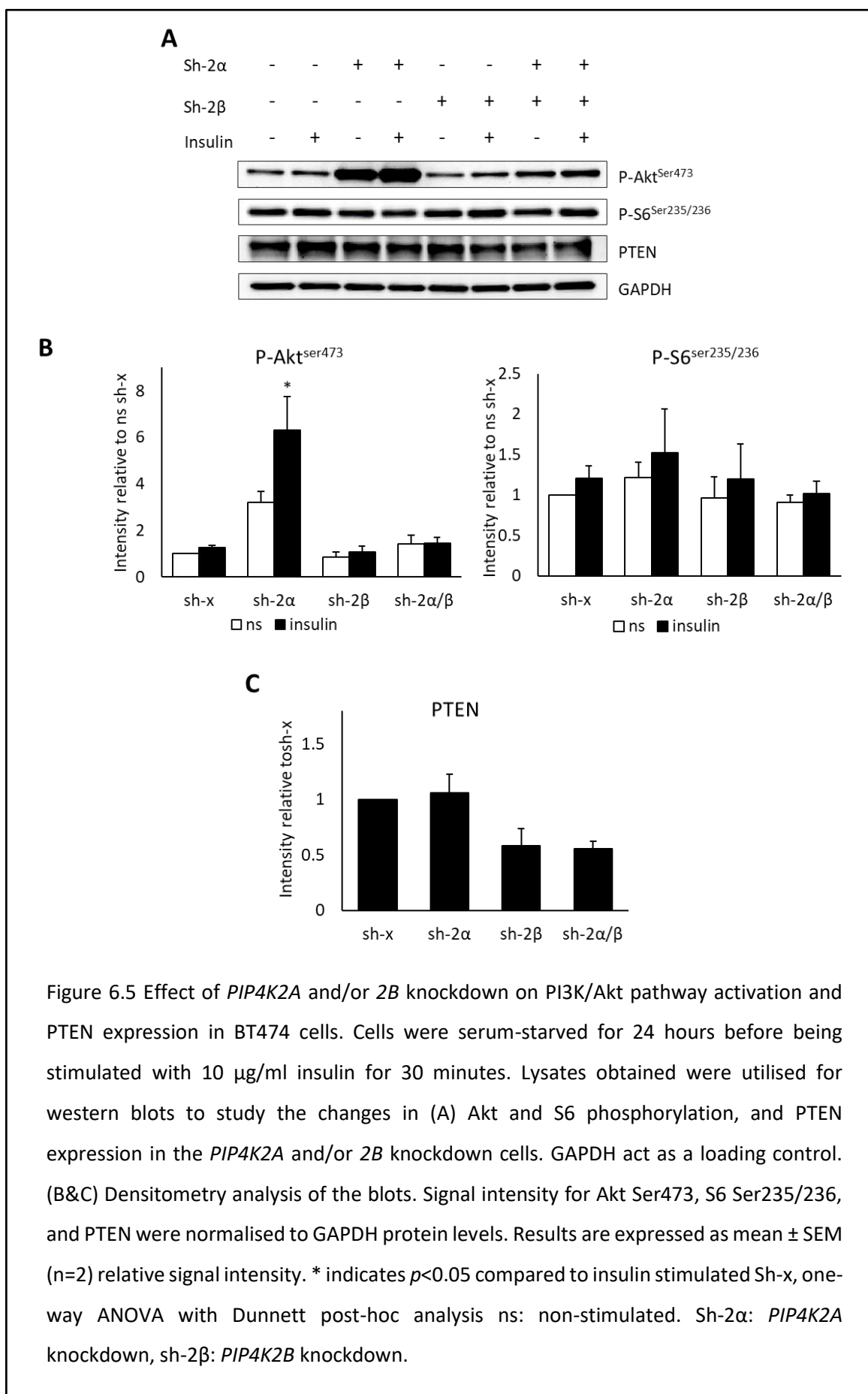


Figure 6.4 Effect of *PIP4K2A* and/or *2B* knockout on PI3K/Akt pathway activation and PTEN expression in BT474 cells. Cells were serum-starved for 24 hours before being stimulated with 10 μ g/ml insulin for 30 minutes. Lysates obtained were utilised for western blots to study the changes in (A) Akt and S6 phosphorylation and (B) PTEN expression in the *PIP4K2A* and/or *2B* CRISPR-Cas9 knockout cells. Actin and GAPDH act as loading controls. 2 α -Ko: *PIP4K2A* knockout, 2 β -Ko *PIP4K2B* knockout. (C&D) Densitometry analysis of the blots. Signal intensity for Akt Ser473, S6 Ser235/236, and PTEN were normalised to actin or GAPDH protein levels. Results are expressed as mean \pm SEM (n=2) relative signal intensity. * indicates $p < 0.05$ compared to insulin stimulated ctrl, one-way ANOVA with Tukey's post-hoc analysis. ns: non-stimulated.

Current data however contradicted the previous finding by Emerling *et al.*, (2013) that showed double depletion of *PIP4K2A/2B* in BT474 by shRNA caused increased Akt phosphorylation. To determine whether the previous finding could be replicated and that the discrepancy could be due to different methods of PIP4K depletion, BT474 cells with *PIP4K2A* and/or *2B* silenced through shRNA were used to study changes in their Akt and S6 phosphorylation. The cells were serum-starved for 24 hours and stimulated with 10µg/ml of insulin for 30 minutes, and the lysates were utilised for western blot analysis. Results showed that there was no significant difference in Akt phosphorylation between insulin stimulated and non-stimulated cells in the control and *PIP4K2B* knockdown group. *PIP4K2A* knockdown resulted in a higher Akt phosphorylation even in the non-stimulated cells compared to the control group, suggesting an increased in the phosphorylation of its basal Akt protein. *PIP4K2A/2B* double knockdown cells on the other hand, showed a trend of increased Akt phosphorylation in the non-stimulated samples compared to the control group, with no significant difference compared to their respective stimulated samples. Explanation regarding this observation is yet to be determined. (Figure 6.5A & B). No prominent changes could be seen in S6 phosphorylation and PTEN expression following the *PIP4K2A* and/or *2B* knockdown (Figure 6.5A & C). There was no clear relationship between changes in Akt phosphorylation and PTEN expression to explain the current finding. However, the differences between findings showed by BT474 cells with PIP4Ks depleted through knockout and knockdown could be due to the different methods of depletion used.



6.2.2 Identifying the effect of *PIP4K2A* and *PIP4K2B* acute depletion on the PI3K/Akt pathway activation and PTEN expression

Previous studies suggested that PIP4K loss could have both a positive and negative effect on the PI3K/Akt/mTOR pathway, depending on the duration of the protein depletion (Bulley *et al.*, 2016). To determine whether different effects on Akt and S6 phosphorylation levels can be seen as the PIP4K is rapidly removed in the U2OS cell line, the same insulin stimulated PI3K/Akt/mTOR experiment was also conducted in U2OS cells that have PIP4K2 α or 2 β degraded by auxin inducible degron (AID) system, as described in Chapter 4. The cells were treated with auxin for either 16 or 24 hours and the protein lysates were obtained for western blot analysis. Initial findings suggested that for both PIP4K2 α and 2 β isoforms, acute depletion of the protein after 16 hours of auxin treatment led to reduced phosphorylation of Akt and S6 (Figure 6.6A). After 24 hours of auxin treatment, PIP4K2 α -mAID cells also showed a reduction in Akt phosphorylation, while PIP4K2 β -AID cells exhibited no or little effect on Akt and S6 phosphorylation (Figure 6.6C). These results however were inconsistent, as in other experiments, 16 hours of auxin treatment led to increased Akt phosphorylation (data not shown). To understand if this inconsistent Akt and S6 phosphorylation patterns are in agreement with PTEN levels in cells, the cells were also probed with a PTEN antibody and analysed by western blot (Figure 6.6B & D). There were only slight changes in PTEN expression except for the 2 α -mAID cells receiving 24 hours of auxin.

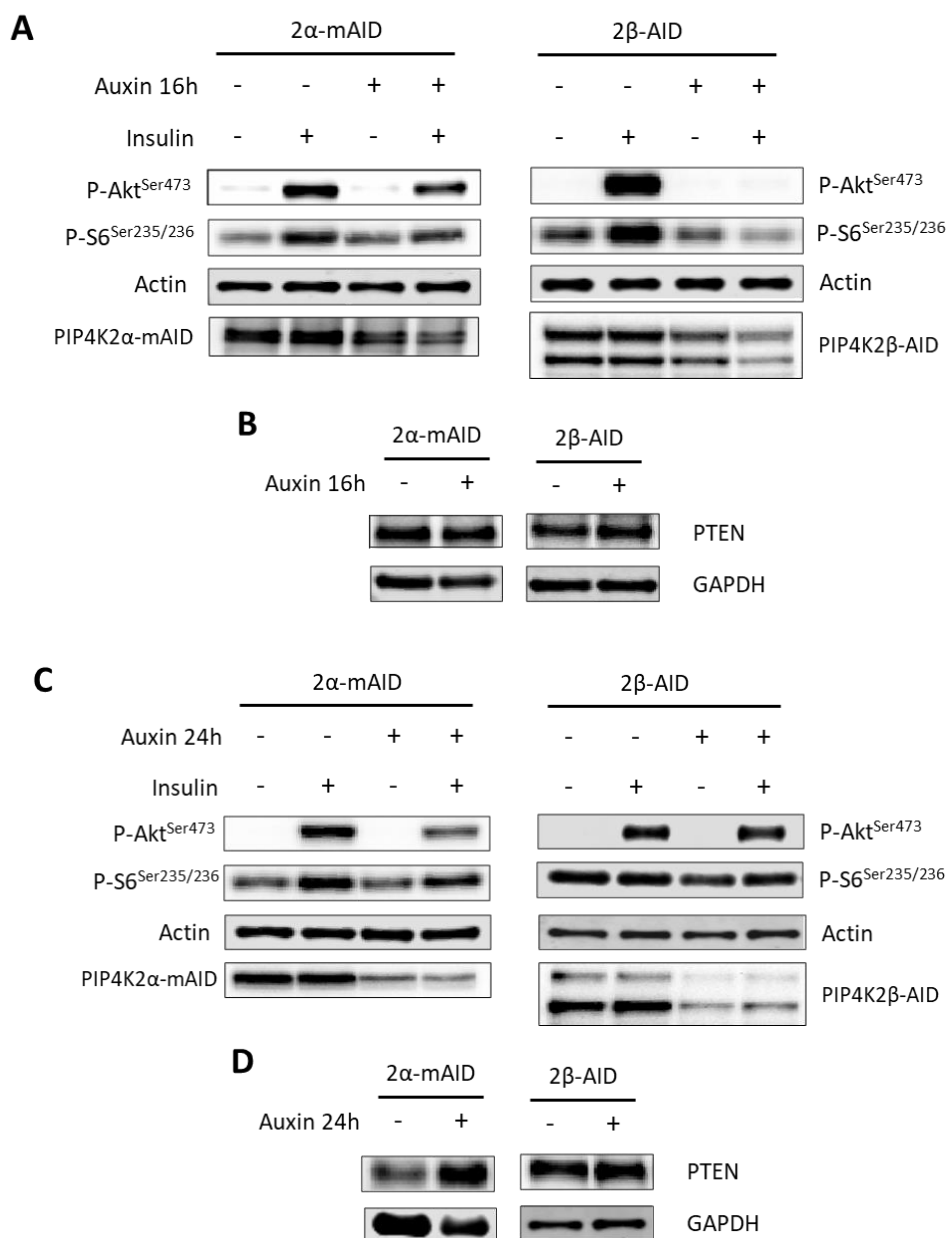
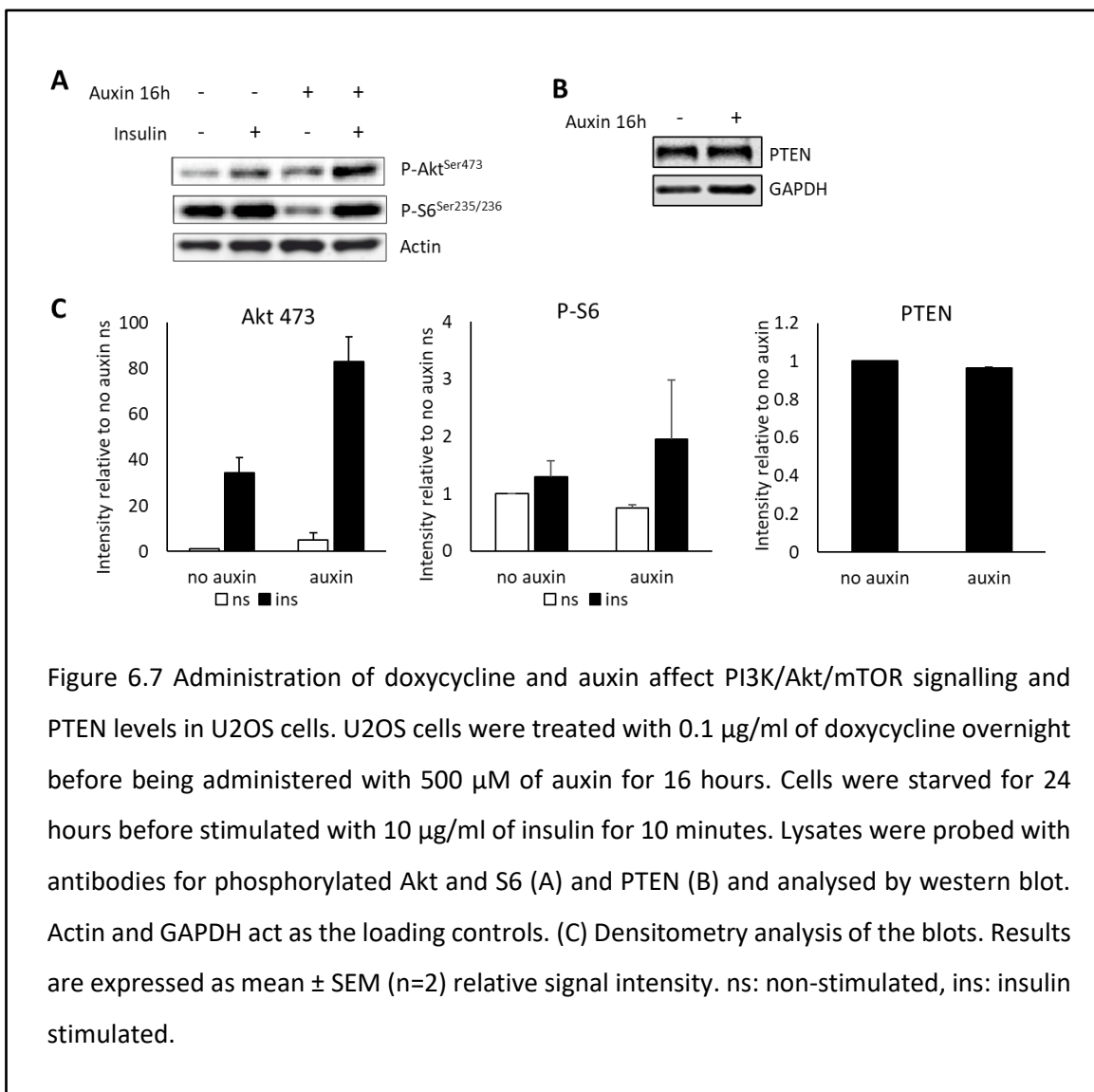


Figure 6.6 Attempts to determine the effects of acute depletion of PIP4K2 α and 2 β on PI3K/Akt/mTOR signalling and PTEN levels. PIP4K2 α -mAID and PIP4K2 β -AID cells were treated with 0.1 μ g/ml of doxycycline overnight prior to administration of 500 μ M of auxin for (A & B) 16 and (C & D) 24 hours before being stimulated with 10 μ g/ml of insulin. Cells were probed with antibodies for phosphorylated Akt and S6 (A & C) and PTEN (B & D) and analysed by western blot. Actin and GAPDH act as loading controls.

Given the inconsistent effect of acute depletion of PIP4K2 α and 2 β on PI3K/Akt/mTOR signalling, attempts to confirm whether the observed effects were due to the loss of PIP4K in the cells or from the administration of doxycycline and auxin (dox-aux) were undertaken. To determine whether dox-aux treatment affected the PI3K/Akt/mTOR signalling, wild type U2OS cells, which are the parental cell line for the two PIP4K-AID tagged cells, were treated with doxycycline overnight followed by auxin for 16 hours before being stimulated with insulin. Protein lysates of the cells were then obtained to study changes in Akt and S6 phosphorylation, including PTEN expression by western blot analysis. Following 16 hours of auxin treatment, the phosphorylation of Akt increased compared to control cells (Figure 6.7A & C). PTEN expression did not show any changes compared to untreated control cells following 16 hours of auxin treatment (Figure 6.7B & C). These data suggested that dox-aux treatment affects PI3K/Akt/mTOR signalling independently.



It is still unclear whether the treatment effect was specifically caused by the auxin or the tet-on activator doxycycline. Therefore, the Akt and S6 phosphorylation, as well as PTEN expression was compared between U2OS wild type, 2 α -mAID, and 2 β -AID cells treated with auxin for 16 or 24 hours. The cells either had the doxycycline removed before the addition of auxin or added together with the auxin. The cells then received insulin stimulation. Western blot analysis showed clear changes in Akt phosphorylation in U2OS wild type cells but not in the AID-tagged cells (Figure 6.8A & B). There was also no specific pattern observed to help in understanding which treatment agent was causing the fluctuation in Akt phosphorylation and PTEN expression. Western blot analysis also showed that the 2 α -mAID cells had stronger phosphorylation of Akt at Ser473 as well as S6 compared to the other two cell lines. This finding could suggest that there is an increase in the activation of PI3K/Akt signalling following auxin treatment in the 2 α -mAID tagged cells irrespective of the changes in PIP4K2 α level. Meanwhile, the unchanged expression of PIP4K2 α and 2 β in the wild type cells indicate that the dox-aux treatment does not affect the endogenous levels PIP4Ks. Based on these data, it is difficult to draw a conclusion regarding the effect of acute PIP4K removal on the PI3K/Akt pathway. Both doxycycline and auxin did not show a consistent effect on PTEN expression and Akt phosphorylation when administered in U2OS cells. However, both PIP4K2 α -mAID and 2 β -AID cells also demonstrated different patterns of changes in Akt phosphorylation and PTEN expression compared to wild type cells. These findings at most could suggest that acute depletion of PIP4K2 α or 2 β exhibits certain effects towards the PI3K/Akt signalling that are unclear due to the possible side effect shown by the doxycycline and auxin treatment.

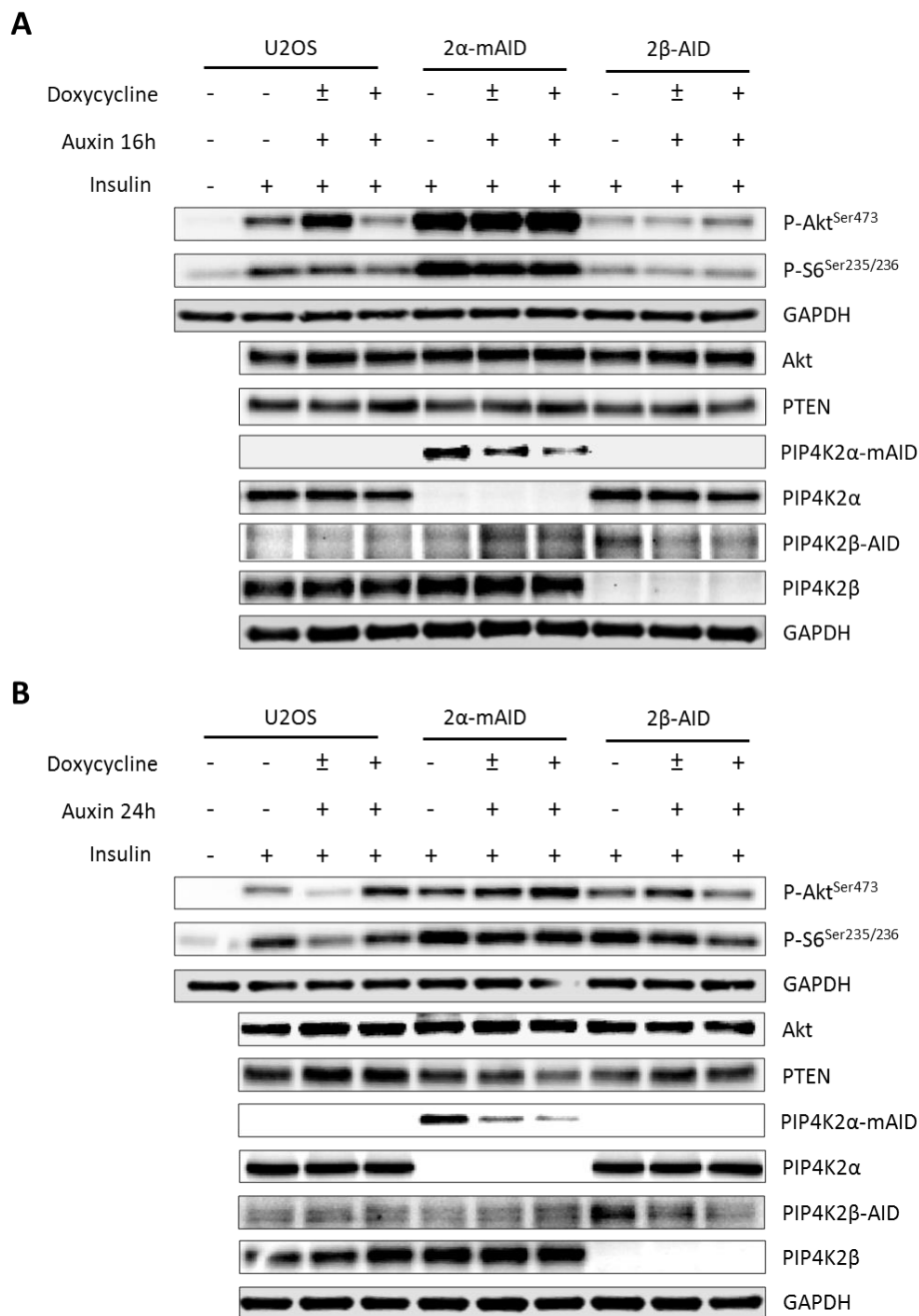


Figure 6.8 Administration of auxin with and without doxycycline being removed show different effects on PTEN expression and Akt and S6 phosphorylation. U2OS, PIP4K2 α -mAID, and PIP4K2 β -AID cells were treated with 0.1 μ g/ml of doxycycline overnight, followed by either removal of doxycycline before (\pm) or added together (+) with 500 μ M of auxin for (A) 16 hours, or (B) 24 hours. Cells were starved for 24 hours within the treatment time before being stimulated with 10 μ g/ml of insulin for 10 minutes. Lysates were utilised for western blot analysis. Actin and GAPDH act as loading controls.

6.3 Discussion

6.3.1 *PIP4K2A* and *PIP4K2B* depletion modulates PI3K/Akt signalling through PTEN.

My experiments indicate that PIP4Ks have a negative effect on the activation of PI3K/Akt pathway in U2OS cells. Similar observations were also shown by other studies conducted in different cells from different organisms (Carricaburu *et al.*, 2003; Lamia *et al.*, 2004; Ramel *et al.*, 2009; Emerling *et al.*, 2013; Jones *et al.*, 2013; Jude *et al.*, 2015; Sharma *et al.*, 2019; Shin *et al.*, 2019; Wang *et al.*, 2019). Previously, the negative effect of PIP4K on this pathway was focused on the role of PtdIns5P in inhibiting PtdIns(3,4,5)P₃ and Akt phosphatases (Carricaburu *et al.*, 2003; Ramel *et al.*, 2009). The more recent studies highlighted the functions of PIP4Ks in destabilising PI3K and suppressing PIP5K actions (Shin *et al.*, 2019; Wang *et al.*, 2019). In this study, the expression of PTEN was also found to be affected by PIP4K silencing. PTEN is a known negative regulator of PI3K/Akt, and its transcription is positively regulated by p53 (Stambolic *et al.*, 2001). Current findings showed that individual knockdown of *PIP4K2A* or *2B* leads to high Akt phosphorylation and low PTEN expression. A similar outcome was also observed in cells with P53 and *PIP4K2B* knockout. Therefore, it could be concluded that together with p53, PIP4K negatively regulates the Akt pathway in U2OS cells partly through decreasing the expression of PTEN.

A previous study reported that p53 has a positive effect on PTEN transcription level (Stambolic *et al.*, 2001). In my experiment, PTEN mRNA expression was reduced in p53 knockout U2OS cells which were also transduced with empty pLenti CRISPR plasmid. However, similar observation was absent in p53 knockout U2OS cells transduced with pLKO.1 vector expressing non-targeting shRNA (Sh-x). It is speculated that the discrepancy comes from the control cells that were transduced with the non-targeting Sh-x sequence. Non-targeting shRNA sequence has been used as a negative control to compare with cells receiving a targeting shRNA sequence. However, studies have shown that continuous presence of non-targeting shRNA or siRNA sequence in cells could affect the expression of several genes involved in inflammatory and stress response (Wei *et al.*, 2012; Raof *et al.*, 2016). Although there was no direct connection with PTEN expression reported, there is a possibility that the reduced expression of PTEN in the control cells was due to the expression of Sh-x sequence that had altered the PTEN normal regulation. The stress induced by the non-targeting shRNA sequence was observed to be dose-dependent (Wei *et al.*, 2012), suggesting that reducing the amount of shRNA used can be useful to decrease undesired effects. In addition, there is no evidence showing that the undesired effects of non-targeting shRNA are similar in all cell lines, and thus the effect of Sh-x expression needs to be carefully observed in different cells.

Data from the PIP4Ks knockout cells set showed that both p53 and *PIP4K2B* control PTEN expression but through a different mechanism. P53 controls PTEN at the transcription level, which is in line with a previous study (Stambolic *et al.*, 2001), while *PIP4K2B* modulates PTEN expression at the protein level, probably causing higher degradation of the protein. It is necessary to confirm this hypothesis and to identify which protein degradation complex is involved in mediating the PIP4K-PTEN interaction. Treating *PIP4K2B* knockout cells with proteasome inhibitor for example could help to determine whether PIP4K2 β modulates PTEN expression through proteasomal activity. Both proteins are known to undergo degradation through the E3 ubiquitin ligase system, and one protein known to mediate the degradation of both proteins is speckle-type POZ protein (SPOP) (Bunce *et al.*, 2008; Li *et al.*, 2014, 2018). Although SPOP was reported to have no effect on PTEN stability in some cells (Ju *et al.*, 2019), being the only known mediator for PIP4K so far could make this protein to be the first to be investigated.

The relationship between PIP4K and p53 in modulating the PI3K/Akt pathway, as shown in this study, might actually involve a more complex mechanism than just co-regulating PTEN. P53, PTEN, and Akt are involved in a regulatory network involving various feedback loops that control the cell and growth of cancer (Review by Nakanishi *et al.*, 2014). In addition to the role of p53 in controlling PTEN's transcription level, PTEN also positively regulates the activity of p53 by inhibiting the oncogenic MDM2 function (Zheng *et al.*, 2010); while Akt aids MDM2 mediated reduction in the level and activity of p53 (Zhou *et al.*, 2001). Findings from the current study could create an additional level of understanding of this regulatory network (Figure 6.9). However, being one of the most frequently mutated protein in cancer cells, the interaction between PTEN and PIP4K in PI3K/Akt signalling should not be generalised to all cancer cells and validations in different tumour cells are necessary.

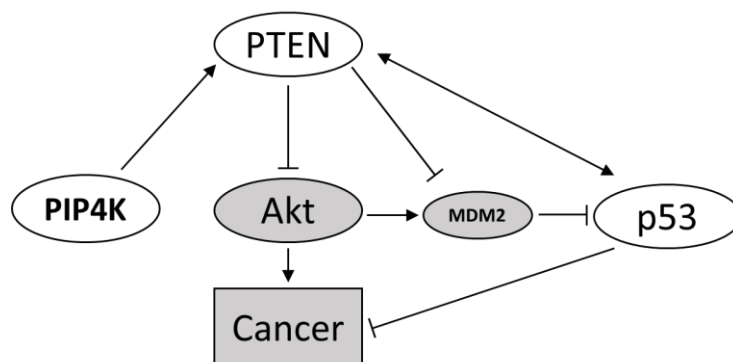


Figure 6.9 Suggested PIP4K involvement in the PTEN-Akt-p53-MDM2 regulatory network in U2OS cells. Simplified pathway showing the relationship between all the components towards cancer growth. Arrows indicate activation, and hammerheads indicate inhibition.

An example of tumour cells that do not always apply to the above theory is the BT474 cell line. Unlike U2OS, *PIP4K2A* and *2B* knockout reduced Akt phosphorylation while increasing PTEN expression in BT474 cells. *PIP4K2B* expression in BT474 cells is high (Emerling *et al.*, 2013), leading to a possibility that this kinase produces a large pool of PtdIns(4,5)P₂ crucial for the PI3K/Akt pathway. Loss of the *PIP4K2B* gene might cause the cells to be deprived of their major PtdIns(4,5)P₂ supply that leads to reduced PI3K/Akt activation. Identifying the changes in PtdIns(4,5)P₂ levels in the cells will be needed to confirm this hypothesis. However, knockdown of *PIP4K2A/2B* enhances PI3K/Akt activation in BT474 cells, which is similar to data previously reported (Emerling *et al.*, 2013). The opposite effects seen between *PIP4K2A/2B* knockdown and knockout could be due to the different levels of PIP4K message present in cells after the two different methods of silencing PIP4K. It is possible that as PIP4K expressions in BT474 cells reached below certain threshold level, Akt activation will be inhibited through a specific mechanism yet to be explored. However, I have not compared the expression of PIP4K in BT474 after knockdown and knockout on the same blot, thus this hypothesis could not be confirmed.

The different effects of PIP4K depletion towards the PI3K/Akt pathway in U2OS and BT474 cells suggested that PIP4Ks have unique roles in different cell lines. Apart from BT474, there are other cells that exhibit a positive relationship between PIP4K and Akt activation as discussed in the introduction (Bulley *et al.*, 2016). Based on the evidence, the synthetic lethal interaction between p53 and PIP4K could probably only take place if both p53 and PIP4K have positive effects on the Akt pathway activity and their co-depletion leads to a reduction in PI3K/Akt activation as observed in BT474 cells. Therefore, it is possible that tumour cells in which PIP4K has a positive effect on the PI3K/Akt pathway should be the next candidates for the p53-PIP4K synthetic lethal interaction studies.

Although the role of PIP4K on Akt pathway activation has been studied, literature that highlighted the opposite effect between acute and chronic removal of PIP4K in cells (Bulley *et al.*, 2016) had motivated us to investigate the same phenomenon in U2OS cells. However, the AID technique currently adopted did not provide convincing coherent data. In addition to the possible chronic degradation issue discussed in the previous chapter, the fluctuating level of PTEN and Akt phosphorylation observed with the doxycycline-auxin (dox-aux) treatment is also a big concern. The variations shown in the level of Akt phosphorylation following the dox-aux treatment were also inconsistent. As this phenomenon was also observed in the cells not bearing any degron-tagged construct, it is therefore believed that the dox-aux treatment could be responsible. Alteration in PI3K/Akt activation, regardless of PTEN expression, could be due to the complicated feedback mechanisms as well as cross-talk with other pathways.

It is unclear how auxin affects either the PTEN or the Akt pathway. The phytohormone auxin by itself was reported to not have any effects on cytotoxicity and the Akt pathway. However, it exhibited toxicity in mammalian cells at high doses through the action of eukaryotic peroxidases (Folkes *et al.*, 1999), and enhanced cell apoptosis in combination with cytokinin partly through the disruption of the Akt pathway (Zhao *et al.*, 2015). The effect on PTEN however, was not specifically discussed in the study. The other component of the treatment, doxycycline, was reported to induce Akt pathway activation in mammalian and murine cells (Wang *et al.*, 2012; Chang *et al.*, 2014). The effect of doxycycline on the signalling pathway is dose-dependent, and the dose used in this study was already ten times less than the previous study. Long-term exposure of low doxycycline in the cells possibly caused the changes in PI3K/Akt pathway activation, and together with the removal of *PIP4K2A/2B*, had caused erratic pathway modulation. Therefore, utilising cells stably expressing the TIR1 construct could be considered in the future to avoid using doxycycline. With the new advancement in the technique, switching to a more powerful AID-TIR1 construct to minimise the amount of auxin required for the degradation (Yamada *et al.*, 2018) is another aspect to take into account.

As there were no observed effects of doxycycline and auxin treatment on PIP4K2 α and 2 β expression, it is at least known that the level of PIP4K was not affected by these treatments. However, the small amount of AID-tagged PIP4K protein relative to the endogenous counterpart could be another reason for inconsistent observations in the experiments. The higher level of Akt phosphorylation in 2 α -mAID cells compared to wild type and β -AID cells suggested that it occurred due to the chronic lack of PIP4K2 α in the cells. Up to this point, we could not make any conclusion regarding the effect of PIP4K acute depletion on the Akt pathway activation.

This chapter shows that in the human osteosarcoma U2OS cells, PIP4K negatively controls the PI3K/Akt pathway activation, partly through PTEN. This has brought PIP4K into an indirect connection with the tumour suppressor p53 in the pathway. The opposite finding from the BT474 cells indicates that the role of PIP4K towards the pathway is cell-dependent. Different cellular dynamics formed following variation in mutations, such as *PIP4K2B* gene amplification in BT474 could be one of the factors that determine the kinase's role in the cells. These findings are important as they illustrate the importance of understanding the role of PIP4Ks toward the PI3K/Akt pathway in different types of cancer cells. The positive effect of PIP4K on the pathway might hint that the kinases could be a good therapeutic target for that particular type of tumour. However, more investigations are required to confirm this hypothesis.

Chapter 7 Final Discussion

7.1 Role of PIP4K in the immune system and cancer cells

PIP4K is a family of phosphoinositide kinases found to be involved in various cellular functions including immune system regulation and tumour growth (Fiume *et al.*, 2015). Initial findings on high expression of PIP4K in hematopoietic cells, together with immune hyperactivity observed in mice lacking PIP4K2 γ isoform (Jude *et al.*, 2015; Shim *et al.*, 2016), had raised the need to further investigate the kinase's function in the immune system. PIP4K has also been reported to control the growth of several types of cancers (Keune *et al.*, 2013; Jude *et al.*, 2015; Shin *et al.*, 2019), and a synthetic lethal interaction has been reported between PIP4K2 α /2 β and p53 in a breast cancer cell line, hinting for future cancer treatments with PIP4K (Emerling *et al.*, 2013). Therefore, this two-part study was conducted to investigate the role of PIP4K in regulating the immune system through regulatory T (Tregs) and naïve T cells, and to investigate the presence and possible molecular mechanism of a PIP4K-p53 synthetic lethal interaction in tumour cells.

The role of PIP4K in immune system regulation was a collaboration project with Dr. Poli from INGM, Milan. Our findings suggested that depletion of PIP4K reduced proliferation, survival, and suppressive activity of Tregs. The mechanism of action proposed is to be partly due to reduced PI3K/Akt activation that also downregulates UHRF1 and the transcription factor FOXP3. This data provides an additional explanation for how deletion of *PIP4K2C* in mice leads to hyperactivation of the immune system (Shim *et al.*, 2016). However, the mechanism of the synthetic lethal interaction between PIP4K and p53 in cancer cells was not elucidated, as this interaction was absent in the two cancer cell line (U2OS and HCT116) models used in this study but could be replicated in BT474 cells which were used in the original study. Our data suggest that the synthetic lethal interaction between PIP4K and p53 in tumour cells is not a universal phenomenon, and several suggestions for possible future studies were given in the discussion of Chapter 5. In addition, current data also demonstrates a novel potential relationship between PIP4K and PTEN in PI3K/Akt signalling.

7.2 Different roles of PIP4K in PI3K/Akt signalling pathway

Data from my experiments for both Tregs and cancer cell studies have shown that PIP4K modulates the PI3K/Akt pathway activation differently. However, the exact mechanism by which PIP4K impact on PI3K/Akt signalling is still not clear. The proposed mechanisms include PIP4K regulation of PI3K activity (Jones *et al.*, 2013; Shin *et al.*, 2019), PtdIns(3,4,5)P₃ phosphatase activity (Carricaburu *et al.*, 2003), and Akt phosphatase activity (Ramel *et al.*, 2009). A more recent study demonstrated that PIP4K regulates PtdIns(4,5)P₂ level by inhibiting the activity of PIP5K (Wang *et al.*, 2019). Current findings also have contributed to this field of knowledge by showing that changes in PIP4K level could affect the expression of PTEN. Depletion of PIP4K in U2OS reduces the level of PTEN leading to an increase in Akt activation. However, BT474 cells showed the opposite effect of PIP4K depletion on both PTEN and Akt phosphorylation. These data suggest that depletion of PIP4K could affect the same downstream protein differently in different cancer cells, suggesting this pathway is highly regulated and complex.

The distinct effect of PIP4K depletion on PI3K/Akt signalling is not only seen between different cancer cell lines but also between T cell lineages expressing different cell surface markers. As shown in Chapter 3 (section 3.2.1 and 3.2.4), depletion of PIP4K2 β and 2 γ in Tregs reduced the phosphorylation of Akt and S6 while similar PIP4K silencing in naïve T cells resulted in higher phosphorylation of the two proteins. This suggested that the role of PIP4K on PI3K/Akt pathway is highly cell-type specific. These observations also raised a question regarding the presence of a specific factor in the cells which determine how PIP4K will affect PI3K/Akt/mTOR signalling. Previous studies in *Drosophila* also reported an opposite effect of dPIP4K loss on mTOR signalling in whole larval extracts compared to an embryonic cell line (Gupta *et al.*, 2013; Sharma *et al.*, 2019). They suggested that the observed discrepancy between the two studies could be due to different levels of TORC1 activation in various cells, and that mTOR activity may not require dPIP4K function in every tissue (Sharma *et al.*, 2019). One study investigated the different effect of inhibition on PI3K/Akt/mTOR pathway activation in Tregs and Tconv cells, which suggested that the higher PTEN levels in Tregs had down-regulated the PI3K/Akt/mTOR signalling causing these cells to have minimal response towards mTOR inhibitor (Strauss *et al.*, 2009). Based on these data, it could be speculated that the different roles of PIP4K on PI3K/Akt/mTOR might depend on up- and down-regulation of the pathway in cells. Different levels of protein(s) regulating the PI3K/Akt pathway, such as PTEN could determine how PIP4K functions in the pathway.

PIP4K plays a minor role in the production of PtdIns(4,5)P₂ compared to another family of kinases, PIP5K. Whether the small pool of PtdIns(4,5)P₂ produced by PIP4K has a special function is still in question (Emerling *et al.*, 2013; Fiume *et al.*, 2015). The effect of PIP4K depletion is stronger

in Tregs known to have a higher PTEN expression compared to the naïve T cells (Strauss *et al.*, 2009). Thus, it is possible that in an environment where PI3K/Akt activation is minimal due to a higher PTEN level, the small pool of PIP4K-produced-PtdIns(4,5)P₂ becomes significant for the PI3K/Akt pathway activation. The higher level of PTEN expression in BT474 compared to U2OS can be one of the reasons to support this theory (Appendix D). This possible PIP4K-PTEN-Akt connection might explain the reason why the synthetic lethal interaction was not seen in all types of cancer with loss of p53 function. However, it is also important to remember that *PIP4K2B* is upregulated in the BT474 cells, which might indicate that the PtdIns(3,4,5)P₃ production in the cells are highly affected by the PtdIns(4,5)P₂ produced by the PIP4K2β.

PTEN has been one of the focus points in studying the differences in Akt phosphorylation/activation in various cancer cells (Georgescu, 2010). High PTEN levels do not always correlate with low Akt phosphorylation and vice versa, suggesting that other novel mechanisms controlling both Akt and PTEN independently may exist (He *et al.*, 2007). *PIP4K2A* and PTEN were also postulated to compete for binding to PI3K, and that the lack of PTEN enables *PIP4K2A* to directly bind and lead to PI3K degradation in glioblastoma cells (Shin *et al.*, 2019). Thus, PTEN may be a good starting point to study the different effects of PIP4K on the PI3K/Akt pathway.

The role of each PIP4K isoform needs to be carefully determined as well when studying the kinase's effect on signalling. The three isoforms of PIP4K, the 2α, 2β, and 2γ were reported to have various degrees of activity, which differ up to thousands of folds (Clarke *et al.*, 2008; Bultsma *et al.*, 2010). Being the most active isoform does not necessarily mean that the 2α will always have more impact compared to the other two. Current findings showed that the effects of 2β depletion in both Tregs and BT474 cells are stronger than 2α. These variations indicate that each isoform might take part in specific physiological processes. In addition, the level of PIP4K isoforms can vary in different cells. For example, *PIP4K2B* is known to be highly expressed in the BT474 cells (Luoh *et al.*, 2004; Emerling *et al.*, 2013; Keune *et al.*, 2013), suggesting that the 2β isoform plays crucial roles in the cells. Thus, identifying the level of PIP4K isoforms in studied cells is also necessary before examining their role.

7.3 The future direction of PIP4K as a target for immune-related disorder and cancer therapy

The distinct effect of PIP4K depletion on specific T cell lineages might suggest its suitability for the treatment of systemic immune-related disease. As shown by the previous study by Shim *et al.* (2016), deletion of *PIP4K2C* in mice leads to hyperactivation of the immune system partly through the increased percentage of Tconv cells and reduced percentage of Foxp3⁺ Tregs compared to wild type mice. Our study has demonstrated how depletion of specific PIP4K in Tregs *via* the effect on Akt pathway activation could lead to low Tregs proliferation and suppressive activity. The fact that our study could not show any changes in the Th1 and Th2 master transcription factors T-BET and GATA3 upon *PIP4K2A* and *2B* silencing in CD4⁺ naïve T cells might indicate that the depletion of these kinases does not impact on differentiation of the Th cells from naïve T cells. However, it is still unknown whether PIP4K silencing could affect the activity of other Tconv cells such as CD8⁺ cytotoxic cells. Therefore, future studies should investigate the role of PIP4K in the PI3K/Akt/mTOR pathway activation of other Tconv cells.

Data from our and other studies indicate that PIP4K removal in cancer cells could either inhibit (Emerling *et al.*, 2013; Keune *et al.*, 2013; Jude *et al.*, 2015) or contribute to (Shin *et al.*, 2019) tumour growth, and the distinct role of PIP4K in PI3K/Akt pathway activation might be one of the reasons behind these differences. Therefore, understanding the role of PIP4K depletion in different types of cancer will be necessary before deciding its suitability for any cancer treatment. In addition, *TP53*^{-/-}, *PIP4K2A*^{-/-}, *PIP4K2B*^{+/-} mice had a dramatic reduction in spontaneous tumour formation caused by the absence of the tumour suppressor p53 (Emerling *et al.*, 2013). Based on the reported functions of PIP4K (discussed in Chapter 1; section 1.2.3), we could postulate that the low *PIP4K2A* and *2B* might partly contribute to the suppression of tumour growth in a cell autonomous way, and the *PIP4K2B* depletion might contribute by enhancing the immunosurveillance activity in the mice. The data suggest a promising systemic effect of PIP4K inhibitor in organisms and its potential to alleviate the chance of developing cancer.

Some inconsistencies in the current study had prevented us from identifying whether acute and chronic depletion of PIP4K produced different effects in cells. Two depletion methods of *PIP4K2A* used in this study, which are shRNA and CRISPR/Cas9, showed different phenotypes in cancer cells, leading us to opt for the third method that is auxin inducible degron (AID). However, the fluctuation of Akt phosphorylation and PTEN expression observed in the AID-tagged cells hampered the investigation. Another possible way to confirm the silencing method of PIP4K in cancer cells will be through suppressing the kinase's activity with inhibitors. Identifying the presence of any differences in acute versus chronic depletion of PIP4K towards the body is crucial,

in order to decide whether any PIP4K drug will be worth developing for long- or short-term treatment. Overall, this study strengthens the idea that PIP4K is a potential target for cancer therapy, and modulation of this kinase can be useful to enhance the immune system.

7.4 Final Conclusion

In conclusion, PIP4K plays multiple roles in regulating the immune system and tumour growth. This study demonstrated that PIP4K modulates the immune system partly through regulatory T cells. The cancer study showed that the synthetic lethality between PIP4K and p53 is not a universal effect and PIP4K depletion can exhibit opposite effects in different types of cancers. In both Tregs and cancer cells, the PI3K/Akt pathway has been shown to be regulated by PIP4K inhibition, while PTEN expression is affected upon PIP4K depletion in cancer cells. It is possible that the different mechanisms of PIP4K regulation on the PI3K/Akt/mTOR pathway are determined by the signalling environment provided by the cells. Therefore, current findings warrant more investigations to validate other possible PIP4K roles in the immune system, especially in effector T cells and its role in different types of cancer cells. Further investigations are also needed to increase our understanding of the relationship between PIP4K and PTEN shown by this study.

Appendix A PIP4K Isoforms Sequence Comparison

A Protein sequences input

PIP4K2A:

```
>sp|P48426|PI42A_HUMAN Phosphatidylinositol 5-phosphate 4-kinase type-2
alpha OS=Homo sapiens OX=9606 GN=PIP4K2A PE=1 SV=2
MATPGNLGSSVLASKTKTKKKHFVAQKVKLFRASDPLLSVLMWGVNHSINELSHVQIPVM
LMPDDFKAYSIIKVDNHLFNKENMPSHFKFKEYCPMVFRLRERFGIDDQDFQNSLTRSA
PLPNDSQARSGARFHTSYDKRYIIKTITSEDVAEMHNILKKYHQYIVECHGITLLPQFLG
MYRLNVDGVEIYVIVTRNVFSHRLSVYRKYDLKGSTVAREASDKEKAKELPTLKDNDFIN
EGQKIYIDDNKKVFLKLEKLDVEFLAQLKIMDYSLLVGIHDVERAEQEVECEENDGEE
EGESDGHVPVGTTPDPSGNTLNSSPPLAPGEFDPNIDVYGIKCHENS PRKEVYFMAIIDI
LTHYDAKKKAAHAAKTVKHGAGAEISTVNPEQYSKRFLDFIGHILT
```

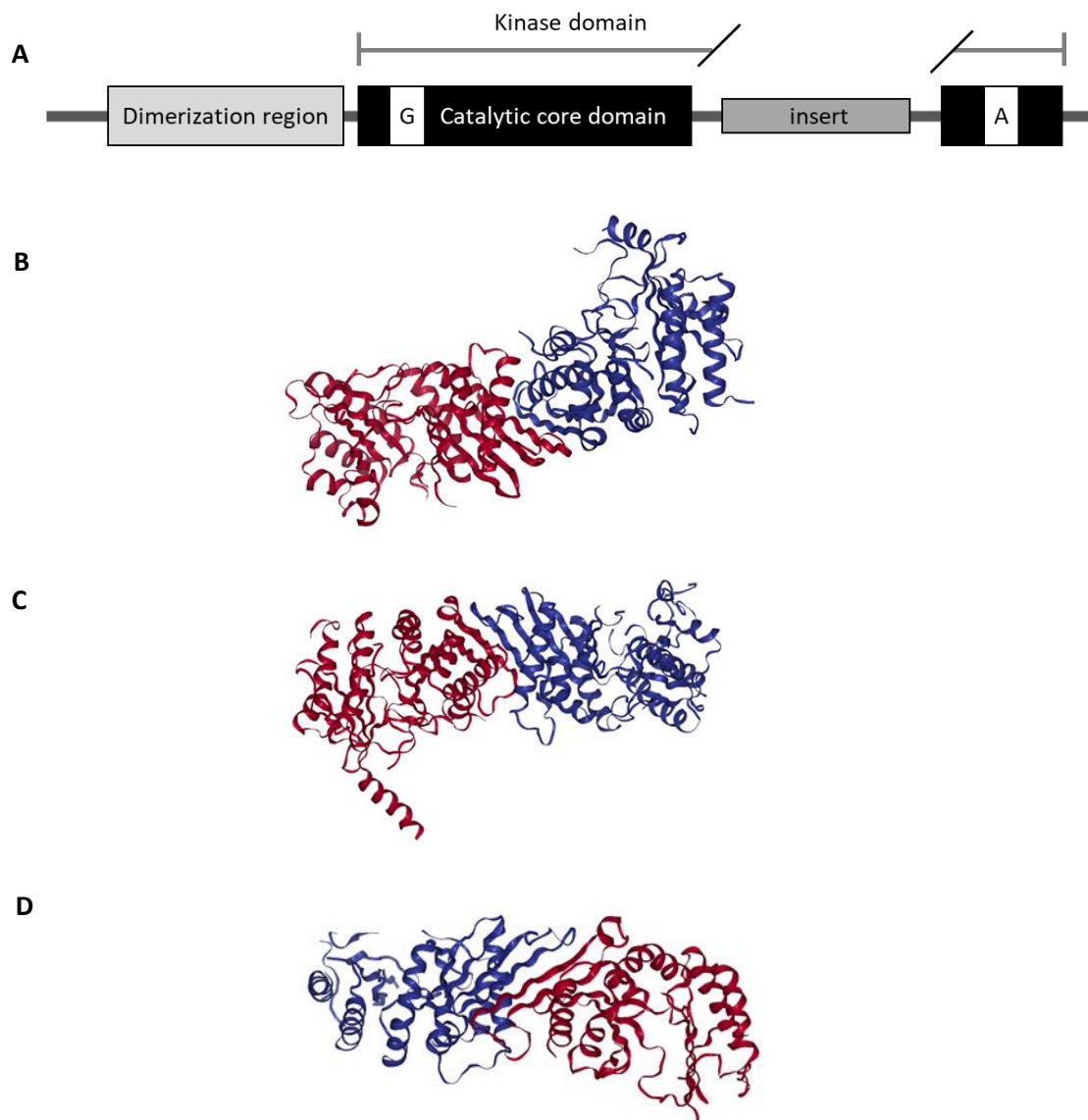
PIP4K2B:

```
>sp|P78356|PI42B_HUMAN Phosphatidylinositol 5-phosphate 4-kinase type-2 beta
OS=Homo sapiens OX=9606 GN=PIP4K2B PE=1 SV=1
MSSNCTSTTAVAVAPLSASKTKTKKKHFVCQKVKLFRASEPILSVLMWGVNHTINELSNV
PVPVMLMPDDFKAYSIIKVDNHLFNKENLPSRFKFKEYCPMVFRLRERFGIDDQDYQNS
VTRSAPINSDSQGRGTRFLTTYDRRFVIKTVSSEDVAEMHNILKKYHQFIVECHGNTLL
PQFLGMYRLTVDGVETVMVTRNVFSHRLTVHRKYDLKGSTVAREASDKEKAKDLPTFKD
NDFLNEGQKLHVGEESKNFLEKLRDVEFLAQLKIMDYSLLVGIHDVDRAEQEEMEVEE
RAEDEECENDGVGGNLLCSYGTTPDPSGNLLSFPRFFGPGFDPVSDVYAMKSHESPCK
EVYFMAIIDILTPYDTKKKAAHAAKTVKHGAGAEISTVNPEQYSKRFFNEFMSNILT
```

PIP4K2C:

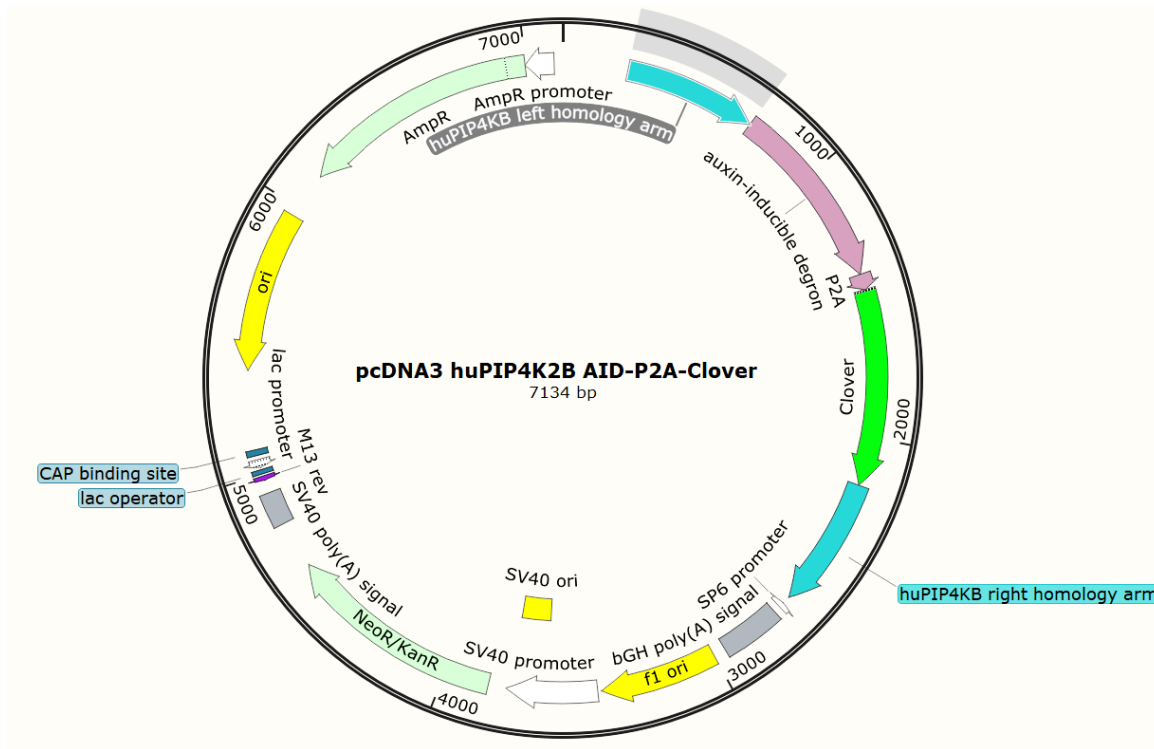
```
>sp|Q8TBX8|PI42C_HUMAN Phosphatidylinositol 5-phosphate 4-kinase type-2 gamma
OS=Homo sapiens OX=9606 GN=PIP4K2C PE=1 SV=3
MASSSVPPATVSAATAGPGPGFGFASKTKKKHFVQKVKVFRAADPLVGVFLWGVVHNSIN
ELSQQVPPVMLLPDDFKASSIKVNNHLFHRENLP SHFKFKEYCPQVFRNLRDRFGIDDQ
DYLVS LTRNPPSESEGS DGRFLISYDRTLVIKEVSEDIADMHSNLSNYHQYIVKCHGNT
LLPQFLGMYRVSVDNEDSYMLVMRNMFSHRLPVHRKYDLKGSLSVREASDKEKVKELPTL
KDMDFLNKNQKVYIGEEEEKIFLEKLRDVEFLVQLKIMDYSLLLGIHDIIRGSEPEEEA
PVREDESEVDGDCSLTGPPALVGSYGTSPGIGGYIHSRPLGPGEFESFIDVYAIRSAE
GAPQKEVYFMGLIDILTQYDAKKKAAHAAKTVKHGAGAEISTVHPEQYAKRFLDFITNIF
A
```


Appendix B Structure of PIP4K Isoforms



Structure of PIP4K. (A) Diagram showing the C-terminal kinase domain of PIP4K contains the activation loop (labelled A), while the N-terminal domain contains the G-loop sequence (labelled G). The kinase catalytic core domain (black) of PIP4K is cut off by the variable insert, which is a region with the least similarity between the three isoforms (Clarke and Irvine, 2018). (B-D) Ribbon diagrams of the crystallographic structure of PIP4K2 α (PDB ID: 2YBX, Tresaugues *et al.*, 2012), 2 β (Rao *et al.*, 1998), and 2 γ (PDB ID: 2GK9, Thorsell *et al.*, 2006) respectively as a dimer. Different colour indicates a different chain.

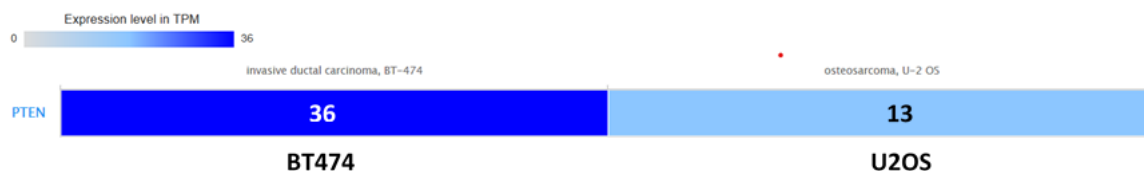
Appendix C Auxin Inducible Degron (AID) Construct



Plasmid map of Auxin Inducible Degron (AID) construct utilised to generate PIP4K2 β -AID cells. The AID construct is fused to neomycin/kanamycin resistant marker, porcine teschovirus-1 2A (P2A), and GFP.

Appendix D Expression of PTEN in U2OS and BT474

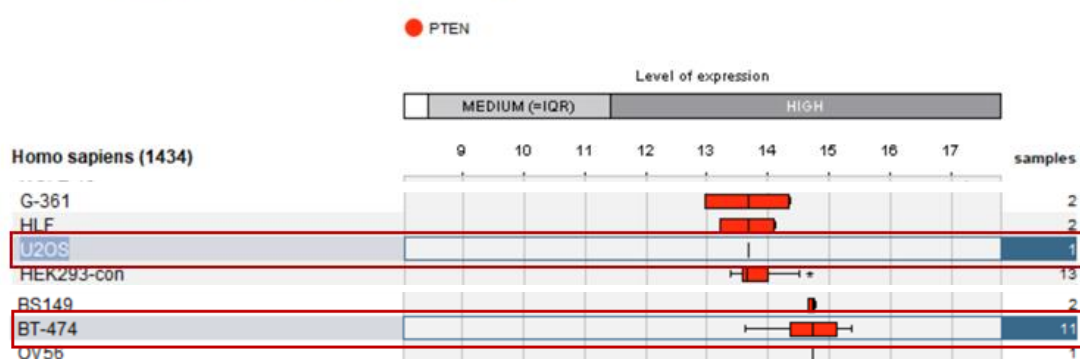
A



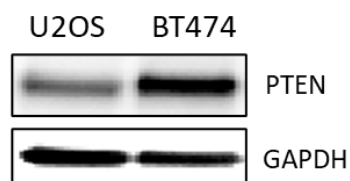
B

Dataset: 1434 cell lines from data selection: HS_AFFY_U133PLUS_2-2

Showing 1 measure(s) of 1 gene(s) on selection: HS-1



C



BT474 has a higher level of PTEN expression compared to U2OS. The level of PTEN expression in U2OS and BT474 were compared across different available online databases and immunoblot experiment. (A) Heat map diagram showing the expression of PTEN in TPM from the Expression Atlas database (Petryszak *et al.*, 2016). (B) Level of PTEN expression from the Gene Investigator database (Hruz *et al.*, 2008). U2OS and BT474 cells are highlighted in red box. (C) Western blot results of U2OS and BT474 lysates probed with PTEN antibody. GAPDH acts as a loading control

List of References

- Abbas, A. K. *et al.* (2013) 'Regulatory T cells: recommendations to simplify the nomenclature', *Nature Immunology*. Nature Publishing Group, 14(4), pp. 307–308. doi: 10.1038/ni.2554.
- Abraham, A. G. and O'Neill, E. (2014) 'PI3K/Akt-mediated regulation of p53 in cancer', in *Biochemical Society Transactions*. Portland Press Ltd, pp. 798–803. doi: 10.1042/BST20140070.
- Abu-Eid, R. *et al.* (2014) 'Selective inhibition of regulatory T cells by targeting the PI3K-Akt pathway.', *Cancer immunology research*, 2(11), pp. 1080–9. doi: 10.1158/2326-6066.CIR-14-0095.
- Agranoff, B. W. (2009) 'Turtles all the way: Reflections on myo-inositol', *Journal of Biological Chemistry*, 284(32), pp. 21121–21126. doi: 10.1074/jbc.X109.004747.
- Al-Ramahi, I. *et al.* (2017) 'Inhibition of PIP4Ky ameliorates the pathological effects of mutant huntingtin protein', *eLife*, 6. doi: 10.7554/eLife.29123.
- Alessi, D. R. *et al.* (1997) 'Characterization of a 3-phosphoinositide-dependent protein kinase which phosphorylates and activates protein kinase Ba', *Current Biology*. Cell Press, 7(4), pp. 261–269. doi: 10.1016/S0960-9822(06)00122-9.
- Ali, K. *et al.* (2014) 'Inactivation of PI(3)K p110 δ breaks regulatory T-cell-mediated immune tolerance to cancer', *Nature*. Nature Publishing Group, 510(7505), pp. 407–411. doi: 10.1038/nature13444.
- Anderson, R. A. *et al.* (1999) 'Phosphatidylinositol phosphate kinases, a multifaceted family of signaling enzymes', *Journal of Biological Chemistry*, 274(15), pp. 9907–9910. doi: 10.1074/jbc.274.15.9907.
- August, A. and Dupont, B. (1994) 'CD28 of T lymphocytes associates with phosphatidylinositol 3-kinase', *International Immunology*, 6(5), pp. 769–774. doi: 10.1093/intimm/6.5.769.
- Bacus, S. S. *et al.* (2002) 'AKT2 is frequently upregulated in HER-2/neu-positive breast cancers and may contribute to tumor aggressiveness by enhancing cell survival', *Oncogene*, 21(22), pp. 3532–3540. doi: 10.1038/sj.onc.1205438.
- Balla, T. (2013) 'Phosphoinositides: tiny lipids with giant impact on cell regulation', *Physiological reviews*, 93(3), pp. 1019–1137. doi: 10.1152/physrev.00028.2012.
- Barretina, J. *et al.* (2012) 'The Cancer Cell Line Encyclopedia enables predictive modelling of anticancer drug sensitivity.', *Nature*, 483(7391), pp. 603–7. doi: 10.1038/nature11003.

- Battaglia, M. *et al.* (2005) 'Rapamycin selectively expands CD4+CD25+FoxP3 + regulatory T cells', *Blood*, 105(12), pp. 4743–4748. doi: 10.1182/blood-2004-10-3932.
- Bennett, C. *et al.* (2001) 'A rare polyadenylation signal mutation of the FOXP3 gene (AAUAAA→AAUGAA) leads to the IPEX syndrome', *Immunogenetics*. Springer, 53(6), pp. 435–439. doi: 10.1007/s002510100358.
- Berridge, M. J. (1984) 'Inositol trisphosphate and diacylglycerol as second messengers.', *The Biochemical journal*, 220(2), pp. 345–60. doi: 10.1101/SQB.1988.053.01.107.
- Biegging, K. T. *et al.* (2014) 'Unravelling mechanisms of p53-mediated tumour suppression', *Nat Rev Cancer*. Nature Publishing Group, a division of Macmillan Publishers Limited. All Rights Reserved., 14(5), pp. 359–370. Available at: <http://dx.doi.org/10.1038/nrc3711>.
- Bilate, A. B. and Lafaille, J. J. (2011) 'It takes two to tango', *Immunity*. Cell Press, pp. 6–8. doi: 10.1016/j.immuni.2011.07.003.
- Borowicz, S. *et al.* (2014) 'The Soft Agar Colony Formation Assay', *Journal of Visualized Experiments*, (92), pp. 1–6. doi: 10.3791/51998.
- Bostick, M. *et al.* (2007) 'UHRF1 plays a role in maintaining DNA methylation in mammalian cells', *Science*. American Association for the Advancement of Science, 317(5845), pp. 1760–1764. doi: 10.1126/science.1147939.
- van den Bout, I. and Divecha, N. (2009) 'PIP5K-driven PtdIns(4,5)P2 synthesis: regulation and cellular functions.', *Journal of cell science*, 122(Pt 21), pp. 3837–3850. doi: 10.1242/jcs.056127.
- Boyton, R. J. and Altmann, D. M. (2002) 'Is selection for TCR affinity a factor in cytokine polarization?', *Trends in Immunology*. Elsevier Current Trends, 23(11), pp. 526–529. doi: 10.1016/S1471-4906(02)02319-0.
- Brown, D. M. *et al.* (1961) '732. Phospholipids. Part VII. The structure of a monophosphoinositide', *Journal of the Chemical Society (Resumed)*, (3774), p. 3774. doi: 10.1039/jr9610003774.
- Brunkow, M. E. *et al.* (2001) 'Disruption of a new forkhead/winged-helix protein, scurfy, results in the fatal lymphoproliferative disorder of the scurfy mouse', *Nature Genetics*. Nature Publishing Group, 27(1), pp. 68–73. doi: 10.1038/83784.
- Bulley, S. J. *et al.* (2016) 'In B cells, phosphatidylinositol 5-phosphate 4-kinase- α synthesizes PI(4,5)P2 to impact mTORC2 and Akt signaling', *Proceedings of the National Academy of Sciences*, 113(38), pp. 10571–10576. doi: 10.1073/pnas.1522478113.

- Bultsma, Y. *et al.* (2010) 'PIP4Kbeta interacts with and modulates nuclear localization of the high-activity PtdIns5P-4-kinase isoform PIP4Kalpha.', *The Biochemical journal*, 430(2), pp. 223–35. doi: 10.1042/BJ20100341.
- Bunce, M. W. *et al.* (2008) 'Coordinated activation of the nuclear ubiquitin ligase Cul3-SPOP by the generation of phosphatidylinositol 5-phosphate', *Journal of Biological Chemistry*. American Society for Biochemistry and Molecular Biology, 283(13), pp. 8678–8686. doi: 10.1074/jbc.M710222200.
- Cannell, I. G. *et al.* (2008) 'How do microRNAs regulate gene expression?', *Biochemical Society Transactions*, pp. 1224–1231. doi: 10.1042/BST0361224.
- Carricaburu, V. *et al.* (2003) 'The phosphatidylinositol (PI)-5-phosphate 4-kinase type II enzyme controls insulin signaling by regulating PI-3,4,5-trisphosphate degradation.', *Proceedings of the National Academy of Sciences of the United States of America*, 100(17), pp. 9867–9872. doi: 10.1073/pnas.1734038100.
- Chang, C.-F. *et al.* (2012) 'Polar Opposites: Erk Direction of CD4 T Cell Subsets', *The Journal of Immunology*, 189(2), pp. 721–731. doi: 10.4049/jimmunol.1103015.
- Chang, M.-Y. *et al.* (2014) 'Doxycycline Enhances Survival and Self-Renewal of Human Pluripotent Stem Cells', *Stem Cell Reports*. Cell Press, 3(2), pp. 353–364. doi: 10.1016/J.STEMCR.2014.06.013.
- Chapman, N. M. and Chi, H. (2014) 'mTOR signaling, Tregs and immune modulation', *Immunotherapy*, 6(12), pp. 1295–1311. doi: 10.2217/imt.14.84 [doi].
- Chatterjee, M. *et al.* (2013) 'The PI3k/Akt signaling pathway regulates the expression of Hsp70, which critically contributes to Hsp90-chaperone function and tumor cell survival in multiple myeloma', *Haematologica*, 98(7), pp. 1132–1141. doi: 10.3324/haematol.2012.066175.
- Chellappa, S. *et al.* (2019) 'The PI3K p110 δ Isoform Inhibitor Idelalisib Preferentially Inhibits Human Regulatory T Cell Function', *The Journal of Immunology*. The American Association of Immunologists, 202(5), pp. 1397–1405. doi: 10.4049/jimmunol.1701703.
- Chen, W. *et al.* (2003) 'Conversion of Peripheral CD4 + CD25 – Naive T Cells to CD4 + CD25 + Regulatory T Cells by TGF- β Induction of Transcription Factor Foxp3', *The Journal of Experimental Medicine*, 198(12), pp. 1875–1886. doi: 10.1084/jem.20030152.
- Choi, S. *et al.* (2015) 'PIP kinases define PI4,5P2 signaling specificity by association with effectors', *Biochimica et Biophysica Acta - Molecular and Cell Biology of Lipids*, 1851(6), pp. 711–723. doi: 10.1016/j.bbalip.2015.01.009.

- Choi, S. *et al.* (2019) 'A nuclear phosphoinositide kinase complex regulates p53', *Nature Cell Biology*. Nature Publishing Group, 21(4), pp. 462–475. doi: 10.1038/s41556-019-0297-2.
- Chow, S. *et al.* (2006) 'Constitutive phosphorylation of the S6 ribosomal protein via mTOR and ERK signaling in the peripheral blasts of acute leukemia patients', *Experimental Hematology*. Elsevier, 34(9), pp. 1182–1190. doi: 10.1016/J.EXPHEM.2006.05.002.
- Christgen, M. *et al.* (2012) 'IPH-926 lobular breast cancer cells harbor a p53 mutant with temperature-sensitive functional activity and allow for profiling of p53-responsive genes', *Laboratory Investigation*, 92(11), pp. 1635–1647. doi: 10.1038/labinvest.2012.126.
- Ciruela, A. *et al.* (2000) 'Nuclear targeting of the beta isoform of type II phosphatidylinositol phosphate kinase (phosphatidylinositol 5-phosphate 4-kinase) by its alpha-helix 7.', *Biochemical Journal*, pp. 587–591.
- Clarke, J. H. *et al.* (2007) 'Type II PtdInsP kinases: location, regulation and function.', *Biochemical Society symposium*, 74(74), pp. 149–59. doi: 10.1042/BSS0740149.
- Clarke, J. H. *et al.* (2008) 'Localization of phosphatidylinositol phosphate kinase IIgamma in kidney to a membrane trafficking compartment within specialized cells of the nephron.', *American journal of physiology. Renal physiology*, 295(5), pp. F1422–F1430. doi: 10.1152/ajprenal.90310.2008.
- Clarke, J. H. *et al.* (2009) 'Distribution and neuronal expression of phosphatidylinositol phosphate kinase IIy in the mouse brain', *The Journal of Comparative Neurology*, 517(3), pp. 296–312. doi: 10.1002/cne.22161.
- Clarke, J. H. *et al.* (2015) 'The function of phosphatidylinositol 5-phosphate 4-kinase γ (PI5P4K γ) explored using a specific inhibitor that targets the PI5P-binding site', *Biochemical Journal*, 466(2), pp. 359 LP – 367. Available at: <http://www.biochemj.org/content/466/2/359.abstract>.
- Clarke, J. H. and Irvine, R. F. (2012) 'The activity, evolution and association of phosphatidylinositol 5-phosphate 4-kinases', *Advances in Biological Regulation*. Elsevier, 52(1), pp. 40–45. doi: 10.1016/j.advenzreg.2011.09.002.
- Clarke, J. H. and Irvine, R. F. (2013) 'Evolutionarily conserved structural changes in phosphatidylinositol 5-phosphate 4-kinase (PI5P4K) isoforms are responsible for differences in enzyme activity and localization.', *The Biochemical journal*, 454(1), pp. 49–57. doi: 10.1042/BJ20130488.

- Clarke, J. H. and Irvine, R. F. (2018) 'Phosphatidylinositol 5-Phosphate 4-Kinase', in Choi, S. (ed.) *Encyclopedia of Signaling Molecules*. Cham: Springer International Publishing, pp. 3940–3949. doi: 10.1007/978-3-319-67199-4.
- Crellin, N. K. *et al.* (2007) 'Altered activation of AKT is required for the suppressive function of human CD4+CD25+ T regulatory cells', *Blood*, 109(5), pp. 2014–2022. doi: 10.1182/blood-2006-07-035279.
- Czech, M. P. (2000) 'PIP2 and PIP3', *Cell*, 100(6), pp. 603–606. doi: 10.1016/S0092-8674(00)80696-0.
- Divecha, N. *et al.* (1995) 'The cloning and sequence of the C isoform of PtdIns4P 5-kinase', *Biochemical Journal*, 309(3), pp. 715–719. doi: 10.1042/bj3090715.
- Divecha, N. (2010) 'Lipid Kinases: Charging PtdIns(4,5)P2 Synthesis', *Current Biology*, 20(4), pp. R154–R157. doi: 10.1016/j.cub.2010.01.016.
- Divecha, N. (2016) 'Phosphoinositides in the nucleus and myogenic differentiation: how a nuclear turtle with a PHD builds muscle', *Biochemical Society Transactions*, 44(1), pp. 299–306. doi: 10.1042/BST20150238.
- Droubi, A. *et al.* (2016) 'Nuclear localizations of phosphatidylinositol 5-phosphate 4-kinases α and β are dynamic and independently regulated during starvation-induced stress', *Biochemical Journal*, 473(14), pp. 2155–2163. doi: 10.1042/BCJ20160380.
- Dudley, M. E. *et al.* (2003) 'Generation of Tumor-Infiltrating Lymphocyte Cultures for Use in Adoptive Transfer Therapy for Melanoma Patients', *Journal of Immunotherapy*. J Immunother, 26(4), pp. 332–342. doi: 10.1097/00002371-200307000-00005.
- Echard, A. (2012) 'Phosphoinositides and cytokinesis: The "PIP" of the iceberg', *Cytoskeleton*, 69(11), pp. 893–912. doi: 10.1002/cm.21067.
- Elouarrat, D. *et al.* (2013) 'Role of phosphatidylinositol 5-phosphate 4-kinase α in zebrafish development', *International Journal of Biochemistry and Cell Biology*. Elsevier Ltd, 45(7), pp. 1293–1301. doi: 10.1016/j.biocel.2013.03.009.
- Emerling, B. M. *et al.* (2013) 'Depletion of a putatively druggable class of phosphatidylinositol kinases inhibits growth of p53-Null tumors', *Cell*. Elsevier, 155(4), pp. 844–857. doi: 10.1016/j.cell.2013.09.057.

- Engelman, J. A. (2009) 'Targeting PI3K signalling in cancer: opportunities, challenges and limitations', *Nature Reviews Cancer*. Nature Publishing Group, 9(8), pp. 550–562. doi: 10.1038/nrc2664.
- Espinosa, J. M. *et al.* (2003) 'p53 functions through stress- and promoter-specific recruitment of transcription initiation components before and after DNA damage', *Molecular Cell*. Cell Press, 12(4), pp. 1015–1027. doi: 10.1016/S1097-2765(03)00359-9.
- Etemire, E. *et al.* (2013) 'Transiently Reduced PI3K/Akt Activity Drives the Development of Regulatory Function in Antigen-Stimulated Naïve T-Cells', *PLoS ONE*. Edited by A. Waisman. Public Library of Science, 8(7), p. e68378. doi: 10.1371/journal.pone.0068378.
- Fabian, L. *et al.* (2010) 'Phosphatidylinositol 4,5-bisphosphate Directs Spermatid Cell Polarity and Exocyst Localization in *Drosophila*', *Molecular Biology of the Cell*, 21(9), pp. 1546–1555. doi: 10.1091/mbc.E09-07-0582.
- Fayard, E. *et al.* (2010) 'Phosphatidylinositol 3-kinase signaling in thymocytes: the need for stringent control.', *Science signaling*, 3(135), p. re5. doi: 10.1126/scisignal.3135re5.
- Feng, Z. (2010) 'p53 regulation of the IGF-1/AKT/mTOR pathways and the endosomal compartment.', *Cold Spring Harbor perspectives in biology*. doi: 10.1101/cshperspect.a001057.
- Fiume, R. *et al.* (2015) 'PIP4K and the role of nuclear phosphoinositides in tumour suppression', *Biochimica et Biophysica Acta - Molecular and Cell Biology of Lipids*. Elsevier B.V., 1851(6), pp. 898–910. doi: 10.1016/j.bbalip.2015.02.014.
- Folkes, L. K. *et al.* (1999) 'Peroxidase-catalyzed effects of indole-3-acetic acid and analogues on lipid membranes, DNA, and mammalian cells in vitro', *Biochemical Pharmacology*. Elsevier, 57(4), pp. 375–382. doi: 10.1016/S0006-2952(98)00323-2.
- Fontenot, J. D. *et al.* (2003) 'Foxp3 programs the development and function of CD4+CD25+ regulatory T cells', *Nature Immunology*. Nature Publishing Group, 4(4), pp. 330–336. doi: 10.1038/ni904.
- Friedland, J. C. *et al.* (2014) 'Targeted inhibition of Hsp90 by ganetespib is effective across a broad spectrum of breast cancer subtypes', *Investigational New Drugs*. Kluwer Academic Publishers, 32(1), pp. 14–24. doi: 10.1007/s10637-013-9971-6.
- Fruman, D. A. *et al.* (2017) 'The PI3K Pathway in Human Disease', *Cell*. Cell Press, pp. 605–635. doi: 10.1016/j.cell.2017.07.029.

- Fruman, D. A. and Rommel, C. (2014) 'PI3K and cancer: lessons, challenges and opportunities', *Nature Reviews Drug Discovery*. Nature Publishing Group, 13(2), pp. 140–156. doi: 10.1038/nrd4204.
- Fung, E. Y. M. G. *et al.* (2009) 'Analysis of 17 autoimmune disease-associated variants in type 1 diabetes identifies 6q23/TNFAIP3 as a susceptibility locus', *Genes and Immunity*. Nature Publishing Group, 10(2), pp. 188–191. doi: 10.1038/gene.2008.99.
- Gelato, K. A. *et al.* (2014) 'Accessibility of Different Histone H3-Binding Domains of UHRF1 Is Allosterically Regulated by Phosphatidylinositol 5-Phosphate', *Molecular Cell*. Cell Press, 54(6), pp. 905–919. doi: 10.1016/J.MOLCEL.2014.04.004.
- Georgescu, M. M. (2010) 'Pten tumor suppressor network in PI3K-Akt pathway control', *Genes and Cancer*. Impact Journals, LLC, pp. 1170–1177. doi: 10.1177/1947601911407325.
- Giaccia, A. J. and Kastan, M. B. (1998) 'The complexity of p53 modulation: Emerging patterns from divergent signals', *Genes and Development*. Cold Spring Harbor Laboratory Press, pp. 2973–2983. doi: 10.1101/gad.12.19.2973.
- Giulino-Roth, L. *et al.* (2017) 'Inhibition of Hsp90 suppresses PI3K/AKT/mTOR signaling and has antitumor activity in Burkitt lymphoma', *Molecular Cancer Therapeutics*. American Association for Cancer Research Inc., 16(9), pp. 1779–1790. doi: 10.1158/1535-7163.MCT-16-0848.
- Gozani, O. *et al.* (2003) 'The PHD Finger of the Chromatin-Associated Protein ING2 Functions as a Nuclear Phosphoinositide Receptor', *Cell*, 114(1), pp. 99–111. doi: 10.1016/S0092-8674(03)00480-X.
- Graeber, T. G. *et al.* (1996) 'Hypoxia-mediated selection of cells with diminished apoptotic potential in solid tumours', *Nature*, 379(6560), pp. 88–91. doi: 10.1038/379088a0.
- Grainger, D. L. *et al.* (2011) 'Involvement of phosphatidylinositol 5-phosphate in insulin-stimulated glucose uptake in the L6 myotube model of skeletal muscle', *Pflügers Archiv - European Journal of Physiology*. Springer-Verlag, 462(5), pp. 723–732. doi: 10.1007/s00424-011-1008-4.
- Grimm, D. *et al.* (2006) 'Fatality in mice due to oversaturation of cellular microRNA/short hairpin RNA pathways', *Nature*. Nature Publishing Group, 441(7092), pp. 537–541. doi: 10.1038/nature04791.
- Grzechnik, A. T. and Newton, A. C. (2016) 'PHLPPing through history: A decade in the life of PHLPP phosphatases', *Biochemical Society Transactions*. Portland Press Ltd, 44(6), pp. 1675–1682. doi: 10.1042/BST20160170.

- Gupta, A. *et al.* (2013) 'Phosphatidylinositol 5-phosphate 4-kinase (PIP4K) regulates TOR signaling and cell growth during *Drosophila* development.', *Proceedings of the National Academy of Sciences of the United States of America*. National Academy of Sciences, 110(15), pp. 5963–8. doi: 10.1073/pnas.1219333110.
- Gupta, S. *et al.* (2007) 'Binding of Ras to Phosphoinositide 3-Kinase p110 α Is Required for Ras-Driven Tumorigenesis in Mice', *Cell*. Cell Press, 129(5), pp. 957–968. doi: 10.1016/J.CELL.2007.03.051.
- Hainaut, P. and Hollstein, M. (1999) 'p53 and Human Cancer: The First Ten Thousand Mutations', *Advances in Cancer Research*. Academic Press, 77(C), pp. 81–86. doi: 10.1016/S0065-230X(08)60785-X.
- Hammond, G. R. V. *et al.* (2012) 'PI4P and PI(4,5)P2 Are Essential But Independent Lipid Determinants of Membrane Identity', *Science*, 337(6095), pp. 727–730. doi: 10.1126/science.1222483.
- Han, J. M. *et al.* (2012) 'The Role of the PI3K Signaling Pathway in CD4+ T Cell Differentiation and Function', *Frontiers in Immunology*, 3(August), p. 245. doi: 10.3389/fimmu.2012.00245.
- Hanahan, D. and Weinberg, R. A. (2000) 'The hallmarks of cancer.', *Cell*, 100(1), pp. 57–70. Available at: <http://www.ncbi.nlm.nih.gov/pubmed/10647931>.
- Hanahan, D. and Weinberg, R. A. (2011) 'Hallmarks of cancer: the next generation.', *Cell*. Elsevier Inc., 144(5), pp. 646–74. Available at: <http://dx.doi.org/10.1016/j.cell.2011.02.013>.
- Harada, Yohsuke *et al.* (2010) 'Transcription factors Foxo3a and Foxo1 couple the E3 ligase Cbl-b to the induction of Foxp3 expression in induced regulatory T cells', *The Journal of Experimental Medicine*, 207(7), pp. 1381–1391. doi: 10.1084/jem.20100004.
- Haxhinasto, S. *et al.* (2008) 'The AKT-mTOR axis regulates de novo differentiation of CD4+Foxp3+ cells.', *The Journal of experimental medicine*, 205(3), pp. 565–74. doi: 10.1084/jem.20071477.
- Hayashi, Y. *et al.* (2016) 'p53 functional deficiency in human colon cancer cells promotes fibroblast-mediated angiogenesis and tumor growth', *Carcinogenesis*. Oxford University Press, 37(10), pp. 972–984. doi: 10.1093/carcin/bgw085.
- He, L. *et al.* (2007) 'Co-existence of high levels of the PTEN protein with enhanced Akt activation in renal cell carcinoma', *Biochimica et Biophysica Acta - Molecular Basis of Disease*. Elsevier, 1772(10), pp. 1134–1142. doi: 10.1016/j.bbadis.2007.07.001.

- Helmin, K. A. *et al.* (2020) 'Maintenance DNA methylation is essential for regulatory T cell development and stability of suppressive function', *Journal of Clinical Investigation*, 130(12), pp. 6571–6587. doi: 10.1172/JCI137712.
- Hlobilkova, A. *et al.* (2000) 'Cell Cycle Arrest by the PTEN Tumor Suppressor Is Target Cell Specific and May Require Protein Phosphatase Activity', *Experimental Cell Research*. Academic Press, 256(2), pp. 571–577. doi: 10.1006/EXCR.2000.4867.
- Hodgkin, M. N. *et al.* (2000) 'Phospholipase D regulation and localisation is dependent upon a phosphatidylinositol 4, 5-bisphosphate-specific PH domain', *Current Biology*, 10(1), pp. 43–46. doi: 10.1016/S0960-9822(99)00264-X.
- Hong, A. W. *et al.* (2020) 'Critical roles of phosphoinositides and NF2 in Hippo pathway regulation', *Genes & Development*, pp. 1–15. doi: 10.1101/gad.333435.119.
- Hopkins, B. D. *et al.* (2020) 'Insulin–PI3K signalling: an evolutionarily insulated metabolic driver of cancer', *Nature Reviews Endocrinology*. Springer US, 16(5), pp. 276–283. doi: 10.1038/s41574-020-0329-9.
- Hruz, T. *et al.* (2008) 'Genevestigator V3: A Reference Expression Database for the Meta-Analysis of Transcriptomes', *Advances in Bioinformatics*, 2008, pp. 1–5. doi: 10.1155/2008/420747.
- Hu-Lieskovan, S. *et al.* (2015) 'Improved antitumor activity of immunotherapy with BRAF and MEK inhibitors in BRAFV600E melanoma', *Science Translational Medicine*. American Association for the Advancement of Science, 7(279), pp. 279ra41-279ra41. doi: 10.1126/scitranslmed.aaa4691.
- Hu, W. *et al.* (2012) 'The Regulation of Multiple p53 Stress Responses is Mediated through MDM2', *Genes and Cancer*. Impact Journals, LLC, pp. 199–208. doi: 10.1177/1947601912454734.
- Huang, S. and Ingber, D. E. (1999) 'The structural and mechanical complexity of cell-growth control', *Nature Cell Biology*, 1(5), pp. E131–E138. doi: 10.1038/13043.
- Huang, T. *et al.* (2011) 'Analysis and prediction of translation rate based on sequence and functional features of the mRNA', *PLoS ONE*. Public Library of Science, 6(1), p. e16036. doi: 10.1371/journal.pone.0016036.
- Ibrahim, E. *et al.* (2009) 'Basal vs. luminal a breast cancer subtypes: A matched case-control study using estrogen receptor, progesterone receptor, and HER-2 as surrogate markers', *Medical Oncology*. Humana Press Inc, 26(3), pp. 372–378. doi: 10.1007/s12032-008-9131-6.

- Ikonomov, O. C. *et al.* (2019) 'Small molecule PI3K inhibitors as cancer therapeutics: Translational promises and limitations', *Toxicology and Applied Pharmacology*. Academic Press Inc., p. 114771. doi: 10.1016/j.taap.2019.114771.
- Im, H. *et al.* (2011) 'The Inoue Method for Preparation and Transformation of Competent *E. coli*: 'Ultra Competent' Cells', *BIO-PROTOCOL*. doi: 10.21769/BioProtoc.143.
- Irvine, R. F. (2005) 'Inositide evolution - towards turtle domination?', *The Journal of Physiology*, 566(2), pp. 295–300. doi: 10.1113/jphysiol.2005.087387.
- Irvine, R. F. (2016) 'A short history of inositol lipids', *Journal of Lipid Research*, 57(11), pp. 1987–1994. doi: 10.1194/jlr.R071712.
- Itahana, K. *et al.* (2007) 'Methods to Detect Biomarkers of Cellular Senescence', in. Humana Press, pp. 21–31. doi: 10.1007/978-1-59745-361-5_3.
- Itahana, Y. and Itahana, K. (2018) 'Emerging Roles of p53 Family Members in Glucose Metabolism.', *International journal of molecular sciences*. Multidisciplinary Digital Publishing Institute (MDPI), 19(3). doi: 10.3390/ijms19030776.
- Itoh, T. *et al.* (1998) 'A novel phosphatidylinositol-5-phosphate 4-kinase (phosphatidylinositol-phosphate kinase Ily) is phosphorylated in the endoplasmic reticulum in response to mitogenic signals', *Journal of Biological Chemistry*, 273(32), pp. 20292–20299. doi: 10.1074/jbc.273.32.20292.
- Jackson, A. L. and Linsley, P. S. (2010) 'Recognizing and avoiding siRNA off-target effects for target identification and therapeutic application', *Nature Reviews Drug Discovery*, pp. 57–67. doi: 10.1038/nrd3010.
- Janku, F. *et al.* (2018) 'Targeting the PI3K pathway in cancer: are we making headway?', *Nature Reviews Clinical Oncology*. Nature Publishing Group, 15(5), pp. 273–291. doi: 10.1038/nrclinonc.2018.28.
- Jeong, I. *et al.* (2018) 'GEMiCCL: Mining genotype and expression data of cancer cell lines with elaborate visualization', *Database*, 2018(2018), pp. 1–8. doi: 10.1093/database/bay041.
- Jia, L.-Q. *et al.* (1997) 'Screening the p53 status of human cell lines using a yeast functional assay', *Molecular Carcinogenesis*. John Wiley & Sons, Ltd, 19(4), pp. 243–253. doi: 10.1002/(SICI)1098-2744(199708)19:4<243::AID-MC5>3.0.CO;2-D.
- Jones, D. R. *et al.* (2006) 'Nuclear PtdIns5P as a Transducer of Stress Signaling: An In Vivo Role for PIP4Kbeta', *Molecular Cell*, 23(5), pp. 685–695. doi: 10.1016/j.molcel.2006.07.014.

- Jones, D. R. *et al.* (2013) 'PtdIns5P is an oxidative stress-induced second messenger that regulates PKB activation', *FASEB Journal*, 27(4), pp. 1644–1656. doi: 10.1096/fj.12-218842.
- Ju, L. G. *et al.* (2019) 'SPOP suppresses prostate cancer through regulation of CYCLIN E1 stability', *Cell Death and Differentiation*. Nature Publishing Group, 26(6), pp. 1156–1168. doi: 10.1038/s41418-018-0198-0.
- Jude, J. G. *et al.* (2015) 'A targeted knockdown screen of genes coding for phosphoinositide modulators identifies PIP4K2A as required for acute myeloid leukemia cell proliferation and survival', *Oncogene*. England, 34(10), pp. 1253–1262. doi: 10.1038/onc.2014.77.
- Kaesler, M. D. *et al.* (2004) 'Regulation of p53 Stability and Function in HCT116 Colon Cancer Cells', *Journal of Biological Chemistry*, 279(9), pp. 7598–7605. doi: 10.1074/jbc.M311732200.
- Kawase, T. *et al.* (2009) 'PH Domain-Only Protein PHLDA3 Is a p53-Regulated Repressor of Akt', *Cell*, 136(3), pp. 535–550. doi: 10.1016/j.cell.2008.12.002.
- Kerdiles, Y. *et al.* (2010) 'Foxo transcription factors control regulatory T cell development and function', *Immunity*, 33(6), pp. 890–904. doi: 10.1016/j.immuni.2010.12.002.Foxo.
- Keune, W.-J. *et al.* (2012) 'Regulation of Phosphatidylinositol-5-Phosphate Signaling by Pin1 Determines Sensitivity to Oxidative Stress', *Science Signaling*, 5(252), pp. ra86–ra86. doi: 10.1126/scisignal.2003223.
- Keune, W.-J. *et al.* (2013) 'Low PIP4K2B Expression in Human Breast Tumors Correlates with Reduced Patient Survival: A Role for PIP4K2B in the Regulation of E-Cadherin Expression', *Cancer Research*, 73(23), pp. 6913–6925. doi: 10.1158/0008-5472.CAN-13-0424.
- Kitagawa, M. *et al.* (2017) 'Dual blockade of the lipid kinase PIP4Ks and mitotic pathways leads to cancer-selective lethality', *Nature Communications*. Nature Publishing Group, 8(1), p. 2200. doi: 10.1038/s41467-017-02287-5.
- Klocke, K. *et al.* (2017) 'CTLA-4 expressed by FOXP3+ regulatory T cells prevents inflammatory tissue attack and not T-cell priming in arthritis', *Immunology*. Blackwell Publishing Ltd, 152(1), pp. 125–137. doi: 10.1111/imm.12754.
- Kunz, J. *et al.* (2000) 'The activation loop of phosphatidylinositol phosphate kinases determines signaling specificity.', *Molecular cell*, 5(1), pp. 1–11. doi: [https://doi.org/10.1016/S1097-2765\(00\)80398-6](https://doi.org/10.1016/S1097-2765(00)80398-6).

- Lacroix, M. and Leclercq, G. (2004) 'Relevance of Breast Cancer Cell Lines as Models for Breast Tumours: An Update', *Breast Cancer Research and Treatment*. Kluwer Academic Publishers, 83(3), pp. 249–289. doi: 10.1023/B:BREA.0000014042.54925.cc.
- Lamia, K. A. *et al.* (2004) 'Increased Insulin Sensitivity and Reduced Adiposity in Phosphatidylinositol 5-Phosphate 4-Kinase *-/-* Mice', *Molecular and Cellular Biology*, 24(11), pp. 5080–5087. doi: 10.1128/MCB.24.11.5080-5087.2004.
- Lane, D. P. (1992) 'p53, guardian of the genome', *Nature*. Nature Publishing Group, pp. 15–16. doi: 10.1038/358015a0.
- Li, G. *et al.* (2014) 'SPOP promotes tumorigenesis by acting as a key regulatory hub in kidney cancer', *Cancer Cell*. Cell Press, 25(4), pp. 455–468. doi: 10.1016/j.ccr.2014.02.007.
- Li, H. *et al.* (2018) 'WWP2 is a physiological ubiquitin ligase for phosphatase and tensin homolog (PTEN) in mice', *Journal of Biological Chemistry*. American Society for Biochemistry and Molecular Biology Inc., 293(23), pp. 8886–8889. doi: 10.1074/jbc.RA117.001060.
- Li, J. *et al.* (1997) 'PTEN, a putative protein tyrosine phosphatase gene mutated in human brain, breast, and prostate cancer', *Science*, 275(5308), pp. 1943–1947. doi: 10.1126/science.275.5308.1943.
- Li, S. *et al.* (2019) 'An efficient auxin-inducible degron system with low basal degradation in human cells', *Nature Methods*. Nature Publishing Group, 16(9), pp. 866–869. doi: 10.1038/s41592-019-0512-x.
- Lima, K. *et al.* (2019) 'PIP4K2A and PIP4K2C transcript levels are associated with cytogenetic risk and survival outcomes in acute myeloid leukemia', *Cancer Genetics*. Elsevier, 233–234, pp. 56–66. doi: 10.1016/J.CANCERGEN.2019.04.002.
- Liu, H. *et al.* (2013) 'ERK differentially regulates Th17- and Treg-cell development and contributes to the pathogenesis of colitis', *European Journal of Immunology*, 43(7), pp. 1716–1726. doi: 10.1002/eji.201242889.
- Liu, M. *et al.* (2019) 'Methodologies for improving HDR efficiency', *Frontiers in Genetics*. Frontiers Media S.A. doi: 10.3389/fgene.2018.00691.
- Liu, Y. and Bodmer, W. F. (2006) 'Analysis of P53 mutations and their expression in 56 colorectal cancer cell lines', *Proceedings of the National Academy of Sciences of the United States of America*, 103(4), pp. 976–981. doi: 10.1073/pnas.0510146103.

- Lowe, S. W. and Earl Ruley, H. (1993) 'Stabilization of the p53 tumor suppressor is induced by adeno virus 5 E1A and accompanies apoptosis', *Genes and Development*. Cold Spring Harbor Laboratory Press, 7(4), pp. 535–545. doi: 10.1101/gad.7.4.535.
- Lu, L. *et al.* (2010) 'Role of SMAD and Non-SMAD Signals in the Development of Th17 and Regulatory T Cells', *The Journal of Immunology*. The American Association of Immunologists, 184(8), pp. 4295–4306. doi: 10.4049/jimmunol.0903418.
- Lui, V. W. Y. *et al.* (2013) 'Frequent mutation of the PI3K pathway in head and neck cancer defines predictive biomarkers', *Cancer Discovery*. American Association for Cancer Research, 3(7), pp. 761–769. doi: 10.1158/2159-8290.CD-13-0103.
- Lundquist, M. R. *et al.* (2018) 'Phosphatidylinositol-5-Phosphate 4-Kinases Regulate Cellular Lipid Metabolism By Facilitating Autophagy', *Molecular Cell*, 70(3), pp. 531-544.e9. doi: 10.1016/j.molcel.2018.03.037.
- Luo, J. *et al.* (2009) 'A Genome-wide RNAi Screen Identifies Multiple Synthetic Lethal Interactions with the Ras Oncogene', *Cell*. Cell Press, 137(5), pp. 835–848. doi: 10.1016/J.CELL.2009.05.006.
- Luo, X. *et al.* (2008) 'Cutting Edge: TGF- β -Induced Expression of Foxp3 in T cells Is Mediated through Inactivation of ERK', *The Journal of Immunology*. The American Association of Immunologists, 180(5), pp. 2757–2761. doi: 10.4049/jimmunol.180.5.2757.
- Luoh, S.-W. *et al.* (2004) 'Overexpression of the amplified Pip4k2 β gene from 17q11–12 in breast cancer cells confers proliferation advantage', *Oncogene*, 23(7), pp. 1354–1363. doi: 10.1038/sj.onc.1207251.
- Ma, X. M. and Blenis, J. (2009) 'Molecular mechanisms of mTOR-mediated translational control', *Nature Reviews Molecular Cell Biology*, 10(5), pp. 307–318. doi: 10.1038/nrm2672.
- Mackey, A. M. *et al.* (2014) 'PIP4ky is a substrate for mTORC1 that maintains basal mTORC1 signaling during starvation', *Science Signaling*, 7(350), pp. ra104–ra104. doi: 10.1126/scisignal.2005191.
- Madeira, F. *et al.* (2019) 'The EMBL-EBI search and sequence analysis tools APIs in 2019', *Nucleic Acids Research*, 47(W1), pp. W636–W641. doi: 10.1093/nar/gkz268.
- Maehama, T. and Dixon, J. E. (1998) 'The tumor suppressor, PTEN/MMAC1, dephosphorylates the lipid second messenger, phosphatidylinositol 3,4,5-trisphosphate', *Journal of Biological Chemistry*. American Society for Biochemistry and Molecular Biology, 273(22), pp. 13375–13378. doi: 10.1074/jbc.273.22.13375.

- Manning, B. D. (2004) 'Balancing Akt with S6K: Implications for both metabolic diseases and tumorigenesis', *Journal of Cell Biology*. The Rockefeller University Press, pp. 399–403. doi: 10.1083/jcb.200408161.
- Marie, J. C. *et al.* (2005) 'TGF- β 1 maintains suppressor function and Foxp3 expression in CD4+CD25+ regulatory T cells', *Journal of Experimental Medicine*. The Rockefeller University Press, 201(7), pp. 1061–1067. doi: 10.1084/jem.20042276.
- Masuda, T. *et al.* (2016) 'Off Target, but Sequence-Specific, shRNA-Associated Trans-Activation of Promoter Reporters in Transient Transfection Assays', *PLOS ONE*. Edited by T. Langmann. Public Library of Science, 11(12), p. e0167867. doi: 10.1371/journal.pone.0167867.
- Mathre, S. *et al.* (2019) 'Functional analysis of the biochemical activity of mammalian phosphatidylinositol 5 phosphate 4-kinase enzymes', *Bioscience Reports*. Portland Press Ltd, 39(2). doi: 10.1042/BSR20182210.
- Mayer, D. *et al.* (2008) 'Proliferative effects of insulin analogues on mammary epithelial cells', *Archives of Physiology and Biochemistry*, 114(1), pp. 38–44. doi: 10.1080/13813450801900645.
- McCrea, H. J. and De Camilli, P. (2009) 'Mutations in Phosphoinositide Metabolizing Enzymes and Human Disease', *Physiology*, 24(1), pp. 8–16. doi: 10.1152/physiol.00035.2008.
- Meriin, A. B. *et al.* (1998) 'Proteasome inhibitors activate stress kinases and induce Hsp72. Diverse effects on apoptosis', *Journal of Biological Chemistry*, 273(11), pp. 6373–6379. doi: 10.1074/jbc.273.11.6373.
- Michalek, R. D. *et al.* (2011) 'Cutting Edge: Distinct Glycolytic and Lipid Oxidative Metabolic Programs Are Essential for Effector and Regulatory CD4+ T Cell Subsets', *The Journal of Immunology*, 186(6), pp. 3299–3303. doi: 10.4049/jimmunol.1003613.
- Michell, R. H. (2011) 'Inositol and its derivatives: Their evolution and functions', *Advances in Enzyme Regulation*. Elsevier Ltd, 51(1), pp. 84–90. doi: 10.1016/j.advenzreg.2010.10.002.
- Milella, M. *et al.* (2015) 'PTEN: Multiple functions in human malignant tumors', *Frontiers in Oncology*. Frontiers Research Foundation. doi: 10.3389/fonc.2015.00024.
- Miskov-Zivanov, N. *et al.* (2013) 'The duration of T cell stimulation is a critical determinant of cell fate and plasticity', *Science Signaling*. American Association for the Advancement of Science, 6(300), pp. ra97–ra97. doi: 10.1126/scisignal.2004217.

- Moore, C. B. *et al.* (2010) 'Short hairpin RNA (shRNA): design, delivery, and assessment of gene knockdown.', *Methods in molecular biology (Clifton, N.J.)*. NIH Public Access, 629, pp. 141–158. doi: 10.1007/978-1-60761-657-3_10.
- Morgens, D. W. *et al.* (2016) 'Systematic comparison of CRISPR/Cas9 and RNAi screens for essential genes', *Nature Biotechnology*. Nature Publishing Group, 34(6), pp. 634–636. Available at: <http://www.nature.com/articles/nbt.3567> (Accessed: 9 December 2019).
- Morrow, A. A. *et al.* (2014) 'The lipid kinase PI4KIII β is highly expressed in breast tumors and activates Akt in cooperation with Rab11a', *Molecular Cancer Research*. American Association for Cancer Research Inc., 12(10), pp. 1492–1508. doi: 10.1158/1541-7786.MCR-13-0604.
- Müller, P. *et al.* (2005) 'Hsp90 is essential for restoring cellular functions of temperature-sensitive p53 mutant protein but not for stabilization and activation of wild-type p53: implications for cancer therapy.', *The Journal of biological chemistry*. American Society for Biochemistry and Molecular Biology, 280(8), pp. 6682–91. doi: 10.1074/jbc.M412767200.
- Muller, P. A. J. and Vousden, K. H. (2014) 'Mutant p53 in cancer: New functions and therapeutic opportunities', *Cancer Cell*. Cell Press, pp. 304–317. doi: 10.1016/j.ccr.2014.01.021.
- Nakanishi, A. *et al.* (2014) 'The tumor suppressor PTEN interacts with p53 in hereditary cancer (Review)', *International Journal of Oncology*. Spandidos Publications, pp. 1813–1819. doi: 10.3892/ijo.2014.2377.
- Nambiar, T. S. *et al.* (2019) 'Stimulation of CRISPR-mediated homology-directed repair by an engineered RAD18 variant', *Nature Communications*. Nature Publishing Group, 10(1), pp. 1–13. doi: 10.1038/s41467-019-11105-z.
- Natsume, T. *et al.* (2016) 'Rapid Protein Depletion in Human Cells by Auxin-Inducible Degron Tagging with Short Homology Donors', *Cell Reports*. Cell Press, 15(1), pp. 210–218. doi: 10.1016/j.celrep.2016.03.001.
- Nelson, W. G. and Kastan, M. B. (1994) 'DNA strand breaks: the DNA template alterations that trigger p53-dependent DNA damage response pathways.', *Molecular and Cellular Biology*. American Society for Microbiology, 14(3), pp. 1815–1823. doi: 10.1128/mcb.14.3.1815.
- Nishimura, K. *et al.* (2009) 'An auxin-based degron system for the rapid depletion of proteins in nonplant cells', *Nature Methods*. Nature Publishing Group, 6(12), pp. 917–922. doi: 10.1038/nmeth.1401.

- Nishimura, K. and Fukagawa, T. (2017) 'An efficient method to generate conditional knockout cell lines for essential genes by combination of auxin-inducible degron tag and CRISPR/Cas9', *Chromosome Research*. Springer Netherlands, 25(3–4), pp. 253–260. doi: 10.1007/s10577-017-9559-7.
- Noch, E. K. *et al.* (2020) 'Distribution and localization of phosphatidylinositol 5-phosphate, 4-kinase alpha and beta in the brain', *bioRxiv*. Cold Spring Harbor Laboratory, p. 2020.01.29.925685. doi: 10.1101/2020.01.29.925685.
- Obata, Y. *et al.* (2014) 'The epigenetic regulator Uhrf1 facilitates the proliferation and maturation of colonic regulatory T cells', *Nature Immunology*. Nature Publishing Group, 15(6), pp. 571–579. doi: 10.1038/ni.2886.
- Oda, K. *et al.* (2005) 'High Frequency of Coexistent Mutations of PIK3CA and PTEN Genes in Endometrial Carcinoma', *Cancer Research*, 65(23), pp. 10669–10673. doi: 10.1158/0008-5472.CAN-05-2620.
- Ohkura, N. and Sakaguchi, S. (2010a) 'Foxo1 and Foxo3 help Foxp3.', *Immunity*. Elsevier, 33(6), pp. 835–7. doi: 10.1016/j.immuni.2010.12.004.
- Ohkura, N. and Sakaguchi, S. (2010b) 'Regulatory T cells: Roles of T cell receptor for their development and function', *Seminars in Immunopathology*, 32(2), pp. 95–106. doi: 10.1007/s00281-010-0200-5.
- Okkenhaug, K. (2002) 'Impaired B and T Cell Antigen Receptor Signaling in p110delta PI 3-Kinase Mutant Mice', *Science*, 297(5583), pp. 7–18. doi: 10.1126/science.1073560.
- Okkenhaug, K. (2013) 'Signaling by the Phosphoinositide 3-Kinase Family in Immune Cells', *Annual Review of Immunology*. Annual Reviews, 31(1), pp. 675–704. doi: 10.1146/annurev-immunol-032712-095946.
- Ouyang, W. *et al.* (2010) 'Foxo proteins cooperatively control the differentiation of Foxp3+ regulatory T cells.', *Nature immunology*. Nature Publishing Group, 11(7), pp. 618–627. doi: 10.1038/ni.1884.
- Pandiyan, P. *et al.* (2007) 'CD4+CD25+Foxp3+ regulatory T cells induce cytokine deprivation-mediated apoptosis of effector CD4+ T cells.', *Nature immunology*, 8(12), pp. 1353–1362. doi: 10.1038/ni1536.
- Papatheodorou, I. *et al.* (2020) 'Expression Atlas update: from tissues to single cells', *Nucleic acids research*, 48(D1), pp. D77–D83. doi: 10.1093/nar/gkz947.

- Patterson, S. J. *et al.* (2011) 'Cutting Edge: PHLPP Regulates the Development, Function, and Molecular Signaling Pathways of Regulatory T Cells', *The Journal of Immunology*, 186(10), pp. 5533–5537. doi: 10.4049/jimmunol.1002126.
- Patton, D. T. *et al.* (2006) 'Cutting Edge: The Phosphoinositide 3-Kinase p110 Is Critical for the Function of CD4+CD25+Foxp3+ Regulatory T Cells', *The Journal of Immunology*, 177(10), pp. 6598–6602. doi: 10.4049/jimmunol.177.10.6598.
- Patton, D. T. *et al.* (2011) 'The PI3K p110 δ Regulates Expression of CD38 on Regulatory T Cells', *PLoS ONE*. Edited by J. Zimmer, 6(3), p. e17359. doi: 10.1371/journal.pone.0017359.
- Pedoux, R. *et al.* (2005) 'ING2 Regulates the Onset of Replicative Senescence by Induction of p300-Dependent p53 Acetylation', *Molecular and Cellular Biology*, 25(15), pp. 6639–6648. doi: 10.1128/MCB.25.15.6639.
- Pendaries, C. *et al.* (2003) 'Phosphoinositide signaling disorders in human diseases', *FEBS Letters*, 546(1), pp. 25–31. doi: 10.1016/S0014-5793(03)00437-X.
- Pennock, N. D. *et al.* (2013) 'T cell responses: naïve to memory and everything in between', *Advances in Physiology Education*. American Physiological Society, 37(4), pp. 273–283. doi: 10.1152/advan.00066.2013.
- Petryszak, R. *et al.* (2016) 'Expression Atlas update - An integrated database of gene and protein expression in humans, animals and plants', *Nucleic Acids Research*, 44(D1), pp. D746–D752. doi: 10.1093/nar/gkv1045.
- Pizer, F. L. and Ballou, C. E. (1959) 'Studies on myo-Inositol Phosphates of Natural Origin', *Journal of the American Chemical Society*, 81(4), pp. 915–921. doi: 10.1021/ja01513a040.
- Poli, A. *et al.* (2020) 'Genetic and pharmacological inhibition of PIP4Ks reprograms human T-reg cell identity and functional output', *Manuscript submitted for publication*.
- Pompura, S. L. and Dominguez-Villar, M. (2018) 'The PI3K/AKT signaling pathway in regulatory T-cell development, stability, and function', *Journal of Leukocyte Biology*. John Wiley & Sons, Ltd, 103(6), pp. 1065–1076. doi: 10.1002/JLB.2MIR0817-349R.
- Powell, S. N. *et al.* (1995) 'Differential sensitivity of p53(-) and p53(+) cells to caffeine-induced radiosensitization and override of G2 delay.', *Cancer research*. American Association for Cancer Research, 55(8), pp. 1643–8. Available at: <http://www.ncbi.nlm.nih.gov/pubmed/7712468> (Accessed: 2 March 2020).

- Qin, J. H. *et al.* (2017) 'Hsp90 inhibitor induces KG-1a cell differentiation and apoptosis via Akt/NF- κ B signaling', *Oncology Reports*. Spandidos Publications, 38(3), pp. 1517–1524. doi: 10.3892/or.2017.5797.
- Rameh, L. E. and Cantley, L. C. (1999) 'The Role of Phosphoinositide 3-Kinase Lipid Products in Cell Function', *Journal of Biological Chemistry*, 274(13), pp. 8347–8350. doi: 10.1074/jbc.274.13.8347.
- Ramel, D. *et al.* (2009) 'PtdIns5P protects Akt from dephosphorylation through PP2A inhibition', *Biochemical and Biophysical Research Communications*. Academic Press, 387(1), pp. 127–131. doi: 10.1016/J.BBRC.2009.06.139.
- Rao, V. D. *et al.* (1998) 'Structure of Type II β Phosphatidylinositol Phosphate Kinase', *Cell*, 94(6), pp. 829–839. doi: 10.1016/S0092-8674(00)81741-9.
- Raof, N. A. *et al.* (2016) 'The effects of transfection reagent polyethyleneimine (PEI) and non-targeting control siRNAs on global gene expression in human aortic smooth muscle cells', *BMC Genomics*. BioMed Central Ltd., 17(1), pp. 1–13. doi: 10.1186/s12864-015-2267-9.
- Raychaudhuri, S. *et al.* (2008) 'Common variants at CD40 and other loci confer risk of rheumatoid arthritis', *Nature Genetics*, 40(10), pp. 1216–1223. doi: 10.1038/ng.233.
- Rincón, M. *et al.* (2001) 'Signal transduction by MAP kinases in T lymphocytes', *Oncogene*, 20(19), pp. 2490–2497. doi: 10.1038/sj.onc.1204382.
- Roberts, S. and Girardi, M. (2008) 'Conventional and Unconventional T Cells', in *Clinical and Basic Immunodermatology*. London: Springer London, pp. 85–104. doi: 10.1007/978-1-84800-165-7_6.
- Rudensky, A. Y. (2011) 'Regulatory T cells and Foxp3', *Immunological Reviews*. Wiley/Blackwell (10.1111), 241(1), pp. 260–268. doi: 10.1111/j.1600-065X.2011.01018.x.
- Rudolph, M. G. *et al.* (2006) 'How TCRs bind MHCs, Peptides, and Coreceptors', *Annual Review of Immunology*, 24(1), pp. 419–466. doi: 10.1146/annurev.immunol.23.021704.115658.
- Saal, L. H. *et al.* (2005) 'PIK3CA Mutations Correlate with Hormone Receptors, Node Metastasis, and ERBB2, and Are Mutually Exclusive with PTEN Loss in Human Breast Carcinoma', *Cancer Research*, 65(7), pp. 2554–2559. doi: 10.1158/0008-5472.CAN-04-3913.
- Sakaguchi, S. *et al.* (2001) 'Immunologic tolerance maintained by CD25+ CD4+ regulatory T cells: their common role in controlling autoimmunity, tumor immunity, and transplantation tolerance', *Immunological Reviews*, 182(1), pp. 18–32. doi: 10.1034/j.1600-065X.2001.1820102.x.

- Sambrook, J. and Russell, D. (2000) *Molecular Cloning: A laboratory Manual*. 3rd Editio. United State: Cold Spring Harbor Laboratory Press.
- Santegoets, S. J. A. M. *et al.* (2015) 'Monitoring regulatory T cells in clinical samples: consensus on an essential marker set and gating strategy for regulatory T cell analysis by flow cytometry', *Cancer Immunology, Immunotherapy*. Springer Berlin Heidelberg, 64(10), pp. 1271–1286. doi: 10.1007/s00262-015-1729-x.
- Sarbassov, D. D. *et al.* (2005) 'Phosphorylation and regulation of Akt/PKB by the rictor-mTOR complex', *Science*. American Association for the Advancement of Science, 307(5712), pp. 1098–1101. doi: 10.1126/science.1106148.
- Sarbassov, D. D. *et al.* (2006) 'Prolonged Rapamycin Treatment Inhibits mTORC2 Assembly and Akt/PKB', *Molecular Cell*, 22(2), pp. 159–168. doi: 10.1016/j.molcel.2006.03.029.
- Sathyan, K. M. *et al.* (2019) 'An improved auxin-inducible degron system preserves native protein levels and enables rapid and specific protein depletion.', *Genes & development*. Cold Spring Harbor Laboratory Press, 33(19–20), pp. 1441–1455. doi: 10.1101/gad.328237.119.
- Schmittgen, T. D. and Livak, K. J. (2008) 'Analyzing real-time PCR data by the comparative CT method', *Nature Protocols*, 3(6), pp. 1101–1108. doi: 10.1038/nprot.2008.73.
- Schulze, H. *et al.* (2006) 'Characterization of the megakaryocyte demarcation membrane system and its role in thrombopoiesis.', *Blood*. The American Society of Hematology, 107(10), pp. 3868–75. doi: 10.1182/blood-2005-07-2755.
- Seo, Y. R. *et al.* (2002) 'Implication of p53 in base excision dna repair: In vivo evidence', *Oncogene*. Nature Publishing Group, 21(5), pp. 731–737. doi: 10.1038/sj.onc.1205129.
- Shalem, O. *et al.* (2014) 'Genome-scale CRISPR-Cas9 knockout screening in human cells', *Science*. American Association for the Advancement of Science, 343(6166), pp. 84–87. doi: 10.1126/science.1247005.
- Sharma, S. *et al.* (2019) 'Phosphatidylinositol 5 Phosphate 4-Kinase Regulates Plasma-Membrane PIP3 Turnover and Insulin Signaling', *Cell Reports*. Cell Press, 27(7), pp. 1979-1990.e7. doi: 10.1016/J.CELREP.2019.04.084.
- Shi, J. *et al.* (2015) 'Discovery of cancer drug targets by CRISPR-Cas9 screening of protein domains', *Nature Biotechnology*. Nature Publishing Group, 33(6), pp. 661–667. doi: 10.1038/nbt.3235.

- Shim, H. *et al.* (2016) 'Deletion of the gene *Pip4k2c*, a novel phosphatidylinositol kinase, results in hyperactivation of the immune system.', *Proceedings of the National Academy of Sciences of the United States of America*. National Academy of Sciences, 113(27), pp. 7596–7601. doi: 10.1073/pnas.1600934113.
- Shin, Y. J. *et al.* (2019) 'PIP4K2A as a negative regulator of PI3K in PTEN-deficient glioblastoma.', *The Journal of experimental medicine*. The Rockefeller University Press, 216(5), pp. 1120–1134. doi: 10.1084/jem.20172170.
- Sivakumaren, S. C. *et al.* (2020) 'Targeting the PI5P4K Lipid Kinase Family in Cancer Using Covalent Inhibitors', *Cell Chemical Biology*. Elsevier Ltd., pp. 1–13. doi: 10.1016/j.chembiol.2020.02.003.
- Somerville, R. P. T. *et al.* (2012) 'Clinical scale rapid expansion of lymphocytes for adoptive cell transfer therapy in the WAVE[®] bioreactor', *Journal of Translational Medicine*. BioMed Central, 10(1), p. 69. doi: 10.1186/1479-5876-10-69.
- Soond, D. R. *et al.* (2012) 'Does the PI3K pathway promote or antagonize regulatory T cell development and function?', *Frontiers in Immunology*, 3(AUG), pp. 1–8. doi: 10.3389/fimmu.2012.00244.
- Stambolic, V. *et al.* (2001) 'Regulation of PTEN Transcription by p53', *Molecular Cell*. Cell Press, 8(2), pp. 317–325. doi: 10.1016/S1097-2765(01)00323-9.
- Strahl, T. and Thorner, J. (2007) 'Synthesis and function of membrane phosphoinositides in budding yeast, *Saccharomyces cerevisiae*', *Biochimica et Biophysica Acta (BBA) - Molecular and Cell Biology of Lipids*, 1771(3), pp. 353–404. doi: 10.1016/j.bbalip.2007.01.015.
- Strauss, L. *et al.* (2009) 'Differential Responses of Human Regulatory T Cells (Treg) and Effector T Cells to Rapamycin', *PLoS ONE*. Edited by D. Unutmaz. Public Library of Science, 4(6), p. e5994. doi: 10.1371/journal.pone.0005994.
- Sun, H. *et al.* (1999) 'PTEN modulates cell cycle progression and cell survival by regulating phosphatidylinositol 3,4,5,-trisphosphate and Akt/protein kinase B signaling pathway', *Proceedings of the National Academy of Sciences*, 96(11), pp. 6199–6204. doi: 10.1073/pnas.96.11.6199.
- Szustak, M. and Gendaszewska-Darmach, E. (2020) 'Extracellular Nucleotides Selectively Induce Migration of Chondrocytes and Expression of Type II Collagen', *International Journal of Molecular Sciences*, 21(15), p. 5227. doi: 10.3390/ijms21155227.
- Tate, J. G. *et al.* (2019) 'COSMIC: The Catalogue Of Somatic Mutations In Cancer', *Nucleic Acids Research*. Oxford University Press, 47(D1), pp. D941–D947. doi: 10.1093/nar/gky1015.

- Thorsell, A. G. *et al.* (2006) 'Structure of Human Phosphatidylinositol-4-phosphate 5-kinase, type II, gamma. PDB ID:2GK9.' doi: 10.2210/PDB2GK9/PDB.
- Toker, A. (1998) 'The synthesis and cellular roles of phosphatidylinositol 4,5-bisphosphate', *Current Opinion in Cell Biology*, 10(2), pp. 254–261. doi: <http://dx.doi.org/10.1007/s00018-002-8465-z>.
- Toker, A. (2002) 'Phosphoinositides and signal transduction', *Cellular and Molecular Life Sciences (CMLS)*, 59(5), pp. 761–779. doi: 10.1007/s00018-002-8465-z.
- Tong, A. A. *et al.* (2019) 'Regulatory T cells differ from conventional CD4+ T cells in their recirculatory behavior and lymph node transit times', *Immunology and Cell Biology*, 97(9), pp. 787–798. doi: 10.1111/imcb.12276.
- Tran, N.-T. *et al.* (2019) 'Enhancement of Precise Gene Editing by the Association of Cas9 With Homologous Recombination Factors', *Frontiers in Genetics*. Frontiers Media S.A., 10(APR), p. 365. doi: 10.3389/fgene.2019.00365.
- Tresaugues, L. *et al.* (2012) 'Crystal Structure of Human Phosphatidylinositol-5-Phosphate 4-Kinase Type-2 Alpha. PDB ID: 2YBX.' doi: 10.2210/PDB2YBX/PDB.
- Uno, J. K. *et al.* (2010) 'Altered Macrophage Function Contributes to Colitis in Mice Defective in the Phosphoinositide-3 Kinase Subunit p110 δ ', *Gastroenterology*, 139(5), pp. 1642-1653.e6. doi: 10.1053/j.gastro.2010.07.008.
- Valerie, K. and Povirk, L. F. (2003) 'Regulation and mechanisms of mammalian double-strand break repair', *Oncogene*, pp. 5792–5812. doi: 10.1038/sj.onc.1206679.
- Vanhaesebroeck, B. *et al.* (2010) 'The emerging mechanisms of isoform-specific PI3K signalling', *Nature Reviews Molecular Cell Biology*. Nature Publishing Group, 11(5), pp. 329–341. doi: 10.1038/nrm2882.
- Viaud, J. *et al.* (2016) 'Phosphoinositides: Important lipids in the coordination of cell dynamics', *Biochimie*, 125, pp. 250–258. doi: 10.1016/j.biochi.2015.09.005.
- Vicinanza, M. *et al.* (2015) 'PI(5)P Regulates Autophagosome Biogenesis', *Molecular Cell*. Cell Press, 57(2), pp. 219–234. doi: 10.1016/J.MOLCEL.2014.12.007.
- Vignali, D. A. A. *et al.* (2008) 'How regulatory T cells work', *Nature Reviews Immunology*, 8(7), pp. 523–532. doi: 10.1038/nri2343.
- Vivanco, I. and Sawyers, C. L. (2002) 'The phosphatidylinositol 3-Kinase–AKT pathway in human cancer', *Nature Reviews Cancer*, 2(7), pp. 489–501. doi: 10.1038/nrc839.

- van der Vliet, H. J. J. and Nieuwenhuis, E. E. (2007) 'IPEX as a result of mutations in FOXP3.', *Clinical & developmental immunology*, 2007, p. 89017. doi: 10.1155/2007/89017.
- Voss, M. D. *et al.* (2014) 'Discovery and pharmacological characterization of a novel small molecule inhibitor of phosphatidylinositol-5-phosphate 4-kinase, type II, beta', *Biochemical and Biophysical Research Communications*. Academic Press, 449(3), pp. 327–331. doi: 10.1016/J.BBRC.2014.05.024.
- Wang, D. G. *et al.* (2019) 'PIP4Ks Suppress Insulin Signaling through a Catalytic-Independent Mechanism', *Cell Reports*. Cell Press, 27(7), pp. 1991-2001.e5. doi: 10.1016/j.celrep.2019.04.070.
- Wang, H. *et al.* (2012) 'Doxycycline regulated induction of AKT in murine prostate drives proliferation independently of p27 cyclin dependent kinase inhibitor downregulation', *PLoS ONE*. Public Library of Science, 7(7). doi: 10.1371/journal.pone.0041330.
- Wang, H. *et al.* (2016) 'Global, regional, and national life expectancy, all-cause mortality, and cause-specific mortality for 249 causes of death, 1980–2015: a systematic analysis for the Global Burden of Disease Study 2015', *The Lancet*. Elsevier, 388(10053), pp. 1459–1544. doi: 10.1016/S0140-6736(16)31012-1.
- Wang, M. *et al.* (2010) 'Genomic tagging reveals a random association of endogenous PtdIns5P 4-kinases IIalpha and IIbeta and a partial nuclear localization of the IIalpha isoform.', *The Biochemical journal*, 430(2), pp. 215–21. doi: 10.1042/BJ20100340.
- Wang, Y. J. *et al.* (2003) 'Phosphatidylinositol 4 phosphate regulates targeting of clathrin adaptor AP-1 complexes to the Golgi', *Cell*, 114(3), pp. 299–310. doi: 10.1016/S0092-8674(03)00603-2.
- Ward, S. G. and Cantrell, D. A. (2001) 'Phosphoinositide 3-kinases in T lymphocyte activation', *Current Opinion in Immunology*, 13(3), pp. 332–338. doi: 10.1016/S0952-7915(00)00223-5.
- Wei, P. C. *et al.* (2012) 'Non-targeting siRNA induces NPGPx expression to cooperate with exoribonuclease XRN2 for releasing the stress', *Nucleic Acids Research*, 40(1), pp. 323–332. doi: 10.1093/nar/gkr714.
- Wilcox, A. and Hinchliffe, K. A. (2008) 'Regulation of extranuclear PtdIns5 P production by phosphatidylinositol phosphate 4-kinase 2 α ', *FEBS Letters*, 582(9), pp. 1391–1394. doi: 10.1016/j.febslet.2008.03.022.
- Williams, L. M. and Rudensky, A. Y. (2007) 'Maintenance of the Foxp3-dependent developmental program in mature regulatory T cells requires continued expression of Foxp3', *Nature Immunology*. Nature Publishing Group, 8(3), pp. 277–284. doi: 10.1038/ni1437.

- Wong, J. *et al.* (2007) 'Adaptation of TCR Repertoires to Self-Peptides in Regulatory and Nonregulatory CD4 + T Cells', *The Journal of Immunology*. The American Association of Immunologists, 178(11), pp. 7032–7041. doi: 10.4049/jimmunol.178.11.7032.
- Yamada, R. *et al.* (2018) 'A Super Strong Engineered Auxin–TIR1 Pair', *Plant and Cell Physiology*. Oxford University Press, 59(8), pp. 1538–1544. doi: 10.1093/pcp/pcy127.
- Yan, D. *et al.* (2015) 'Imbalanced signal transduction in regulatory T cells expressing the transcription factor FoxP3', *Proceedings of the National Academy of Sciences of the United States of America*. National Academy of Sciences, 112(48), pp. 14942–14947. doi: 10.1073/pnas.1520393112.
- Yao, R. and Cooper, G. (1995) 'Requirement for phosphatidylinositol-3 kinase in the prevention of apoptosis by nerve growth factor', *Science*, 267(5206), pp. 2003–2006. doi: 10.1126/science.7701324.
- Yesbolatova, A. *et al.* (2019) 'Generation of conditional auxin-inducible degron (AID) cells and tight control of degron-fused proteins using the degradation inhibitor auxinole', *Methods*. doi: 10.1016/j.ymeth.2019.04.010.
- Yokosuka, T. *et al.* (2010) 'Spatiotemporal Basis of CTLA-4 Costimulatory Molecule-Mediated Negative Regulation of T Cell Activation', *Immunity*. Elsevier Inc., 33(3), pp. 326–339. doi: 10.1016/j.immuni.2010.09.006.
- Yoon, S. and Seger, R. (2006) 'The extracellular signal-regulated kinase: Multiple substrates regulate diverse cellular functions', *Growth Factors*. Informa UK Limited, 24(1), pp. 21–44. doi: 10.1080/02699050500284218.
- Zhao, L. *et al.* (2015) 'Combination of cytokinin and auxin induces apoptosis, cell cycle progression arrest and blockage of the Akt pathway in HeLa cells', *Molecular Medicine Reports*. Spandidos Publications, 12(1), pp. 719–727. doi: 10.3892/mmr.2015.3420.
- Zhao, W. *et al.* (2017) 'Class I phosphatidylinositol 3-kinase inhibitors for cancer therapy', *Acta Pharmaceutica Sinica B*. Elsevier, 7(1), pp. 27–37. doi: 10.1016/j.apsb.2016.07.006.
- Zheng, L. and Conner, S. D. (2018) 'PI5P4Ky functions in DTX1-mediated notch signaling', *Proceedings of the National Academy of Sciences of the United States of America*. National Academy of Sciences, 115(9), pp. E1983–E1990. doi: 10.1073/pnas.1712142115.

- Zheng, T. *et al.* (2010) 'PTEN- and p53-mediated apoptosis and cell cycle arrest by FTY720 in gastric cancer cells and nude mice', *Journal of Cellular Biochemistry*. John Wiley & Sons, Ltd, 111(1), pp. 218–228. doi: 10.1002/jcb.22691.
- Zhou, B. P., Liao, Y., Xia, W., Spohn, B., *et al.* (2001) 'Cytoplasmic localization of p21Cip1/WAF1 by Akt-induced phosphorylation in HER-2/neu-overexpressing cells', *Nature Cell Biology*, 3(3), pp. 245–252. doi: 10.1038/35060032.
- Zhou, B. P., Liao, Y., Xia, W., Zou, Y., *et al.* (2001) 'HER-2/neu induces p53 ubiquitination via Akt-mediated MDM2 phosphorylation', *Nature Cell Biology*. Nature Publishing Group, 3(11), pp. 973–982. doi: 10.1038/ncb1101-973.
- Zhou, H. and Zeng, X. (2009) 'Energy profile and secondary structure impact shRNA efficacy', *BMC Genomics*, 10(Suppl 1), p. S9. doi: 10.1186/1471-2164-10-S1-S9.
- Zhou, X. *et al.* (2019) 'Noteworthy prognostic value of phospholipase C delta genes in early stage pancreatic ductal adenocarcinoma patients after pancreaticoduodenectomy and potential molecular mechanisms', *Cancer Medicine*. John Wiley & Sons, Ltd, p. cam4.2699. doi: 10.1002/cam4.2699.
- Zilfou, J. T. and Lowe, S. W. (2009) 'Tumor suppressive functions of p53.', *Cold Spring Harbor perspectives in biology*. doi: 10.1101/cshperspect.a001883.